

**Mineralogical, Chemical, and Isotopic (Sr, Pb) Composition of
Atmospheric Mineral Dusts in an Ombrotrophic Peat Bog,
Southern South America**

INAUGURAL – DISSERTATION

Zur
Erlangung der Doktorwürde
Der
Naturwissenschaftlich-Mathematischen
Gesamtfakultät
Der
Ruprecht-Karls-Universität
Heidelberg

Vorgelegt von

M.Sc. Atindra Sapkota
aus Nepal

Tag der mündlichen Prüfung:
08.12.2006

**Mineralogical, Chemical, and Isotopic (Sr, Pb) Composition of
Atmospheric Mineral Dusts in an Ombrotrophic Peat Bog,
Southern South America**

Gutachter: Prof. Dr. William Shotyk
Institute für Umwelt-Geochemie
Ruprechts-Karls-Universität Heidelberg
Im Neuenheimer Feld 236
D-69120 Heidelberg

Prof. Dr. Heinz Friedrich Scholer

-Table of contents-

Summary	3
Zusammenfassung	5
Acknowledgements	7
Chapter 1	
1-1 Introduction and background	11
Importance of mineral dusts	14
1-2 Tracing the sources of atmospheric dusts	15
1-2.1 Mineralogy	16
1-2.2 Trace elements	17
1-2.3 Radiogenic isotopes (Sr, Nd, Pb)	19
1-3 Archives of atmospheric dusts	21
1-3.1 Polar snow and ice	21
1-3.2 Marine sediments	23
1-3.3 Peat bogs	23
1-3.3.1 Peatlands	24
- Definitions	24
- Formation	25
- Bog environments	26
1-3.3.2 Peat as an archive of environmental change	27
- Geochemistry	27
- Mineralogy	28
- Composition of peat ash	30
- Peat bogs as archives of atmospheric dusts	31
1-4 Atmospheric deposition of Pb in southern Hemisphere	32
1-5 Aims of the study	33
1-6 Materials and methods	34
1-6.1 Study site	34
1-6.2 Sampling procedure	35
1-6.3 Sample handling and analytical methods	36
1-6.3.1 Modified sample handling and analytical methods	36
- Peat slice and volume/density calculation	36
- Ash and AIA contents	37
1-6.3.2 Summary of sample handling and analytical methods	38
1-7 Results	40
1-8 Conclusions and perspectives	40
Chapter 2	
Six millennia of atmospheric dust deposition in southern South America (Isla Navarino, Chile). (Submitted to The Holocene, 2006)	51
Chapter 3	
Characterization of atmospheric mineral dusts preserved in an ombrotrophic peat bog from southernmost Southern Hemisphere, Oreste Bog, Tierra del Fuego, Chile. (Submitted to Quaternary Research, 2006)	71

Chapter 4

Holocene record of $^{87}\text{Sr}/^{86}\text{Sr}$ ratios in dust components of an ombrotrophic bog at the southernmost edge of South America: volcanic inputs, atmospheric soil dust, and comparison with ice core dust of the Eastern Antarctic Plateau. (Submitted to Earth and Planetary Science Letters, 2006) 93

Chapter 5

The Paradigm of natural Pb in the atmosphere: 6,000 years of soil dust deposition recorded by the Oreste peat bog, southern Patagonia. (Submitted to Global Biogeochemical Cycles, 2006) 113

Appendix I

Suggested protocol for collecting, handling and preparing peat cores and peat samples for physical, chemical, mineralogical and isotopic analysis. (Journal of Environmental Monitoring, 6 (2004) 481-492) 129

Appendix II

Analytical procedures for the determination of selected major (Al, Ca, Fe, K, Mg, Na and Ti) and trace (Li, Mn, Sr, and Zn) elements in peat and plant samples using inductively coupled plasma optical emission spectrometry. (Analytica Chimica Acta, 540 (2005) 247-256) 149

Appendix III

Atmospheric deposition of trace elements (Cr, Cu, Zn, and Rb) in southern South America (a brief overview). 163

Appendix IV

Cleaning of Acid Insoluble Ash (AIA) for Sr isotope measurements. 169

Appendix V

Titanium in an ombrotrophic peat profile from Valle de Andorra (Ushuaia, Tierra del Fuego) as an indicator of atmospheric deposition of mineral dust for the last ca. 1300 years. 173

Summary

Peat bogs are excellent environmental archives of atmospheric deposition of many major and trace elements and of mineral dusts. Geochemical studies of major and trace elements, mineralogy of atmospheric dust and their radiogenic isotope compositions in the peat, provide important information about the mineralogical host phases of major and trace elements transported through the atmosphere, grain size fractionation during transport, and their possible source areas (PSAs). To date, no peat bog records of atmospheric dust depositions in southern South America have been reported. Therefore, the major and trace elements, and mineralogical and radiogenic isotopic compositions of inorganic fraction in a peat bog from southern South America were investigated. The main goal was to characterize the atmospheric dust deposition in southern South America, and to identify their PSA. For this purpose, a 542 cm long core from the Oreste bog in southern Chile, Isla Navarino (55°13'13" S, 67°37'28" W), was used. The peat formation at the Oreste bog began at ~ 11160 ¹⁴C yr before present (BP) (13 ka cal. BP).

Because of the limited amount of mineral material available from thinly sliced cores (~ 2 – 3 mg from a 2 cm slice), an analytical method was developed to extract, isolate, and chemically characterize atmospheric dusts from ombrotrophic peat. About 2 g of dried peat was combusted overnight at 550 °C that on ashing yielded ca. 20 mg. 1M HCl was allowed to react for 15 min to dissolve soluble minerals such as carbonates, sulphates, and oxides which were mainly formed during combustion. Acid insoluble ash (AIA) was then separated from the solution (acid soluble ash: ASA) by using polycarbonate filters of pore size 0.2 μm. The analytical procedure effectively extracted and isolated the AIA fraction which was composed of silicates and refractory oxides derived from crustal weathering, as well as volcanic ash and glass particles. The residue obtained was analyzed directly on the filters using the TITAN and EMMA XRF spectrometers for major (Al, Ca, Fe, K, Si, and Ti) and trace (Cr, Mn, Pb, Sr, and Zr) elements. Although the AIA amounts to no more than a thin layer (ca 2-3 mg) of atmospheric dust, excellent XRF spectra were obtained. Afterwards, Scanning Electron Microscopy (SEM) was used to identify the predominant minerals in selected AIA samples. Similarly, radiogenic isotopes of Pb and Sr compositions in selected AIA and ASA were measured by Multicollector Thermal Ionization Mass Spectrometer (MC-TIMS).

The concentration of titanium (Ti) was used as a surrogate of mineral input in the peat because of its association with accessory minerals which are generally resistant to chemical weathering. The mineral accumulation rate (MAR) was calculated by using Ti concentration in bulk peat, dry bulk density, and long term peat accumulation rate. The distribution of calcium (Ca), manganese (Mn) and strontium (Sr) in bulk peat, and ⁸⁷Sr/⁸⁶Sr compositions in the ASA indicate that the peat was truly ombrotrophic above ~ 300 cm. The distribution of Ca, Mn, Sr, and Ti in the bulk peat were used to show that the mineral dust accumulation for the last ca. 6000 yrs were predominantly atmospheric and effectively constant ($0.43 \pm 0.12 \text{ g m}^{-2} \text{ yr}^{-1}$) except at ca. 4200 cal yr BP. This was further supported by the Ti and zirconium (Zr) concentrations in the acid insoluble ash (AIA). At ca. 4200 cal yr BP where the dust abundance was elevated, Zr was enriched relative to Ti. The SEM micrographs showed that most of the minerals above ca. 400 cm of the peat profile were fine (10 – 20 μm or less) and rounded, except at ~ 300 cm where volcanic tephra grains (> 20 – 40 μm) were predominant. Combined together with the relatively stable amount of AIA, they reflect long-range transport of atmospheric mineral dust and the climate stability for the past ca. 6000 yrs.

The Sr isotope compositions of AIA for the last six millennia (above ~ 420 cm) varied within a narrow range of $0.7087 < ^{87}\text{Sr}/^{86}\text{Sr} < 0.7090$ (average: 0.70884 ± 0.00014 ; n = 9), except at ca. 50 – 60 cm, 160 cm, and 300 cm. At ~ 300 cm, where the tephra grains were predominant and at the other two exceptional points, the Sr isotope compositions deviated towards less radiogenic composition. Similar deviation was also observed in the fen peat before six millennia (at ~ 490 cm). The available age dates, Sr isotope compositions of AIA, elemental concentration of silica (Si) and potassium (K) (expressed in the oxide form and used as a K₂O/SiO₂ ratio), and the published volcanic eruption records in southern South America collectively indicated four episodes of tephra input from the Mt. Burney volcano (⁸⁷Sr/⁸⁶Sr = 0.7042) to the Oreste bog. For the rest of the profile,

the Sr isotope compositions indicate that the atmospheric dusts were derived from the Patagonian belt (southern South America). In general, they collectively supported the previously held view that the atmospheric mineral dusts were well mixed and relatively stable for the last ca. 6000 yrs.

In addition, the observed average value of Sr isotope compositions in the Oreste bog ($^{87}\text{Sr}/^{86}\text{Sr} = 0.70884 \pm 0.00014$) were identical to the Eastern Antarctic ice core dust (ICD) deposited during the Last Glacial Maximum (LGM) and Glacial Stage 2 ($^{87}\text{Sr}/^{86}\text{Sr} = 0.7088 \pm 0.0002$). Therefore, various Anrgentinian sediment (southern South America) deposits accounted for the dust deposition in the Eastern Antarctic ice at least since the Late Pleistocene.

Zusammenfassung

Torfmoore sind ausgezeichnete Umweltarchive für atmosphärische Deposition vieler Haupt- und Spurenelemente und Mineralstäube. Geochemische Untersuchungen der Haupt- und Spurenelemente, der Mineralogie der Stäube sowie deren Isotopenverhältnisse im Torf liefern wichtige Informationen über die Korngrößenverteilung während des Transports, das Ursprungsgestein und mögliche Herkunftsgebiete (PSAs).

Bis heute wird nichts über Torfmoore als Archive für atmosphärische Stäube im Süden Südamerikas berichtet. Daher wurde in dieser Arbeit die anorganische Fraktion eines 542 cm langen Torfkerns aus dem Süden Südamerikas mineralogisch und geochemisch untersucht. Der Kern stammt aus dem Oreste-Torfmoor, Isla Navarino (55°13'13''S, 67°37'28''W), Südpazifik, das seit ~ 11160 ¹⁴C-Jahren (13000 Kalenderjahre) gebildet wird. Das Hauptziel war, die atmosphärische Deposition zu charakterisieren und ihre möglichen PSAs herauszufinden.

Da durch die hochaufgelöste Präparation (2 cm dicke Scheiben) des Kernes nur wenig (2 – 3 mg) Material zur Verfügung stand, musste eine Methode entwickelt werden, um den Staub vom ombotrophen Torf zu trennen, damit er chemisch und mineralogisch analysiert werden kann. Dazu wurden ca. 2 g getrockneter Torf über Nacht bei 550°C verbrannt. Zu der verbliebenen Asche (ca. 20 mg) wurde 1M HCl gegeben und 15 min reagieren lassen, um Karbonate, Sulfate und Oxide, die sich während der Verbrennung bildeten, zu lösen. Die säureunlösliche Asche (AIA) wurde von der Lösung (säurelösliche Asche, ASA) durch Filtration über Polycarbonatmembranfilter (0,2 µm) getrennt. Die so gewonnene AIA-Fraktion bestand aus Silikaten, Refraktären Oxiden und Gläsern, die von Verwitterung und Vulkanausbrüchen stammten. Dieser Rückstand wurde direkt auf den Filtern mit den RFA-Spektrometern TITAN auf Hauptelemente (Al, Ca, Fe, K, Si und Ti) und mit EMMA auf Spurenmetalle (Cr, Mn, Pb, Sr und Zr) untersucht. Obwohl die Asche nur dünne Schichten ausbildete, wurden sehr gute Spektren erhalten. Zusätzlich wurden bei ausgewählten Proben die Hauptmineralphasen mit Hilfe eines Rasterelektronenmikroskops (SEM) identifiziert. Des Weiteren wurden bei einigen Proben die Isotopenverhältnisse für Pb und Sr mit dem Multikollektor-Thermoionisationsmassenspektrometer (MC-TIMS) bestimmt.

Die Verteilung von Ti wurde als Stellvertreter für den Staubeintrag gewählt, da es in vielen Mineralien vorkommt, die der chemischen Verwitterung widerstehen. Die Mineralakkumulationsrate (MAR) wurde über die Titankonzentration im Gesamttorf, dessen Dichte und Akkumulationsrate, berechnet. Die Elementverteilung von Calcium (Ca), Mangan (Mn) und Strontium (Sr) im Torf und das Strontiumisotopenverhältnis in der ASA zeigen, dass der Torf oberhalb von ~300 cm ombotroph ist. Über die Verteilung von Ca, Mn, Sr und Ti im Torf wurde gezeigt, dass die MAR für die letzten ca. 6000 Jahre bei $0,43 \pm 0,12 \text{ gm}^{-2} \text{ a}^{-1}$ lag und atmosphärisch dominiert war. Eine Ausnahme bildet eine Lage vor ca. 4200 Kalenderjahren (BP), die an Staub angereichert ist und deren Ti/Zr-Verhältnis (AIA) zum Zirkonium verschoben ist. SEM-Bilder zeigten, dass die meisten Minerale oberhalb ~ 400 cm zur Feinfraktion (10-20µm oder kleiner) gehören und abgerundet sind. Nur bei ca. 300 cm herrscht eine Tephralage (>20-40 µm) vor. Zusammen mit dem relativ gleich bleibenden Gehalt an AIA weist das auf einen weiträumigen Transport und Klimastabilität für die letzten 6000 Jahre hin.

Das Strontiumisotopenverhältnis der AIA der letzten 6000 Jahre (oberhalb ~420 cm) variiert in einen engen Bereich von $0,7087 < ^{87}\text{Sr}/^{86}\text{Sr} < 0,7090$ mit einem Mittelwert von $0,70884 \pm 0,00014$, n=9. Ausnahmen bilden die zwei Lagen bei ca. 55 cm und 160 cm und die Tephralage bei ca. 300cm. Dort sind die Verhältnisse weniger radiogen geprägt. Eine ähnliche Abweichung zeigt sich im älteren Teil des Kernes bei ca. 490 cm. Die vorhandenen Altersbestimmungen, Strontiumisotopenverhältnisse der AIA, Elementverteilungen von Silizium (Si) und Kalium (K) (ausgedrückt als Verhältnis ihrer Oxide $\text{K}_2\text{O}/\text{SiO}_2$) und veröffentlichte Daten über Vulkanausbrüche ergeben zusammengenommen vier Tephraeinträge durch den Vulkan Mt. Burney ($^{87}\text{Sr}/^{86}\text{Sr}=0,7042$) in das Oreste-Torfmoor. Für den Rest des Profils zeigen die Daten, dass die Stäube aus dem Patagonischen Gürtel im Süden Südamerikas stammen. Insgesamt stützen die Ergebnisse die These, dass die Deposition der letzten 6000 Jahre homogen und relativ konstant war.

Der Mittelwert des Strontiumisotopenverhältnisses im Oreste-Torfmoor ($^{87}\text{Sr}/^{86}\text{Sr}=0,70884\pm 0,00014$) ist identisch zu dem des Staubs des Eiskerns (ICD) aus der Ostantarktis, der während des letzten glazialen Maximums und der zweiten Eiszeit akkumulierte ($^{87}\text{Sr}/^{86}\text{Sr}=0,7088 \pm 0,0002$). Somit kann man verschiedene argentinische (Süd-Südamerika) Sedimentablagerungen als Quelle für den atmosphärischen Staubeintrag in der Ostantarktis seit dem Spätpleistozän ansehen.

Acknowledgements

I am grateful to many people who came along to help with my PhD.

Bill Shotyk! – I thank you for being my supervisor and giving me the opportunity to introduce myself to such an interesting area of research. Your “homely and friendly” environment at the institute and during the field work, workshops and conferences are simply the best. I am grateful for your energetic and enthusiastic support which kept me running. And still do so. I always remember your words: “...if you have any question or problem, just drop by to my office; seven days of the week and any time around.” I thank you once again **Bill**.

I thank **Vera Markgraf** for providing the peat samples and her valuable suggestions, comments, information on my many questions. Thank you for being on another side of the net and quick answers/reviews/suggestions, whenever I sent emails. It is because of your help I was able to stick to the objectives of my PhD and Patagonia, though I could not collect the peat sample from Patagonia as planned.

Andriy Cheburkin and **Helen Kurzel!** – I thank you both for XRF analysis and SEM analysis of numerous samples. I am fortunate to have you there for help and providing me incredible results for both XRF and SEM, no matter how small the sample amount was. I thank you for your painstaking efforts.

My very heartfelt thanks to **Bernd Kober** for his “load off the shoulder” help on Sr isotopes. You and your mechanical horse (TIMS) “smoked them (Sr) out” from their 13000 years long hideout. It is because of you; those dusts came to know their roots and their migration path. And it is because of you that a remarkable paper was written. I thank you once again **Bernd!** I also thank **Dietlinde Pingel** for her support on TIMS analysis.

I extend my sincere gratitude and appreciation to: **Christian Scholz** for help during the ICP-OES analysis; **Michael Krachler** for introducing me to the clean lab and help during ICP-OES analysis; **Stefan Rheinberger** for many technical questions and for translating my “long” summary to “zusammenfassung”; **Torsten Hoffman** for administrative work.

I thank **Stephanie Jansen** and **Frank Schäbitz** from Köln, **George Bonani** and **Irka Hajdas** from ETH Zürich for their help with age dating.

I thank **Jutta, Nicole, Gael, Zyare, Bin, Asher** and **Nicolas** for being there to help, talk, laugh or answer my questions whenever I needed. You people are great.

I thank **Srinivas** and I will always remember the time we spent, the walk on the snow field in January and our discussions. I thank all others in Heidelberg especially “**Gastaldi** - the Italiano” for espresso early in the morning and our tour to the “pond of peace frog.”

I thank Sapkota family and other friends back in Nepal for their moral support, encouragement and understanding throughout the years. I admire your patience though I always kept myself on the other side of the phone. You people are always close to me. Finally yet importantly, I thank **Tanja** and other **friends** for always being there.

Once again, I “**Thank you all!**”

Financial support: the Deutsche Forschungsgemeinschaft (DFG; grants SH 89/1-3 to W. Shotyk) provided funding for this work, including the salary to the author. National Science Foundation (NSF-EAR-9709145), USA to Vera Markgraf, provided funding for the collection of the peat core.

Chapter 1

Introduction and Background

This doctoral dissertation contains five chapters. The first chapter briefly describes the background of the study, its objectives and the summary of work done during the doctoral study. Chapters 2, 3, 4 and 5 are in the form of manuscripts, which have been submitted to journals for publication. The appendixes consist of two co-authored papers (I and II) and supplement data (III, IV, and V).

-Chapter 1-

1-1 Introduction and Background

“A History of the small and invisible”

J. A. Amato

Atmospheric aerosols are solid or liquid particles smaller than 100 μm and suspended in the air (Manahan, 1991). These particles are mainly composed of a carbonaceous fraction (sooty carbon), plus a water soluble ionic fraction (sulfate, nitrate, ammonium ions) and a mostly-insoluble inorganic fraction (elements, oxides, etc.) (Rahn, 1976). The clear difference between

To simplify the classification of various aerosols, Fuchs (1964) differentiated them into three categories, irrespective of particle size: a) mists (liquid particles), b) dusts (solid particles), and c) smoke (both solid and liquid particles of condensation origin which is generally formed by incomplete combustion of fuel).

Atmospheric dusts can further be identified as natural dusts or anthropogenic dust, depending on their nature of origin. Natural dusts are derived from soils and

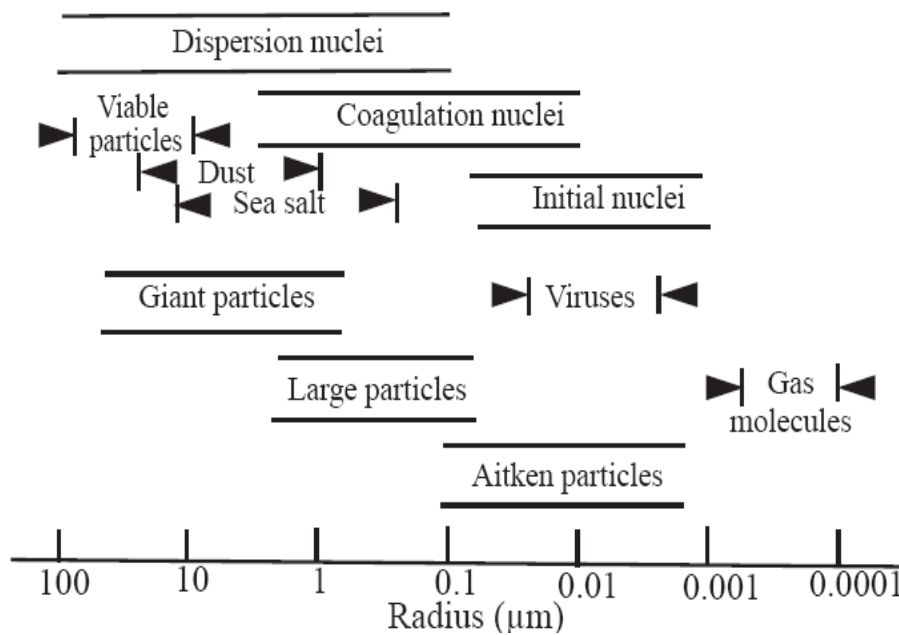


Figure 1: Nomenclature of atmospheric aerosols and their particle sizes. Initial nuclei are formed by condensation of vapours or chemical reactions and on coagulation form slightly larger particles (redrawn from Brimblecome, 1996).

the liquid and solid aerosol particles is that the liquid aerosols are spherical and on collision they may fuse to produce a single spherical particle. On the other hand, solid particles are varied in shapes and may coagulate with other particles of varied shapes to form more or less loose aggregates (Fuchs, 1964). The types of atmospheric particles and their sizes are shown in Figure 1.

sediments that are not subjected to human action. In natural environments fine particles are most commonly formed by gradual weathering and / or glacial abrasion/crushing of rocks (Pye, 1989). Additionally, abrasion and crushing during fluvial, eolian and marine transport may also produce some fine materials. Alternatively, dusts generated by human activities are referred to as anthropogenic dust. Human activities can

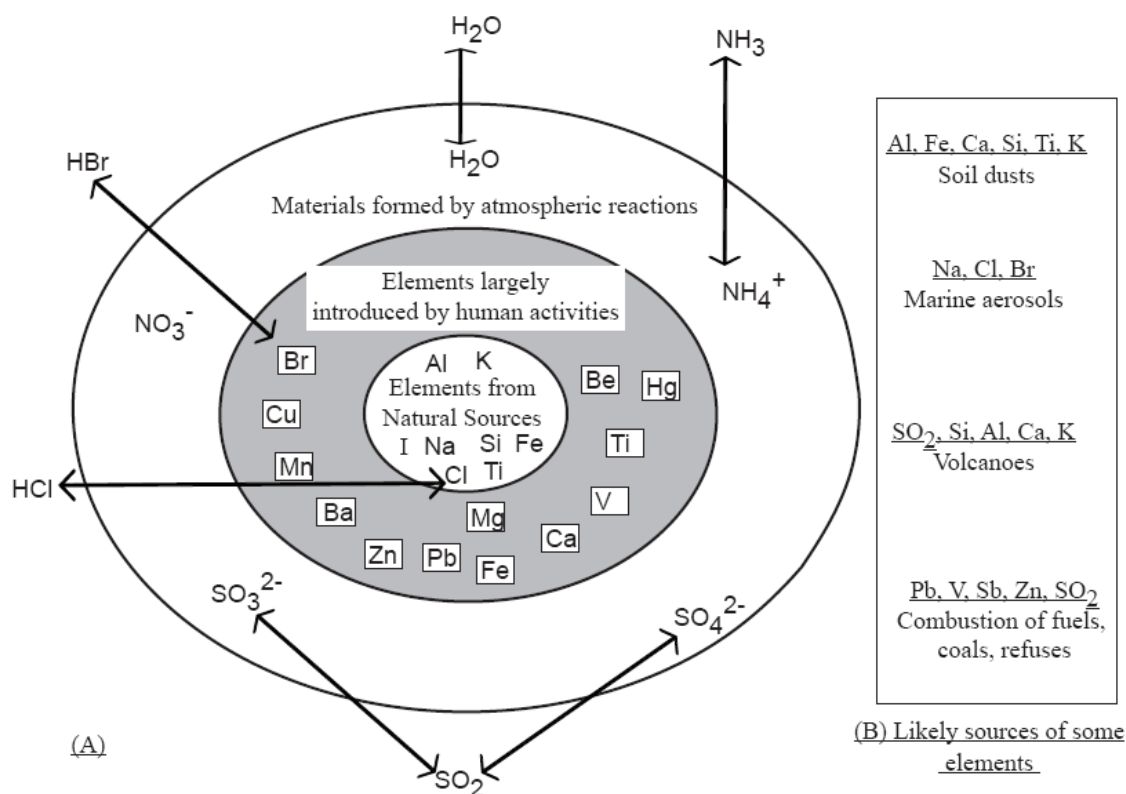


Figure 2: Some of the components of inorganic atmospheric particles (A) and their likely sources (B) (redrawn from Manahan, 1991).

influence dust emissions either by changing the land uses which changes the soil surface conditions and /or by modifying the climate, which in turn modifies dust emissions (Zender et al., 2004). For example, in an estimation of dust emission in the Sahara/Sahel region of Africa, land altered by human practices (e.g. deforestation, over-cultivation) shows a 30 – 50 % increase in dust emissions compared to the natural dusts (Tegen and Fung, 1995). Other activities, which affect land use practices and therefore the generation of dusts, include construction work, mining and smelting, livestock, and vehicles. Figure 2 shows some of the components of inorganic atmospheric particles and their origins (Manahan, 1991).

To trace the early history of atmospheric dust, the Chinese have already documented the atmospheric mineral aerosol for over three thousand years (Zhang, 1984). Nevertheless, the early 18th century drew our attention to the possibility of the atmospheric transport of dust. In the 18th century, Dobson (1781) mentioned the Harmattan periodical winds blowing from the interior parts of Africa towards the Atlantic Ocean. Dobson (1781) wrote: “A fog or haze is one of the

peculiarities which always accompanies the Harmattan”. Probably mentioning the dust in the fog, Dobson (1781) further stated: “As the particles which constitute the fog, are deposited on the grass, the leaves of trees, and even on the skin of the negroes, so as to make them appear whitish.” About 50 years later, Darwin (1845) wrote about his visit to the Cape Verde Islands in January 1832 (Figure 3): “Generally the atmosphere is hazy; and this is caused by the falling of impalpably fine dust, which was found to have slightly injured the astronomical instruments.” “Professor Ehrenberg...” to whom Darwin had given collected dust samples “...finds that this dust consists in great part of infusoria with siliceous shields, and of the siliceous tissue of plants.” Darwin further thought about the source “From the direction of the wind whenever it has fallen, and from its having always fallen during those months when the Harmattan is known to raise clouds of dust high into the atmosphere, we may feel sure that it all comes from Africa.” A summary of his findings was published few years later (Darwin, 1846). In the early 1960s, Brownlow et al. (1965) established a dust collection station at Barbados with the aim of studying

cosmic dust (Delany et al., 1967). Continuing the earlier work of Brownlow et al. (1965), Delany et al. (1967) modified the sampling station; a 14 m wooden tower replaced the existing ground level station to minimize interference (or contamination) from local land.

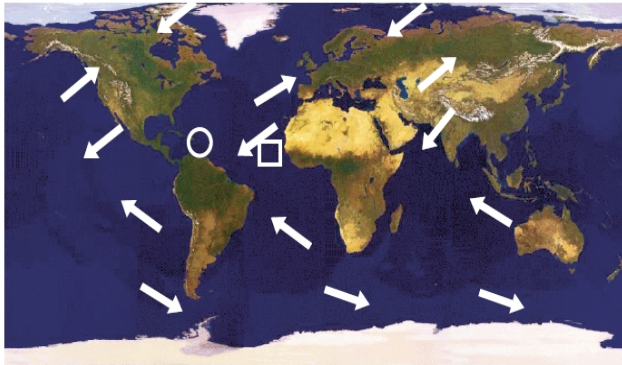


Figure 3: A satellite picture of vegetation patterns and arid and semi-arid areas of the world. Also shown on the map are the major wind directions. The white circle and white square represent Barbados and Cape Verde Islands, respectively. (source: Center for Air Pollution Impact and Trend analysis (CAPITA), Washington University, USA)

Initially, it was thought that significant amount of dust could not be transported across some 5000 km of Atlantic Ocean (Delany et al., 1967). Instead of cosmic dust, Delany et al. (1967) found that “...the enormous quantity of fine reddish-brown dust being caught on the collector meshes could possibly be coming from the European-African continents.” They further noticed that the fungus and magnetic contents of the dust, which show a marked seasonal variation, are in accordance with the shift in wind patterns off the African coast. These findings stimulated further studies to understand the importance of long range transport of mineral dust and to quantify the amount of dust coming from Africa. Based on measurements and models describing the movement of Saharan air outbreaks, Prospero and Carson (1972) estimated that 25 to 37 Terragrams (Tg) of dust are transported through the longitude of Barbados each year. Recently, Kaufman et al. (2005) estimated that 240 ± 80 Tg of dust is transported from Africa to the Atlantic Ocean annually; of this, 140 ± 40 Tg

is deposited in the Atlantic Ocean, 50 Tg fertilize the Amazon Basin, 50 Tg reach the Caribbean, and 20 Tg return to Africa and Europe. In fact, Africa and the Sahara are not the only active sources of dust - arid and semi-arid areas cover more than 30 % of the earth’s land surface (Figure 3) (Thomas, 1989) and cannot be neglected as a predominant dust source. With respect to Asia, Uematsu et al. (1983) estimated that 6 – 12 Tg of Asian dust are transported annually towards the central North Pacific, and the main recipient is the North Pacific Ocean. On a global scale, the estimated inputs of mineral aerosols from arid and semiarid areas (natural source) to the atmosphere range from 1000 – 3000 Tg yr⁻¹ (Table 1).

Table 1: Estimated rates of annual global dust emission

Global emission rate (Tg yr ⁻¹)	References
3000	Tegen and Fung (1994)
1000-2000	Duce (1995)
3000	Mahowald et al. (1999)
1814	Ginoux et al. (2001)
1060 ± 194	Werner et al. (2002)
1654	Mahowald and Luo (2003)
1921	Tegen et al. (2004)

(1 Tg = 10¹² g)

In a natural environment, wind erosion is predominantly responsible for the entrainment of dust in the atmosphere. Four possible mechanisms (Figure 4) may carry the soil particles from the exposed soil surfaces into the air stream: a) creep (rolling) b) saltation (bouncing) c) true suspension (Nickling, 1983) and d) sand blasting (Gomes et al., 1990). Generally, particles with diameters of less than 10 – 20 μm are able to remain suspended long enough (Figure 5) such that they are capable to travel long distances (Schütz, 1989; Herrmann et al., 1999). For example, Figure 6 shows observed grain size fractionation of different aeolian materials such as Harmattan dust and dune sands in NW-Egypt in the size range < 20 μm, and the distances they could possibly travel (Herrmann et al., 1999). Generally, the amount of material and the particle sizes to be transported are a function of the extent of source areas (e.g. rock and soil type, particle

size distribution, organic matter content, moisture content, vegetation cover and soil compaction), the strength of atmospheric circulation (wind strength), and the removal process (settling velocity) (Nickling, 1983). For example, Betzer et al. (1988) found giant mineral particles ($> 75 \mu\text{m}$) in atmospheric dust samples collected at North Pacific (26°N , 155°W). They suggested that these giant mineral particles come from major dust outbreaks in China and have been transported more than 10000 km over the North Pacific Ocean.

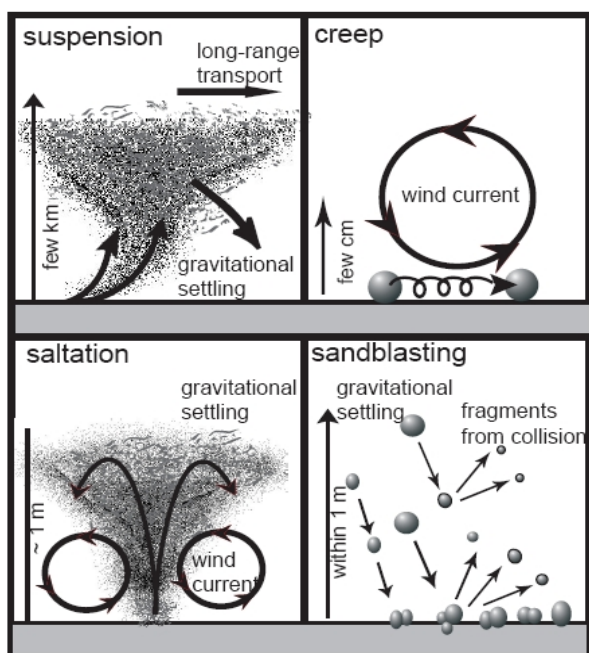


Figure 4: Illustration of possible mechanisms of dust entrainment and transportation by wind into the atmosphere (Usher et al., 2003).

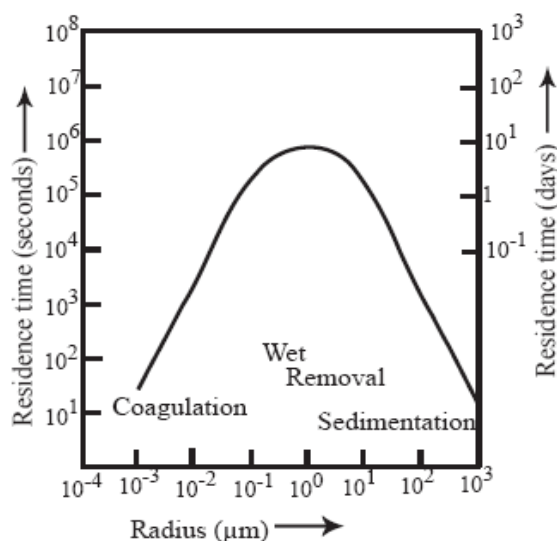


Figure 5: The average residence time for aerosol particles as a function of their size and the dominant sink for each size range (Baird, 1995).

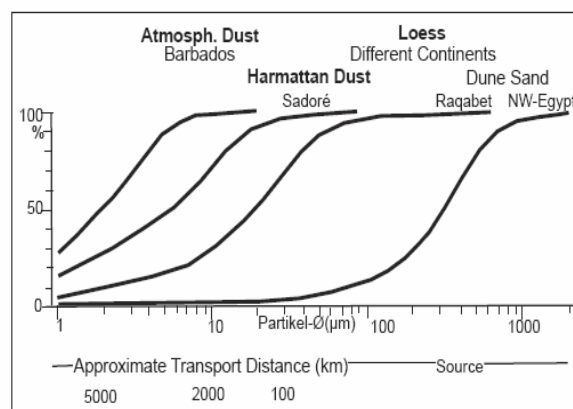


Figure 6: Grain size fractionation of different aeolian materials during atmospheric transport (Herrmann et al., 1999).

Why is it so important to study atmospheric dusts?

“From cosmos to the kitchen counter. The big consequences of little things” H. Holmes

Starting with Darwin, he mentioned that because of the dust the atmosphere was hazy and the visible horizon on the Cape Verde Islands was only one mile distant. Dust did not only play an important role in the formation of the earth (supernova hypothesis); it continues to affect the Earth’s climate system, the chemistry of the atmosphere, and the global biogeochemical cycles of many elements (Figure 7). Studies have shown that mineral aerosols in the atmosphere play an important role in radiative effects (Miller and Tegen, 1998) and cloud condensation nuclei (Yin et al., 2002; Wurzler et al., 2000). “The year without a summer”, or 1816, is probably a good example of how dust can affect the climate. The average summer temperatures fell by as much as 3°C across much of western and central Europe in that year (Oppenheimer, 2003). The massive volcanic dust (ash) released into the atmosphere as a result of the Mt. Tambora eruption also affected places such as northern Europe, northeast America and eastern Canada.

In the global biogeochemical cycles, mineral dust has both positive and negative consequences. Atmospheric mineral dust from arid and semi-arid areas is the major source of iron (Fe) to remote areas of the oceans, which is necessary for photosynthesis by phytoplankton (Duce and Tindale, 1991;

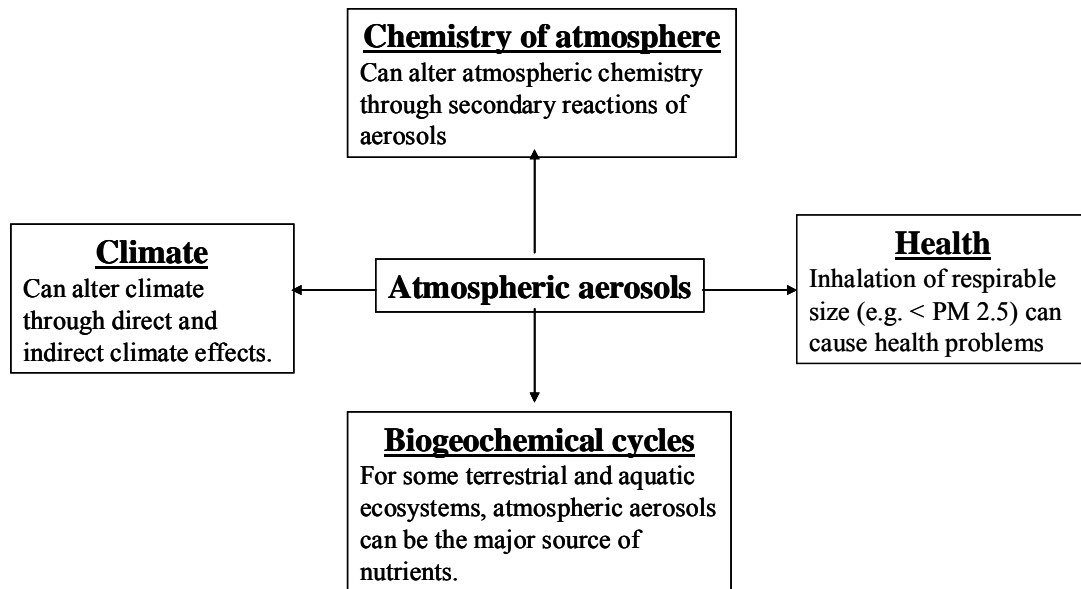


Figure 7: Importance of atmospheric aerosols (based on Usher et al., 2003).

Meskhidze et al., 2003). Similarly, the ecosystems of Hawaii rely on the phosphorus in the atmospheric mineral dust transported over 6000 km from Asia (Chadwick et al., 1999; Vitousek, 2006). On the other hand, large amounts of transatlantic dusts deposited in the Caribbean are damaging the coral reefs (Shinn et al., 2000). Similarly, Prospero (2001) cautioned about the possible effect on human health by the Trade winds carrying North African dust storms into the Caribbean and over North America.

The source identification methods and archives of atmospheric dust such as snow and ice, marine sediments and peat bogs are summarized in the following section.

1-2 Tracing the sources of atmospheric dust

“Billions of tons of tiny particles rise into the air annually—the dust of deserts and forgotten kings mixing with volcanic ash, sea salt, leaf fragments, scales from butterfly wings, shreds of T-shirts, and fireplace soot. And eventually, of course, all this dust must settle” H. Holmes

There are two possible ways to identify the predominant sources of atmospheric dust: a) monitoring (tracking) air-mass trajectories (e.g. field observation and satellite images) and b) analytical techniques (e.g. mineralogy, elemental concentration and isotope fingerprinting). Darwin (see 1-1) showed one of the earliest

examples of tracking air mass trajectories. Based on the observed wind direction, Darwin (1846) predicted an African source for the fine dust, which fell on his vessel while he was at Cape Verde Islands. The early 1970s are probably the beginning of the first estimates (quantification) of dust emission from Africa (100 Tg of dust for a latitude belt 5° - 25 °N) with the help of meteorological observations, *in situ* data and satellite images (Kaufman et al., 2005). With the advancement of technology during the past decades, sophisticated monitoring techniques have evolved to allow atmospheric dust trajectories to be monitored directly (e.g. Figure 8).

On the other hand, analytical techniques provide a more indirect method of tracing the dust sources by comparing certain tracers or fingerprints (minerals, elemental concentration and isotope ratios) in the collected dust, soils, and sediments from possible source areas (PSA). To be useful, tracers must be: a) representative of a specific geographical region, b) distinctive from other areas and c) must remain unaltered (chemically) during atmospheric transport (from source to sink) (Delmonte et al., 2004). When analytical techniques are applied to geological archives, they can take us back to historical times, allowing us to reconstruct the atmospheric history (determination of dust source and palaeoclimatic reconstruction); some of these techniques can take us many thousands years back in time. As an example

of this combination, Kohfeld and Harrison (2001) have summarized the dust accumulation rates derived from loess, sediment and ice cores during different climatic stages covering the past 400 kyr (Figure 9).

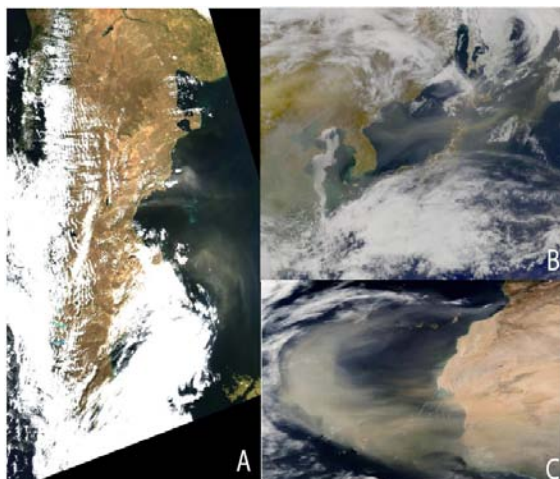
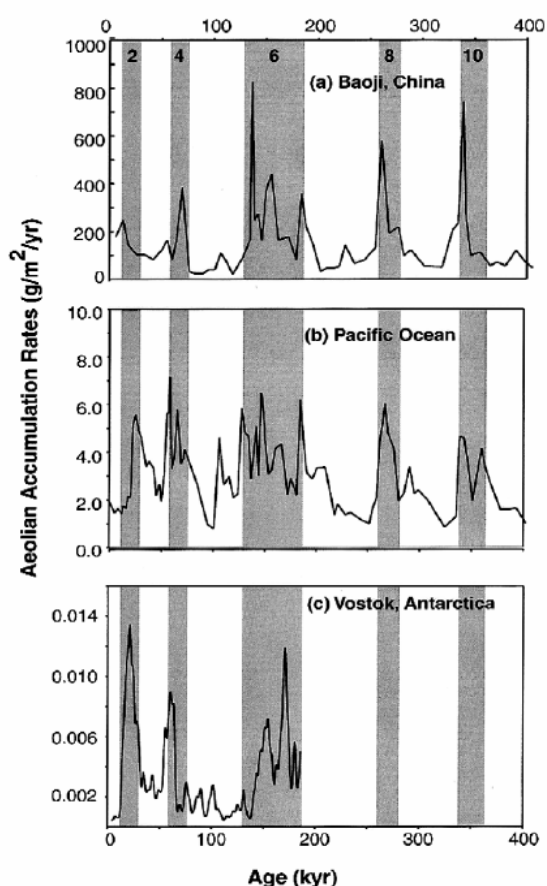


Figure 8: Satellite images of a dust event (brownish color): (A) Patagonian dust on 3rd July 2005, (B) Trail of dust streaming east over North Korea and Japan and heading out over the Pacific Ocean on 17th April 2001, and (C) Sharan dust stream on 26th February 2000. All pictures are obtained in NASA SeaWiFS (Sea-viewing Wide Field-of-view Sensor) project. (source: NASA SeaWiFS Project/Goddard Space Flight Center and Orbital Imaging Corporation- [ORBIMAGE](#)).



← **Figure 9:** Eolian accumulation rates during glacial-interglacial cycles based on (a) the Chinese Loess Plateau, (b) Pacific Ocean marine sediment record (V21-146), and (c) the Vostok ice core. The Cold Glacial Stages are shown by grey shaded area (Kohfeld and Harrison, 2001).

1-2.1 Mineralogy

Both Dobson (1781) and Darwin (1946) attempted to determine the composition of the haze and the fine dust. Therefore, Dobson (1781) “...recommended Mr Norris the use of a good microscope...” and that “...might possibly discover something concerning the nature of the particles” in the Harmattan wind. Mr Norris replied “...neither could I discover anything by taste, or by exposing plates covered thinly with melasses, for when I had dropped an acid or alkali into the water in which I had dissolved the melasses.” Mr. Norris was not able “...to judge the nature of the particles.” Darwin also tried to find out the mineralogy of the excessively fine-grained and reddish-brown dust he had collected (Darwin, 1846). What he found was that the fine-grained dust did not effervesce with acids, but rather it easily fused under the blowpipe into a black or gray bead. This time, Darwin was able to identify a few components, but only microorganisms (Darwin 1846). Professor Ehrenberg, who studied the dust samples given to him by Darwin, also analyzed other dust samples that were collected near the African continent. Based on 37 species of microorganisms that were common in many packets of dust that Professor Ehrenberg analyzed, Darwin (1846) thought that these dusts “...must certainly have come from same source.”

The development of X-ray diffraction (XRD) (between the 1900s and the 1960s) and the Scanning Electron Microscope (SEM) (between the 1930s and the 1960s) have made the mineralogical study of coarse and fine fraction (clay minerals) much easier (Moore and Reynolds, 1997). Biscaye (1965) used mineralogical analysis of the fine fraction of deep-sea sediments to track the dust source to the Atlantic Ocean. Minerals in fine fraction

such as kaolinite, gibbsite, pyrophyllite, mixed layer minerals and chlorite can provide information about their sources, because their distribution is varied on the continent (Chester et al., 1972). Chester et al. (1972) compared the mineralogy of clay size dust (< 2 μm) to those of source-area soils and deep-sea sediments at different latitudes. Among the identified minerals, Chester et al. (1972) concluded that chlorite is relatively independent of latitude, montmorillonite, illite and kaolinite vary along the latitudes (Figure 10). Similarly, Blank et al. (1989) studied the mineralogy of aerosols and sediments of < 2 μm size fraction from the Pacific Ocean. The similarity in the mineral weight percentage of quartz, plagioclase, illite, kaolinite and chlorite between aerosols and sediments suggested that the arid and semi arid regions of Asia are the main sources of mineral aerosol (Blank et al., 1989).

1-2.2 Trace element concentrations

Studies of trace elements in erodible soils have shown that elements such as titanium (Ti) and zirconium (Zr), which are associated with minerals highly resistant to chemical weathering such as zircon and rutile, are enriched in radius range 10 – 60 μm . On the other hand, other elements such as silica (Si) and aluminum (Al) have no size preferences (Figure 11) (Eltayeb et al., 2001; Schütz and Rahn, 1982).

Elements such as Si and Al are found in major rock-forming minerals, for example quartz, feldspars, micas and other aluminosilicate minerals (clay minerals such as illite, kaolinite, smectite). Therefore, the ratio of Ti to Al can provide information about changes in mineralogy such as the relative abundance of heavy minerals, particle sizes and/or changes in sources. The major and trace elements of clay and silt size particles derived from the earth's crust are expected to have a similar composition to the average crustal materials (Rahn, 1976; Schütz, 1989). Enrichment factors (EF) are useful for estimating the changes in source area or mineralogical composition. This is done by using the appropriate reference

element and the following equation (Rahn, 1976):

$$EF \text{ of } X = ([X] / [Y])_{\text{sample}} / ([X] / [Y])_{\text{source}} \quad (1)$$

where [X] and [Y] are the concentration of elements of interest and the reference element in both the sample and source (e.g. crust, soil) respectively. Generally, the elements derived predominantly from soil dust and with no marine input or pollution source such as Si, Al, scandium (Sc) and Ti are chosen as the reference elements. Elements with EF values greater than about five are considered to be from sources other than crustal derived, soil dust (Schütz, 1989).

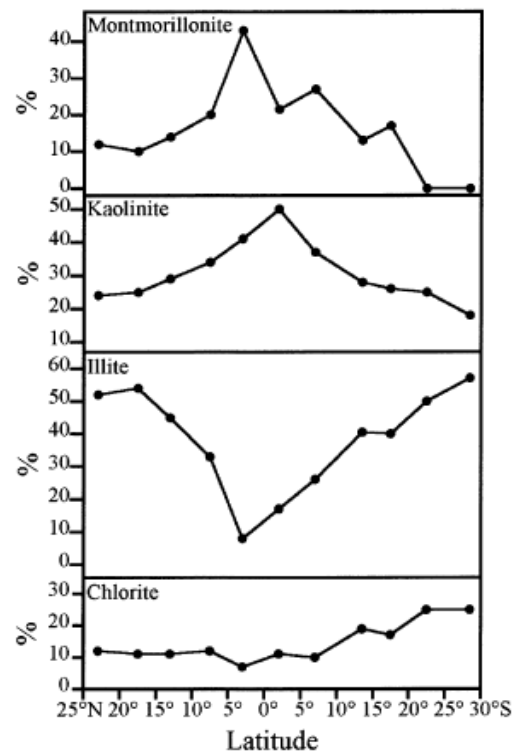


Figure 10: Changes in the clay mineralogy of fine dust (< 2 μm) along latitude. The percentages of clay minerals are of the total < 2 μm fraction and all values are averaged for each 5° of latitude. The plot is based on the eolian dust collected from the marine atmosphere along the eastern margins of the Atlantic Ocean between ~ 27 °N and ~ 34 °S (Chester et al., 1972).

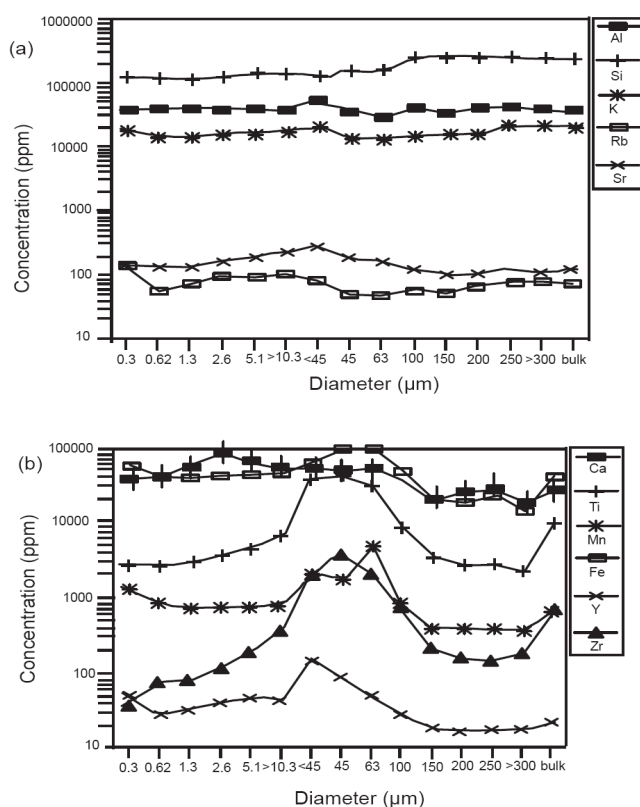


Figure 11: Average elemental concentration and grain size fractionation for Namib soil and its mineral aerosols (Eltayeb et al., 1993)

For example, Boyle (1983) used the Ti/Al ratio of marine sediments to reconstruct eolian transport fluctuations during the Pleistocene (Figure 12). He suggested that the variation in the Ti/Al ratios for the past 130 kyr reflects the changes in the average grain size of eolian material (aluminosilicates) caused by changes in wind speed, direction, and the distribution of arid source areas (Figure 12). Muhs (1990) used Ti and Zr and their enrichment relative to Al to show that most of the silicate minerals in soils of the Caribbean Island are transported from the Sahara-desert (Figure 13). In another study, Gatz and Prospero (1996) collected aerosol samples in central Illinois, (mid west USA) during a summer field campaign held in 1979 and compared the Si/Al and Ca/Al ratio of aerosol to the PSAs. Elemental ratios combined with the meteorological data (air trajectories) suggested that North African dust is the most likely source of dust in central Illinois which was collected in July 1979. Another useful reference element, which has not been used as much in the atmospheric aerosol, is Sc (Shotyk et al., 1998; Shotyk et al., 2001).

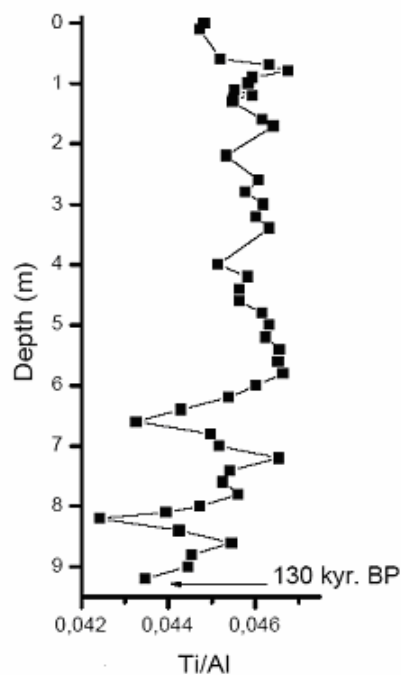


Figure 12: Ti/Al ratio of a marine sediment core (Peru Current; core V19-29; 3°35'S, 83°56'W, 3070m). The changes in the Ti/Al ratio are attributed to changes in the grain size due to changes in wind speed, direction, and source areas (Boyle, 1983).

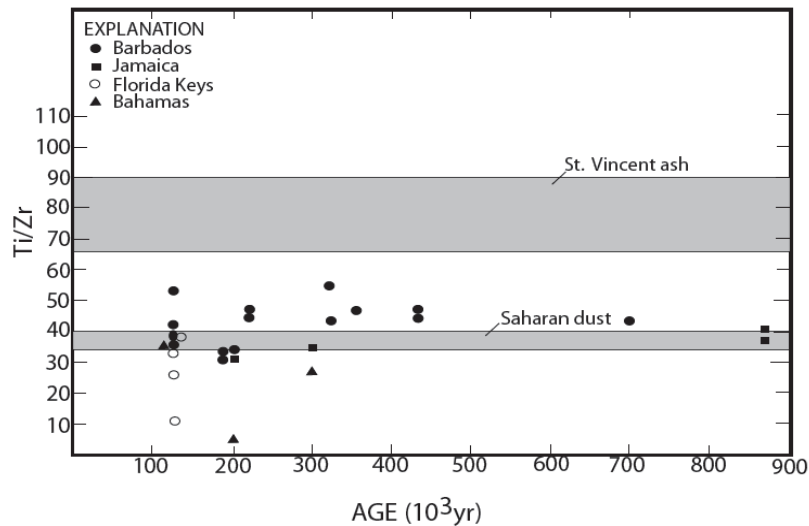


Figure 13: Ti/Zr ratios in soils, St. Vincent volcanic ash and Saharan dust used as a geochemical evidence to show Saharan dust as a parent material for soils developed on Quaternary limestones of Caribbean and Western Atlantic Islands (Muhs, 1990). St. Vincent is ~ 150 km west of Barbados (Figure 3).

1-2.3 Radiogenic isotopes (Pb and Sr)

Strontium (Sr) has four natural and stable isotopes (^{88}Sr , ^{87}Sr , ^{86}Sr and ^{84}Sr), where ^{87}Sr and ^{86}Sr are of particular importance. The isotopic abundance of ^{87}Sr is variable because of the formation of radiogenic ^{87}Sr produced by the decay of naturally occurring ^{87}Rb (rubidium) (Faure, 1986). Strontium is a dispersed element largely controlled by the extent to which Sr^{2+} (1.13 Å) can substitute for Ca^{2+} (calcium) of slightly lower ionic radius (0.99 Å) in Ca-bearing minerals. The common sources of Sr are Ca-bearing minerals such as plagioclase, apatite, calcium carbonate and clay minerals (e.g. smectite). Similarly, Rb (1.48 Å) is also a dispersed element controlled by substitution with K^+ (1.33 Å) (potassium). Rubidium is found commonly in K-bearing minerals such as micas, K-feldspar and certain clay minerals (e.g. kaolinite) (Faure, 1986). In any geological samples such as sediment and atmospheric dust, the relative abundance of ^{87}Sr , which is expressed as $^{87}\text{Sr}/^{86}\text{Sr}$ ratios, depends on the age and the Rb/Sr ratio of the parent rock or mineral.

Dash et al. (1966) measured Sr isotopes in deep-sea sediments with the purpose of establishing geological provenance for deep-sea sediments, distinguishing between authigenic and detrital components, and exploring the possibility of dating

sediment material by Rb-Sr method. Subsequently, Dasch (1969) presented the distribution of $^{87}\text{Sr}/^{86}\text{Sr}$ ratios from the detrital, aluminosilicate minerals in major oceans. He showed that the $^{87}\text{Sr}/^{86}\text{Sr}$ of aluminosilicates (fine and coarse fraction) deposited in the ocean may be used as tracers for source provenance as they were not affected by the marine strontium concentration. Later, Biscaye et al. (1974) used the Sr isotope ratios of air-sampled dust over the ocean as an index for the provenance of dust. The measurements of Sr isotopes on provenance of Antarctic dust were initially done by Grousset et al. (1992). For the provenance of dust, they analyzed the Sr isotopes in both Antarctic ice core dust and the samples such as soil and loess from the PSAs. By using the isotopic ratios of Sr ($^{87}\text{Sr}/^{86}\text{Sr}$) and neodymium (Nd) ($^{143}\text{Nd}/^{144}\text{Nd}$), Grousset et al. (1992) showed that the dust source for Antarctica for the Last Glacial Maximum (LGM) is Argentinian Patagonia (Figure 14). Later, Basile et al. (1997) and Delmonte et al. (2004) used the same isotope system to show that Patagonia is the predominant source of dust for Antarctica. Similarly, using the isotopic ratios of Sr and Nd, Biscaye et al. (1997) and Svensson et al. (2000) showed that eastern Asia is the predominant source of dust for the Greenland ice cap.

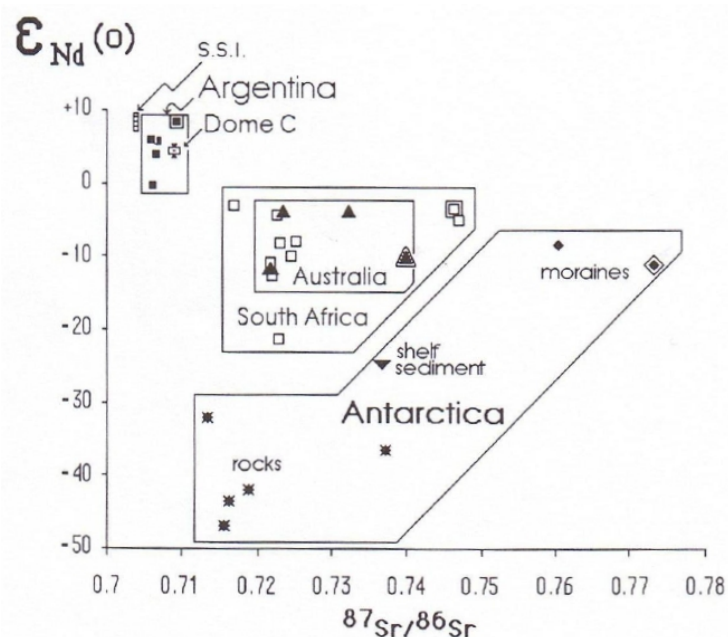


Figure 14: $^{87}\text{Sr}/^{86}\text{Sr}$ ratios vs. $\epsilon_{\text{Nd}}(\text{O})$ for samples from possible source area of dust to ice cores from Dome C (Antarctica). (■ = Argentine loess; ▲ = Australian samples; □ = South African samples. Antarctica: ◆ = moraines; ▼ = shelf sediment; ● = rocks. S.S.I = South Sandwich Island Volcanoes. Less than 5 μm fraction is “framed” by identical symbols.) (Grousset et al., 1992).

Another useful element to fingerprint the atmospheric aerosol is lead (Pb). Lead has three radiogenic isotopes (^{206}Pb , ^{207}Pb and ^{208}Pb) and one non-radiogenic isotope (^{204}Pb), all of which are naturally occurring isotopes. The radiogenic isotopes ^{206}Pb , ^{207}Pb , and ^{208}Pb are the product of the radioactive decay of ^{238}U , ^{235}U , and ^{232}Th respectively. Only non-radiogenic ^{204}Pb is used as a stable reference isotope and it is generally reported as the ratio of a radiogenic to a non-radiogenic isotope ($^{208}\text{Pb}/^{204}\text{Pb}$, $^{207}\text{Pb}/^{204}\text{Pb}$ and $^{206}\text{Pb}/^{204}\text{Pb}$) (Faure, 1986; Barreiro, 1984). The Pb isotope system is a sensitive method for tracing particle origins and can therefore be used to identify both natural and anthropogenic inputs of Pb (Grousset and Biscaye, 2005). The first use of Pb isotopes to identify the sources of atmospheric lead deposition was done by Chow and Johnstone (1965). They used them to identify the sources of anthropogenic lead on snow. Nevertheless, the use of Pb isotopes is not

restricted to the study of the current impact of human activities. The measurement of Pb isotopes in any geological archive (e.g. ice cores, peat bog) combined with the precise age dating can help us to identify the sources of Pb and their variation with time (e.g. pre-industrial, industrial). By using the Sc as a reference element, combined with lead (Pb) isotopes and age dating in a peat profile from Switzerland, Shotyk et al. (1998) showed that human activities have altered lead input in the environment (Figure 15). For example, Shotyk et al. (1998) showed the $^{206}\text{Pb}/^{207}\text{Pb}$ ratios in a peat profile from Switzerland and the factors responsible (e.g. Roman Pb mining, introduction of gasoline etc.) for the observed Pb isotopic ratios (Figure 15). Similarly, in a recent study of peat profile from England, LeRoux et al. (2004) used the $^{208}\text{Pb}/^{206}\text{Pb}$ and $^{206}\text{Pb}/^{207}\text{Pb}$ ratios and showed that the English ores were the predominant sources of Pb during the Pre-Roman, Roman, and Medieval periods.

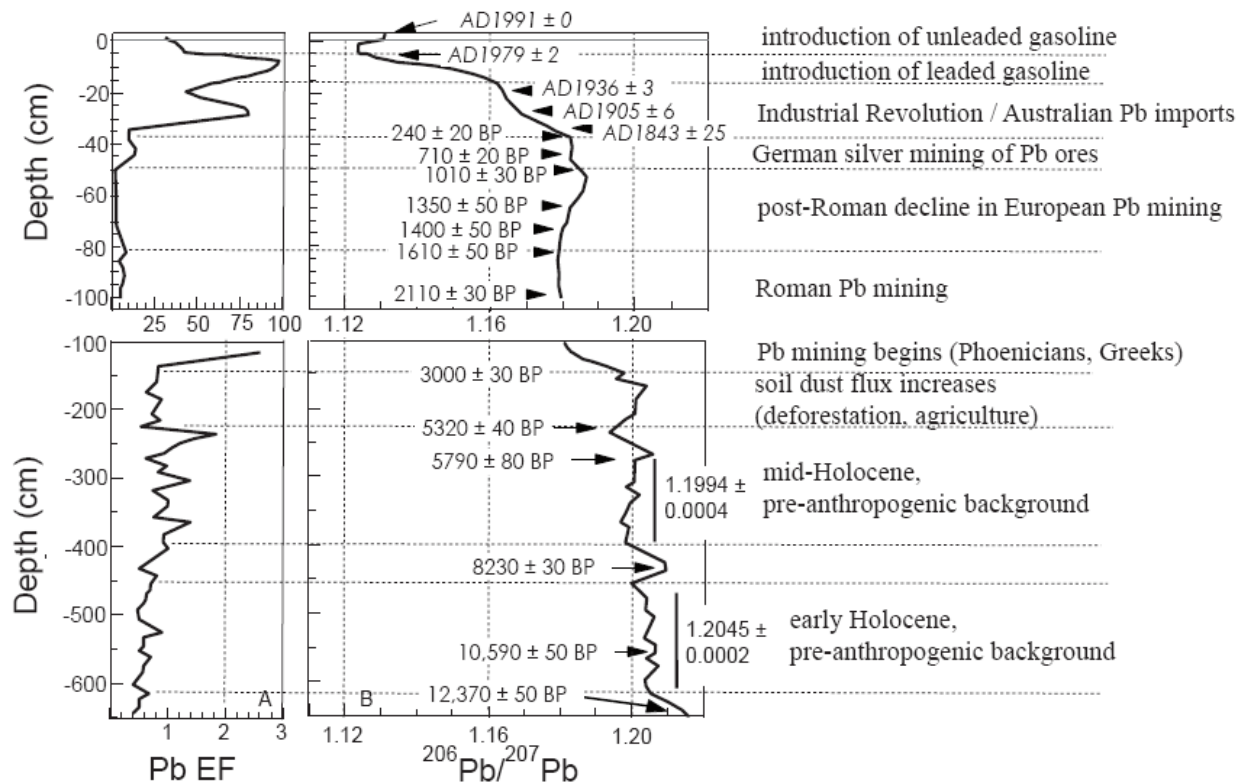


Figure 15: (A) Enrichment of Pb in a peat profile calculated using Sc as a reference element. An EF of less than two suggests that the sample is not enriched. (B) $^{206}\text{Pb}/^{207}\text{Pb}$ isotopic ratios vs. the depth of the peat profile with a record of atmospheric Pb deposition since 12370 ^{14}C yr BP (Shotyk et al., 1998).

1-3 Archives of atmospheric dusts

1-3.1 Polar snow and ice

Snow and ice cores receive eolian inputs of trace elements and minerals derived from soil dust (Marino et al., 2004), marine aerosols (Hinkley and Matsumoto, 2000), volcanic eruptions (Basile et al., 2001) and anthropogenic activities (Wolff and Suttie, 1994). Some of the examples of ice core studies are GISP2 (Greenland Ice Sheet Project), EPICA (European Project for Ice Coring in Antarctica), and Dome C and Vostok Ice cores from Antarctica (Biscaye et al., 1997; Delmonte et al., 2002; Gabrielli et al., 2005; Röthlisberger et al., 2002; Svenson et al., 2000; Vallelonga et al., 2005). The insoluble dust particles in the ice cores are useful proxies for palaeoclimatic reconstructions. For Antarctica, both EPICA (Dome C) and Vostok ice cores (Figure 16)

show a higher dust input during glacial periods, which has been attributed to the increased aridity of continental shelves, higher wind speed and lower sea level (Delmonte et al., 2004). A general overview of the atmospheric circulation of wind at mid-high latitudes, which are dominated by a westerly circumpolar vortex (Thompson and Solomon, 2002), and the land mass at a higher latitude of the southern hemisphere suggests that all the continental areas of the southern hemisphere are possible sources of dust to the Antarctica (Figure 16) (Iriando, 2000; Delmonte et al., 2004). However, isotopic studies (Sr-Nd isotopes) show South America (Patagonia) as the predominant source of dust during the LGM and glacial periods (Grousset et al., 1992; Basile et al., 1997; Delmonte et al., 2004).

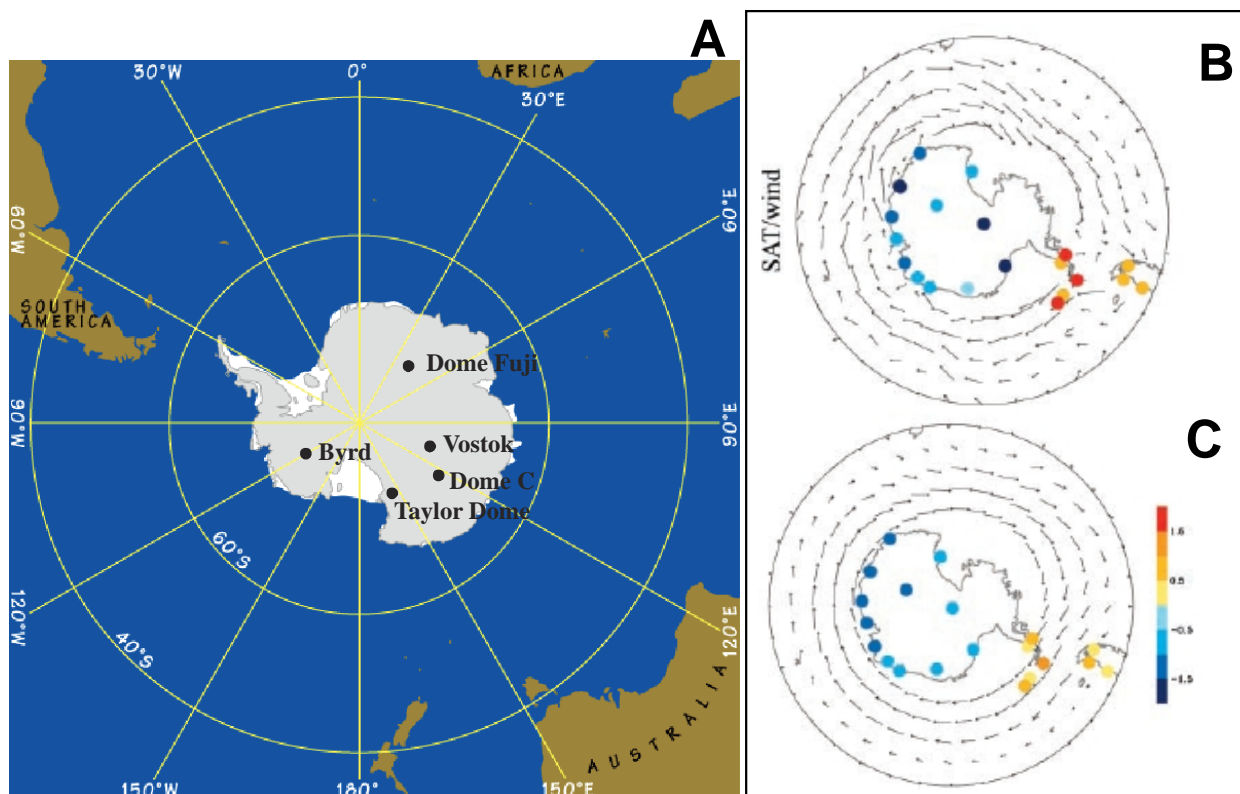


Figure 16: A) Major land masses surrounding Antarctica and the sites used for ice core studies – indicated by (●). B) Trends of polar vortex during December-May and C) the southern hemisphere annular mode (SAM) (Thompson and Solomon, 2002). (source of photo A – Australian Government Antarctic Division).

Compared to the LGM, Antarctic ice cores show a decrease in dust content by almost a factor of 25 to 50 during the Holocene (Delmonte et al., 2002). It is worth mentioning that the particle sizes were relatively larger during the Holocene compared to the dusts deposited during LGM. This has been attributed to the possibility of different transport mechanisms during the Holocene and glacial periods and the contribution of an additional source of dust that was absent during the LGM period (Delmonte et al., 2002). Therefore, in order to understand the possible changes in source area between LGM and Holocene, further studies are required. However, the difficulties lie in the extremely low concentrations of dust (few $\mu\text{g} / \text{kg}$, Figure 17) in ice cores that can make any measurements of elemental concentration, mineralogy and isotopic composition extremely challenging (Delmonte et al., 2002). In addition, there are also some disagreements about the sources of mineral dust in the Antarctic ice cores. For example, Gaudichet et al. (1992) used

kaolinite in mineral dust as a tracer of low latitude soils for the east Antarctic dust. They interpreted the variation of kaolinite in dust recovered from snow as a change in the concentration of the Australian source with climate (Gaudichet et al. 1992). They further used modelling of the desert dust cycle (Atmospheric General Circulation Model) and suggested Australia as a dust source for east Antarctica under both present-day and LGM conditions (Gaudichet et al., 1992). This corresponds with the findings of Mahowald et al. (1999). Based on the atmospheric modeling of dust transport and deposition, Mahowald et al. (1999) suggested that about half the dust in Antarctica is derived from Australia. On the other hand, isotopic studies (Sr and Nd isotopes) have shown Patagonia (South America) as the predominant source (Grousset et al., 1992; Basile et al., 1997; Delmonte et al., 2004). Therefore, a possible solution is to use an alternative environmental archive from both continents (South America and Australia) to evaluate both hypotheses.

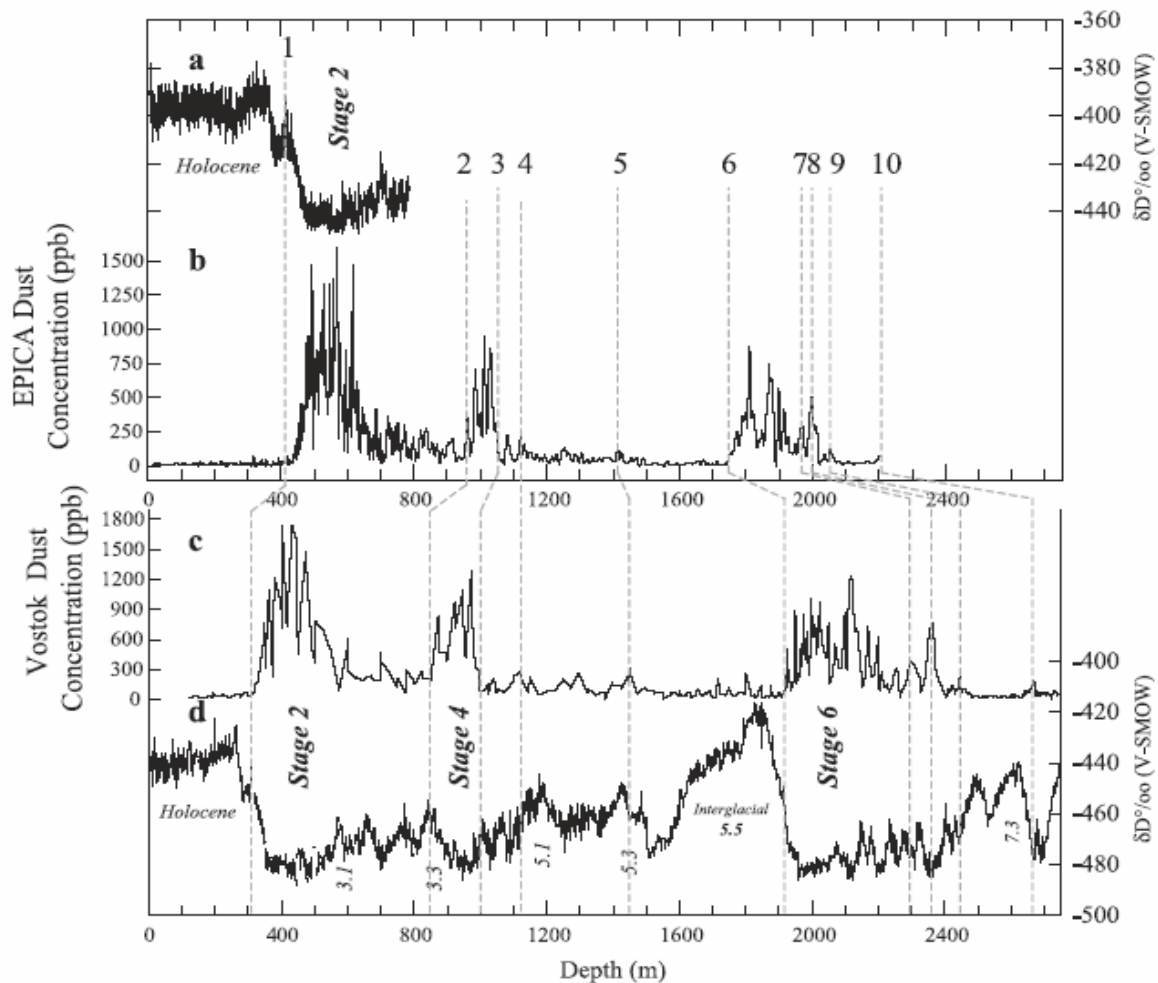


Figure 17: Dust concentration ($\mu\text{g} / \text{kg}$ or ppb) observed at EPICA-Dome C (b) and Vostok ice cores (c) (Delmonte et al., 2004).

1-3.2 Marine sediments

Deep-sea sediments are also a useful archive of eolian deposition and can be used as a proxy of past continental climates and atmospheric transport processes (Nakai et al., 1993). However, sedimentary processes or hemipelagic deposition (rapidly accumulating hemipelagic muds) near continents, turbidite sedimentation, and ice rafting especially in high latitudes can mask the much more slowly accumulating dust along hundreds of kilometers of coastline (Nakai, 1993; Rea et al., 1985). Because of the low sedimentation rate (e.g. $\sim 3 \text{ cm kyr}^{-1}$) (Hovan et al., 1989) even isolating glacial-interglacial changes in

dust deposition is challenging (Kohfeld and Harrison, 2001). In addition, the possible changes in riverine input and / or ocean circulation during glacial-interglacial cycles can disturb even the best record of dust accumulation.

1-3.3 Peat Bogs

Peatlands are widespread in areas of cool, moist climates, and account for ca. 3 to 5 % of the earth's land area (Figure 18). Before discussing the peat bog as an archive of atmospheric elements and mineral matter, the nature and formation of peat bogs will be briefly described.

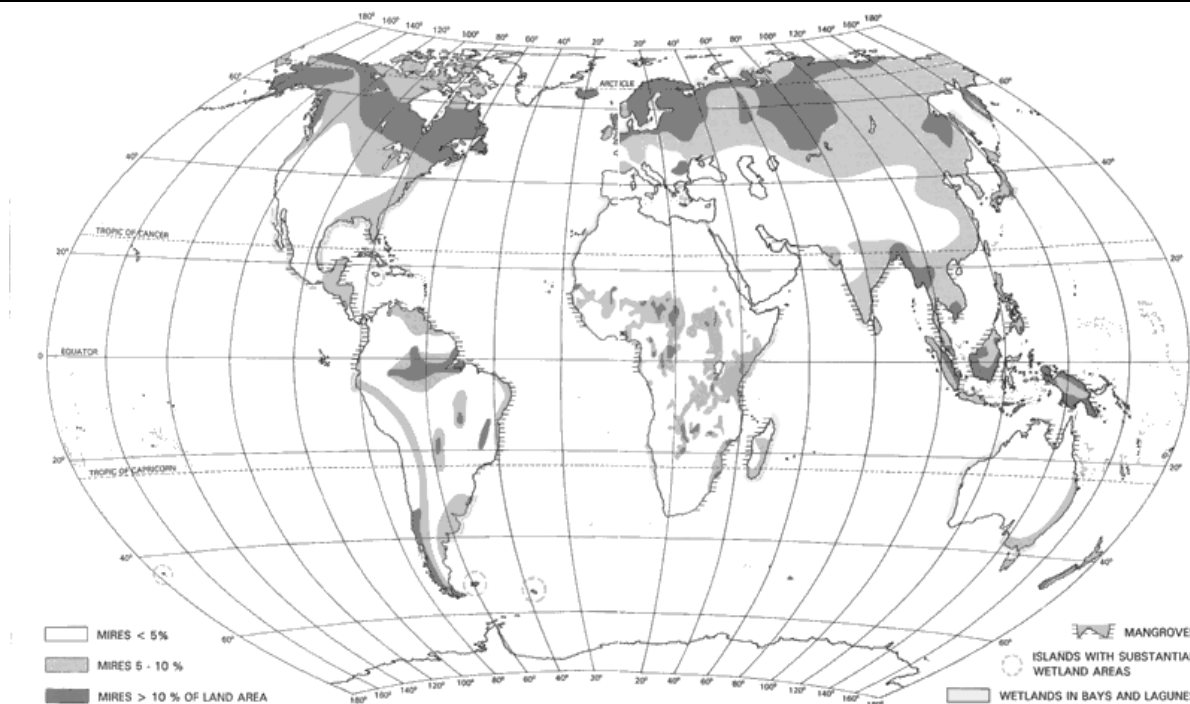


Figure 18: Distribution of peatlands (Charman 2002).

1-3.3.1 Peatland

Definition

Peat can be defined as a “light brown (almost blond) to black organic sediment” predominantly composed of dead vegetation (partially decomposed) (Shotyk, 1988) along with various amounts of inorganic materials. According to the American Society of Testing Materials (ASTM) deliberation peat contains less than 25 wt% inorganic material (Andrejko et al., 1983). This inorganic fraction (ash) is composed of both distinct mineral forms and organically complexed metals and cations (Andrejko et al., 1983). The ecosystems in which at least 30 cm of peat have accumulated are called peatlands (*Mires* in English and *Moor* in German) (Shotyk, 1988). Based on the sources of nutrients, peatlands are divided broadly into fens and bogs (Gore, 1983). The **fens** are peatlands influenced by water derived predominantly from outside of their own immediate limits. Therefore, they may be eutrophic, minerotrophic or oligotrophic. On

the other hand, **bogs** are hydrologically isolated from the ground waters and surface waters and are fed solely by atmospheric deposition (dry deposition and precipitation) (Gore, 1983; Charman, 2002). Therefore, bogs are also referred to as “ombrotrophic” (Greek meaning: “*Ombros*” = rain shower, “*trophe*” = nourishment) (Shotyk, 1988). A cross-section of the key hydrological mire types (bog and fen) is shown in Figure 18. Bogs can be further identified as raised bogs or blanket bogs (Charman, 2002). Raised bogs, as the name suggests, are peatlands with a convex profile (dome structure) (Figure 19 A). Because of the raised profile the dome receives inputs only from the atmosphere and is frequently surrounded by a ring of fen (lagg) zone. On the other hand, blanket bogs cover virtually the entire surface of a particular area, including slopes and mounds (Charman, 2002). Some of the general terms used to describe the peatlands based on the sources of nutrient and vegetation are summarized in Table 2 (Charman, 2002).

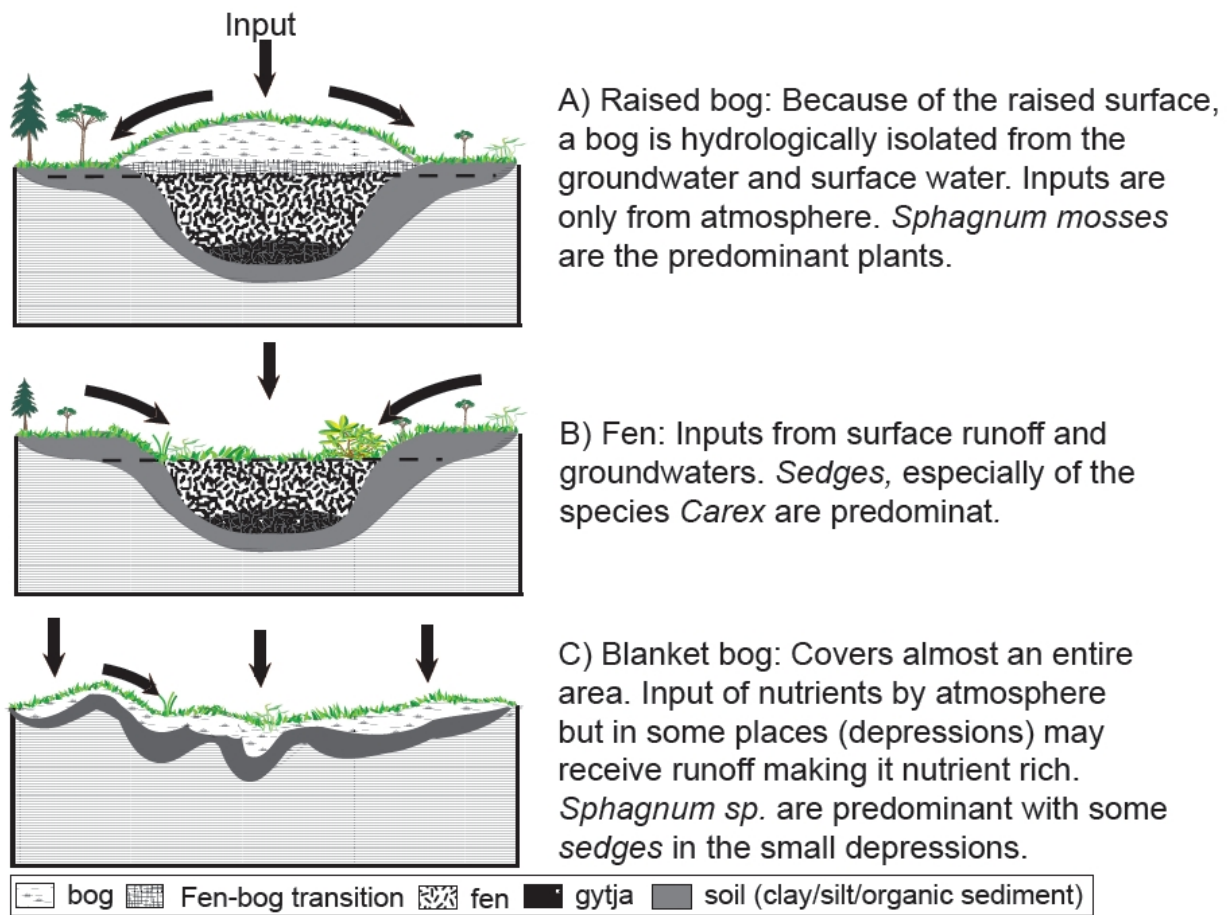


Figure 19: Cross-section of bogs (raised and blanket) and a fen (Based on Charman, 2002).

Table 2: Main terms used in the English-language peatland literature (Charman, 2002).

Wetland	Land with the water table close to or above the surface or which is saturated for a significant period of time. Includes most peatlands but also ecosystems on mineral substrates, flowing and shallow waters
Peatland	Any ecosystem where in excess of 30-40 cm of peat has formed. Includes some wetlands but also organic soils where aquatic processes may not be operating (e.g. drained or afforested peatlands)
Mire	All ecosystems described in English as swamp, bog, fen, moor, muskeg and peatland (Gore 1983c), but often used synonymously with peatlands (Heathwaite et al, 1993b). Includes all peatlands, but some mires may have a mineral substrate
Fen	A mire which is influenced by water from outside its own limits
Bog	A mire which is influenced by water from rain and/or snow falling onto its surface
Marsh	Loose term usually referring to a fen with tall herbaceous vegetation often with a mineral substrate
Swamp	Loose term with very wide range of usage. Usually referring to a fen and often implying forest cover

Formation

Waterlogging and low oxygen content are the main factors for the initiation of peat formation (Charman, 2002). Similarly, there needs to be an excess of precipitation over evapotranspiration and surface runoff. For the peat to accumulate, the rate of decay of

biomass must be less than the rate of growth of plant matter. Peat formation takes place either by the in-filling of shallow lakes (**terrestrialization**) or by the swamping of forested land and / or grassland (**paludification**) (Frenzel, 1983; Charman, 2002). The paludification process can occur

on predominantly flat topography (even on bare rocks) or any wet soil underlying the bedrock. However, the waterlogging condition balancing the rate of decay and rate of biomass accumulation is required for the paludification process. One possible way to achieve waterlogging is by the formation of a chemical pan derived from the illuviation (ie process of redepositing soil material removed from one horizon to another) of iron oxides in an acid medium. Another way is by a gleying. An impermeable substratum such as rocks underlying the thin organic soil can also initiate the paludification process (Frenzel, 1983). In any shallow lakes, pools or hollow basins which can collect water, terrestrialization can occur naturally over time (successive in-filling of aquatic environment). However, the paludification process may require an external factor such as a change in the climate (e.g. change in hydrology and transformation of dry soil to wet soil) for the initiation and accumulation of peat (Charman, 2002). Figure 20 illustrates the process of bog development.

Bog environments

Because of atmospheric inputs and isolation from local groundwater and surface water, the bog environment is oligotrophic, acidic, and generally anoxic (Shotyk, 1988; Shotyk, 1996). The plant communities in such nutrient deficient and acidic environments are dominated by *Sphagnum species*, which have high cation exchange capacities (Clymo, 1983). Some vascular plant species such as *Eriophorum* and dwarf shrubs that are able to withstand acidic, oligotrophic and wet conditions may also a proportion of the bog plant communities (Clymo, 1983). Generally, a peat bog contains a living surface layer (acrotelm) of *Sphagnum* and a dead (decomposed) material, below which diagenesis and humification occurs (catotelm) (Ingram, 1983). The acrotelm is an oxic layer where microbial activity (aerobic) is higher, causing a rapid decay of plant materials. The catotelm is an anoxic layer and with increasing depth and prevailing anaerobic condition the process of diagenesis by humification is extremely slow (Ingram, 1983).

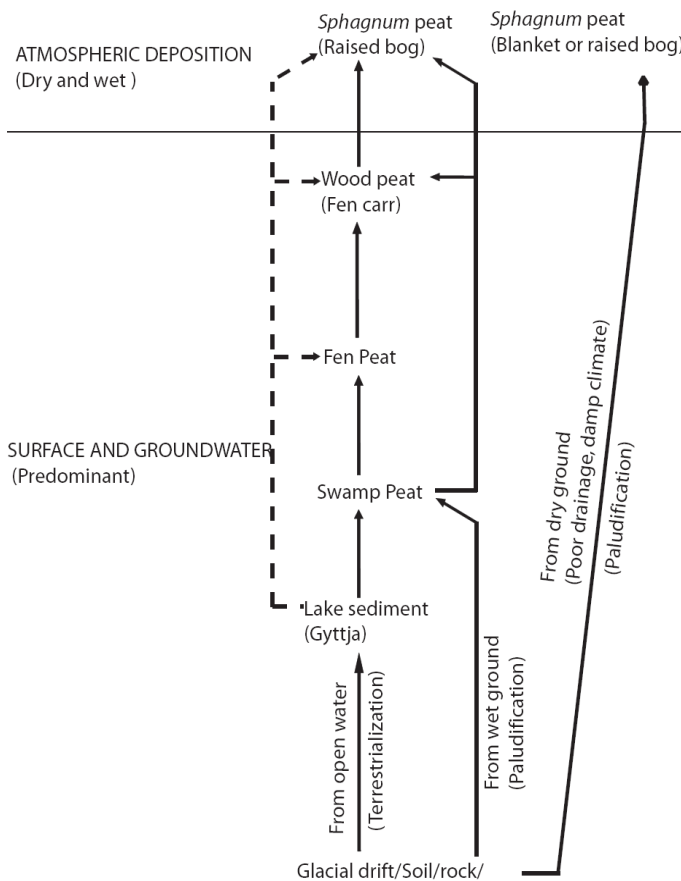


Figure 20: Process of bog development (based on Tallis, 1983 and Charman, 2002).

1-3.3.2 Peat as an archive of environmental change

Geochemistry

In an early work on elemental geochemistry, Schneider (1963) attributed the increasing Fe, Al and Si content in the peat profiles from north-west Germany to the intensified agricultural activities and therefore, the wind erosion of neighboring mineral soils after the Bronze age. Similarly, Chapman (1964) showed a correlation between the elevated wind blown material from deforested land and the increased Al and Si in the peat profile. In weathering profiles, the concentrations of lithogenic elements such as Ti and Zr are enriched in minerals of comparatively dense phases such as rutile, zircon, and monazite (Milnes and Fitzpatrick, 1989; Nesbit and Markovics, 1997). In the soil-derived aerosols, these elements are preferentially enriched in particles of intermediate size (10 – 60 μm) (Eltayeb et al., 2001; Schütz and Rahn, 1982), which can be transported long distances (Schütz, 1989) (see Figure 6 and 11). Therefore, in a peat profile, the elemental concentration of these elements (e.g. Zr to Ti) and their relative abundance can indicate either changes in particle size and mineralogy due to changes in wind strength, or changes in the predominant source area (Shotyk et al., 2002). Hölzer and Hölzer (1998) used Si and Ti concentration in peat as an indicator of soil erosion. Because the concentration of these lithogenic elements depends on the amount and the nature of mineral material deposited on the bog at the time of peat formation, they can reflect past

atmospheric deposition rates. This can be done by using the elemental concentration, peat accumulation rate and bulk peat density (equation 2).

$$\text{AR } (\mu\text{g} / \text{cm}^2 / \text{yr}) = \text{E } (\mu\text{g} / \text{g}) \times \rho \text{ (g} / \text{cm}^3) \times \text{I (cm} / \text{yr)} \quad (2)$$

where E is the elemental concentration, ρ is the dry bulk density and I is the peat accumulation rate. Similarly, using the Ti as a surrogate of mineral matter deposited on the peat, the mineral accumulation rate (MAR) can be calculated as follows (Shotyk et al., 2002) (Chapter 2):

$$\text{MAR } (\mu\text{g} / \text{cm}^2 / \text{yr}) = 250 \times \text{Ti } (\mu\text{g} / \text{g}) \times \rho \text{ (g} / \text{cm}^3) \times \text{I (cm} / \text{yr)} \quad (3)$$

where 250 is the concentration factor used to convert the Ti concentration to an equivalent mineral dust concentration, assuming an average Ti crustal abundance of 0.40 % ($4010 \mu\text{g g}^{-1}$) (Wedepohl, 1995). Shotyk et al. (2001) and (2002) used lithogenic elements such as Ti and Sc in the bulk peat as an indicator of past atmospheric changes in soil dust. For example, using the Ti concentration as surrogate of soil dust Shotyk et al. (2002) (Figure 21) showed that increased soil dust corresponds with the Young Dryas cold climate (10590 ^{14}C yr BP), volcanic emissions (8230 ^{14}C yr BP) and Holocene climate changes (5320 ^{14}C yr BP).

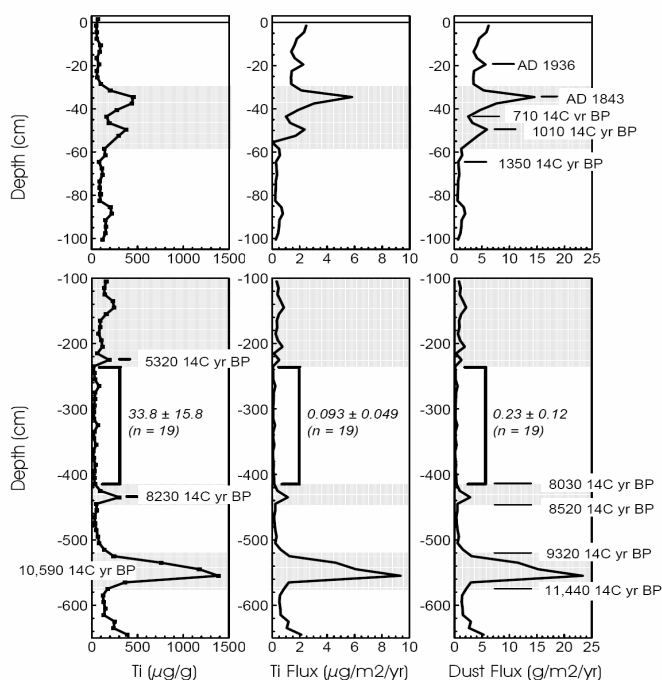


Figure 21: Ti concentration in bulk peat from Switzerland and the calculated atmospheric soil dust deposition rate (Shoty et al., 2002).

However, elemental mobilization should be accounted for before calculating the past accumulation rates of any elements of interest. The concentration of elements deposited in a peat profile can be affected by several factors such as surface runoff, groundwater flow and/or upward diffusion of mobile elements in the ombrogenic peat from the underlying minerogenic peat. Therefore, before calculating the atmospheric deposition rates of trace elements, it is necessary to identify the truly ombrotrophic zone (Shoty, 1996). This can be done by using some elements such as Ca and Sr, which are mobile in peat profiles (Shoty, 1996; Shoty et al., 2001). However, other elements such as Pb (Weiss et al., 1999; Shoty et al., 1998; Shoty et al., 2002) and antimony (Sb) (Shoty et al., 2004) are considered immobile in the peat profile. More than just atmospheric dust, ombrotrophic bogs have been successfully used to study the atmospheric deposition of many trace elements such as Pb (Shoty et al., 1998; Shoty et al., 2005), mercury (Hg) (Roos-Barracough et al., 2006), chromium (Cr) (Krachler et al., 2003) and Sb (Shoty et al., 2004).

Mineralogy

The mineral matter in a peat can be divided into three fractions (Andrejko et al., 1983): a) biogenic components; b) terrigenous

mineral components (soil dusts and volcanoes); and c) authigenic components (minerals formed *in situ*). Inputs of terrigenous minerals can be either from the atmosphere (wind-borne) and/or from surface runoff (washed in), or both. Fens receive terrigenous components predominantly from surface runoff, whereas in bogs the terrigenous components are atmospheric (see Figure 19). In the case of biogenic components in both bogs and fens, they may either have been supplied by the atmosphere or formed *in situ*. Similarly, authigenic components can be formed in both bogs and fens due to peat diagenesis and biomineralization.

Achard (1786) may have been the first scientist to start work on quantitative studies of mineral matter in peat, followed by Zailer and Wilk (1907), who initiated the modern studies of the mineralogy of peat (c.f. Shoty, 1988). In the past (1970s), the spatial and temporal variation in the ash content have been used to study the history of land use (e.g. agriculture, human settlement). Because of atmospheric inputs of mineral matter, the ignition residue (ash content) of an ombrotrophic peat alone has been useful for studying the human activities in the past (Aaby, 1986). For example, in a study of *Sphagnum fuscum* from various sites in mid-western North America, Gorham and Tilton

(1978) found the effect of agricultural activity in the ash content, which was attributed to the wind-blown soil. Similarly, in a study of mires from Finland, Tolonen (1984) observed a correlation between the variation in the ash content and the quantity of wind-blown mineral particles derived from the fields and other bare soils. A number of other studies on the effects of human activities (e.g. agriculture, settlement, etc.) on ash content were done by Bahnson (1973) (c.f. Aaby, 1983) and Vuorela (1983). Vuorela (1983) found that the ash content in *Sphagnum* peat from Finland is a better indicator of changes in agriculture than biological indicators such as Cereals pollen and weeds seeds. Therefore, Vuorela recommended using the ash content of peat deposits over the selected pollen types as indicators of the expansion of arable land. Similarly, Kramm (1978) counted the number of dust particles using optical microscopy in a 0.01 mm² area of a slide preparation in ombrotrophic peat from north-west Germany, and correlated it with past human activities (Figure 22). Recently, Björck and Clemmenson (2004) used the number of

quartz grains (between 0.2 – 0.35 mm and > 0.35 mm), in the inorganic fraction of peat from Sweden which were identified under optical microscopy, and attributed them to the variations in aeolian sand flux and winter climate.

Despite all the earlier efforts, the mineralogy of the inorganic fraction of peat has not been studied extensively. Because of high concentrations of dissolved organic acids and low pH (~ 4), peat bogs can be active agents in the weathering of atmospherically deposited minerals (Shotyk, 1992). However, few studies have been done about the weathering of minerals in peat (Steinmann and Shotyk, 1997; Bennet et al., 1991; LeRoux et al., 2006). Recent studies show that minerals such as apatite and phosphates dissolve rapidly on the surface of the peat, whereas silicate and aluminosilicate minerals are remarkably well preserved, including relatively reactive mineral phases such as feldspars and micas (LeRoux et al., 2006; Steinmann and Shotyk, 1997). Possible reasons given for the preservation of silicate minerals are formation of a siliceous residual

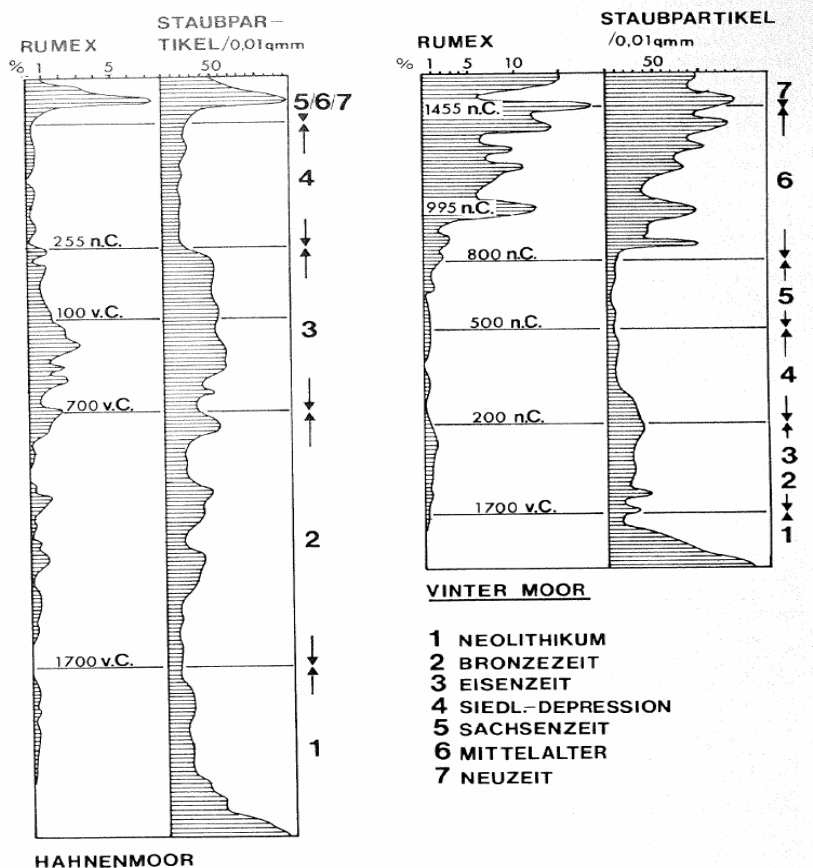


Figure 22: Relationship between *Rumex* curve and inorganic dust particles in Hahnen bog and Vinter bog from Germany (Kramm, 1978).

surface layer on the mineral grains (Steinmann and Shotyck, 1997; LeRoux et al., 2006) and / or the formation of surface coating on mineral grains by humic acid (Ochs et al., 1993; Ochs, 1996). Therefore, recovery of intact, insoluble minerals from the peat should be possible, allowing the identification of their mineralogical composition to be used to infer past atmospheric changes in mineral dust deposition and their provenance.

A mineralogical study of peat can be done either by direct observation in bulk peat (*in situ*) (Kramm, 1978; Raymond et al., 1983) or by the isolation of the minerals from the peat (Andrejko et al., 1983; Raymond et al., 1983; Givelet et al., 2004). One possible way suggested by Raymond et al. (1983) is to impregnate the peat containing abundant minerals with molten paraffin and slice it sufficiently thin (15 – 25 μm). The thinner section (15 μm) and the “adjacent” thicker section (25 μm) can then be used for light microscopy and SEM respectively. Kramm (1978) counted the dust particles directly on peat placed on a slide (*in situ*) under the optical microscope, although he did not mention the nature of these dust particles. Nonetheless, for the ombrotrophic peat with extremely low mineral matter, this procedure may be difficult. Raymond et al. (1983) wrote: “Another problem of major consequences in studying mineral matter in peat is that...” referring to the low or high temperature ash content “...some inorganic fractions may be so scarce that they will not be observable either in thin section or in the X-ray diffraction.” “However, the peats contain some non-biogenic mineral particles of both siliceous and non-siliceous composition...”, and the alternative approach is “...that can be separated from the organic peat material for SEM analysis by ashing and acid bath techniques.” (Raymond et al., 1983) One example is the acid bath (wet digestion) technique to separate the minerals from organic fraction of peat, as used by Finney and Farnham (1968): they added H_2O_2 in a controlled reaction environment (e.g. pH 3 – 4 and/or temperature 65 – 80 $^\circ\text{C}$) to a peat sample until no traces of organic matter were visible. The main reason given by Finney and

Farnham for using this method is that “...oxidation of peat by ashing does not sufficiently clean the mineral fraction for optical study”. However, depending on the amount and nature of organic matter (highly decomposed or not), this method can be time-consuming, requiring from a few days to several weeks of continuous treatment with a reagent. Another method of wet digestion used by Malmer (1988), which has not become common, is destroying the organic fraction by using $\text{HNO}_3 + \text{HClO}_4$ (4:1). The main component of Malmer’s (1988) uncolored acid insoluble ash (AIA) was SiO_2 . However, the common method used for mineralogical analysis is to ash the peat at 550 $^\circ\text{C}$ (generally between 12 – 16 hours), and to dissolve soluble minerals (see following paragraph) such as carbonates, oxides and phosphates formed during peat ashing by using hydrochloric acid (HCl) (Chapman, 1964; Andrejko et al., 1983; Steinmann and Shotyck, 1997; Givelet et al., 2004; Björck and Clemmensen, 2004).

Composition of peat ash

When peat is ashed, the ignition residue contains carbonates (e.g. CaCO_3), phosphates ($\text{Ca}_3(\text{PO}_4)_2$), oxides (CaO), hydroxides (KOH), sulphates (CaSO_4), mineral grains and particles of biogenic origin. Cations (e.g. Ca^{2+} , Mn^{2+} , Mg^{2+} , K^{2+}), associated predominantly with the organic fraction of peat, may be responsible for the formation of most of these amorphous carbonates, phosphates, oxides/hydroxides and sulphates during combustion (Steinmann and Shotyck, 1997). These minerals are readily soluble in acidic media such as HCl. On the other hand, most of the silicates and refractory oxides such as feldspar ($\text{XAl}_{(1-2)}\text{Si}_{(3-2)}\text{O}_8$)^a, mica ($\text{AB}_{2-3}(\text{X}, \text{Si})_4\text{O}_{10}(\text{O}, \text{F}, \text{OH})_2$)^b, sphene (CaTiSiO_5), zircon (ZrSiO_4), and clay minerals (e.g. illite, smectite), originally derived from atmospheric soil dust, are stable during combustion (residual minerals). Biogenic particles such as phytoliths and diatoms that

^a X: Na, Na and/or K, K and/or Ca, Ca

^b A: K (usually), Na, Ca, Ba, and Ce; B: either Al, Li, Fe, Zn, Cr, V, Ti, Mn and/or Mg; X: Al (usually), Be, B, and/or Fe

may either be airborne or *in situ* formed are also stable during high temperature ashing. These stable silicate and oxide minerals and biogenic particles are not easily dissolved in acidic media, giving rise to a residue referred to as “Acid Insoluble Ash” (AIA). A detailed description of mineralogy of Oreste bog is presented in Chapter 3.

Chapman (1964) measured total Si in AIA in a bog from Northumberland and found increased concentrations in the basal peats and in the upper layers. Based on microscopic observations, Chapman (1964) classified the peat silica (insoluble ash) into two categories. The first category included wind-blown quartz and the second included opaline silica of plant origin. He found that the first category (mineral quartz) was abundant in the upper layers. He concluded that the increased supply of wind-blown material was responsible for the abundant mineral quartz affected by deforestation and the creation of open habitats. The mineralogical study of the inorganic fraction of peat from selected layers by Finney and Farnham (1968) was probably the earliest attempt at a detailed study of minerals in peat. Finney and Farnham (1968) divided the AIA into four particle sizes: $< 2 \mu\text{m}$ (45 %), $2 - 6 \mu\text{m}$ (~ 15 %), $6 - 20 \mu\text{m}$ (~ 30 %), and $> 20 \mu\text{m}$ (~ 10 %). The instruments used were optical microscopy for the mineral grains $> 2 \mu\text{m}$, and X-ray diffraction for the mineral grains $< 2 \mu\text{m}$. Kaolinite, illite, vermiculite, quartz and feldspar dominated the $< 2 \mu\text{m}$ size fraction (Finney and Farnham, 1968). Quartz, orthoclase, plagioclase and mica were abundant in the $> 2 \mu\text{m}$ mineral grains. In a study of dust particles, Kramm (1978) counted the particles in peat, but did not mention the mineralogy and particle sizes. Steinman and Shotyk (1997) observed quartz (60 – 90 %), feldspar (5 – 15 %) and muscovite (5 – 15 %) with various other minerals (5 – 10 %) (e.g. biotite, zircon), which were identified by using optical microscopy and SEM (EDS-spectra), in the ash fraction of a peat from the Jura Mountains, Switzerland. Based on the vertical profiles of relatively constant mineralogy with depth, Steinmann and Shotyk (1997) concluded that for the past two millennia the

fine-grained silicates supplied by soil dust have not been measurably weathered.

Peat bogs as archives of atmospheric dusts

Peat bogs can be used as an alternative to the ice cores as archives of dust deposition. Unlike glacial ice which is restricted to alpine and polar regions, peatlands are found nearly all over the world (Figure 18). As mentioned previously, that there is a clear need of alternative archive to complement the Antarctic ice core studies of atmospheric dust deposition (see Chapter 1-3.1), and peat bogs can be utilized for this purpose. Peat bogs, compared to Antarctic ice cores have two advantages: an abundance of mineral matter and adequate temporal resolution. For example, the abundance of mineral matter in Antarctic ice cores is generally on the order of $\mu\text{g} / \text{kg}$ (Figure 17) (Delmonte et al., 2002). Additionally, the mean temporal resolution is between ~ 135 years (EPICA) and ~ 900 years (Dome C) for the Holocene. On the other hand, the abundance of mineral matter in peat is generally on the order of g / kg (Figure 23). For peat bogs with an average long term peat accumulation rate of ca. 1mm per year, peat cores cut into 1cm slices can provide a record of atmospheric changes on a decadal timeframe. Therefore, studies of many parameters such as elemental chemistry, mineralogy and isotopic composition of atmospheric dust can be much easier and with better temporal resolution by using peat cores than by using Antarctic ice cores.

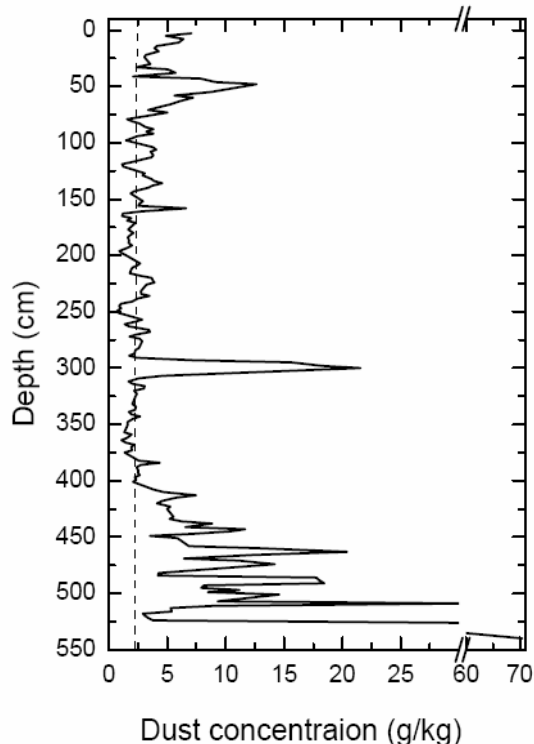


Figure 23: Dust concentration observed at Oreste bog peat profile (Chapter 2) which averages ~ 2 g/kg

1-4 Atmospheric deposition of Pb in southern hemisphere

Significantly fewer studies on the atmospheric deposition of Pb are available for the southern hemisphere than the northern hemisphere. Most of the studies on the atmospheric deposition of Pb are from Antarctic ice cores. In a recent study, Planchon et al. (2003) showed Pb concentrations and isotope ratios in ice cores (Coats Land, Antarctica) for the past 150 years (between 1840 and 1990 AD). In another study of the EPICA ice cores from Dome C, Antarctica, Vallelonga et al. (2005) measured Pb concentration and Pb isotopes between 6.9 kyr BP and 210 kyr BP. They found that soil dust and volcanic emission were responsible for 70 % and 30 % of Pb deposition. However, they could not determine the sources of Pb because of the

scarcity of Pb isotopes data from the possible source areas to be compared to the data from the ice-core. In the early studies of the Pb concentration in ice cores (Antarctic Dome C), Boutron and Patterson (1986) measured 14 Pb concentrations representing the last ~ 27 ka BP, and showed concentration changes during the Wisconsin/Holocene transition. However, only one sample was measured for the last 6000 years, and five other samples were measured between 7 Ka and 13 Ka BP. Due to the extremely low concentration of trace elements in the Antarctic ice, all analytical work with trace elements in ice cores is tedious, time consuming and expensive. For example, Pb is present in Antarctic ice at pg / g concentration or below which is six or seven orders of magnitude lower than in the earth's crust ($14.8 \mu\text{g} / \text{g}$ for the earth's crust and $17 \mu\text{g} / \text{g}$ for the earth's upper continental crust) (Wedepohl, 1995). Vallelonga et al. (2005) found Pb concentrations less than 1 pg / g during the Holocene and the last interglacial periods compared to higher Pb concentration (> 10 pg / g) during cold climatic periods. Therefore, the measurement of trace and ultratrace elements in Antarctic snow and ice is problematic and vulnerable to severe contamination. For example, in the early studies of Antarctic ice cores, the overall lead contamination correction ranged from < 10 % for Wisconsin ice cores containing 5 to 30 pg / g of Pb, to 75 % for Holocene ice cores containing 0.3 to 1 pg / g of Pb (Boutron and Patterson, 1986). In AIA fraction of peat, Pb concentrations are generally in the range of $\mu\text{g} / \text{kg}$ or more ($\mu\text{g} / \text{g}$) (e.g. $15 \pm 8 \mu\text{g} / \text{g}$ in Oreste bog, Chapter 5). Therefore, the reliable measurements of Pb concentrations and the isotopic composition are easier with peat compared to ice, and there is less risk of contamination. Hence, peat bogs have great potential as archives of atmospheric dust and trace elements in the southern hemisphere.

1-5 Aims of the study

compositions of Sr and Pb (Chapter 4 and 5)

Though the radiogenic isotopic data (Sr, Nd) available to date have shown that southern South America is the most important dust source for Antarctica during the Glacial Stages, possible contributions from other sources have not been excluded. This is because of the observed partial overlap of radiogenic isotopes between southern South America, New Zealand and the Antarctic dry valleys. Meanwhile for the Holocene, the sources of dust are not well-defined by isotopic fingerprinting as for the LGM dust samples probably because of the recovery of extremely lower abundance of mineral dusts (15 – 23 $\mu\text{g}/\text{kg}$). However, despite the decrease in particle sizes and increase in dust concentrations, southern South America is still considered as the main source of dusts during the Holocene. Therefore, further studies are required to verify the assumption that the dust source to Antarctica has remained constant irrespective of climatic changes and transport mode.

Southernmost South America is the only major land mass that extends beyond 45 °S, contains abundant peatlands and lies between the extensive loess plains of Argentina and the Antarctic continent. Therefore, atmospheric dusts on its way to Antarctica from Argentinian loess plains are possibly being deposited and possibly preserved for thousands of years in peat bogs from southernmost South America. Hence, a peat bog from Southern South America is used with the following objectives:

- a) to reconstruct the changing rates of atmospheric dust deposition using the accumulation rates of conservative, lithogenic elements (e.g. Ti) (Chapter 2)
- b) to identify the predominant minerals and to characterize the size and morphology of these materials to evaluate source strength (relative importance of local versus long-range and soil dust versus volcanic tephra). (Chapter 3)
- c) to identify the predominant source areas of these materials using precise measurements of the isotopic

6 Materials and methods

1-6.1 Study site

The Oreste bog is located in Bahía Windhound, Southern Isla Navarino, Chile (55°13'13''S and 67°37'28'' W 35m) (Figure 24). It is a Magellanic moorland bog (maritime climate), with an average precipitation of 800 mm / yr (Rabassa et al., 1996). The climate of the area is determined by prevailing westerlies (Tuhkanen, 1992) with seasonal shifts of the storm tracks that cross the belt of westerlies, poleward in summer and equatorward in winter (Pendall et al., 2001). The ombrotrophic bogs, including Oreste bog, within this maritime climate zone show rapid growth and are of recent origin overlying minerotrophic peat (Rabassa et al., 1996). The dominant moorland taxa are

Sphagnum magellanicum, *Drepanocladus* spp., and *Astelia pumila* accompanied by *Carex*, *Ericaceae* (*Empetrum*) and *Marrsippospermum grandiflorum*.

The central part of Isla Navarino is mountainous. This central belt is part of a Late Jurassic-Early Cretaceous marginal basin (the Rocas Verdes Marginal Basin) with the following rock types: Upper Jurassic silicic volcanic rocks, Lower Cretaceous deep-marine volcanoclastic turbidites and slope mudstones, and Upper Cretaceous plutonic rocks (Olivero and Martinioni, 2001). Mesozoic quartzites, slates, phyllites, and low-grade schists dominate the geology of the area. A geological map of the study area is shown in Figure 25.

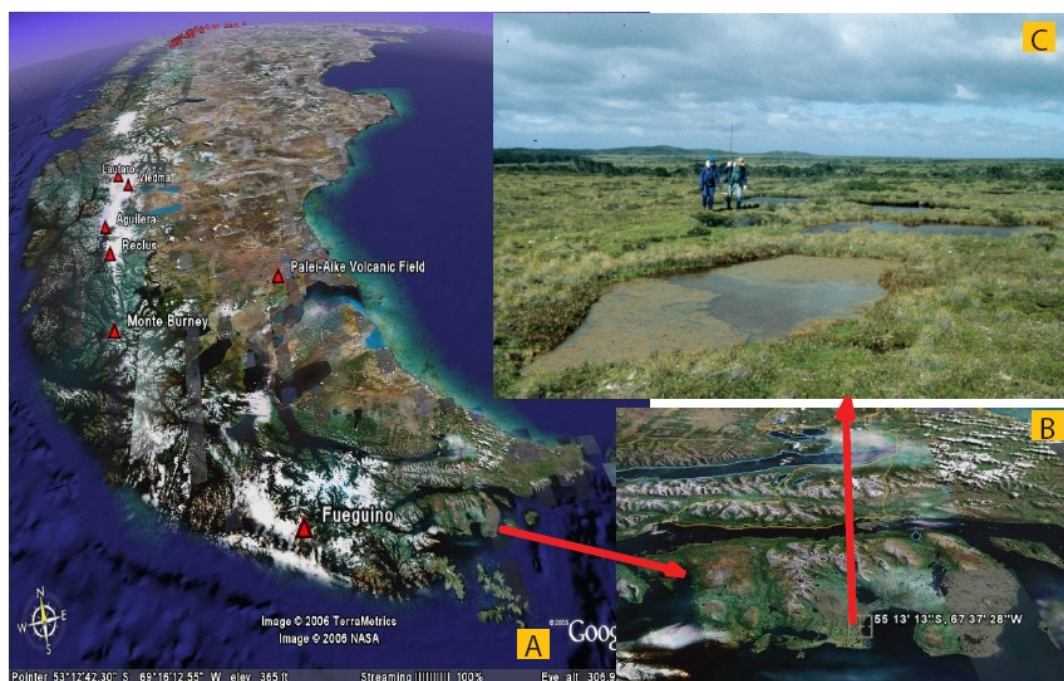


Figure 24: (A) Photo of southern South America, (B) Isla Navarino where the Oreste bog is located, and (C) photo of the Oreste bog. Photos A and B are from Google Earth. Photo C was taken by Vera Markgraf.

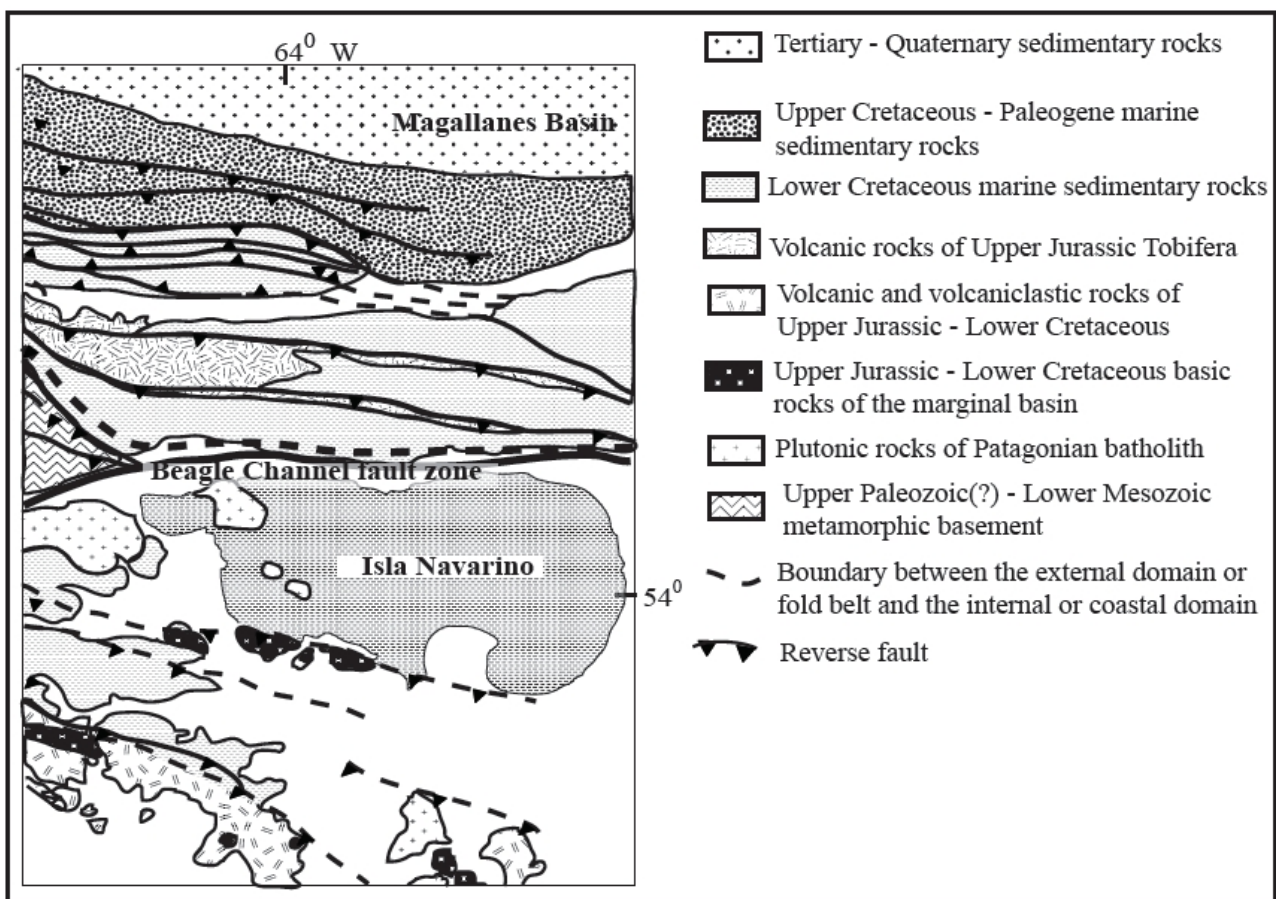


Figure 25: Geological setting of the Isla Navarino (Kraemer, 2003)

Some of the bogs in this region have been used for paleobotanical studies but to date, no geochemical studies have been reported. The Oreste bog has not previously been the subject of botanical or geochemical studies.

1-6.2 Sampling procedure

The Oreste bog was cored with a Livingston piston sampler of 7.5 cm diameter to a depth of 542 cm. Cores were recovered at intervals of 100 cm, but immediately sectioned into increments of 25 cm in the field using a knife. Afterwards, in the laboratory, each of the core sections was cut precisely into 2 cm increments and $\sim 6 \text{ cm}^{-3}$ volumetric plugs were taken from each slice for paleobotanical / macrofossil studies (see 1-6.3) (Chapter 2). The remaining subsamples were used for chemical analysis, mineralogical characterization (Chapter 2 and 3) and radiogenic isotope fingerprinting (Chapter 4 and 5). The peat stratigraphy based on the visual inspection and trophic status of peat is shown in Figure 26 (Chapter 2).

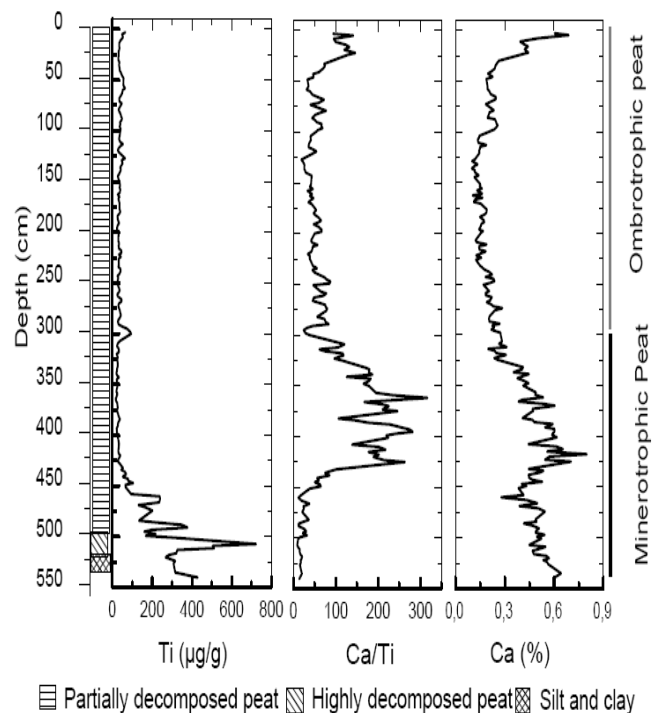


Figure 26: Peat stratigraphy and the trophic status of peat core from Oreste bog

1-6.3 Sample handling and analytical methods

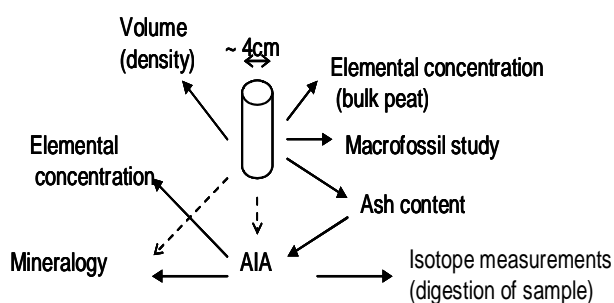


Figure 27: Illustration of parameters determined in the peat samples.

In the Oreste bog, two types of samples were required a) bulk peat powder and b) peat ash. Bulk peat powder was required to determine elemental concentrations in bulk peat. Peat ash was required for ash content, but also for chemical, mineralogical and isotopic analysis of AIA (Figure 27).

Highlighting the importance of the thickness of a peat slice, Givelet et al. (2004) wrote: “The resolution and magnitude of any given peak depends on the thickness of slice”. The suggested thickness of a peat slice is 1 cm in order to improve the accuracy, reproducibility and reliability of peat bog archives (Givelet et al., 2004). In the Oreste bog, early calculations using the average peat diameter (~ 4 cm) and the assumption of 80 – 90 % water content in the peat (Charman, 2002) suggested that the 1 cm slice would yield about 1 g of dry peat. This would be correspondingly less if a sample were to be removed for macrofossil analysis.

As previously mentioned concerning the general characteristics of an ombrotrophic peat containing 1 – 2 % ash content, previous studies have shown that insoluble minerals (AIA) account for only 17 – 50 % of the ash content (Finney and Farnham, 1968; Björck and Clemenson, 2004; Steinmann and Shotyck, 1997). Because of the low AIA content,

Finney and Farnham (1968) used samples of peat sufficiently large to yield approximately 2 – 3 g of insoluble mineral matter for their mineralogical studies. Referring to the problem of low ash content, Givelet et al. (2004) wrote: “Moreover in the case of a general study also including bulk peat geochemistry, there may be only a small quantity of peat available for mineralogical analysis.” Therefore, geochemical and mineralogical studies of atmospheric mineral dust using peat require either large sample volumes to obtain enough mineral matter, or the use of precise and sensitive analytical approaches to work with small quantities of mineral matter. However, with the available coring equipment and the need for adequate temporal resolution, sample size is limited (Appendix I) (Givelet et al., 2004).

Assuming a 2 % ash content in Oreste peat, 1 g of peat (1 cm slice) might yield ~ 20 mg of ash, which, in turn, would yield only 4 – 10 mg of AIA. With this material required for chemical, mineralogical, and isotopic analyses, sample handling and analytical methods need to be optimized.

1-6.3.1 Modified sample handling and analytical methods

Peat slice and volume/density calculations

Because of the limited amount of AIA to be expected from 1 cm peat slices, peat sub-samples were cut into 2 cm increments. Givelet et al. (2004) showed that the precision of bulk density measurements, which require volume measurements, is very important in order to calculate the element accumulation and soil dust fluxes. The irregular shape of peat slices (Figure 28), however, made it difficult to calculate the volume and thus the density. Therefore, open source “imageJ” software was used to calculate the volume of the peat slices (Figure 28) (Chapter 2). Afterwards, ~ 6 cm³ sub-samples were taken for macrofossil studies.

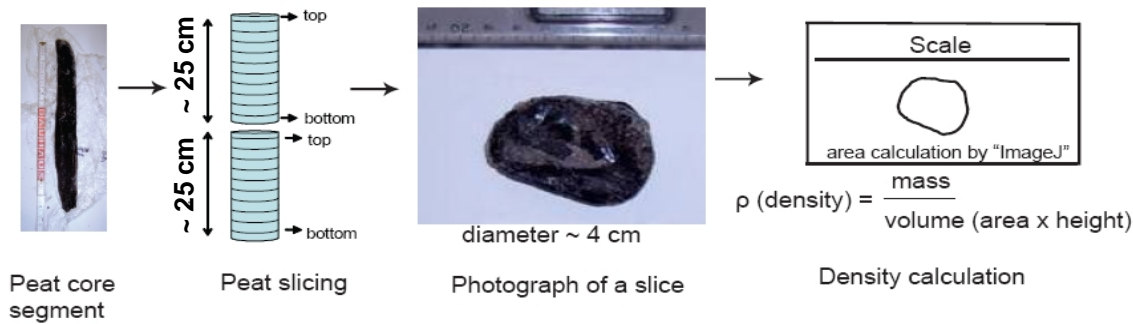


Figure 27: Illustration of sample handling for density calculation by using “ImageJ” software. The top and bottom slice of each peat section were used for age dating.

Ash and AIA content

The dry weight of bulk peat obtained was approximately 2 g and the ash content typically 1 % (550 °C, overnight). The soluble fraction of the peat ash was dissolved by using 1M HCl for 15 minutes. With an ash content of approximately 1 %, the yield of AIA was approximately 3 – 10 mg (~ 20 % of ash content) (Figure 29).

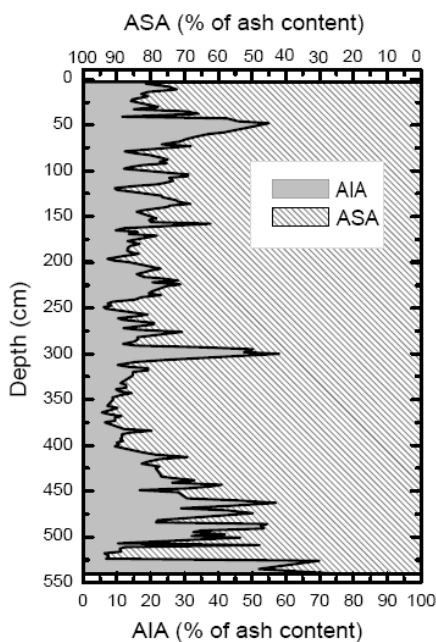


Figure 29: Acid Insoluble Ash (AIA) and Acid Soluble Ash (ASA) as a percentage of the total amount of ash in the Oreste peat profile (chapter 2). 1M HCl was used as a reagent with a reaction time of 15 minutes.

Reaction time for 1M HCl

The dissolution of soluble minerals, formed during combustion, in the peat ash by using acid (HCl), has been attempted in the past. Nevertheless, there are variations in the

strength of acid and duration of the reaction time used (Damman et al., 1992; Steinmann and Shoty, 1997; Björck and Clemmensen, 2004). Previous studies on sediments have shown that acid concentrations are sometimes inadequate for complete leaching of soluble phases from carbonate-bearing sediments (Snape et al., 2004; Sutherland et al., 2004). Similarly, excessive acid concentrations can dissolve or leach some of the target phases (silicates and aluminosilicates). Selection of the strength of acid required to minimize the dissolution of aluminosilicates also depends on reaction time. The optimized leaching procedures recommended are 4hrs with 1M HCl and 1h (shaken) with 0.5M HCl and employing a solid-to-solution ratio of 1g : 20 ml for two different sediment matrixes (Snape et al., 2004; Sutherland et al., 2004).

The reaction time required for 1M HCl to dissolve the soluble fraction was optimized using a series of tests at an earlier stage of the work. Similar amounts of peat ash were leached with 1M HCl using different reaction times (15 min, 30 min, 45 min, 120 min, 160 min, and overnight). The solutions were filtered after each reaction time and the filtrate was analyzed using inductively coupled plasma-optical emission spectrometry (ICP-OES). The concentration obtained for each of the elements after the first 15 minutes of reaction time was established as the reference level (100 % abundance) and other reaction times were calculated relative to this point (Figure 30). The elemental concentration was almost constant for 45 minutes and started to increase after that. Therefore, it could be inferred that as the peat matrix contains only ca. 1 % of mineral

materials, 1M HCl (1 : 10 w / v) with a shorter reaction time (15 minutes) was sufficient to dissolve the soluble fraction and isolate the silicates in peat ash (Figure 30).

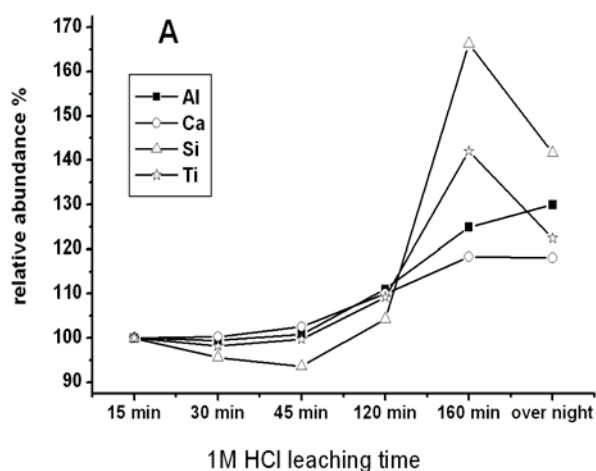


Figure 30: Relative abundance of Al, Ca, Si and Ti, observed in 1M HCl leachate of bulk peat ash using ICP-OES (n = 2). The concentration of the element at 15 minutes was established as reference level (100 % abundance).

1-6.3.2 Summary of sample handling and analytical methods

To maximize the use of available peat material (~ 2 g dry weight) for determination of ash content, elemental concentration in bulk peat and AIA, mineralogy and isotope fingerprinting, the analytical procedures outlined in the following Figure (31) were employed.

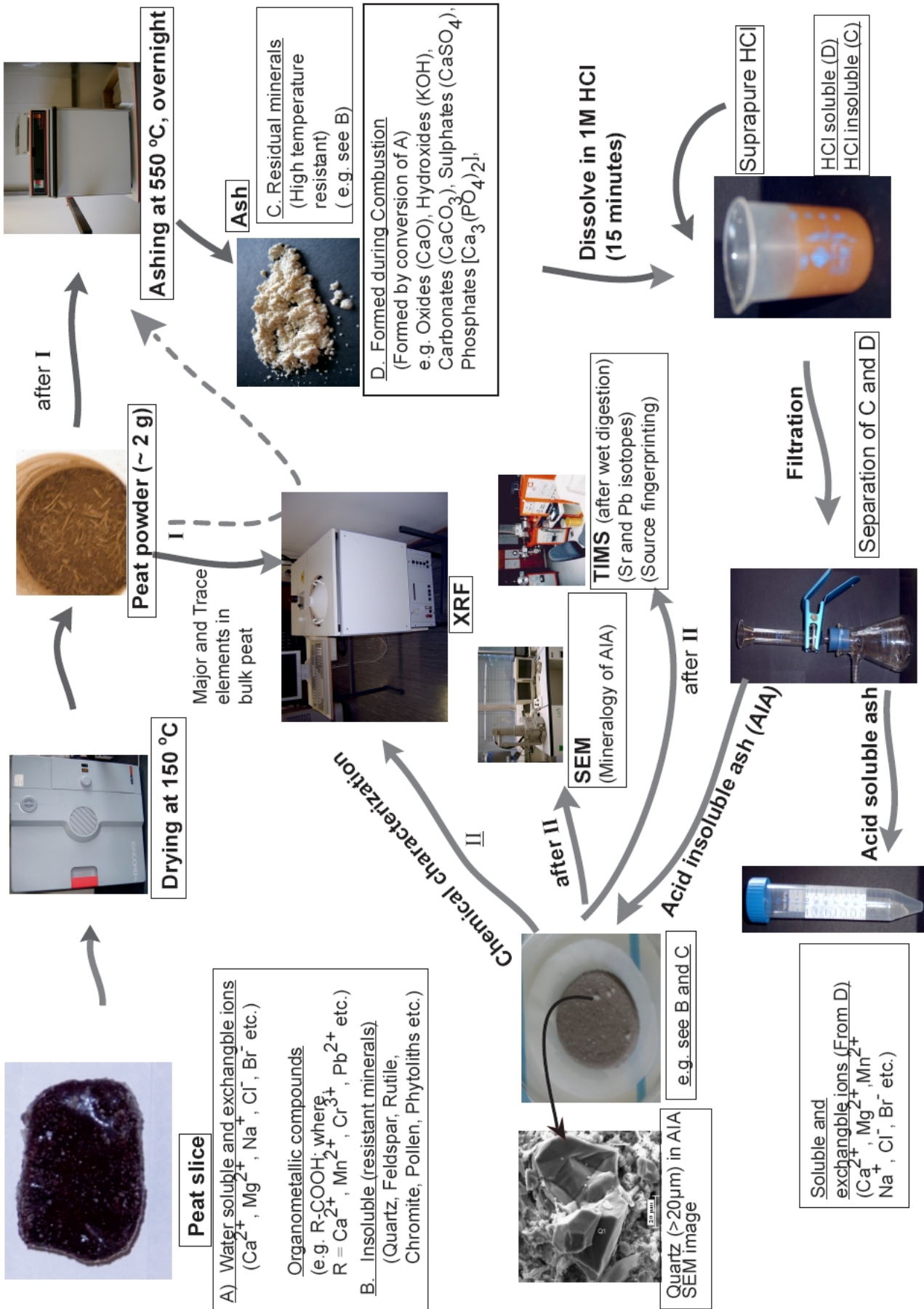


Figure 31: Illustration of sample handling and analytical procedures for Oreste peat.

1-7 Results

The geochemical studies of Ca, Mn, and Ti showed that the accumulation of mineral matter during the last ca. 6000 yrs was predominantly atmospheric with a record of effectively constant deposition ($0.43 \pm 0.12 \text{ g / m}^2 \text{ / yr}$) (Chapter 2). The lithogenic mineral particles found in the majority of samples were predominantly composed of weathered particles of quartz, plagioclase, potassium feldspars, pyroxenes, mica, amphiboles and few grains of heavy minerals such as zircon and monazite (Chapter 2 and 3). Effectively constant dust deposition combined with predominantly fine grained ($< 20 \text{ }\mu\text{m}$) and rounded mineral particles (Chapter 2 and 3) reflected the long-range atmospheric transport of soil dust and the climate stability for the past 6000 yrs.

The isotopic composition of Sr ($^{87}\text{Sr}/^{86}\text{Sr}$) in the AIA showed the atmospheric dust was of Patagonian origin (Chapter 4). The close proximity of the isotopic signature of Sr in the AIA and the Antarctic ice core dust suggests that southern South America was the predominant dust source not only during the LGM but also continuously to the present (Chapter 4).

The similarity between the Pb concentration in the AIA ($15.2 \text{ }\mu\text{g g}^{-1}$) and the crustal values ($14.8 \text{ }\mu\text{g / g}$ for the Earth's crust and $17 \text{ }\mu\text{g / g}$ for the Earth's upper continental crust) (Wedepohl, 1995) suggests that soil dust particles could account for effectively all of the natural inputs of atmospheric Pb (Chapter 5). The enrichment of Pb relative to Ti and $^{206}\text{Pb}/^{207}\text{Pb}$ ratio indicates inputs of anthropogenic Pb during the the 20th century.

1-8 Conclusions and perspectives

Mineralogical and chemical studies (major and trace elements) in bulk peat and insoluble ash provides valuable information about the mineralogical host phases which constitute silicate dusts in the atmosphere. Analysis of radiogenic isotopes (Pb, Sr) provides insight into the predominant source areas of these dusts.

In most of the palaeoclimatic studies of atmospheric dust and its provenance, polar ice cores have been used. This study is the

first attempt at using the peat bog as an environmental archive to reconstruct the past atmospheric dust and its provenance in southern South America.

Additionally, this research work complements the ice core studies of atmospheric dust deposition in the Antarctic Peninsula and its source characterization. Further, the work presented here opens up new possibilities of using peat bogs as archives of atmospheric dust to precisely characterize the source areas, the mineralogical, chemical and isotopic composition of mineral dusts.

However, for the trace elements (e.g. Pb, Zn, Cr, Cu, etc.) further studies are required to understand their input into the atmosphere of South America. Because the peat core was collected for a botanical study and not for geochemical studies, detailed and more precise studies of trace elements were not possible. For this, peat cores especially aimed at geochemical studies are required for the reconstruction of past atmospheric deposition of trace elements. Specifically, larger cores are needed to provide sufficient sample material for high resolution reconstructions of recent changes (i.e. the past century) in atmospheric depositions

References

- Aaby B. (1986) Palaeoecological studies of mires. In *Handbook of Holocene Palaeoecology and Palaeohydrology* (ed. B. E. Berglund), 145-164. John Wiley and Sons Ltd.
- Amato J. A. (2000) Dust: A history of the small and the invisible. University of California Press, Berkeley and Los Angeles, California, USA.
- Andrejko M. J., Raymond Jr., R., and Cohen A. D. (1983) Biogenic silica in peats: possible source for chertification in lignites. *Mineral Matter in peat: Its occurrence, form and distribution*, 25-37.
- Baird C. (1995) *Environmental Chemistry*, 2nd Edition, W.H. Freeman, pp. 528.
- Barreiro B. A. (1984) Lead isotopes and Andean magmagenesis. In *Andean Magmatism: Chemical and isotopic constraints* (ed. R. S. Harmon and B.

- A. Barreiro), 21-30. Shiva Publishing Limited
- Basile I., Grousset F. E., Revel M., Petit J. R., Biscaye P. E., and Barkov N. I. (1997) Patagonian origin of glacial dust deposited in east Antarctica (Vostok and Dome C) during glacial stages 2, 4, and 6. *Earth and Planetary Science Letters* **146**, 573-589.
- Basile I., Petit J. R., Tournon S., Grousset F. E., and Barkov N. I. (2001) Volcanic layers in Antarctic (Vostok) ice cores: source identification and atmospheric implications. *Journal of Geophysical Research* **106**, 31915-31931.
- Bennett P. C., Siegel D. I., Hill B. M., and Glaser P. M. (1991) Fate of Silicate minerals in a peat bog. *Geology* **19**, 328-331.
- Betzer P. R., Carder K. L., Duce R. A., Merrill J. T., Tindale N. W., Uematsu M., Costello D. K., Young R. W., Feely R. A., Breland J. A., Bernstein R. E., and Greco A. M. (1988) Long-range transport of giant mineral aerosol particles. *Nature* **336**, 568-571.
- Biscaye P. E. (1965) Mineralogy and sedimentation of recent deep-sea clay in the Atlantic Ocean and adjacent seas and oceans. *Geological Society of America Bulletin* **76**, 803-832.
- Biscaye P. E., Chesselet R., and Prospero J. M. (1974) Rb-Sr, $^{87}\text{SR}/^{86}\text{SR}$ isotope system as an index of provenance of continental dusts in the open Atlantic ocean. *Journal de Recherches Atmospheriques* **viii**(3-4), 819-829.
- Biscaye P. E., Grousset F. E., Revel M., Gaast S. V., Zielinski G. A., Vaars A., and Kukla G. (1997) Asian provenance of glacial dust (stage 2) in the Greenland Ice Sheet Project 2 Ice core, summit, Greenland. *Journal of Geophysical Research* **102**, 26765-26781.
- Björck S. and Clemmensen L. B. (2004) Aeolian sediment in raised bog deposits, Halland, SW Sweden: a new proxy record of Holocene winter storminess variation in southern Scandinavia? *The Holocene* **14**, 677-688.
- Blank M., Leinen M., and Prospero J. M. (1989) Major Asian aeolian inputs indicated by the mineralogy of aerosols and sediments in the western North Pacific. *Nature* **314**, 84-86.
- Boutron C. F. and Patterson C. C. (1986) Pb concentration changes in Antarctic ice during the Wisconsin/Holocene transition. *Nature* **323**, 222-225.
- Boyle E. A. (1983) Chemical accumulation variations under the Peru Current during the past. *Journal of Geophysical Research* **88**, 7667-7680.
- Brimblecombe P. (1996) *Air composition and chemistry*, 2nd Edition, Cambridge University Press, pp. 267.
- Brownlow A. E., Hunter W., and Parkin D. W. (1965) Cosmic dust collections at various latitudes. *Geophysics Journal* **9**, 337-368.
- Casey W. H., Westrich H. R., Banfield J. F., Ferruzzi G., and Arnold G. W. (1993) Leaching and reconstruction at the surfaces of dissolving chain-silicate minerals. *Nature* **366**, 253-256.
- Chadwick O. A., Derry L. A., Vitousek P. M., Huebert B. J., and Hedin L. O. (1999) Changing sources of nutrients during four million years of ecosystem development. *Nature* **397**, 491-497.
- Chapman S. B. (1964) The ecology of Coom Rigg Moss, Northumberland. II. The Chemistry of peat profiles and the development of the bog system. *Journal of Ecology* **52**, 315-321.
- Charman D. (2002) *Peatlands and Environmental Change*. John Wiley and Sons Ltd.
- Chester R., Elderfield H., Griffin J. J., Johnson L. R., and Padgham R. C. (1972) Eolian dust along the eastern margins of the Atlantic Ocean. *Marine Geology* **13**, 91-105.
- Chow T. J. and Johnstone M. S. (1965) lead isotopes in gasoline and aerosols of Los Angeles Basin, California. *Science* **147**, 502-503.
- Clymo R. S. (1983) Peat. In *Mires: Swamp, bog, fen and moor (Ecosystems of the world 4A)* (ed. A. J. P. Gore), 159-224. Elsevier Scientific Publishing Company.

- Damman A. W. H., Tolonen K., and Sallantaus T. (1992) Element retention and removal in ombrotrophic peat of Häädetkeidas, a boreal Finish peat bog. *Suo* **43**, 137-145.
- Darwin C. (1845) *Journal of Researches into the Natural History and Geology of the countries visited during the voyage round the world of H.M.S. Beagle round the world, under the Command of Capt. Fitz Roy, R.N.*, 2nd Edition, London: John Murray, pp. 520.
- Darwin C. (1846) An account of the fine dust which often falls on the vessels in the Atlantic Ocean. *Proceedings of the Geological Society* **2**, 26-30.
- Dasch E. J. (1969) Strontium isotopes in weathering profiles, deep-sea sediments, and sedimentary rocks. *Geochimica et Cosmochimica Acta* **33**, 1521-1552.
- Dasch E. J., Hills F. A., and Turekian K. K. (1966) Strontium isotopes in deep-sea sediment. *Science* **153**, 295-297.
- Delany A. C., Delany A. C., Parkin D. W., Griffin J. J., Goldberg E. D., and Reimann B. E. F. (1967) Airborne dust collected at Barbados. *Geochimica et Cosmochimica Acta* **31**, 885-909.
- Delmonte B., Basile-Doelsch I., Petit J.-R., Maggi V., Revel-Rolland M., Michard A., Jagoutz E., and Grousset F. (2004) Comparing the EPICA and Vostok dust records the last 220,000 years: stratigraphical correlation provenance in glacial periods. *Earth-Science Reviews* **66**, 63-87.
- Delmonte B., Petit J.-R., and Maggi V. (2002) Glacial to Holocene implications of the new 27000-year dust record from the EPICA Dome (East Antarctica). *Climate Dynamics* **18**, 647-660.
- Dobson M. (1781) An account of the Harmattan, a singular African Wind. *Philosophical Transactions of the Royal Society of London* **LXXI**, 46-57.
- Duce R. A. (1995) Sources, distributions, and fluxes of mineral aerosols and their relationship to climate. In *Aerosol Forcing of Climate: report of the Dahlem Workshop on Aerosol forcing of climate Berlin 1994, April 24-29* (ed. R. J. Charlson and J. Heintzenberg), 43-72. John Wiley and Sons.
- Duce R. A. and Tindale N. W. (1991) Atmospheric transport of iron and its deposition in the Ocean. *Limnological Oceanography* **36**, 1715-1726.
- Eltayeb M. A. H., Grieken R. E. V., Maenhaut W., and Annegran H. J. (1993) Aerosol-soil fractionation for Namib desert samples. *Atmospheric Environment* **27A**, 669-678.
- Eltayeb M. A. H., Injuk J., W. Maenhaut, and Grieken R. E. V. (2001) Elemental composition of mineral aerosol generated from Sudan Sahara sand. *Journal of Atmospheric Chemistry* **40**, 247-273.
- Faure G. (1986) *Principles of Isotope Geology*. John Wiley and Sons.
- Finney H. R. and Farnham R. S. (1968) Mineralogy of the inorganic fraction of peat from two raised bogs in northern Minnesota. *Proceedings of the 3rd International Peat Congress*, Canada, 102-108.
- Frenzel B. (1983) Mires - Repositories of climatic information of self-perpetuating ecosystems? In *Mires: Swamp, bog, fen and moor (Ecosystems of the world 4A)* (ed. A. J. P. Gore), 35-66. Elsevier Scientific Publishing Company.
- Fuchs N. A. (1964) *The mechanics of aerosols*. (Translation from Russian by R. E. Daisley and M. Fuchs) (ed. C. N. Davies), Revised and enlarged edition (1989), Dover Publication, Inc., New York.
- Gabrielli P., Planchon F. A. M., Hong S., Lee K. H., Hur S. D., Barbante C., Ferrari C. P., Petit J. R., Lipenkov V. Y., Cescon P., and Boutron C. F. (2005) Trace elements in Vostok Antarctic ice during the last four climatic cycles. *Earth and Planetary Science Letters* **234**, 249-259.
- Gaudichet A., Angelis M. D., Joussaume S., Petit J. R., Korotkevitch, Y. S., and Petrov V. N. (1992) Comments on the

- origin of dust in east Antarctica for present and ice age conditions. *Journal of Atmospheric Chemistry* **14**, 129-142
- Ginoux P., Chin M., Tegen I., Prospero J. M., Holben B., Dubovik O., and Lin S.-J. (2001) Sources and distributions of dust aerosols simulated with the GOCART model. *Journal of Geophysical Research* **106**, 20255-20273.
- Givelet N., Roux G. L., Cheburkin A., Chen B., Frank J., Goodsite M. E., Kempter H., Krachler M., Noernberg T., Rausch N., Rheinberger S., Roos-Barraclough F., Sapkota A., Schölz C., and Shotyk W. (2004) Suggested protocol for collecting, handling and preparing peat cores and peat samples for physical, chemical, mineralogical and isotopic analyses. *Journal of Environmental Monitoring* **6**, 481-492.
- Gomes L., Bergametti G., Coude-Gaussen G., and Rognon P. (1990) Submicron desert dusts: A sandblasting process. *Journal of Geophysical Research* **95**, 13927-13935.
- Gore A. J. P. (1983) Introduction. In *Mires: Swamp, bog, fen and moor (Ecosystems of the world 4A)* (ed. A. J. P. Gore), 1-34. Elsevier Scientific Publishing Company.
- Gorham E. and Tilton D. L. (1978) The mineral content of *Sphagnum fuscum* as affected by human settlement. *Canadian Journal of Botany* **56**, 2755-2759.
- Grousset F. E. and Biscaye P. E. (2005) Tracing dust sources and transport patterns using Sr, Nd and Pb isotopes. *Chemical Geology* **222**, 149-167.
- Grousset F. E., Biscaye P. E., Revel M., Petit J.-R., Pye K., Joussaume S., and Jouzel J. (1992) Antarctic (Dome C) ice-core dust at 18 k.ya. B.P.: Isotopic constraints on origins. *Earth and Planetary Science Letters* **111**, 175-182.
- Holmes H. (2001) The secret life of dust: from cosmos to the kitchen counter, the big consequences of little things. John Wiley and Sons, Inc. New York, USA.
- Herrmann L., Stahr K., and Jahn R. (1999) The importance of source region identification and their properties for soil-derived dust: the case of Harmattan dust sources for eastern West Africa. *Contributions to Atmospheric Physics* **72**, 141-150.
- Hinkely T. K. and Matsumoto A. (2000) Atmospheric regime of dust and salt through 75,000 years of Taylor dome ice core: refinement by measurement of major, minor and trace metal suites. *Journal of Geophysical Research* **106**, 18487-18493.
- Hölzer A. and Hölzer A. (1998) Silicon and titanium in peat profiles as indicators of human impact. *The Holocene* **8**, 685-696.
- Hovan S. A., Rea D. K., Piasias N. G., and Shackleton N. J. (1989) A direct link between the china loess and marine? ¹⁸O records: aeolian flux to the north Pacific. *Nature* **340**, 296-298.
- Ingram H. A. P. (1983) Hydrology. In *Mires: Swamp, bog, fen and moor*, Vol. 4A (ed. A. J. P. Gore), 67-158. Elsevier Scientific Publishing Company.
- Iriondo M. (2000) Patagonian dust in Antarctica. *Quaternary International* **68**, 83-86.
- Junge C. (1979) The importance of mineral dust as an atmospheric constituent. In *Saharan dust* (ed. C. Morales), 49-60. John Wiley and Sons, Chichester.
- Kaufman Y. J., Koren I., Remer L. A., Tanre D., Ginoux P., and Fan S. (2005) Dust transport and deposition observed from the Terra-Moderate Resolution Imaging Spectroradiometer (MODIS) spacecraft over the Atlantic Ocean. *Journal of Geophysical Research* **110** (doi:10.1029/2003JD004436).
- Kohfeld K. E. and Harrison S. P. (2001) DIRTMAP: the geological record of dust. *Earth-Science Reviews* **54**, 81-114.
- Krachler M., Mohl C., Emos H., and Shotyk W. (2003) Atmospheric deposition of V, Cr, and Ni since the Late Glacial: Effects of climatic cycles, human

- impacts and comparison with crustal abundances. *Environmental Science and Technology* **37**, 2658-2667.
- Kraemer P. E. (2003) Orogenic shortening and the origin of the Patagonian orocline (56 °S. Lat). *Journal of South American Earth Sciences* **15**, 731-748.
- Kramm E. (1978) Pollenanalytische Hochmooruntersuchungen zur Floren- und Siedlungsgeschichte zwischen Ems und Hase. *Abhandlungen aus Landesmuseum für Naturkunde zu Münster in Westfalen* **40**, 1-49.
- LeRoux G., Laverret E., and Shotyk W. (2006) Fate of calcite, apatite and feldspars in peat bogs. *Journal of the Geological Society of London* **163**, 641-646.
- LeRoux G., Weiss D., Grattan J., Givelet N., Krachler M., Cheburkin A., Rausch N., Kober B., and Shotyk W. (2004) Identifying the sources and timing of ancient and medieval atmospheric lead pollution in England using a peat profile from Lindow bog, Manchester. *Journal of Environmental Monitoring* **6**, 502-510.
- Mahowald N., Kohfeld K. E., Hansson M., Balkanski Y., Harrison S. P., Prentice I. C., Schulz M., and Rodhe H. (1999) Dust sources and deposition during the last glacial maximum and current climate: a comparison of model results with paleodata from ice cores and marine sediments. *Journal of Geophysical Research* **104**, 15895-15916.
- Mahowald N. M. and Luo C. (2003) A less dusty future? *Geophysical Research Letters* **30**, doi:10.1029/2003GL017880.
- Malmer N. (1988) Patterns in the growth and the accumulation of inorganic constituents in the Sphagnum cover on ombrotrophic bogs in Scandinavia. *Oikos* **53**, 105-120.
- Manahan S. E. (1991) *Environmental chemistry*, 5th Edition, CRC Press Inc., pp. 600.
- Marino F., Maggi V., Delmonte B., Ghermandi G., and Petit J. R. (2004) Elemental composition (Si, Fe, Ti) of atmospheric dust over the last 220 kyr from the EPICA ice core (Dome C, Antarctica). *Annals of Glaciology* **39**, 110-118.
- Meskhidze N., Chameides W. C., Nenes A., and Chen G. (2003) Iron mobilization in mineral dust: Can anthropogenic SO₂ emissions affect ocean productivity? *Geophysical Research Letters* **30**, doi:10.1029/2003GL018035.
- Miller R. L. and Tegen I. (1998) Climate response to soil dust aerosols. *Journal of Climate* **11**, 3247-3267.
- Milnes A. R. and Fitzpatrick R. W. (1989) Titanium and Zirconium Minerals. In *Minerals in Soil Environments* (ed. J. B. Dixon and S. B. Weed), 1131-1205. Soil Science Society of America.
- Moore D. M. and Robert C. Reynolds J. (1997) *X-ray diffraction and the identification and analysis of clay minerals*. Oxford University Press, Inc., New York.
- Muhs R. D., Bush A. C., Stewart C. K., Rowland T. R., and Crittenden R. C. (1990) Geochemical evidence of Saharan dust parent material for soils developed on quaternary limestones of Caribbean and western Atlantic islands. *Quaternary Research* **33**, 157-177.
- Nakai S., Halliday A. N. and Rea D. K. (1993) Provenance of dust in the Pacific Ocean. *Earth and Planetary Science Letters* **119**, 143-157.
- Nesbitt H. W. and Markovics G. (1997) Weathering of granodioritic crust, long-term storage of elements in weathering profiles, and petrogenesis of siliciclastic sediments. *Geochimica et Cosmochimica Acta* **61**, 1653 -1670.
- Nickling W. G. (1983) Grain-size Characteristics of sediment transported during dust storms. *Journal of Sedimentary Petrology* **53**, 1011-1024.
- Ochs M. (1996) Influence of humified and non-humified natural organic compounds on mineral dissolution. *Chemical Geology* **132**, 119-124.

- Ochs M., Brunner I., Stumm W., and Cosovic B. (1993) Effects of root exudates and humic substances on weathering kinetics. *Water, Air, Soil Pollution* **68**, 213-229.
- Olivero E. B. and Martinioni D. R. (2001) A review of the geology of the Argentinean Fuegian Andes. *Journal of South American Earth Sciences* **14**, 175-188.
- Oppenheimer C. (2003) Climatic, environmental and human consequences of the largest known historic eruption: Tambora volcano (Indonesia). *Progress in Physical Geography* **27**, 230-159.
- Pendall E., Markgraf V., White J. W. C., and Dreier M. (2001) Multiproxy record of Late Pleistocene-Holocene climate and vegetation changes from a peat bog in Patagonia. *Quaternary Research* **55**, 168-178.
- Planchon F. A. M., Velde K. V. D., Rosman K. J. R., Wolff E. W., Ferrari C. P., and Boutron C. F. (2003) One hundred fifty-year record of lead isotopes in Antarctic snow from Coats Land. *Geochimica et Cosmochimica Acta* **67**, 693-708.
- Prospero J. M. (2001) African dust in America. *Geotimes*, 24-27.
- Prospero J. M. and Carson T. N. (1972) Vertical and aerial distribution of Saharan dust over the Western Equatorial North Atlantic Ocean. *Journal of Geophysical Research* **77**, 2555-2565.
- Rabassa J., Coronato A., and Roig C. (1996) The Peat bogs of Tierra del Fuego, Argentina. In *Global Peat Resources* (ed. E. Lappalainen). International Peat Society, Finland.
- Rahn K. A. (1976) The chemical composition of the atmospheric aerosol (Technical Report), Graduate School of Oceanography, University of Rhode Island.
- Rea D. K., Leinen M., and Janecek T. R. (1985) Geologic approach to the long-term history of atmospheric circulation. *Science* **227**, 721-725.
- Raymond Jr, R., Andrejko M. J., and Bardin S. W. (1983) Techniques for applying scanning electron microscopy to the study of mineral matter in peat. In *Minerals in Peat: Its occurrence, form and distribution*, (ed. R. Jr, Raymond and M. J. Andrejko), 169-177. US DOE, Los Alamos, USA.
- Roos-Barraclough F., Givélet N., Cheburkin A. K., Shotyk W., and Norton S. A. (2006) A ten thousand year record of atmospheric mercury accumulation in peat from Caribou Bog, Maine, and its correlation to bromine and selenium. *Environmental Science and Technology* **40**, 3188-3194.
- Röthlisberger R., Mulvaney R., Wolf E. W., Hutterli M. A., Bigler M., Sommer S., and Jouzel J. (2002) Dust and sea salt variability in central East Antarctica (Dome C) over the last 45 kyrs and its implications for southern high-latitude climate. *Geophysical Research Letters* **29**, doi:10.1029/2002GL015186.
- Schneider S. (1963) Chemical and stratigraphical investigations of high-moor profiles in North-west Germany. *Proceedings of the 2nd International Peat Congress*, U.S.S.R, 75-90.
- Schütz L. (1979) Saharan dust transport over the North Atlantic Ocean-Model calculations and measurements. In *Saharan dust* (ed. C. Morales), 233-242. John Wiley and Sons.
- Schütz L. (1989) Atmospheric mineral dust-properties and source makers. In *Paleoclimatology and Paleometeorology: Modern and past patterns of global atmospheric transport* (ed. M. Leinen and M. Sarnthein) 359-383. Kluwer Academic Publishers.
- Schütz L. and Rahn K. A. (1982) Trace-element concentrations in erodible soils. *Atmospheric Environment* **16**, 171-176.
- Shinn E. A., Smith G. W., Prospero J. M., Betzer P., Hayes M. L., Garrison V., and Barber R. T. (2000) Africa dust and the demise of Caribbean Coral reefs. *Geophysical Research Letters* **27**, 3029-3032.

- Shotyk W. (1988) Review of the inorganic geochemistry of peats and peatland waters. *Earth-Science Reviews* **25**, 95-176.
- Shotyk W. (1992) Organic Soils. In *Weathering, soils and paleosols* (ed. I. P. Martini and W. Chesworth), 203-224. Elsevier Science Publishers.
- Shotyk W. (1996) Peat bog archives of atmospheric metal deposition: geochemical evaluation of peat profiles, natural variations in metal concentrations, and metal enrichment. *Environmental Reviews* **4**, 149-183.
- Shotyk W., Goodsite M. E., Barraclough F. R., Gievelet N., Roux G. L., Weis D., Cheburkin A. K., Knusden K., Heinemeier J., Knaap W. O. V. d., Norton S. A., and Lohse C. (2005) Accumulation rates and predominant atmospheric sources of natural and anthropogenic Hg and Pb on the Faroe Islands since 5400 ¹⁴C yr BP recorded by a peat core from a blanket bog. *Geochimica et Cosmochimica Acta* **69**, 1-17.
- Shotyk W., Krachler M., Martinez-Cortizas A., Cheburkin A. K., and Emons H. (2002) A peat bog record of natural, pre-anthropogenic enrichments of trace elements in atmospheric aerosols since 12370 ¹⁴C yr BP, and their variation with Holocene climate change. *Earth and Planetary Science Letters* **6180**, 1-17.
- Shotyk W., Weiss D., Appleby P. G., Cheburkin A. K., Frei R., Gloor M., Kramers J. D., Reese S., and Knaap W. O. V. (1998) History of atmospheric lead deposition since 12,370 ¹⁴C yr BP from a peat bog, Jura Mountains, Switzerland. *Science* **281**, 1635-1640.
- Shotyk W., Weiss D., Kramers J. D., Frei R., Cheburkin A. K., Gloor M., and Reese S. (2001) Geochemistry of the peat bog at Etang de La Gruère, Jura Mountains, Switzerland, and its record of atmospheric Pb and lithogenic trace metals (Sc, Ti, Y, Zr, and REE) since 12370 ¹⁴C yr BP. *Geochimica et Cosmochimica Acta* **65**, 2337-2360.
- Snape I., Scouller R. C., Stark S. C., Stark J., Riddle M. J., and Gore D. B. (2004) Characterisation of the dilute HCl extraction method for the identification of metal contamination in Antarctic sediments. *Chemosphere* **57**, 491-504.
- Steinmann P. and Shotyk W. (1997) Geochemistry, mineralogy, and geochemical mass balance on major elements on two peat bog profiles (Jura Mountains, Switzerland). *Chemical Geology* **138**, 25-53.
- Sutherland R. A., Tack F. M. G., Ziegler A. D., and Bussen J. O. (2004) Metal extraction from road-deposited sediments using nine partial decomposition procedures. *Applied Geochemistry* **19**, 947-955.
- Svensson A., Biscaye P. E., and Grousset F. E. (2000) Characterization of late glacial continental dust in the Greenland Ice Core Project ice core. *Journal of Geophysical Research* **105**, 4637-4656.
- Tallis J. H. (1983) Changes in wetland communities. In *Mires: Swamp, bog, fen and moor (Ecosystems of the world 4A)* (ed. A. J. P. Gore), 311-347. Elsevier Scientific Publishing Company.
- Tegen I. and Fung I. (1994) Modelling of mineral dust in the atmosphere: Sources, transport, and optical thickness. *Journal of Geophysical Research* **99**, 22897-22914.
- Tegen I. and Fung I. (1995) Contribution to the atmospheric mineral aerosol load from land surface modification. *Journal of Geophysical Research* **100**, 18707-18726.
- Tegen I., Werner M., Harrison S. P., and Kohfeld K. E. (2004) Relative importance of climate and land use in determining present and future global soil dust emission. *Geophysical Research Letters* **31**, L05105, doi:10.1029/2003GL019216.
- Thomas D. S. G. (1989) The nature of arid environments. In *Arid Zone Geomorphology* (ed. D. S. G. Thomas), 1-8. Belhaven Press.

- Thompson D. W. J. and Solomon S. (2002) Interpretation of recent southern Hemisphere climate change. *Science* **296**, 895-899.
- Tolonen K. (1984) Interpretation of changes in the ash content of ombrotrophic peat layers. *Bulletin of Geological Society of Finland*. **56**, 207-219.
- Tuhkanen S. (1992) The climate of Tierra del Fuego from a vegetation geographical point of view and its ecoclimatic counterparts elsewhere. *Acta Botanica Fennica* **145**, 1-64.
- Uematsu M., Duce R. A., Prospero J. M., Chen L., Merrill J. T., and McDonald R. L. (1983) Transport of Mineral aerosol from Asia over the North Pacific Ocean. *Journal of Geophysical Research* **88**, 5343-5352.
- Usher C. R., Michel A. E., and Grassian V. (2003) Reactions on Mineral Dust. *Chemical Reviews* **103**, 4883-4939.
- Vallelonga P., Gabrielli P., Rosman K. J. R., Barbante C., and Boutron C. F. (2005) A 220 kyr record of Pb isotopes at Dome C Antarctica from analyses of the EPICA ice core. *Geophysical Research Letters* **32**, doi:10.1029/2004GL021449.
- Vitousek P. (2006) Ecosystem science and human-environment interactions in the Hawaiian archipelago. *Journal of Ecology* **94**, 510-521.
- Vuorela I. (1983) Field erosion by wind as indicated by fluctuations in the ash content of sphagnum peat. *Bulletin of Geological Society of Finland* **55**, 25-33.
- Wedepohl K. H. (1995) The composition of the continental crust. *Geochimica et Cosmochimica Acta* **59**, 1217-1232.
- Werner M., Tegen I., Harrison S. P., Kohfeld K. E., Prentice I. C., Balkanski Y., Rodhe H., and Roelandt C. (2002) Seasonal and interannual variability of the mineral dust cycle under present and glacial climate conditions, *Journal of Geophysical Research* **107**, doi:10.1029/2002JD002365.
- Wurzler S., Reisin T. G., and Levin Z. (2000) Modification of mineral dust particles by cloud processing and subsequent effects on drop size distributions. *Journal of Geophysical Research* **105**, 4501-4512.
- Wüst R. A. J., Ward C. R., Bustin R. M., and Hawke M. I. (2002) Characterization and quantification of inorganic constituents of tropical peats and organic-rich deposits from Tasek Bera (Peninsular Malaysia): implication for coals. *International Journal of Coal Geology* **49**, 215 – 249.
- Yin Y., Wurzler S., Levin Z., and Reisin T. G. (2002) Interactions of mineral dust particles and clouds: Effects on precipitation and cloud optical properties. *Journal of Geophysical Research* **107**, doi:10.1029/2001JD001544.
- Zhang D. (1984) Synoptic-climatic studies of dust fall in China since historic times. *Scientia Sinica (Series B)* **XXVII**(8), 825-836.

Chapter 2

Atmospheric Dust Deposition Rates

-Chapter 2-
**Six millennia of atmospheric dust deposition in southern South
America (Isla Navarino, Chile)**

Atindra Sapkota¹, Andriy K. Cheburkin¹, Georges Bonani² and William Shotyk*¹

¹Institute of Environmental Geochemistry, University of Heidelberg, Im Neuenheimer Feld 236, D-69120, Heidelberg, Germany

²Institute for Particle Physics, ETH Zurich, Switzerland

*Corresponding author, Tel: + 49 (6221) 54 4803; Fax: + 49 62 21 54 52 28,

Email: shotyk@ugc.uni-heidelberg.de

Submitted to The Holocene, 2006

Abstract

To characterize dust deposition in southern South America, a 542 cm long core from a peat bog in southern Chile (Oreste bog, Isla Navarino) was studied. Peat formation started ~ 11160 ¹⁴C yr before present (BP). The titanium (Ti) concentration in bulk peat, combined with dry bulk density, and peat accumulation rate, were used to calculate the mineral accumulation rate (MAR) in the Oreste bog. The distribution of calcium (Ca), manganese (Mn) and titanium (Ti) showed that mineral accumulation for the last ca. 6000 yrs was predominantly atmospheric with a record of effectively constant deposition (0.43 ± 0.12 g m⁻² yr⁻¹). Similarly, Ti and zirconium (Zr) concentrations in the acid insoluble ash (AIA) were also effectively constant and agreed well with the MAR for the last six millennia, except at ca. 4200 cal yr BP, where Zr was enriched relative to Ti. Here, Scanning Electron Microscope (SEM) micrographs showed that the AIA was dominated by volcanic particles ($> 20 - 40$ μ m), with the Mt. Burney eruption identified as the most likely source. In contrast to this anomalous zone, SEM studies showed that the mineral particles found in the majority of the sample were predominantly fine grained (< 20 μ m) and rounded. Derived from soils and supplied by long-range atmospheric transport, they reflect the climate stability for the past 6000 yrs.

Keywords: *atmospheric mineral dust, ombrotrophic bog, acid insoluble ash, titanium, zirconium*

Introduction

The fluxes, particle size distribution, mineralogy, and chemistry of atmospheric mineral dusts are important because of their impacts on the earth's climate system, the chemistry of the atmosphere, and the global biogeochemical cycles of many elements (Goudie and Midelton, 2001; Harrison and Kohfeld, 2001). Arid and semi-arid areas, which cover more than 30 % of the earth's land surface, are important sources of soil-derived dust to the atmosphere (Thomas, 1989). Geological archives such as ice cores, peat bogs, sediments, and loess deposit are important in the determination of the predominant dust sources and allow detailed palaeoclimatic reconstructions.

Like polar ice caps, ombrotrophic peat bogs are fed solely by atmospheric deposition (dry and wet) and can provide reliable records of the changing rates of atmospheric dust deposition. In addition, many mineralogical and chemical changes are preserved over time (Shotyk et al., 2002; Shotyk et al., 2001; Steinmann and Shotyk, 1997). Complete records derived from peat cores in Switzerland and Indonesia have effectively shown the relationship between chemical composition of ombrotrophic peat, changing climate and long-range transport of the atmospheric mineral aerosols (Shotyk et al., 2002; Weiss et al., 2002). Even in the anaerobic, organic-rich acidic environment of peat bogs (~ pH 4), atmospherically deposited, fine-grained silicate and resistate oxide mineral fraction such as quartz, feldspar, ilmenite and rutile reveal little evidence of chemical attack subsequent to deposition (Finney and Farnham, 1968; Le Roux et al., 2006; Steinmann and Shotyk, 1997). These minerals can be separated either by dry ashing or wet digestion of the organic fraction of peat material. Dry ashing is a common procedure to destroy the organic materials in peat, leaving behind oxides, hydroxides, carbonates, sulphates, refractory mineral grains, and particle of biogenic origin. Hydrochloric acid is commonly used to dissolve the soluble ash fraction such as carbonates and phosphates and to separate the acid insoluble ash (AIA), which is mainly

composed of insoluble silicate and resistate oxide minerals.

In contrast to the studies of atmospheric dust deposition in the Northern Hemisphere using archives such as ice cores (Biscaye et al., 1997; Bory et al., 2002; Zdanowicz et al., 2000) and peat bogs (Björck and Clemmensen, 2004; Shotyk et al., 2002; Shotyk et al., 2001), few comparable, quantitative data is available for Southern Hemisphere. In addition, the palaeoclimatic study of dust deposition in the Southern Hemisphere is mainly based on the ice cores from Antarctica with a focus on the last glacial maximum and earlier times (Grousset et al., 1992), possibly because of very low dust content in the ice cores during the Holocene (Delmonte et al., 2002). Although, the considerable change in atmospheric dust deposition seen in Antarctic ice cores is attributed to long-range transport and continental source strength, there is no consensus about the dominant source areas (Basile et al., 1997; Grousset et al., 1992; Mahowald et al., 1999). Some groups have investigated loess from possible source areas, and others have used computer modeling to identify the source area of the dust. The extent of source areas, strength of atmospheric circulation, and atmospheric removal process determine the dust deposition rate at any particular location (Bory et al., 2002). Hence, a suitable, long-term continental geochemical archive of atmospheric dust found in peat bogs from the Southern Hemisphere would supplement the polar ice core studies. Unlike ice cores, peat bogs have certain advantages as archives including their global distribution, easy access, and relatively easier and far less expensive sample handling and analytical procedures.

We know of no peat bog records of atmospheric dust deposition in southernmost South America. Thus, as a first attempt to characterize dust deposition, we used a peat core from Oreste bog, Isla Navarino, southern Chile. Our main goals were to (a) determine the extent of the ombrotrophic zone of the peat profile, (b) quantify the mineral accumulation rate (MAR), (c) using Ti and Zr in the AIA fraction, determine the predominant sources of silicate and oxide

minerals, and d) using SEM and XRD methods, to identify the dominant minerals present and to determine their size and morphology.

All of these approaches were employed in an effort to reconstruct the changing rates of atmospheric dust deposition in southern South America. We also present the first use of X-ray fluorescence spectrometry to provide quantitative analysis of major and trace elements in the AIA fraction.

Material and methods

Sample collection and preparation

The Oreste bog is part of an extensive lowland bog area, located near the Fondeadero Orestes anchoring spot on the west side of Bahia Windhound, Southern Isla Navarino, Chile ($55^{\circ}13'13''\text{S}$ and $67^{\circ}37'28''\text{W}$ 35m) (Figure 1). It is a Magellanic Moorland bog located behind a *Nothofagus*

betuloides forest belt lining the bay. The climate of the area has an average precipitation of 800 mm yr⁻¹ (Rabassa et al., 1996), under the influence of the Westerlies circulation (Tuhkanen, 1992) whose storm tracks shift seasonally, poleward in summer and equatorward in winter (Pendall et al., 2001). Ombrotrophic bogs in this maritime climate region, including Oreste bog show rapid growth and are of late Holocene origin overlying minerotrophic peatlands (Rabassa et al., 1996). The dominant moorland taxa are the mosses *Sphagnum magellanicum* and *Drepanocladus sp.*, the cushion plants *Astelia pumila* and *Donatia fascicularis*, accompanied by *Carex sp.*, *Empetrum nigrum* (*Ericaceae*) and *Marrisspospermum grandiflorum*. A Livingston piston sampler of 7.5 cm diameter was used to core the Oreste bog to a depth of 542 cm, with cores recovered in lengths of 100 cm. The cores were sectioned in the field into increments of

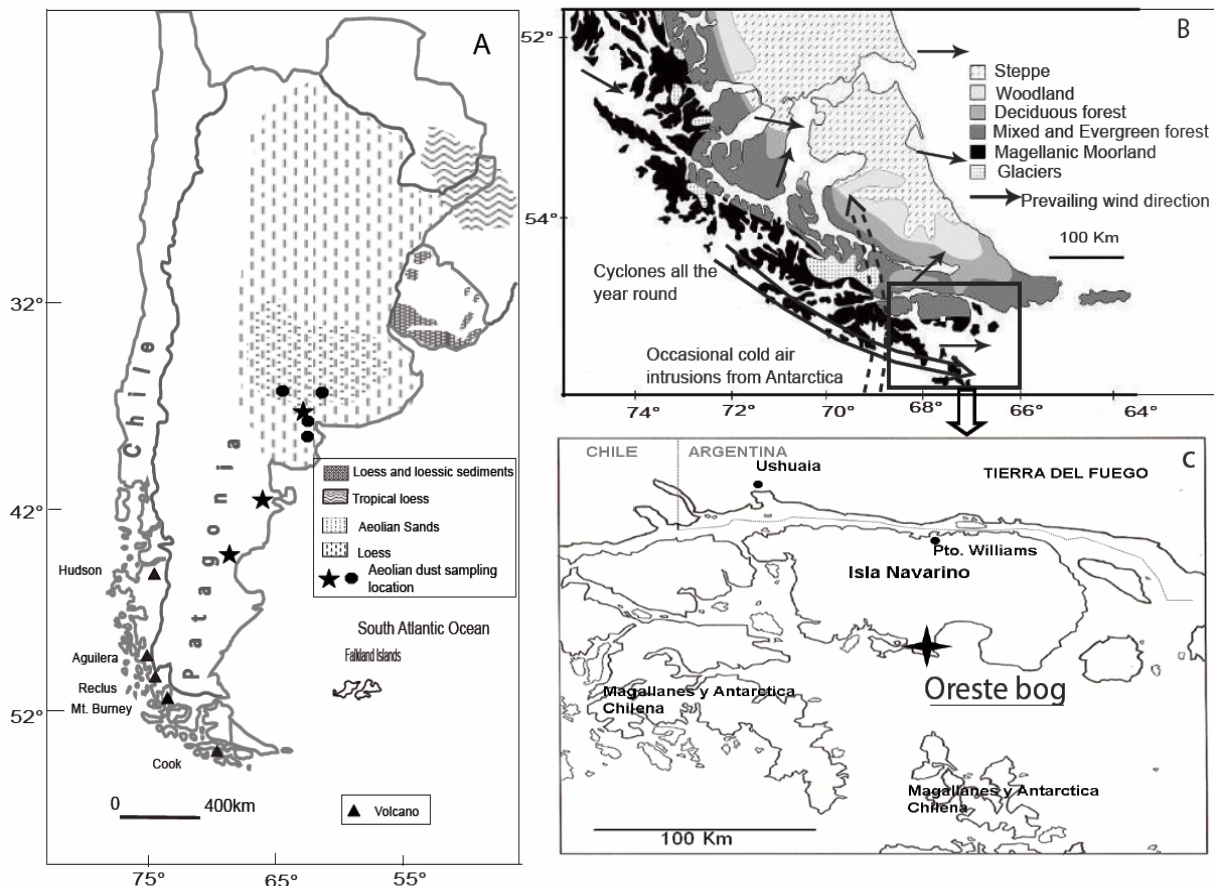


Figure 1: Map of South America showing distribution of loess (Zarate, 2003) and location of volcanoes with Late Pleistocene / Holocene eruption (Kilian et al., 2003)(A). Also shown in the map is the aeolian dust sampling sites in order to measure the dust flux (Ramsperger et al., 1998; Gaiero et al., 2003) (A). Southern South America with major vegetation zone (Huber and Markgraf, 2003), wind direction (Tuhkanen, 1992), and peat sampling site (B). More detailed map of the Oreste bog (C).

25 cm using a knife, wrapped in clean plastic foil and kept refrigerated after shipping to the University of Colorado. The peat between 0 and 505 cm was well preserved whereas between 505 and 530 cm it was highly decomposed. Between 530 and 542 cm the peat was minerogenic, containing silt and clay.

The site is exposed to the ocean to the south and west, while to the north, the central part of Isla Navarino is mountainous. This central belt is part of a Late Jurassic-Early Cretaceous marginal basin (the Rocas Verdes Marginal Basin) with the following rock types: Upper Jurassic silicic volcanic rocks, Lower Cretaceous deep-marine volcanoclastic turbidites and slope mudstones, and Upper Cretaceous plutonic rocks (Olivero and Martinioni, 2001). Mesozoic quartzites, slates, phyllites, and low-grade schists dominate the geology of the area.

Sample preparation

Dry weight, density and macrofossil collection

After freezing, each core section was cut precisely into 2 cm increments using a stainless steel band saw. Peat sub-samples obtained were irregular in shape, making it difficult to calculate volume and density. A photograph of each of the peat sub-sample was used to calculate the volume of the irregular slices using open source software “ImageJ”. An object of known volume was used to evaluate the accuracy of the volume measurement and the error was less than ~ 1 %. Similarly, about 6 cm⁻³ volumetric plugs were taken from each slice for paleobotanical / macrofossil studies but were frozen until further use. Then, the remaining sub-samples were dried overnight at 105 °C in clean polyethylene vessels. Afterwards, the oven-dried samples were crushed gently by a porcelain mortar in a clean polyethylene vessel.

Ash content and acid insoluble ash

A high temperature muffle furnace (mls 1200 pyro, MLS GmbH, Germany) operated at 550 °C overnight was used to combust approximately 2 g of dried peat, which typically yielded ca. 20 mg ash. After

determination of the ash content, 1M HCl (Suprapure, Merck, Darmstadt, Germany) was allowed to react for 15 minutes to dissolve soluble minerals such as carbonates, phosphates, sulphates and oxides. The insoluble mineral particles were separated from the HCl mixture using a 0.2 µm membrane filter (nuclepore polycarbonate, Ø 25 mm, Whatman International Ltd., Kent, UK) under vacuum (Milipore filtration kit, Milipore, MA, USA). New petri dishes were first leached in 10% HNO₃ (analytical reagent grade) for 2 – 3 days and then rinsed extensively followed by drying in a class 100 laminar flow clean air cabinet. Before use, the filters were kept in the previously cleaned petri dishes and leached in 1 % HNO₃ (ultrapure, prepared in-house). Afterwards, they were rinsed 3 – 4 times with deionized water. High purity water (18.2 MΩ) obtained from a MilliQ-system (Millipore, Milford, MA, USA) was used for the required solution preparation and rinsing. All the procedures of acid leaching, filtration, and sample drying were done in class 100 clean lab facilities.

Chemical analysis

XRF analysis of bulk peat

A non-destructive, energy-dispersive XRF analyzer was used to measure calcium (Ca), manganese (Mn), potassium (K), and titanium (Ti) in dried, milled bulk peat powders. The design of the TITAN instrument (Cheburkin and Shotykh, 2005) consists of a Co target, conventional X-ray tube and monochromator adjusted on the Co K-alpha line (6.93 keV). A high purity Ge X-ray detector having resolution of 115 eV at 5.9 keV is employed. Acquisition time was 600 seconds. Powdered peat samples (0.5 – 1 g) were placed in 1530 Spectro XRF sample cups with a thin piece (4 micrometers) of Prolene film serving as the bottom. Standard reference materials such as NIST 1515 (apple leaves), NIST 1547 (peach leaves), NIST 1575 (pine needles), NIST 1632b (coal), NIST 1635 (coal), and BCR-60 (aquatic mosses) were used to calibrate the instrument. The detection limits for Ca, Mn, K, and Ti were 10 µg g⁻¹, 0.9 µg g⁻¹, 20 µg g⁻¹, and 1.5 µg g⁻¹, respectively.

XRF analysis of AIA

The TITAN XRF analyzer was used to measure Ti in the AIA. Similarly, the EMMA XRF analyzer (Cheburkin and Shotykh, 1996) was used to measure Zr concentrations in the AIA. XRF spectra of a thin film of the AIA obtained using the TITAN and EMMA instrument, showed not only the major elements such as Ca, K, and Ti, but also trace elements such as Pb and Zr could be easily measured in the AIA fraction (Figure 2). In contrast, in bulk peat it was not possible to quantify either Pb or Zr because their concentrations were below the detection limit $0.6 \mu\text{g g}^{-1}$ and $2 \mu\text{g g}^{-1}$, respectively. The combustion of organic fraction from a peat

and the cleaning of silicate fraction by HCl had made the AIA free of matrix effects yielding better sensitivity to X-ray intensities.

The design of EMMA analyzer is similar to the TITAN analyzer and uses monochromatic X-ray excitation. The main difference compared to the TITAN analyzer is the Mo target, conventional X-ray tube with Si(Li) detector and the monochromator adjusted on the Mo K-beta line (19.6 keV). Power supplies were 17kV and 2mA in the case of the TITAN analyzer, and 45 kv and 10 mA for the EMMA analyzer. The acquisition time was 600 seconds for the TITAN and 1200 seconds for the EMMA analyzer.

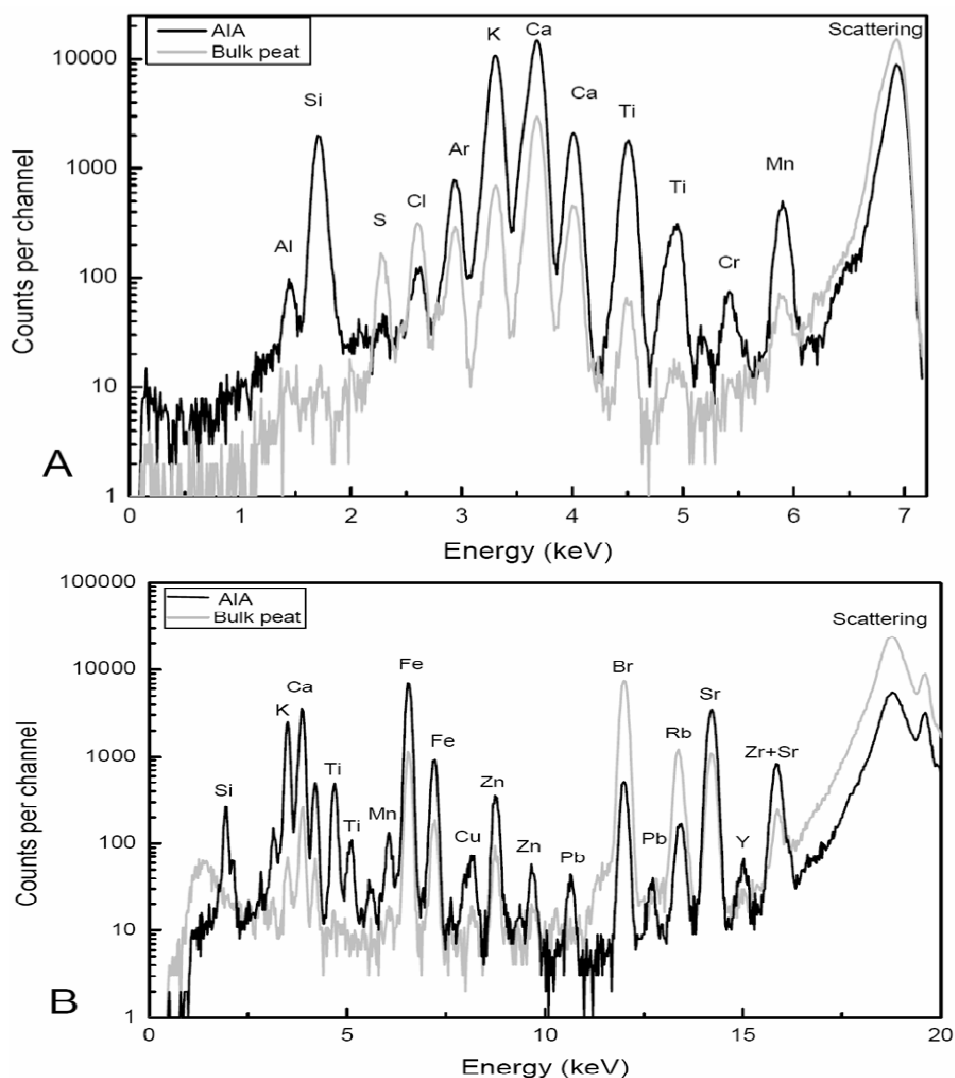


Figure 2: Typical XRF spectra of major and trace elements measured in filtrate residue (AIA) and bulk peat using the TITAN (A) and EMMA (B) spectrometers. Sample was taken from a depth of 25 cm.

The amount of AIA collected on filters varied from 0.7 to 100 mg on the 1.8 cm² deposition area. In other words, the amount of AIA on the filter varied from 0.4 to 55 mg cm⁻². Such high variation of sample mass makes XRF analysis rather complicated. It was not possible to reduce the variation in sample mass using additives such as boric acid, because it was necessary to use the same sample materials later, for mineralogical and isotopic studies.

Standard reference materials such as W-1 (diabase), DTS-1 (dunite), G2 (granite) and MAG1 (marine sediment) from USGS; 1633a (coal fly ash) and 2710 (Montana I soil) from NIST; LKSD-1 (lake sediment) and LKSD-4 (lake sediment) from CCRMP helped to prepare working standards and calibrate the instrument for XRF analysis of AIA. To that end, varying amounts (2 to 100 mg) of each SRM material was mixed with distilled water and deposited on the same polycarbonate membrane filters as for the AIA. The TITAN and EMMA XRF analyzers were then used to measure three SRM samples of density comparable to AIA. The data were used to make two types of calibration-curves: (1) peak area as a function of the mass of the sample (the element concentration being constant) and (2) peak area as a function of the element concentration (the sample mass being nearly constant). The complete description of this calibration procedure will be described in a separate, specialized publication. In brief, it was possible to analyze the AIA samples with an uncertainty of $\pm 12 - 15\%$ (relative) for all elements of the interest. The sensitivity of the analysis was dependent on the amount of material deposited on the filters and was sufficient to analyze all elements of interest. The absolute sensitivities for some trace elements obtained using NIST 2783 SRM (atmospheric dust collected on filter media) using the EMMA XRF (ng cm⁻²) were 67 Fe, 0.45 Ni, 0.5 Cu, 0.9 Zn, 0.2 Rb, 0.3 Sr, and 0.8 Pb.

Mineralogical study of AIA

A Siemens D501 diffractometer was used to determine the mineralogy of AIA directly on the filters. The step-scanning size was from 2.5 to 70° with a step size of 0.02° and a counting time of two seconds per step. Background stripping, indexation of the diffraction peaks, and mineral identification were done using MacDiff 4 Software (Petschick, 2005).

A LEO 440 Scanning Electron Microscope (SEM) coupled with Energy-Dispersive X-Ray Spectrometer (EDS) helped to study the morphology and chemical composition of individual mineral dust particles from selected AIA samples, which had been carbon coated. High tension of 20 kV and probe current from 0.5 to 6 nA was used to operate the SEM. Similarly, an OXFORD EDS system having an energy resolution of 133 eV at 5.9 keV allowed X-ray microanalysis of elements heavier than carbon.

Chronology of peat accumulation

A bulk peat sample at 540 – 542 cm depth was dated using ¹⁴C AMS (Accelerator Mass Spectrometry) at the Arizona AMS Laboratory, University of Arizona, USA. Sixteen samples from other levels in the core were selected for additional ¹⁴C age dating (AMS) at the Institute of Particle Physics, ETH (Zürich, Switzerland) (Table I). The limited amount of sample material (few mg) and the extent of its decomposition in samples below 500 cm limited the number of macrofossils which could be dated. A modified cleaning procedure of the acid-alkali-acid method (Hajdas et al., 2004) was used to prepare samples for age dating. CALIB Rev. 5.0.2 (Stuiver and Reimer, 1993) and INTCAL 04.14C (Reimer et al., 2004) converted the radiocarbon dates to calibrated years BP (cal yr BP).

Table I: Radiocarbon dates of peat from Oreste Bog, Isla Navarino, Chile (with 1σ deviation)

Depth (cm)	AMS ^{14}C yr BP ($\pm 1\sigma$)	Calibrated ages (yr $\pm 1\sigma$)	Cal yr BP (median)	Sample material	Lab no.
24.5	190 \pm 50	(-)2 - 281	177	Stem	ETH- 30888
149.5	2020 \pm 50	1898 - 2039	1976	Bulk (> 100 μm)	ETH- 31600
175	305 \pm 65	301 - 457	379	Leaves (<i>Nothofagus</i>)	ETH-30889
229.5	1225 \pm 50	1047 - 1235	1155	Bulk (> 100 μm)	ETH-31601
255.5	1455 \pm 50	1306 - 1379	1350	Bulk (> 100 μm)	ETH-31602
279.5	3700 \pm 55	3934 - 4145	4040	Stem	ETH- 30890
305.5	3985 \pm 60	4300 - 4529	4459	Stem	ETH- 30891
380.5	3955 \pm 60	4297 - 4517	4409	Bulk (> 100 μm)	ETH- 30892
405.5	5010 \pm 65	5657 - 5886	5755	Bulk (> 100 μm)	ETH- 30893
454.5	5170 \pm 60	5769 - 5994	5929	Stem	ETH- 30894
479.5	5300 \pm 60	5995 - 6180	6085	Leaves (<i>Nothofagus</i>)	ETH- 31603
479.5	5200 \pm 60	5901 - 6170	5967	Stem	ETH-30895
480.5	5105 \pm 60	5752 - 5917	5828	Bulk (> 100 μm)	ETH- 31604
480.5	5170 \pm 75	5754 - 6000	5929	Stem	ETH-30896
505.5	5330 \pm 60	6002 - 6189	6111	Leaves (<i>Nothofagus</i>)	ETH- 31605
505.5	5175 \pm 60	5769 - 5997	5997	Stem	ETH-30897
541.5	11 160 \pm 110	12 951 - 13 149	13 063	Bulk peat	AA-18818

Results

Age dating and chronology of peat accumulation

The AMS ^{14}C dates were calibrated and used to calculate peat accumulation rates (Table I). Peat formation started at ~ 11160 ^{14}C yr before present (BP), which corresponds to ~ 13000 calibrated years BP (cal yr BP). Two age-depth models were reconstructed in cal yr using a third-degree polynomial regression (Figure 3A and 3B). Three dates between ~ 175 and 256 cm were not used for either age depth model, as they appear far too young in comparison with the other dates (Figure 3A and 3B).

The first age-depth model (Figure 3A) suggests a hiatus in peat accumulation

between 11000 and 6000 cal yr BP (~ 0.05 mm yr $^{-1}$). Above 500 cm (~ 6000 cal yr BP) peat growth became rapid (0.83 mm yr $^{-1}$), which is in agreement with many other records from this region (Rabassa et al., 1989, Pendall et al., 2001). Similar rates are also found in other maritime bogs, such as the blanket bogs of NW Scotland and the Island of Foula in Shetland (Shotyk, 1997).

The early Holocene, in the high southern latitudes, despite the forest expansion at ~ 9000 cal yr BP, was drier than the late Holocene with presence of significant proportion of open ground, steppe elements, high fire frequency and precipitation below modern levels (Pendall et al., 2001; Markgraf, 1993, Huber et al., 2004). The Oreste bog

located in the southern lowlands of Isla Navarino, without any significant input from mountain drainage, might have experienced this early Holocene dry period especially strong, resulting in insufficient moisture for peat to grow.

In the second age-depth model, eight dates between 505 and 405 cm were not used, assuming them too young. The reason for this assumption is the presence of a tephra layer at 60 cm, 158 cm, between 293 and 300 cm and ~ 490 cm thought to represent the Mt. Burney eruption dated 95 cal yr BP (Global volcanism Program,

<http://www.volcano.si.edu>), between 2026 ± 48 and 2063 ± 90 cal yr BP, 4245 ± 125 cal yr BP and between 9009 ± 17 and 9175 ± 111 cal yr BP (Kilian et al., 2003) and the Sr isotope signature of AIA (unpublished data).

The portion of the core between ~ 420 and 542 cm, characterized by high bulk density, high ash content and high AIA content, indicating minerotrophic peat, is not discussed further in the context of this paper. For the section of the peat profile above ~ 420 cm which is the focus of this study, the two age depth models yield similar peat accumulation rates.

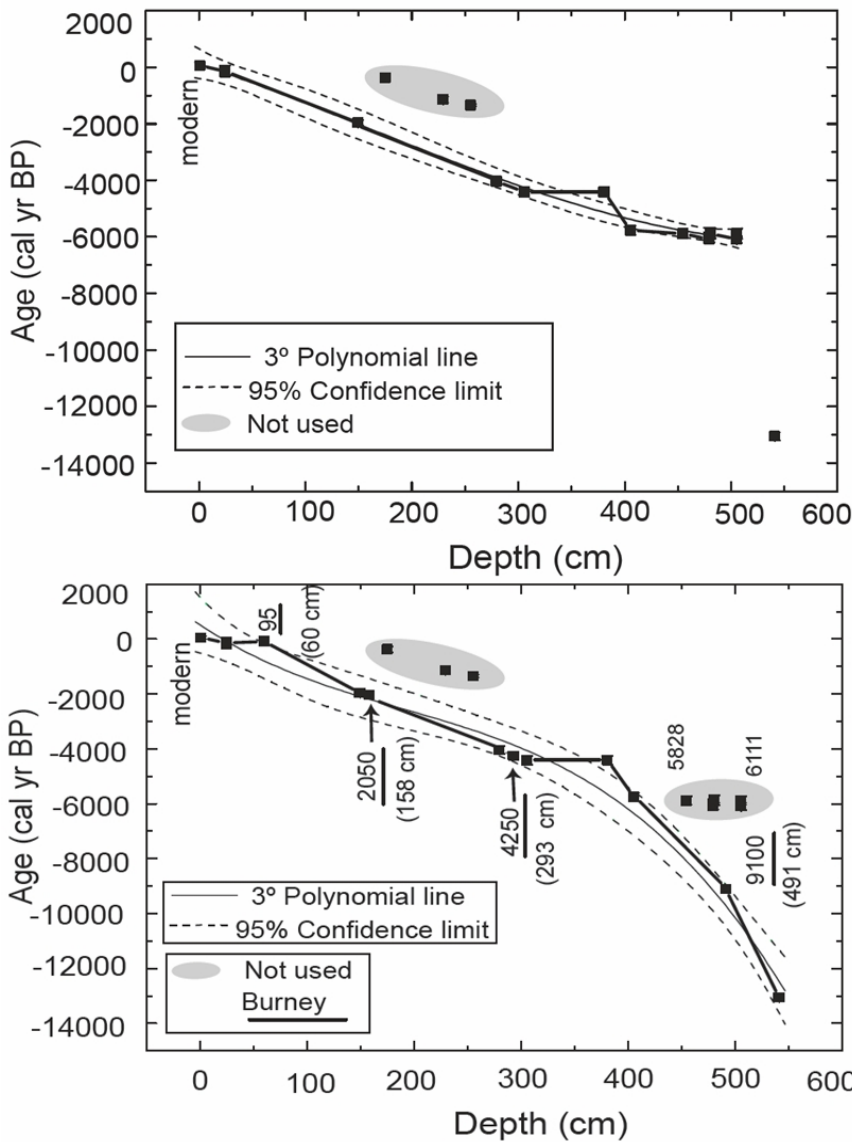


Figure 3: Age-depth model and the 3° polynomial regression curve of calibrated ages as a function of the peat bog depth. The reported four eruptions of the Mt. Burney volcano were (a) between 9009 ± 17 and 9175 ± 111 cal yr BP, (b) 4254 ± 120 cal yr BP, (c) between 2026 ± 48 and 2063 ± 90 cal yr BP (Kilian et al., 2003), and (d) 95 cal yr BP (Global volcanism Program,. The regression equation were $y= 601.90558 - 30.47615x + 0.10549x^2 - 1.74063 E-4x^3$ ($r^2=0.97249$) and $y= 119.62752 - 12.01393x + 0.01393x^2 + 3.02118 E-4x^3$ ($r^2=0.98292$) for model 3A and 3B, respectively. The ^{14}C age dates shown in the shaded eclipse were not used in the age-depth model, for the reasons given in the text.

Bulk density, Ash content, and AIA

The average density, ash content, and AIA content of the Oreste peat profile were 0.06 g cm^{-3} , 2% and 0.7%, respectively, based on dry weight (Figure 4). The bulk density and ash content are elevated at both the upper and lower end of the peat profiles. The most notable peak in ash and AIA (4 % and 2%, respectively) is found at 293 – 300 cm (Figure 4).

Titanium concentration and mineral accumulation

The mineral accumulation rate (MAR) can be calculated using the Ti concentration in the bulk peat (Figure 5), bulk density of the peat, and the average, long term peat accumulation rate (Shotyk et al., 2002).

$$\text{MAR} (\mu\text{g cm}^{-2} \text{ yr}^{-1}) = 250 \times \text{Ti} (\mu\text{g g}^{-1}) \times \rho (\text{g cm}^{-3}) \times I (\text{cm yr}^{-1}) \quad (1)$$

where ρ represents the dry bulk density, and the peat accumulation rate. The Ti

concentration and the calculated MAR showed far greater values below 420 cm than above (Figure 5). The variation in Ti concentration and the calculated MAR (Figure 5) resemble those of ash content and AIA, i.e. they both peak at $\sim 300 \text{ cm}$ and increase below 420 cm.

Calcium, Mn, and K in bulk peat

The concentrations of Ca, Mn, are elevated at the top, and at the bottom of the profile (Figure 6). Potassium reveals a peak at a depth of $\sim 300 \text{ cm}$ (Figure 6), corresponding to that of ash and AIA.

Elemental concentrations in AIA (Ti and Zr)

The Ti and Zr concentrations in AIA (Figure 7) show two distinct profiles: relatively constant concentration above 420 cm ($\sim 0.29 \%$ Ti, and $103 \mu\text{g g}^{-1}$ Zr) and elevated concentration below 420 cm (0.66% Ti, and $250 \mu\text{g g}^{-1}$ Zr).

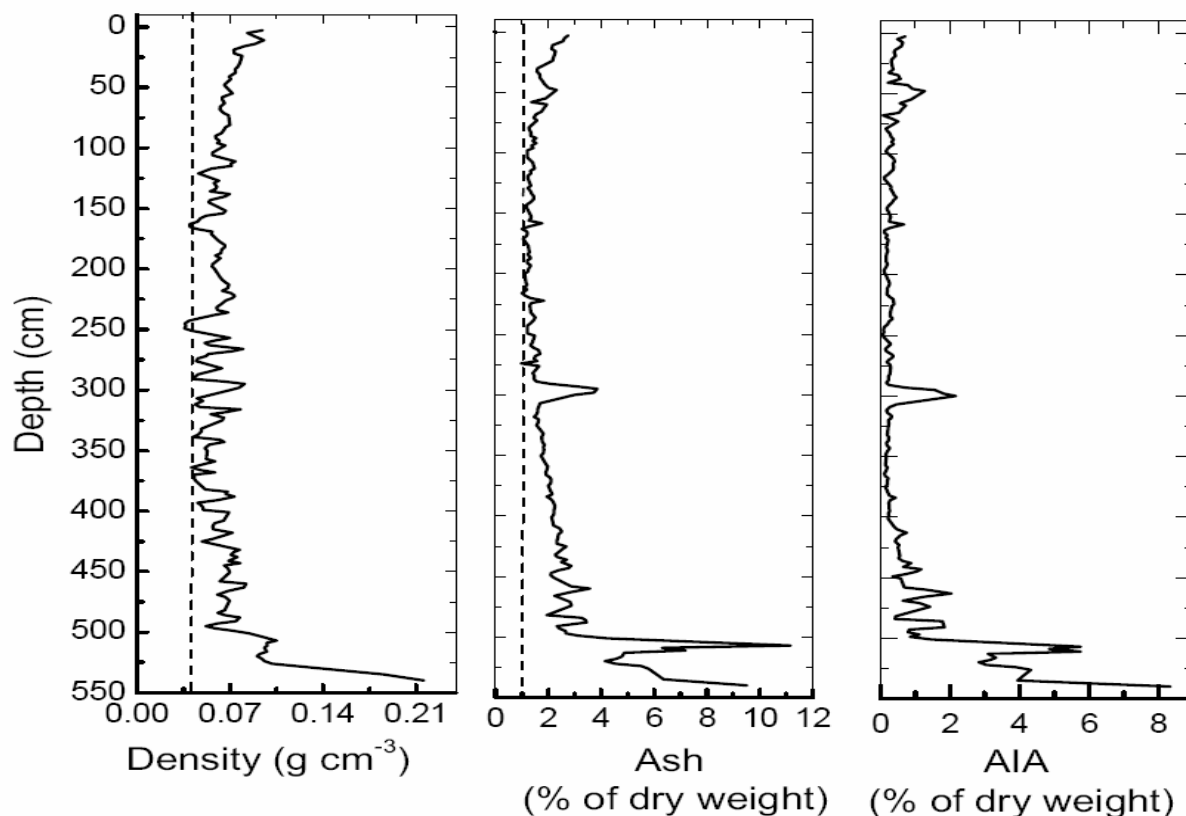


Figure 4: Density (g cm^{-3}), ash content (%), and acid insoluble ash (AIA, %) of the complete vertical peat profile.

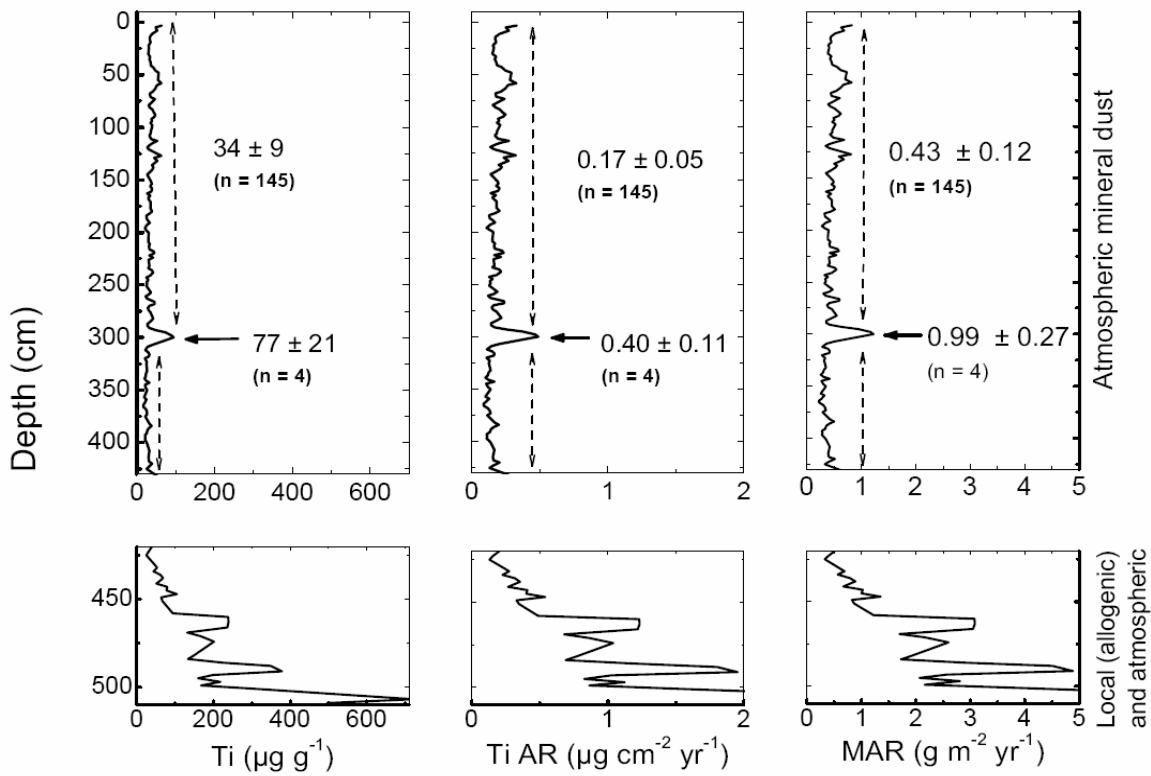


Figure 5: Ti concentration ($\mu\text{g g}^{-1}$) and calculated accumulation rates of Ti (Ti AR) and mineral matter (MAR); the AR are given in units of $\mu\text{g cm}^{-2} \text{yr}^{-1}$ and $\text{g m}^{-2} \text{yr}^{-1}$ for Ti AR and MAR, respectively.

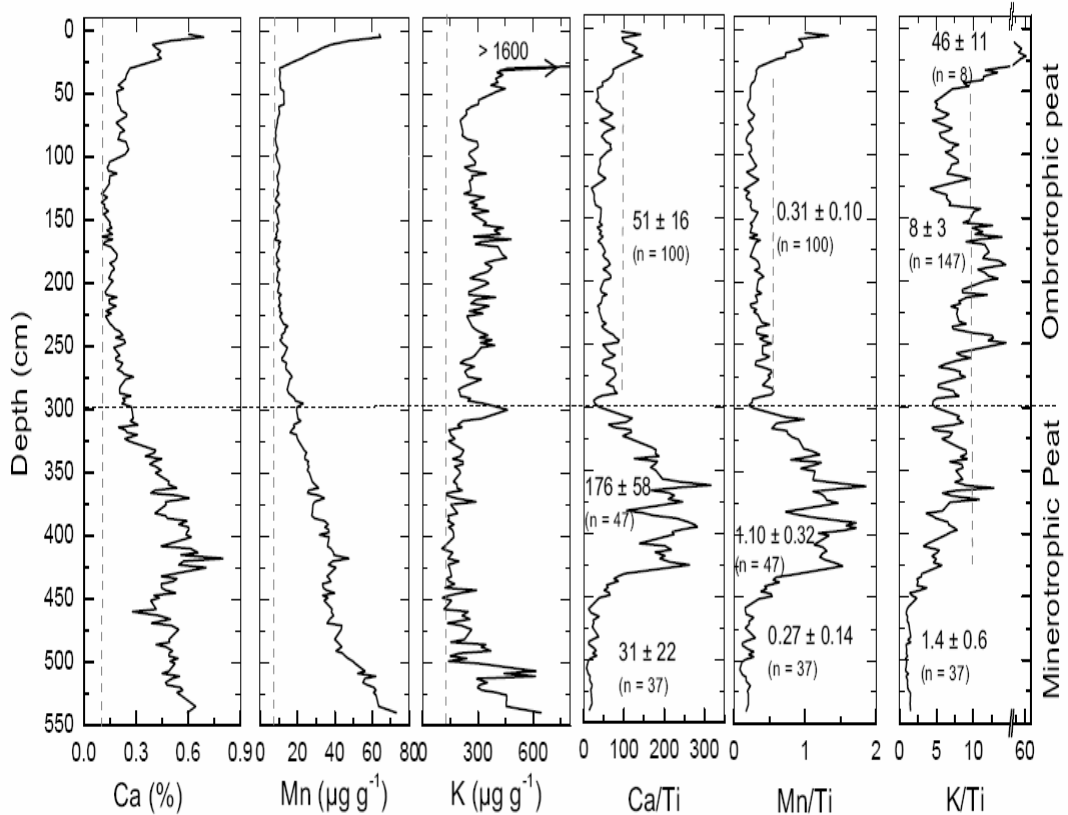


Figure 6: Concentration profiles of Ca (%), Mn ($\mu\text{g g}^{-1}$) and K ($\mu\text{g g}^{-1}$) and their ratio to Ti (bulk peat).

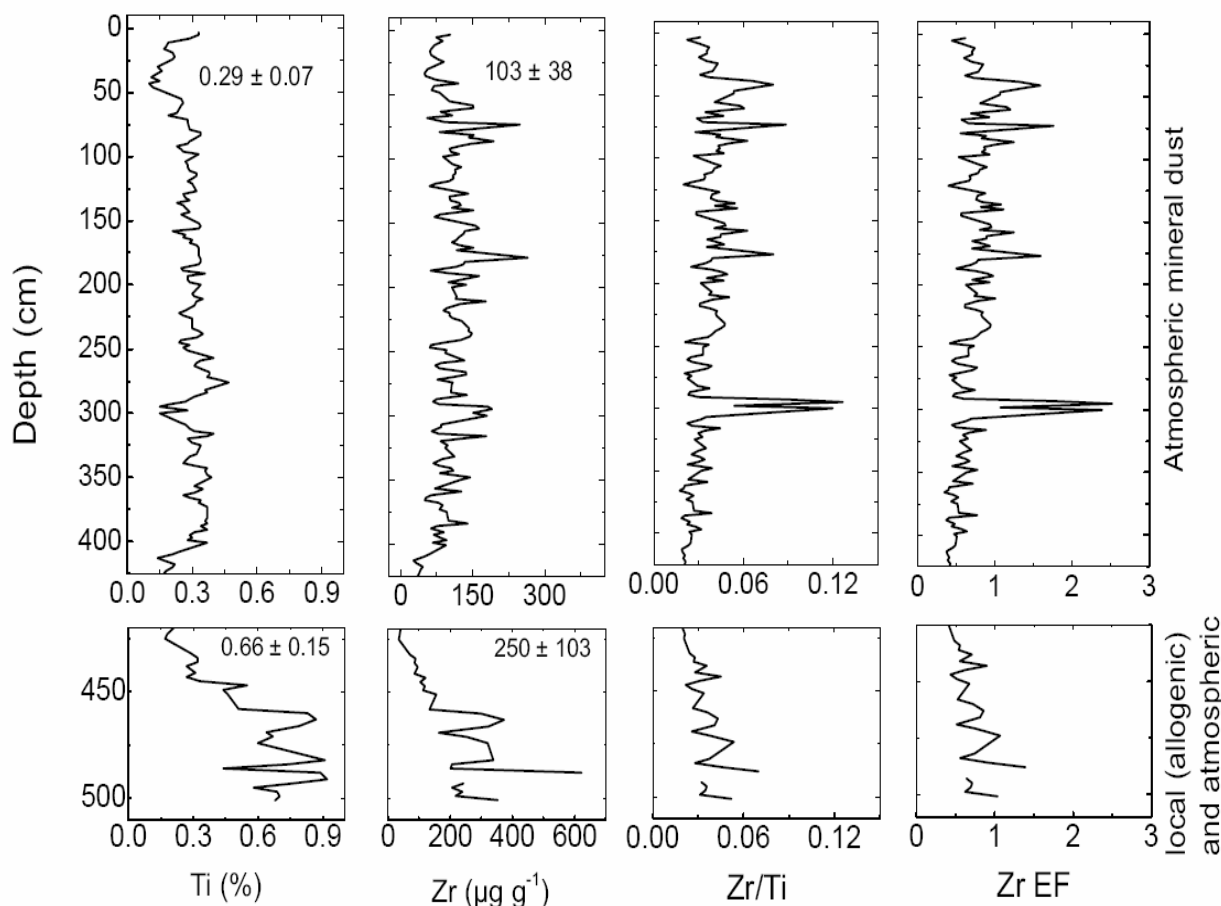


Figure 7: Concentration of lithogenic elements Ti (%) and Zr ($\mu\text{g g}^{-1}$) in the AIA; ratio of Zr/Ti and EF of Zr calculated using Ti as reference element (see text).

Components of AIA

Several AIA samples from different depths were chosen for XRD and SEM analysis, including the peak in ash and Ti at ~ 300 cm (Figure 4 and 5). The XRD analysis identified only quartz, albite and minor illite (Figure 8) possibly because of the low amount of mineral material used and the poor sensitivity of XRD. However, SEM analyses showed that the AIA consisted of both lithogenic and biogenic mineral materials.

Biogenic components

The biogenic components identified were composed primarily of amorphous silica such as phytoliths and diatoms (Figure 9A). They were found in the AIA at all depths above 420 cm, but were predominant near the surface (for example, Figure 9A: depth of 50 cm). It is not possible to tell whether, these were produced by plants growing in the bog, surrounding the bog, or from long range atmospheric transport.

Lithogenic components

Input from soil dust

The mineralogical composition of the AIA between the surface and 420 cm was mostly weathered particles of quartz, plagioclases, potassium feldspars, pyroxenes, mica, and amphiboles (Figure 9B). Also found in the AIA were rounded ilmenite, needle shaped rutile, and mesh shaped illite of soil-derived dust. In addition, a few weathered grains ($\sim 10 - 20 \mu\text{m}$) of heavy minerals such as zircon and monazite were also present. The predominant particle sizes of the AIA components in the upper 420 cm were mostly in the range of 0.5 and $10 \mu\text{m}$ (Figure 9B).

Volcanic input

Notably, AIA samples from 43 to 66 cm (Figure 4) and from 156 to 158 cm also showed a few pumice fragments of particle sizes $> 40 \mu\text{m}$ (Figure 9C). Similarly, the

mineralogical composition of AIA samples from 293 – 300 cm contained relatively larger (more than 20 – 40 μm , up to 150 μm) particles of typical angular to sub-angular pumice pyroclasts of andesitic to dacitic

composition (Figure 9D). All of these zones containing pumice fragments correspond to peaks in ash, AIA and Ti, (except at ~ 156 cm) (Figure 4 and 5).

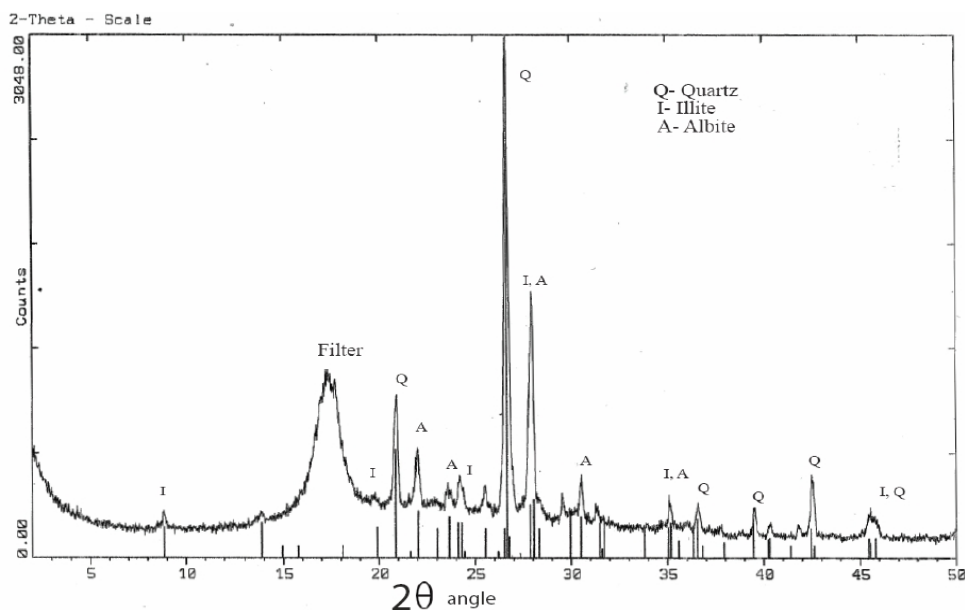


Figure 8: XRD spectrum of AIA taken from a depth of 63 cm.

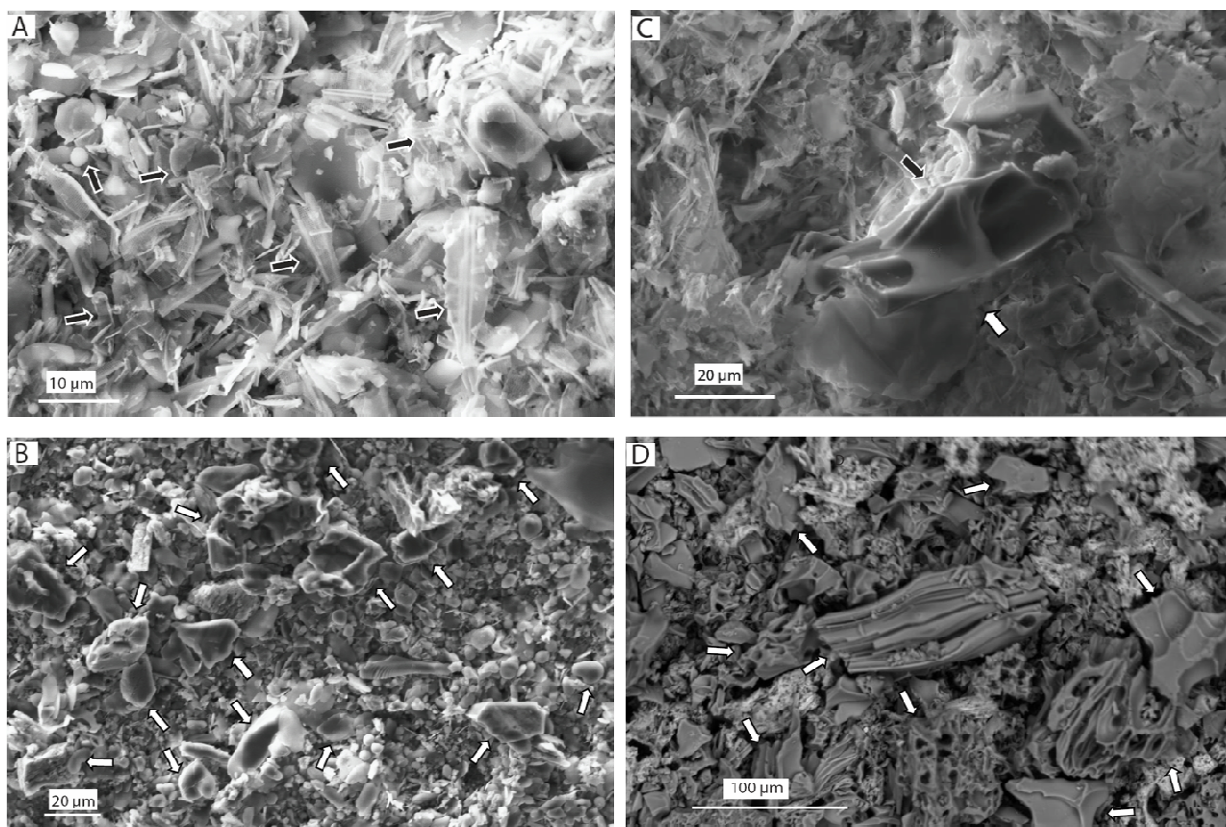


Figure 9: Grain sizes and textures of AIA components (indicated by arrows): (A) Biogenic components (phytoliths and diatoms; $< 20 \mu\text{m}$, depth of 50 cm); (B) Silicate minerals (feldspar, quartz, etc., $< 20 \mu\text{m}$, depth of 190 cm); (C) Volcanic particles (pumice fragments, $> 40 \mu\text{m}$, depth of 63 cm); (D) Volcanic particles (pumice fragments, $> 40 \mu\text{m}$, depth of 298 cm).

Discussion

Ombrotrophic character of the peat deposit

The low ash content above 450 cm ($\leq 3\%$) and low density (typically 0.05 to 0.1 g cm⁻³) in the Oreste bog peat profile are well within the range characteristic of ombrotrophic peat bogs (Steinmann and Shotytk, 1997; Tolonen, 1984). In contrast, the abundance of ash (Figure 4) and Ti (Figure 5) show that peat below 450 cm is minerotrophic. However, the Ca/Ti ratio (Figure 6) shows that the peat between 300 cm and 450 cm has become enriched in Ca, out of proportion with Ti. The addition of Ca (and Mn) to the overlying peats is probably due to mineral dissolution in deeper peat layers, combined with upward diffusion of Ca²⁺ and Mn²⁺. Taken together, the Ca and Mn concentrations and the Ca/Ti plus Mn/Ti ratios, show clearly that truly ombrotrophic peats are found only above ~ 300 cm.

The enrichment of Ca, Mn and K relative to Ti in the top part (above 30 cm) indicates the influence of vegetation on the distribution of these elements, which are essential elements for plant growth.

Changing rates of mineral matter input

Based on the trophic status of the Oreste peat bog and the Ti concentrations in bulk peat, inputs of mineral particles above 420 cm were predominantly of atmospheric origin. Below 420 cm, the minerals were predominantly from local sources having been transported by flowing surface waters.

The relatively constant MAR above 420 cm (0.43 g m⁻² yr⁻¹), corresponding to ca. 6000 yrs, suggests stable climatic conditions with a relatively constant dust supply. Based on the vegetation records from southern South America (Heusser, 1998; Markgraf et al., 1992), this time period is characterized by environmental conditions comparable to those found today. Specifically, this interval represents the establishment of Magellanic Moorland (Heusser, 1998; Stephanie Janssen, pers. Comm.). Taken together, dust circulation and deposition in southernmost South America were already stable beginning by 6000 – 5500 cal yrs BP (Figure 5) (Table I). The predominance of rounded, fine-

grained mineral particles in the AIA since ca. 6000 yrs suggests long-range atmospheric transport (Figure 9 A and B).

The mineralogical study of the AIA at 293 – 300 cm, motivated by the peak of ash content, AIA, K, and Ti concentration in bulk peat and the calculated MAR (Figure 4, 5, and 6), showed predominantly glassy pumice fragments of volcanic origin with predominantly larger particle sizes (Figure 9D). Hence, a volcanic eruption must have been responsible for the abrupt change in dust accumulation at ~ 300 cm. The elevated K concentrations at depth from 293 cm to 300 cm is consistent with andesitic to dacitic composition which is predominant in the Austral volcanic zone (49 – 56°S) (Stern et al., 1984).

Abundance of Ti and Zr in the AIA

Concentrations and size distributions of particles in the atmosphere depend not only on availability within the source area, but also on transport, transformation, deposition, and resuspension processes (Schütz, 1989). The lower concentration of Ti ($\sim 25\%$) and Zr ($\sim 40\%$) in AIA above 420 cm, compared to the crustal values (Wedepohl, 1995), reflect selective segregation of heavy minerals in atmospheric dust during transportation. Titanium and Zr are most commonly found in dense mineral phases which behave conservatively during chemical weathering. Analyses of Ti and Zr in highly weathered, winnowed soils have revealed lower concentrations in the smaller particle sizes ($< 10\ \mu\text{m}$) compared to larger particles ($\sim 45 - 100\ \mu\text{m}$) (Eltayeb et al., 2001; Schütz and Rahn, 1982). Similarly, the smaller particles ($< 10\ \mu\text{m}$) can be transported thousands of kilometers, and much further than larger particles ($> 10\ \mu\text{m}$) (Schütz and Seibert, 1987) with higher sedimentation velocities (Nickling, 1983). Hence, the lower concentration of Ti and Zr seen in the Oreste bog suggests a fine fraction of soil-derived atmospheric dust of clay and silt sized material. In addition, relatively constant Ti and Zr concentrations in the AIA, parallel to Ti in the bulk peat and the calculated MAR, indicate that the atmospheric dust for the last 6000 yrs (above 420 cm) was predominantly

supplied by a specific source area, or constant series of sources with similar particle sizes.

Enrichment factors are useful to assess the contribution of a specific source area to the dust and to the fractionation of the mineral particles undergone during transport (Rahn, 1976; Schütz and Rahn, 1982). The Zr/Ti ratio in the Earth's Continental Crust is 0.05 (Wedepohl, 1995) and this ratio was used to calculate the crustal enrichment factor (EF) in mineral dust deposited on the peat bog (Figure 7) as follows:

$$EF = (Zr / Ti)_{\text{sample}} / (Zr / Ti)_{\text{crust}} \quad (2)$$

The Zr/Ti ratios and EFs of Zr were relatively constant with values similar to crustal proportions above 420 cm, except at ca. 300 cm. The enrichment of Zr relative to Ti at ca 300 cm indicates a different source. The AIA samples from this depth are dominated by tephra (Figure 9D) which shows that this period witnessed mineral dust inputs being dominated by a volcanic source.

Comparison with other studies in southern South America

In the absence of relevant studies on long-term dust deposition in the southernmost southern hemisphere, we tried to compare the atmospheric MAR with other short-term dust accumulation data calculated using direct air measurements and modeling studies. A recent study on dust deposition in SW Pampa (~38 – 40°S) has shown deposition rates of 40 to 80 g m⁻² yr⁻¹ (averaged over 3 years) (Ramsperger et al., 1998), which are more than 100 times higher than the MAR calculated in the Oreste bog. Similarly, the dust accumulation rate calculated using direct measurements (averaged over 2 years) in SW Pampa (~ 38 – 45°S) yielded deposition rates on the order of 35 g m⁻² yr⁻¹ (Gaiero et al., 2003). The difference between those two reports and the data presented here for Oreste bog (0.43 ± 0.12 g m⁻² yr⁻¹) can be explained by the distances involved; the Pampa sampling sites are more than 1000 km further north of the Oreste bog (55°S). Though the MAR for Oreste bog is ~ 40% of the model by Tegen and Fung (1994) (1 to 10 g m⁻² yr⁻¹, averaged over 13 months), it is within the

range estimated by the GOCART model (0.1 to 0.5 g m⁻² yr⁻¹, averaged over 5 years) (Ginoux et al., 2001). Notably, the MAR calculated here was a long-term average (6000 yrs), while the atmospheric deposition estimated by models and observations are based on present day values. Hence, the short-term observations and the model estimates might not account for long-term climatic variables, such as seasonal shift in wind direction and storminess. Furthermore, the difference in observed versus modeled dust deposition might also be affected by the predominant influence of westerlies and the separation of the Oreste bog from the unforested Patagonian lowlands by the mountain belts. The most likely source of the atmospheric dust to the Oreste bog is arid and semi arid areas of continental Patagonia (38°S to 52°S) (Gaiero et al., 2003) and the pampas lying further north (Zárate, 2003).

Possible source of volcanic input

We tried to estimate the age of the tephra found at ca. 300 cm. The dated sample closest to the described tephra (293 - 300 cm) was 3985 14C yr BP (4300 - 4529 cal yr BP); this sample was 5 cm below the tephra layer. Similarly, another sample was dated at 3700 14C yr BP (3934 – 4145 cal yr BP); this sample was 13 cm above the tephra. Both of these age dates are consistent with the published value (4254 ± 120 cal yr BP) for the Mid-Holocene eruption of Mt. Burney (Kilian et al., 2003). Mt. Burney is located approximately 400 km north-west (52°S) of the Oreste bog and is known to have deposited tephra as far south as Tierra del Fuego.

Conclusions

Measurements of ash, AIA, Ti and Zr in peat cores from the Oreste Bog show that in the southernmost Southern Hemisphere, atmospheric mineral dust deposition was effectively constant for approximately the last 6000 years. The mineralogical composition, size, and morphology of the dust particles show that long range atmospheric transport dominated the dust inputs for six millennia. The only significant exception to this general statement was found in peat dating to ca. 4200

ys ago, when elevated concentrations of ash, AIA, Ti, and Zr document additional dust inputs. Those peat samples also contain larger, angular particles of pumice, which are probably derived from the Mt. Burney eruption.

Acknowledgements

Financial support from the Deutsche Forschungsgemeinschaft (SH 89 /2-2 and SH 89/2-3) is gratefully acknowledged. We are grateful to Dr. Vera Markgraf who provided us with the peat core which she had collected in 1995 from the Oreste bog under a grant from the National Science Foundation (NSF-EAR-9709145), USA, and for her valuable input. Thanks to Ms. Stephanie Janssen (University of Köln) for preparing the samples for age dating and Ms. Helen Kurzel for expert XRF and SEM analyses. Thanks also to Marc Petras for XRD analysis.

References

- Basile, I.A., Grousset F.E., Revel, M., Petit, J.-R., Biscaye, P.E. and Barkov, N.I.** 1997: Patagonian origin of glacial dust deposited in east Antarctica (Vostok and Dome C) during glacial stages 2, 4, and 6. *Earth and Planetary Science Letters* 146, 573-589.
- Biscaye, P.E., Grousset, F.E., Revel, M., Gaast, S.V., Zielinski, G.A., Vaars, A., and Kukla, G.** 1997: Asian provenance of glacial dust (stage 2) in the Greenland Ice sheet project 2 Ice core, summit, Greenland. *Journal of Geophysical Research* 102, 26765-26781.
- Björck, S. and Clemmensen, L.B.** 2004: Aeolian sediment in raised bog deposits, Halland, SW Sweden: a new proxy record of Holocene winter storminess variation in southern Scandinavia? *The Holocene* 14, 677-688.
- Bory, A.J.M., Biscaye, P.E., Svensson, A. and Grousset, F.E.** 2002: Seasonal variability in the origin of recent atmospheric mineral dust at NorthGRIP, Greenland. *Earth and Planetary Science Letters* 196, 123-134.
- Cheburkin, A. and Shotyk, W.** 1996: An Energy-dispersive Miniprobe Multielement Analyzer (EMMA) for direct analysis of Pb and other trace elements in peats. *Fresenius. Journal of Analytical Chemistry* 354, 688-691.
- 2005 Energy-dispersive XRF spectrometer for Ti determination (TITAN). *X-Ray Spectrometry* 34, 69-72.
- Delmonte, B., Petit, J.-R. and Maggi, V.** 2002: Glacial to Holocene implications of the new 27000-year dust record from the EPICA Dome (East Antarctica). *Climate Dynamics* 18, 647-660.
- Eltayeb, M.A.H., Injuk, J., Maenhaut, W. and Grieken R.E.V.** 2001: Elemental Composition of Mineral Aerosol generated from Sudan Sahara Sand. *Journal of Atmospheric Chemistry* 40, 247-273.
- Finney, H.R. and Farnham, R.S.** 1968: Mineralogy of the inorganic fraction of peat from two raised bogs in northern Minnesota. *Proceedings of 3rd International Peat Congress Quebec, Canada*, 102-108.
- Gaiero, D.M., Probst, J.-L., Depetris, P.J., Bidart S.M. and Leleyter, L.** 2003: Iron and other transition metals in Patagonian riverborne and windborne materials: Geochemical control and transport to the southern South Atlantic Ocean. *Geochimica Cosmochimica Acta* 67, 3603-3623.
- Ginoux, P., Chin, M., Tegen, I., Prospero, J.M., Holben, B., Dubovik, O. and Lin, S.-J.** 2001: Sources and distributions of dust aerosols simulated with the GOCART model. *Journal of Geophysical Research* 106, 20255-20273.
- Goudie, A.S. and Midelton, N.J.** 2001: Saharan dust storms: nature and consequences. *Earth Science Reviews* 56, 179-204.
- Grousset, F.E., Biscaye, P.E., Revel, M., Petit, J.-R., Pye, K., Joussaume, S. and Jouzel, J.** 1992: Antarctic (Dome C) ice-core dust at 18 k.ya. B.P.:

- Isotopic constraints on origins. *Earth and Planetary Science Letters* 111, 175-182.
- Hajdas, I., Bonani, G., Thut, J., Leone, G., Pfenninger, R. and Maden, C.** 2004: A report on sample preparation at the ETH/PSI AMS facility in Zurich. *Nuclear Instruments and Methods in Physics Research B* 223-224, 267-271.
- Harrison, S.P. and Kohfeld, K.E.** 2001: The role of dust in climate changes today, at the last glacial maximum and in the future. *Earth Science Reviews* 54, 43-80.
- Heusser, C.J.** 1998: Deglacial palaeoclimate of the American sector of the Southern Ocean: Late Glacial-Holocene records from the latitude of Canal Beagle (55°S), Argentine Tierra del Fuego. *Palaeogeography, Palaeoclimatology, Palaeoecology* 141, 277-301.
- Heusser, C.J. and Rabassa, J.** 1987: Cold climatic episode of Younger Dryas age in Tierra del Fuego. *Nature* 328, 609-611
- Huber, U.M., Markgraf, V., Schaebitz, F.** 2004: Geographical and temporal trends in Late Quaternary fire histories of Fuego-Patagonia, South America. *Quaternary Science Reviews* 23, 1079-1097.
- Kilian, R., Hohner, M., Biester, H., Wallrabe-Adams, H.J. and Stern, C.R.** 2003: Holocene peat and lake sediment tephra record from the southernmost Chilean Andes (53-55oS). *Revista Geologica de Chile* 30, 23-37.
- Le Roux, G., Laverret, E. and Shoty, W.** 2006: Fate of calcite, apatite and feldspars in an ombrotrophic peat bog, Black forest, Germany. *Journal of the Geological Society* 163, 641-646.
- Mahowald, N., Kohfeld, K.E., Hansson, M., Balkanski, Y., Harrison, S.P., Prentice, I.C., Schülz, M. and Rodhe H.** 1999: Dust sources and deposition during the last glacial maximum and current climate: a comparison of model results with paleodata from ice cores and marine sediments. *Journal of Geophysical Research* 104, 15895-15916.
- Markgraf, V.** 1993: Paleoenvironments and paleoclimates in Tierra del Fuego and southernmost Patagonia, South America. *Palaeogeography, Palaeoclimatology, Palaeoecology* 102, 53-68.
- Markgraf, V., Dodson, J.R., Kershaw, A.P., McGlone, M.S. and Nicholls, N.** 1992: Evolution of late Pleistocene and Holocene climates in the circum-South Pacific land areas. *Climate Dynamics* 6, 193-211.
- Nickling, W.G.** 1983: Grain-size characteristics of sediment transported during dust storms. *Journal of Sedimentary Petrology* 53, 1011-1024.
- Olivero, E.B. and Martinioni, D.R.** 2001: A review of the geology of the Argentinean Fuegian Andes. *Journal of South American Earth Sciences* 14, 175-188.
- Pendall, E., Markgraf, V., White, J.W.C. and Dreier, M.** 2001: Multiproxy record of Late Pleistocene-Holocene climate and vegetation changes from a peat bog in Patagonia. *Quaternary Research* 55, 168-178.
- Petschick, R.** 2005: MacDiff Software.
- Rabassa, J., Coronato, A. and Roig, C.** 1996: *The peat bogs of Tierra del Fuego, Argentina*. In Lappalainen, E., editor, *Global Peat Resources*, Finland: International Peat Society.
- Rabassa, J., Heusser, C.J. and Coronato, A.** 1989: Peat/bog accumulation rate in the Andes of Tierra del Fuego and Patagonia (Argentina and Chile) during the last 43,000 years. *Prineos* 138, 113-122.
- Rahn, K.A.** 1976: *The chemical composition of the atmospheric aerosol*. Technical Report, University of Rhode Island: Graduate School of Oceanography.
- Ramsperger, B., Peinemann, N. and Stahr, K.** 1998: Deposition rate and characteristics of aeolian dust in the semi-arid and sub-humid regions of the Argentinean Pampa. *Journal of Arid Environment* 39, 467-476.

- Reimer, P.J., Baillie, M.G.L., Bard, E., Bayliss, A., Beck, J.W., Bertrand, C., Blackwell, P. G., Buck, C.E., Burr, G., Cutler, K.B., Damon, P.E., Edwards, R.L., Fairbanks, R.G., Friedrich, M., Guilderson, T.P., Hughen, K.A., Kromer, B., McCormac, F.G., Manning, S., Ramsey, C.B., Reimer, R.W., Remmele, S., Southon, J.R., Stuiver, M., Talamo, S., Taylor, F.W., Plicht, J.V. and Weyhenmeyer, C.E.** 2004: INTCAL04 Terrestrial radiocarbon age calibration, 0-26 Cal Kyr BP. *Radiocarbon* 46, 1029-1058.
- Schütz, L.** 1989: *Atmospheric mineral dust-properties and source makers*. In Leinen, M. and Sarnthein, M., editors, *Paleoclimatology and Paleometeorology: Modern and Past Patterns of Global Atmospheric Transport*, Dordrecht: Kluwer Academic Publishers, 359-383.
- Schütz, L. and Rahn, K.A.** 1982: Trace-element concentrations in erodible soils. *Atmospheric Environment* 16, 171-176.
- Schütz, L. and Seibert, M.** 1987: Mineral aerosols and source identification. *Journal of Aerosol Science* 18, 1-10.
- Shotyk, W.** 1997: Atmospheric deposition and mass balance of major and trace elements in two oceanic peat bog profiles, northern Scotland and the Shetland Islands. *Chemical Geology* 138, 55-72.
- Shotyk, W., Krachler, M., Martinez-Cortizas, A., Cheburkin, A.K. and Emons, H.** 2002: A peat bog record of natural, pre-anthropogenic enrichments of trace elements in atmospheric aerosols since 12370 ¹⁴C yr BP, and their variation with Holocene climate change. *Earth and Planetary Science Letters* 6180, 1-17.
- Shotyk, W., Weiss, D., Kramers, J.D., Frei, R., Cheburkin, A.K., Gloor, M. and Reese, S.** 2001: Geochemistry of the peat bog at Etang de La Gruère, Jura Mountains, Switzerland, and its record of atmospheric Pb and lithogenic trace metals (Sc, Ti, Y, Zr, and REE) since 12,370 ¹⁴C yr BP. *Geochimica Cosmochimica Acta* 65, 2337-2360.
- Steinmann, P. and Shotyk, W.** 1997: Geochemistry, mineralogy, and geochemical mass balance on major elements on two peat bog profiles (Jura Mountains, Switzerland). *Chemical Geology* 138, 25-53.
- Stern, C.R., Futa, K. and Muehlenbachs, K.** 1984: *Isotope and trace element data for Orogenic Andesites from the Austral Andes*. In Harmon, R.S. and Barreiro B.A., editors, *Andean Magmatism: Chemical and Isotopic constraints*, UK: Shiva Publishing Limited, 31-46.
- Stuiver, M. and Reimer, P.J.** 1993: Radiocarbon calibration program Rev.3.0.3. *Radiocarbon* 35, 215-230.
- Tegen, I. and Fung, I.** 1994: Modeling of mineral dust in the atmosphere: Sources, transport, and optical thickness. *Journal of Geophysical Research* 99, 22897-22914.
- Thomas, D.S.G.** 1989: *The nature of arid environments*. In Thomas D.S.G., editor, *Arid Zone Geomorphology*, London: Belhaven Press, 1-8.
- Tolonen, K.** 1984: Interpretation of changes in the ash content of ombrotrophic peat layers. *Bulletin of Geological Society of Finland* 56, 207-219.
- Tuhkanen, S.** 1992: The climate of Tierra del Fuego from a vegetation geographical point of view and its ecoclimatic counterparts elsewhere. *Acta Botanica Fennica* 145, 1-64.
- Wedepohl, K.H.** 1995: The composition of the continental crust. *Geochimica Cosmochimica Acta* 59, 1217-1232.
- Weiss, D., Shotyk, W., Rieley, J., Page, S., Gloor, M., Reese, S. and Martinez-Cortizas, A.** 2002: The geochemistry of major and selected trace elements in a forested peat bog, Kalimantan, SE Asia, and its implications for past atmospheric dust deposition. *Geochimica Cosmochimica Acta* 66, 2307-2323.
- Zárate, M.A.** 2003: Loess of southern South America. *Quaternary Science Reviews* 22, 1987-2006.

Zadnowicz, C.M., Zielinski, G.A., Wake, C.P., Fisher, D.A. and Koerner, R.M. 2000: A Holocene record of atmospheric dust deposition on the Penny Ice Cap, Baffin Island, Canada. *Quaternary Research* 53, 62-69.

Chapter 3

Mineralogy of Dusts

-Chapter 3-
Characterization of atmospheric mineral dusts preserved in an ombrotrophic peat bog from southernmost Southern Hemisphere, Oreste Bog, Tierra del Fuego, Chile

Olena Kurzel, Atindra Sapkota, William Shotyk*

Institute of Environmental Geochemistry, University of Heidelberg, Im Neuenheimer Feld 236, D-69120, Heidelberg, Germany

*Corresponding author, Tel: + 49 (6221) 54 4803; Fax: + 49 62 21 54 52 28,

Email: shotyk@ugc.uni-heidelberg.de

Submitted to Quaternary Research, 2006

Abstract

The ombrotrophic (ie rain-fed) section of the Oreste Bog (Isla Navarino, Chile) from southernmost South America, has been accumulating atmospheric mineral dusts for more than six thousand years. After extracting and isolating the Acid Insoluble Ash (AIA) fraction of the peat samples, individual mineral grains were identified, and their size and morphology characterized, using Scanning Electron Microscopy (SEM) employing energy-dispersive XRF analysis. The mineralogy of the samples (typically 2 to 3 mg) was dominated by primary, rock-forming minerals such as quartz, plagioclase, and mica, but accessory minerals including zircon, monazite, rutile, ilmenite, and titanite, were also common. A diverse array of siliceous particles of biogenic origin, especially phytoliths and diatoms, as well as tephra grains, were found throughout the profile. A zone of anomalous concentrations of AIA at a depth of 300 cm is dominated by particles of volcanic ash. Dating the peat profile using ^{14}C and the development of an age-depth model suggest that these tephra grains can be attributed to the Mt. Burney eruption at ca. 4200 cal yr BP. The low abundance of AIA combined with the size, morphology and uniform distribution of primary, rock-forming minerals, indicates that relatively stable climatic conditions have prevailed for the past ca. 6000 yrs., with dusts supplied both by local as well as long range atmospheric transport.

Keywords: *ombrotrophic peat, inorganic fraction, soil dust, tephra, southern South America*

1 Introduction

Arid and semi-arid areas which cover more than 30 % of the earth's land surface are important sources of dust in the atmosphere (Thomas, 1989), generated predominantly by wind erosion of soil particles. The fluxes, particle size distribution, mineralogy, and chemistry of atmospheric mineral dusts are important because of their impacts on the earth's climate system, their influence on chemical processes in the atmosphere, and the global biogeochemical cycles of many elements (Goudie, 2001; Harrison and Kohfeld, 2001). The proportion of dust entrained in the atmosphere and its transportation is a function of the extent of source areas, strength of atmospheric circulation, and removal processes (Nickling, 1983). Distances from the dust source and wind speed are the dominant factors affecting the average particle size of suspended materials. With increased transport distances combined with reduced wind speeds, the average particle sizes in the atmospheric dust decreases (Schütz, 1989). Compared to larger particles ($> 10 - 20 \mu\text{m}$), smaller particles ($< 10 \mu\text{m}$) can be transported thousands of kilometers (Schütz, 1989) because of differential settling velocity of material during atmospheric transport (Leinen et al. 1994; Nickling, 1983). The mineralogical and chemical properties of soil-derived atmospheric dust are important to understanding the behaviour of deflated dust (Prospero, 1996).

Snow and ice cores are valuable archives of atmospheric deposition of soil derived dust, volcanic ash particles, marine aerosols, and trace elements (natural and/or anthropogenic) (Biscaye et al. 1997; Delmonte et al., 2002; Gabrielli et al., 2005; Röthlisberger et al., 2002; Svensson et al., 2000; Vallelonga et al., 2005). However, very few attempts have been made at mineralogical studies of dusts in ice cores (Svensson et al., 2000; Gaudichet et al., 1986) partly because of the tremendous challenge posed by the very low concentrations of dusts ($\mu\text{g} / \text{kg}$) which render any studies of mineralogy or chemistry most difficult (Delmonte et al., 2002).

Like ice cores, ombrotrophic peat bogs are a valuable archive of atmospheric mineral dust deposition as they receive these particles exclusively from air. The inorganic fraction of peat can be divided into three components (Andrejko et al., 1983): a) biogenic components (allochthonous and autochthonous); b) terrigenous mineral components (allogenic mineral matter from dust and/or flooding); and c) authigenic components (ie minerals formed *in situ*). Even in the anaerobic, organic-rich acidic environment of peat bogs ($\sim \text{pH } 4$), atmospherically deposited, fine-grained silicate minerals (quartz, feldspar) as well as the resistate oxides (ilmenite, rutile) appear not to dissolve after deposition (Steinmann and Shoty, 1997). These minerals can be separated by either dry ashing or wet digestion of the organic fraction of peat material. Dry ashing is a common procedure to destroy the organic materials in peat, leaving behind oxides, hydroxides, carbonates, sulphates, refractory mineral grains, and particles of biogenic origin in the ash. Hydrochloric acid is commonly used to dissolve the acid-soluble ash fraction (ASA) dominated by carbonates, sulphates and phosphates, and separate the acid insoluble ash (AIA), which is mainly composed of insoluble silicate and resistate oxide minerals.

The mineralogy of the inorganic fraction in peat material from two raised bogs in Northern Minnesota, USA, has shown that most of the minerals (about 80 - 90 %) were composed of fine grained particles ($< 20 \mu\text{m}$) of aeolian origin (Finney and Farnham, 1968). Similarly, the number of quartz grains in the ignition residue has been used to determine variations in aeolian sand influx and winter climate through time (Björck and Clemmensen, 2004). However, except for these studies, the mineralogical composition and size fractionation of the inorganic material in peat has not been studied extensively.

Using peat cores from a complete vertical section of a bog from southernmost South America, the objectives of this study are to: (1) identify the predominant mineral phases present in the acid-insoluble fraction, in particular to distinguish between atmospheric

particles derived from soils, volcanoes, and biological sources, (2) characterize the size and morphology of these materials, to estimate the relative importance of local versus long range sources of atmospheric dusts, and (3) using an appropriate age-depth model, to identify any climate-dependent changes in the relative abundance of mineral particles over time.

2 Study area

2.1 Site description

The Oreste bog is situated near the Fondeadero Orestes on the west side of the Bahía Windhound, southern part of Isla Navarino, Chile ($55^{\circ}13'13''$ S and $67^{\circ}37'28''$ W; at an altitude of 35m (Figure 1). The Isla Navarino is a part of the Tierra del Fuego archipelago. Biogeographically, the area can be termed 'antarctic', 'subantarctic' and so forth, following varying interpretations (Tuhkanen, 1992; Heusser, 1998). The temperature conditions in this region average above freezing point in the coldest months and 9°C during the warmest months. Annual precipitation in the region is approximately 600 mm.

This territory is within the path of eastward moving cyclones. Strong westerly wind directions occur at least 75 % of the time in the Magellanic region. Another direction is cold southerly air stream of Antarctic origin (Figure 1) (Tuhkanen, 1992). The direct oceanic influence is also present. During the Quaternary, this territory was ice-covered and now has typical post-glacier

relief with extensive lakes.

The Oreste bog is a Magellanic moorland bog located behind a *Nothofagus betuloides* forest. In the bog, the dominant plant species at the present time are: *Sphagnum magellanicum*, *Drepanocladus sp.*, and *Astelia pumila*, accompanied by *Carex*, *Ericaceae* (*Empetrum*) and *Marsippospermum grandiflorum* (Vera Markgraf, personal communication).

2.2 Geological setting

Isla Navarino is a part of the Patagonian Andes orocline. The structure of this territory is defined by the Beagle Channel fault zone at the southern edge of the Cordillera Darwin. The oldest unit recognized is a sedimentary metamorphic basement of Late Paleozoic-Early Mesozoic age. Plutonic bodies of tonalites, granites, granodiorites, diorites, and gabbros of the Patagonian batholith, are interpreted as exposed roots of a Middle Jurassic - Neogene magmatic composition. Upper Jurassic-Lower Cretaceous pillow lavas, sheeted dikes, and gabbros of the Tortuga complex unconformably cover the basement. The Yahgan Formation is well exposed and consists of a complex association of coarse conglomerates, sandstones, sandy and silty turbidites, black tuffaceous mudstones and tuffs. The metamorphism reaches chlorite-biotite grade. The outcrops of all of the above-mentioned rocks are present at the Isla Navarino and vicinity (Kraemer, 2003;

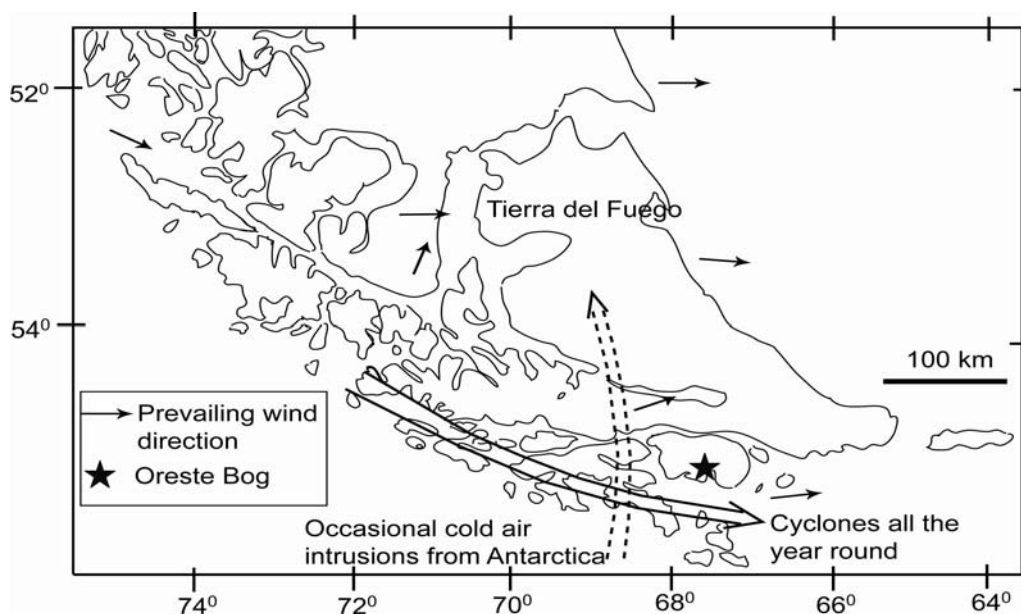


Figure 1: Map of southern South America, location of core site of the Oreste peat bog at Isla Navarino of southern Tierra del Fuego and main direction of the wind (Tuhkanen, 1992).

Olivero et al., 2001). All of these complexes are covered by Quaternary sand, gravel, clay and till (Clapperton, 1993). The Andean Austral Volcanic Zone (AVZ) is located to the north-west of the described territory with six volcanoes active during the Holocene (Stern et al., 1996).

3 Materials and Methods

The Oreste bog was cored in 1995 to a depth of 542 cm using a Livingston piston corer of 7.5 cm diameter. A ^{14}C age date (AMS) of a *Nothofagus* leaf taken from a depth of 506 cm yielded an age of 6100 ± 132 calibrated years BP (ETH-31605). The complete peat profile was sliced into 2 cm sections for physical, chemical and mineralogical analyses. The ash content of the samples were determined by combustion overnight at 550 °C. The determination of acid insoluble ash (AIA) was done by leaching peat ash with 1M HCl for 15 min. During this reaction time the soluble minerals such as carbonates, sulphates, phosphates, and oxides were dissolved. The AIA was collected on polycarbonate membrane filters of 0.2 μm pore size using vacuum filtration.

The morphology, size and chemical composition of inorganic particles were investigated using high resolution Scanning Electron Microscopy (SEM) (LEO-440), equipped with OXFORD Energy-Dispersive X-ray Spectrometer (EDS). The acceleration voltage was 20 kV, and beam current 0.8 to 2 nA. All samples were coated with graphite before SEM analysis. The chemical composition was determined directly in particles of varying size and shape, without any further sample preparation. As a result, the chemical compositions of the particles presented here, are not quantitative.

4 Results and Discussion

Components of insoluble inorganic matter

The amount of AIA in peat samples from the Oreste bog profile varies from 1 mg at the depth of 245 cm to 100 mg at a depth of 266 cm (Figure 2). The fine material ($< 10 \mu\text{m}$) is dominated by small particles of quartz, some accessory minerals, and small grains which are rhyolitic in composition. The former is of variable origin, such as fragments

of larger grains, particles which have been removed from colloidal suspension, and debris of biogenic material.

The coarse fraction ($> 30 \mu\text{m}$), is represented by grains of minerals from rocks and biogenic minerals such as phytoliths.

The extremely low mass of material obtained in the AIA fraction indicates that all mineral components of this bog are derived from atmospheric deposition. At a depth of 403 cm there is a profound increase in mass per sample slice. This change indicates a transition from the ombrotrophic to increasingly minerotrophic conditions with increasing depth.

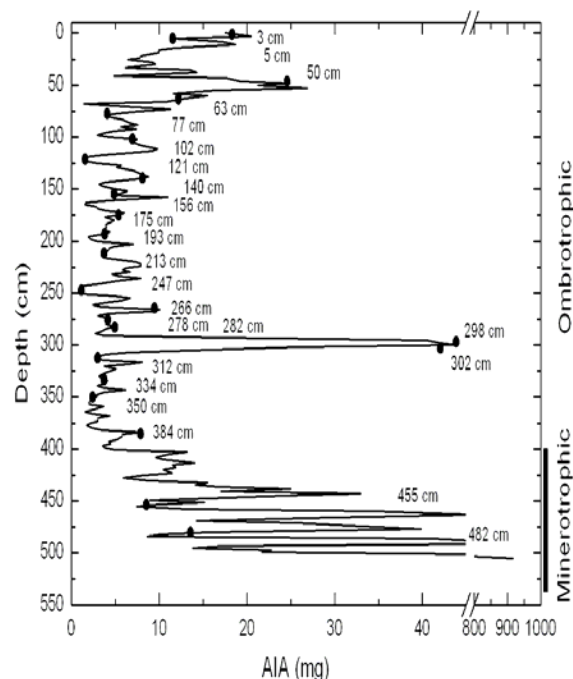


Figure 2: Distribution of Acid Insoluble Ash (AIA) in the Oreste peat profile. Samples used for the SEM study are indicated by the solid circle (●).

4.1 Biogenic materials

Biogenic mineral matter in the Oreste peat profile, formed as a result of biologic and metabolic activities by plants and animals, is represented by phytoliths, diatoms, sponge spicules, and mineralized plant tissue (Figure 3 and 4). These components are found in varying abundance in most of the Oreste peat profile except at depths of 298 – 302 cm. These diverse forms of biogenic silica are commonly found in peat (Wüst et al., 2003; Wüst et al., 2002; Carnelli et al., 2004; Kondo et al., 1994; Piperno, 1988). However, it is not

possible to tell whether these were produced *in situ* within the peatland environment, or whether they were derived from external

sources, and delivered by the atmosphere. Therefore, the biogenic phases are not discussed further.

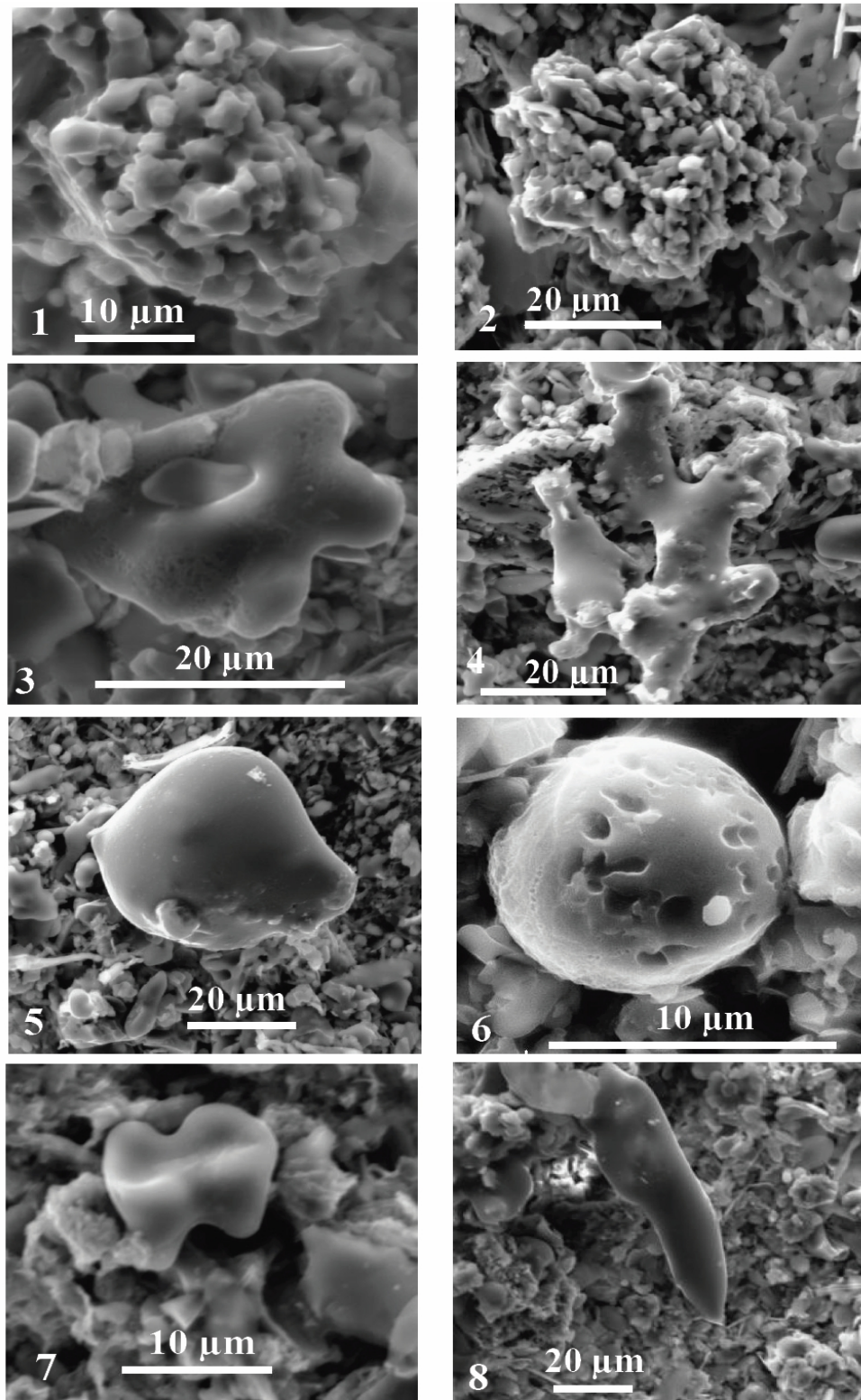


Figure 3: SEM photographs showing shapes of phytoliths: 1) and 2) - phytoliths from a aggregate class from a depth 156 and 175 cm; 3) and 4) - phytoliths from a anticlinal class from a depth 156 and 175 cm respectively; 5) - phytoliths from a depth 175 cm; 6) - phytoliths from a spherical smooth class from a depth of 5 cm; 7) - phytoliths from a depth of 334 cm; 8) - phytoliths from a depth of 5 cm;

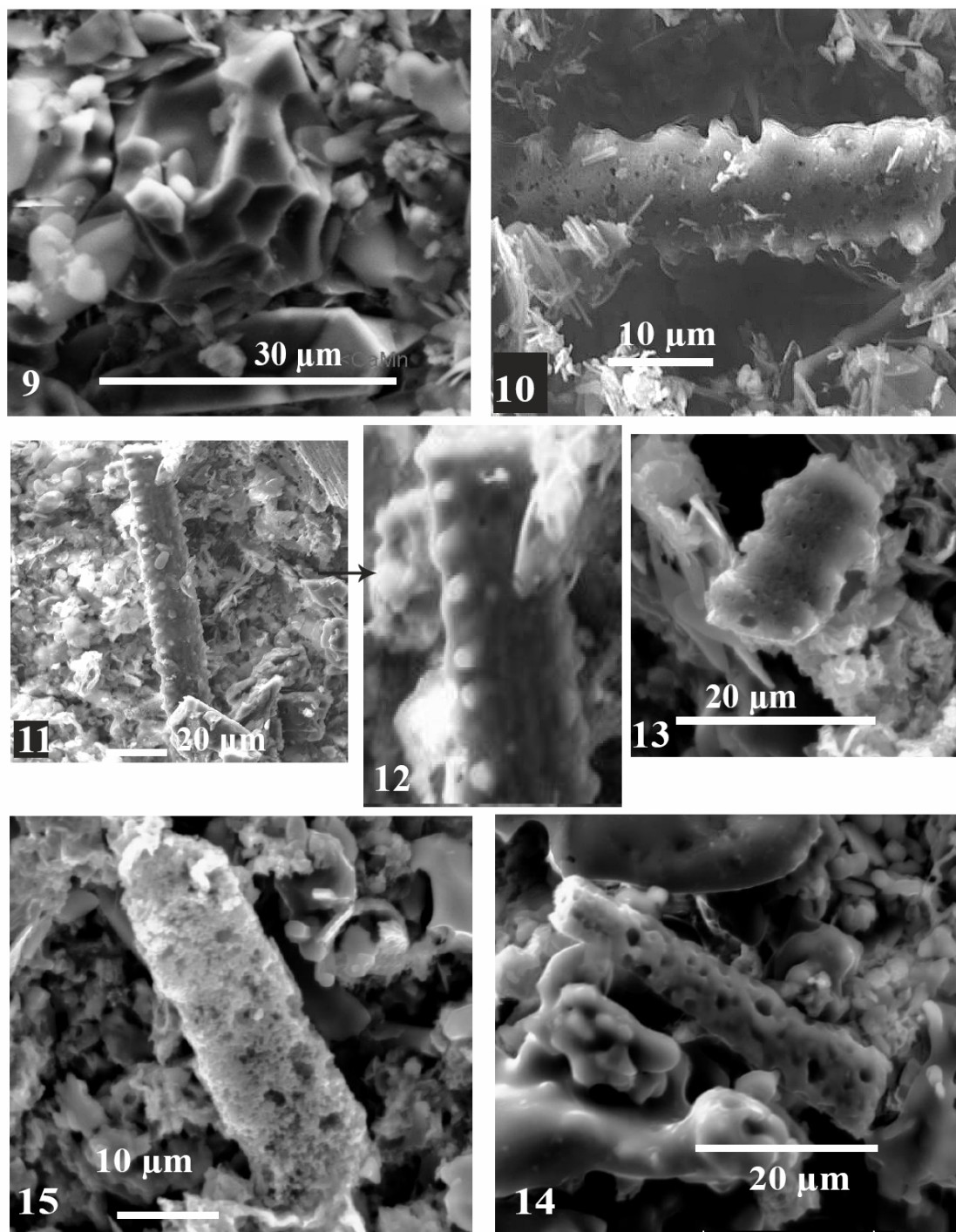


Figure 3 (continued): SEM photographs showing shapes of phytoliths: 9) - phytoliths from a polygonal shape from a depth of 140 cm; 10) - elongate phytoliths from a depth of 50 cm; 11) - elongate phytoliths from a depth of 77 cm; 12) enlargement of 11; 13) - phytoliths from a depth of 282 cm; 14) - elongate phytoliths from a depth of 175 cm; 15) - elongated with small pit from a depth of 283 cm.

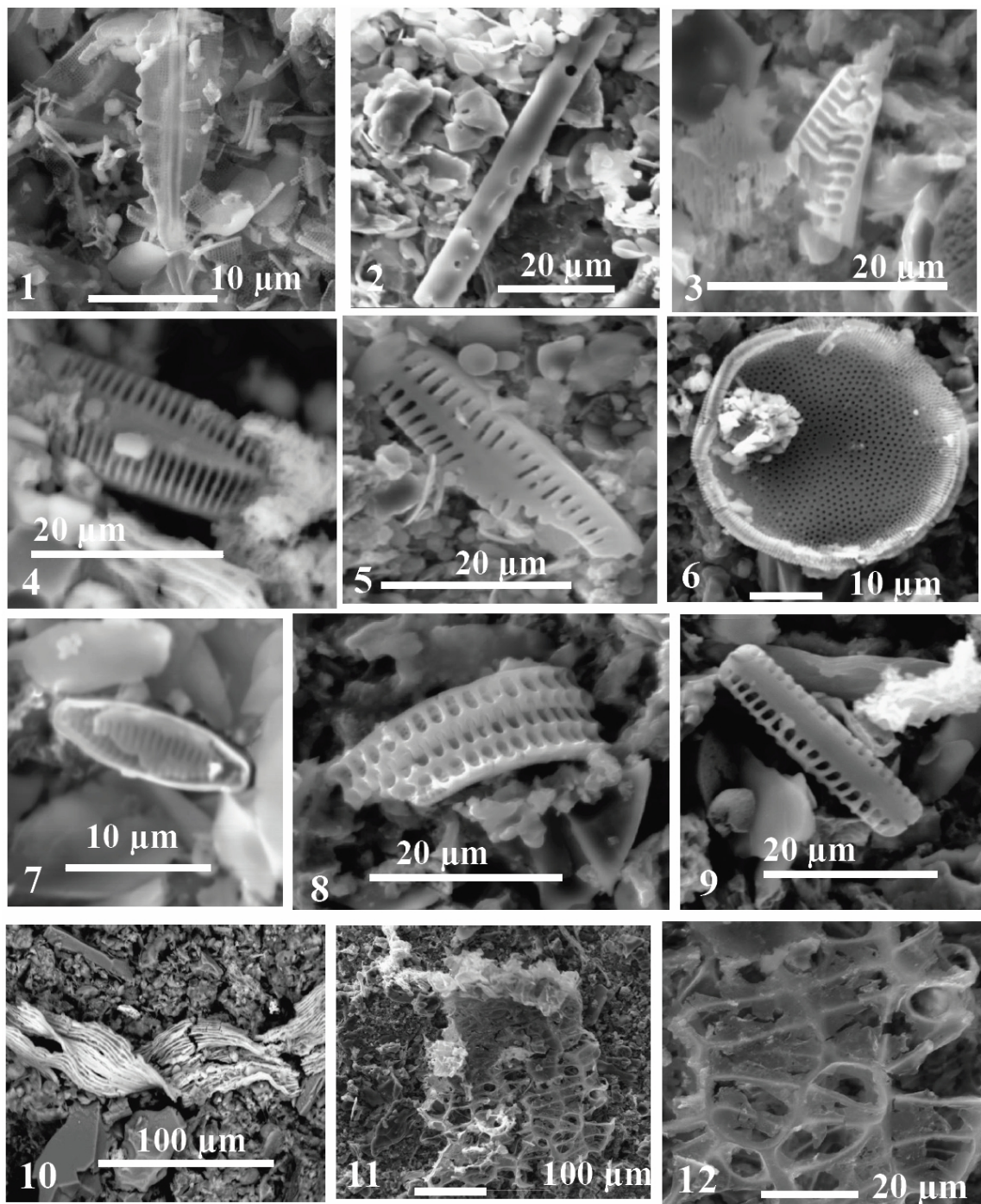


Figure 4: SEM images of the biogenic inorganic matter: 1, 3-9) different species of diatoms collected throughout the profile), 2) debris of the sponge spikules (depth 63 cm), 10) mineralized plant tissue, depth 77 cm (back scattering electrons detector), 11) mineralized plant tissue, depth 350 cm and 12) enlargement of 11.

4.2 Terrigenous or detrital mineral

The terrigenous or detrital mineral matter in the AIA can be divided into a) primary rock-forming minerals, b) accessory minerals, and c) volcanic ash (tephra and pumice). The approximate distribution of these minerals in the peat profile is shown in

Table 1 and 2. These materials were supplied by atmospheric inputs in the ombrotrophic sections of the peat profile (above ~ 400 cm). In the minerotrophic zone, however, these materials were derived from both atmospheric and local, aquatic sources. The identified terrigenous minerals are described below.

Table 1: Distribution of rock-forming minerals, identified using SEM, in the inorganic fraction (AIA) of the Oreste peat profile.

Depth (cm)	Rock-forming minerals					
	Quartz	Mica	Feldspar	Na-Ca plagioclase	Pyroxene +amphibole	Amphibole
0-3	*	*	*	-	-	-
5	*	*	*	*	*	-
50	*	*	*	*	*	*
63	*	*	*	*	-	-
77	*	*	*	*	*	*
102	*	*	-	-	-	-
121	*	*	*	*	*	*
140	*	*	*	*	*	-
156	-	*	-	*	*	*
175	*	*	-	*	*	-
193	*	*	*	*	-	-
213	*	*	*	*	*	*
247	*	*	*	*	-	-
266	*	*	-	*	-	-
278	*	*		*	*	*
282	*	*	*	*	*	-
298	-	-	-	-	-	-
302	-	-	-	-	-	-
312	-	*	*	-	-	-
334	*	*	*	*	-	-
350	*	*	-	*	-	-
384	*	*	*	*	-	-
455	*	*	*	*	-	-
482	*	*	*	-	*	-

Note: - absent; *present; **common; ***abundant

Table 2: Distribution of accessory minerals and volcanic ash particles, identified using SEM, in the inorganic fraction (AIA) of the Oreste peat profile.

Depth (cm)	Accessory minerals							Volcanic ash
	Zircon	Monazite	Titanite	Chromite	Rutile	Ilmenite	Ilmenite with MnO	(pumice/tephra)
0-3	-	*	-	*	-	*	-	*
5	*	*	*	*	*	*	*	*
50	*	-	*	*	*	*	*	*
63	-	-	*	*	*	*	-	*
77	-	-	*	*	*	*	-	*
102	*	*	-	-	-	*	-	*
121	-	-	**	-	**	*	-	*
140	*	*	*	-	*	*	-	*
156	*	-	*	-	-	*	-	*
175	*	*	*	*	*	*	*	*
193	*	*	*	-	*		*	*
213	*	-	**	-	**	*	-	*
247	*	*	-	-	*	*	*	*
266	-	*	-	-	-	-	-	*
278	-	-	-	-	-	-	-	*
282	*	-	-	-	*	*	-	*
298	-	-	-	-	*	*	-	***
302	-	-	-	*	*	-	-	***
312	-	-	-	-	-	-	-	*
334	*	*	-	-	-	-	-	*
350	*	*	-	-	*	*	-	*
384	*	-	-	-	-	*	-	*
455	-	-	-	-	-	-	-	*
482	*	-	-	-	-	-	-	*

Note: - absent; *present; **common; ***abundant

4. 2.1 Rock-forming minerals

The rock-forming minerals identified in the AIA are quartz, mica, plagioclase feldspar, potassium feldspar, plagioclase, pyroxene and amphiboles (Figure 5); all are found throughout the entire core.

Quartz - SiO₂

Quartz is common throughout the entire profile except at a depth of 293 - 305 cm where pumice is predominant (Table 1 and 2). In the Oreste bog, three kinds of quartz with different size and morphology are

observed (Figure 5: 1 - 3). The first group contains larger grains, with dimensions ranging from 100 x 80 µm to 50 x 40 µm with fresh, angular shapes, frequently with irregular and rarely with conchoidal fractures. The second group consists of the fragments of prismatic crystals with a maximum dimension of 40 µm. The third group is composed of the fine fraction with particle dimensions < 10 µm and made up of angular to rounded fragments.

Mica - KAl₂(OH)₂(Al,Si₃O₁₀)

Micas are represented by large, thin flakes which range in size from 60 x 40 µm up to 200 x 150 µm with smooth and foliated surfaces (Figure 5: 4). Mica grains are found in all AIA samples from the Oreste peat profile, except at a depth of 289 - 302 cm where tephra is found. The analyses show that all grains have the chemical composition of a muscovite.

Plagioclase – $Na(Al,Si)_3O_8$ - $Ca(Al_2Si_2O_8)$ and Potassium Feldspar– $K(Al,Si)_3O_8$

Plagioclase feldspar is essentially a complete solid solution series from pure albite ($NaAlSi_3O_8$) to pure anorthite ($CaAl_2Si_2O_8$). In the Oreste peat profile, 12 grains of albite and 11 grains of andesine were observed. Plagioclases are more widely distributed and more abundant than alkali K-feldspars. Plagioclases are found at different stages of dissolution (Figure 5: 5 - 10).

As a rule, both types of minerals have a tabular habit, usually striated, often with typical etch pits (Huang, 1989). The size of the feldspars ranges from 20 µm to 150 µm and they are distributed evenly throughout the entire profile.

Minerals such as **Pyroxene** ($Ca(Mg,Fe,Al)(Al,Si)_2O_6$) and **Amphibole** ($NaCa_2(Mg,Fe)_4(Fe,Al)OH_2(Al_2Si_6O_{22})$), are also present throughout the entire profile in the form of single grains and are frequently weathered (Figure 5: 11 and 12). The size of these minerals ranges from 10 µm to 60 µm. Most of them have the shape of well formed thick, short prisms with sharp edges. Crystals with subhedral stripes are also found.

4. 2.2 Accessory minerals

Accessory minerals were observed throughout the entire profile (Table 2). The identified accessories minerals include zircon, chromite, monazite, titanite, rutile, and ilmenite (Figure 6). The size of these minerals varies from less than 10 up to 50 µm, with most specimens in the range of 15 - 20 µm.

Magnetite - $FeFe_2O_4$

Magnetite with high concentrations of Cr_2O_3 is a mineral from the spinel group. The minerals of this group form a solid solution from magnetite to chromite - $(Fe,Mg,Zn,Mn)(Al,Fe,Cr)_2O_4$. Magnetites are present in all samples down to a depth of

77 cm, but are found only in two samples in deeper layers (175 and 302 cm). The identified magnetite grains are irregular in shape, sometimes with small dust particles adhering (Figure 6: 1). In total, eleven grains of magnetite were observed, ranging in size from 2 µm to 50 µm (Figure 6: 1). All of them show a variable composition of Cr_2O_3 component (6 – 43 %) and extremely high FeO (53 – 67 %). Grains with admixture of Ni (up to 6 %) and Zn (up to 3 %) are also present.

Zircon - $ZrSiO_4$

Zircon, a common mineral in detrital deposits, is found throughout the profile without recognizable variation with respect to depth. More than 40 grains were observed and 15 analyses were made. The description of zircon habits are divided into four groups: a) fine prismatic crystals varying in shape with particle size (< 10 up to 30 µm); b) curved, elongated grains that are 15 – 30 µm in length; c) fragments of both types with sizes ranging from 10µm to 60 µm; and d) metamictic grains with rounded shapes, approximately 15 µm in size. The latter form of zircon implies that the crystal was destroyed under the influence of Th and U that are commonly present in small amounts in zircons. The chemical compositions of the zircons are relatively constant with ZrO_2 (61 – 66 %) and HfO_2 (0.95 - 1.50 %). At a depth of 140 cm, a zircon was found containing Y_2O_3 (14 %). The images of zircon habit are presented at the Figure 6: 2 – 6.

Monazite - $(REE)PO_4$

Monazite has been found in some samples (Table 2) and eight analyses of them were made. The monazite grains are irregular angular or rounded in shape and usually have a small size varying from <10 µm up to 30 µm (Figure 6: 7 - 9). Metamictic grains of monazite were also found. The contents of P_2O_5 fluctuate from 24 to 35%, La_2O_3 - 12 to 18%, Ce_2O_3 – from 29 to 42%. Small amounts of Pr_2O_3 (up to 2%) and Nd_2O_3 (up to 12%) are also present. In addition, Fe, Al, and Si were detected.

Rutile - TiO_2

Rutile or anatase (trimorph of rutile) minerals are commonly found throughout the peat profile (Table 2). Ten grains of rutile

(Figure 6: 10 - 13) and anatase (Figure 6: 14) in the peat profile are divided into two groups. The first group contains rounded, sometimes elongated grains, frequently covered by a crust of leucoxene, ranging in size from 20 μm to 70 μm . The second group contains crystals of the rutile with needle-like habit. A cluster of rutile crystals is observed in the sample from a depth of 298 cm, corresponding to the greatest abundance of tephra. The rutile crystals are 70 μm in length and observed with glass of rhyolitic composition. Slender acicular single crystals from 5 μm to 20 μm also are present at depths of 140, 175 and 193 cm. The irregular, angular debris of the Ti-bearing minerals with sizes ranging from < 5 μm up to 30 μm are found. Typical crystals of anatase with dipyrnidal habit are found at a depth of 350 cm.

Ilmenite - FeTiO_3

Ilmenite is abundant in the peat profile of the Oreste bog (Table 2). The ilmenite grains ranging from 5 μm to 50 μm in length, characteristically as irregular massive, sometimes rounded grains. Some ilmenites have conchoidal fracture. The surface of the grains is frequently weathered with etch pits. The images of ilmenite are presented in Figure 6: 15 -18. Grains with small, adhering dust particles were also found; these are probably leucoxene. Aggregates of ilmenite with Na-Ca plagioclase are also observed. Fragments of ilmenite grains are also abundant in the samples.

Based on the chemical composition, the ilmenite grains can be divided into two

groups. The chemical composition of the first group (18 samples) is TiO_2 (48 – 61 %) and FeO (34 - 48 %), with admixture of MnO (up to 5 %), MgO (up to 4 %), SiO_2 (up to 5 %), Al_2O_3 (up to 2 %), and sometimes CaO (2 – 3 %). The second group (8 samples) yielded the following chemical composition: TiO_2 (41 - 58 %), FeO (18 – 37 %), MnO (8 – 29 %), and an admixture of SiO_2 (up to 3%). The presence of these two groups of ilmenite can be explained by the fact that ilmenite (FeTiO_3) and pyrophanite (MnTiO_3) form a solid solution.

However, ilmenite with low MnO component is found throughout the entire profile, while ilmenites with large MnO contents (high pyrophanite mole fraction) are found in the upper part of the profile down to ca. 50 cm and then again in the interval of 175 - 282 cm.

Titanite - $\text{CaTiO}(\text{SiO}_4)$

Titanite or sphene is observed above 213 cm in the peat profile (Table 2). The chemical composition of sphene consists of TiO_2 (33 – 37 %) and CaO (27 – 30 %), with no detectable admixtures. The shapes of the sphene are a) elongated with smooth curves, b) isometric rounded, and c) irregular angular debris with traces of weathering, sometimes with small adhering dust particles. All grains are between 10 μm and 30 μm in size. SEM images of titanite are shown in Figure 6: 19 – 22.

In addition, few other rare minerals are also found in the profile: Mn-bearing garnet at a depth of 282 cm; ksenotime and the orthite at depths of 140 and 213 cm.

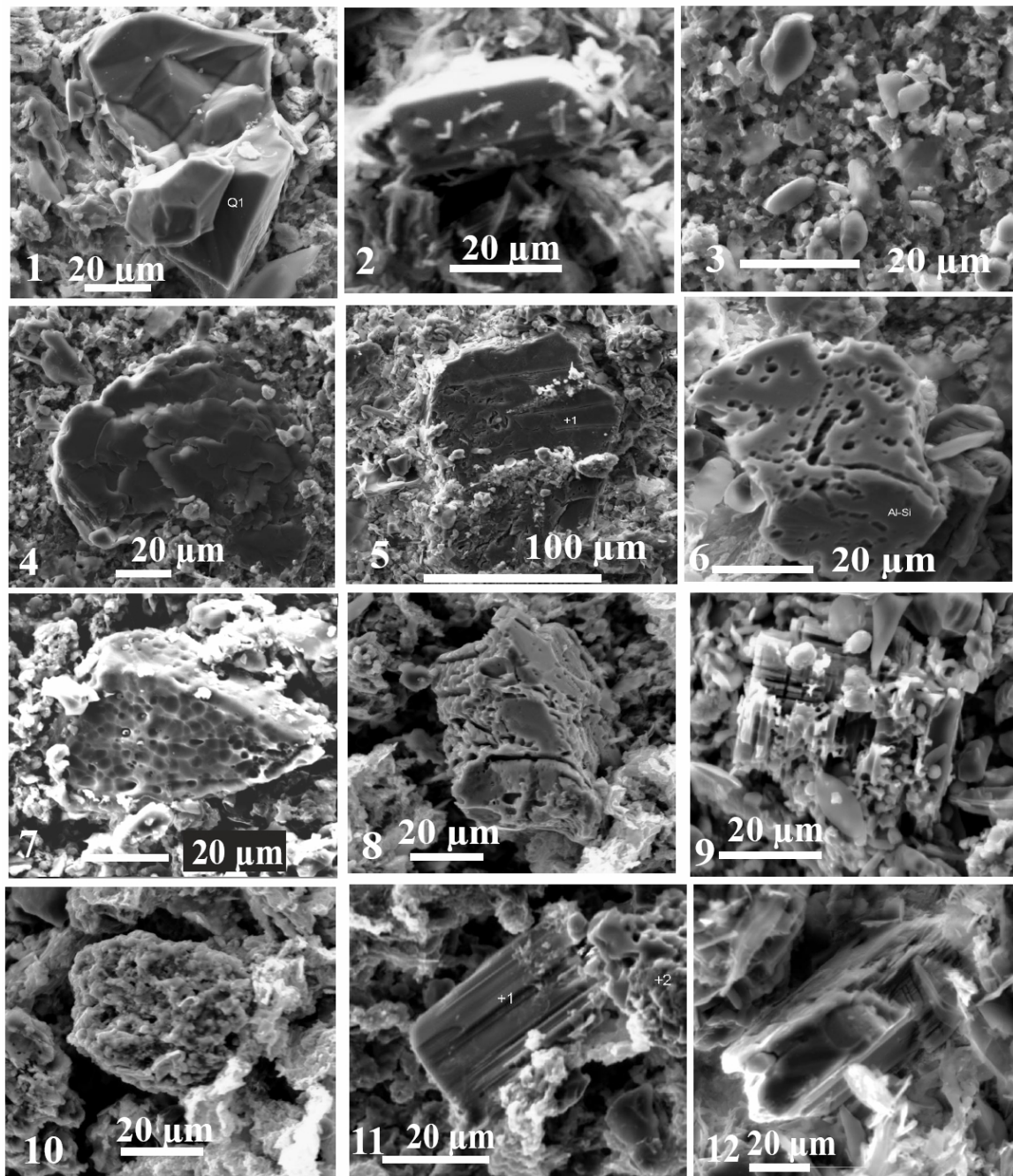


Figure 5: SEM images showing the primary rock-forming minerals: **quartz** 1) angular shapes with irregular fracture, depth 350 cm, 2) fragment of a prismatic crystal, depth 50 cm, 3) a fine fraction of angular, rounded grains, depth 140 cm, 4) flake of **mica**, depth 350 cm; plagioclase grains with different stages of weathering: 5) **Na-Ca plagioclase**, at the depth of 5 cm, 6) Na-Ca plagioclase, at depth of 350 cm, 7) pronounced etch-pitting, depth of 384 cm, 8) advance stage of weathering, depth of 282 cm, 9) grain of the **K-feldspar**, depth of 175 cm, 10) aggregate with chemical composition of K-feldspar, depth of 282 cm; 11) probably grain of **pyroxene** from the depth at 278 cm, 12) grain of **amphiboles**, possibly grunerite $(\text{Fe,Mg})_7(\text{OH})[\text{Si}_8\text{O}_{22}]$ at the depth 50 cm.

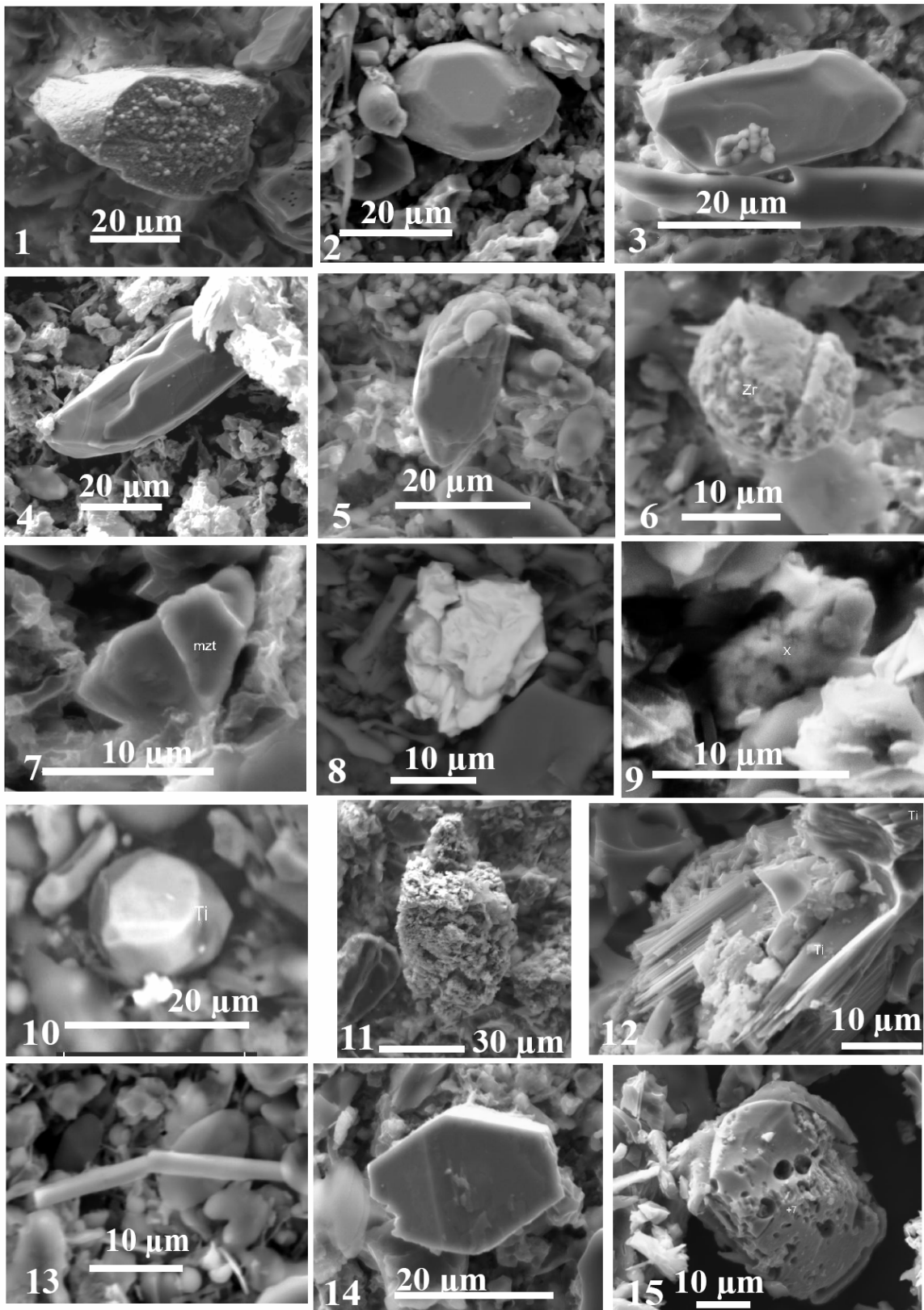


Figure 6: SEM images of representative accessory minerals. Some of the images are obtained by using back scattering electrons for the better mass contrast. **Magnetite:** 1) the grain of the magnetite with adhering dust particles at the depth of 77 cm. **Zircon** grains: 2) and 3) fine crystals with different habits are observed at depths of 175 and 350 cm respectively, 4) and 5) curved, elongate grains at depths of 282 and 175 cm, 6) rounded metamict grains from the depth of 5 cm. **Monazite** grains: 7) elongate, rounded grain from the depth of 350 cm, 8) irregular angular grain with conchoidal fracture, depth of 5 cm (back scattered electron detector), 9) metamict grains of monazite from the depth of 102 cm. **Rutile** grains: 10) isometric, rounded

(Fig 6; continued) crystal of the rutile from the depth of 5 cm (back scattered electron detector), 11) rutile covered by leucoxene at the depth of 77cm, 12) cluster of needle-like rutile crystals with volcanic glass, depth at of 298 cm, 13) a single needle-like rutile crystal from depth of 175 cm, 14) crystal of anatase at depth 350 cm.

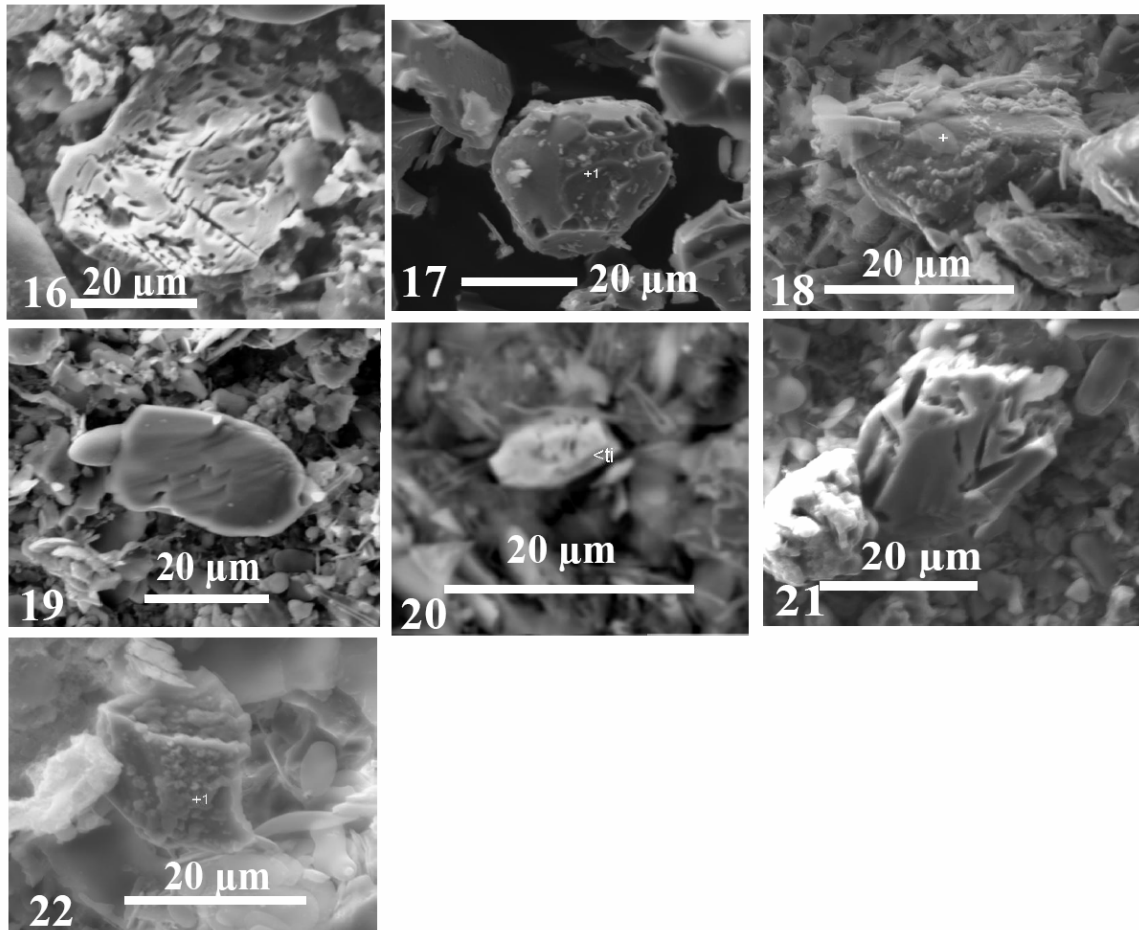


Figure 6 (continued): **Ilmenite** grains: 15) and 16) irregular massive shape, frequently dissolved with pits at depths of 298 and 384 cm respectively, 17) massive rounded grains of ilmenite from depth of 298 cm, 18) the grains of ilmenite with small adhering particles, perhaps leucoxene, depth of 63 cm. The shapes of grains of **Titanite** are 19) elongated with smooth curved, at depth of 175 cm, 20) isometric crystal, depth of 63 cm (back scattered electron detector), 21) and 22) irregular angular debris with traces of weathering, with adhering dust particles at depths of 193 and 5 cm, respectively.

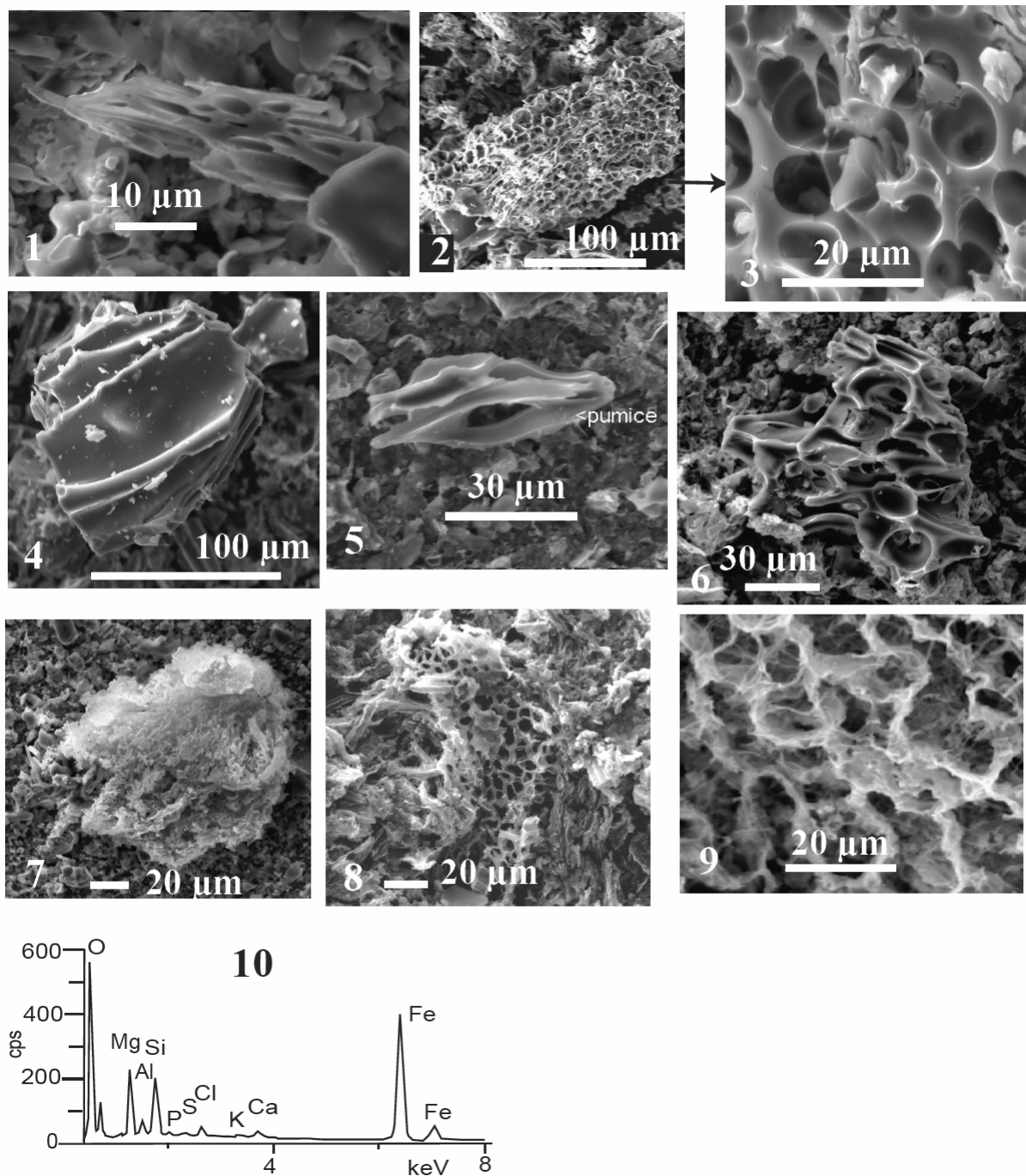


Figure 7: SEM images showing grains of pumice: 1) grains with well-developed, ovoid vesicles, 2) highly vesicular grains of pumice and 3) same pumice, magnified, 4) nonvesicular pumice, 5) grains with sharp edges, 6) pumice grain with trace of vesicle, 7) and 8) sponge-like smectite from depths of 175 cm and 278 cm, respectively, 9) increased magnification of the smectite from the depth of 175 cm, 10) EDS-spectra of sponge-like smectite from the depth of 278 cm.

4. 2.3 Volcanic ash

The Oreste bog is located on the territory bordering with the Andean Austral Volcanic Zone (AVZ) (Stern et al., 1984). Six active volcanoes in the AVZ have erupted andesites and dacites (Stern et al. 1996, Kilian et al., 2003). Because of ash falls, volcanic glasses or pumices are expected to occur

commonly. Thirty-six pumices from Oreste bog were investigated using EDS. They have a rhyolitic and dacitic in composition. The distribution of pumices in the profile of the Oreste bog and SEM micrographs of volcanic glasses or pumices are shown in Table 2 and Figure 7: 1 - 6, respectively. Pumices with

rhyolitic compositions are distributed in all samples throughout the entire core.

Pumices are angular to subangular grains with diverse, well-developed ovoid vesicular and thin vesicle walls. In the Oreste bog the pumice is highly vesicular with elongated vesicles and delicate irregular surfaces. Some pumice, apparent on grain surfaces, has sharp vesicle edges. The nonvesicular grains, consisting of small, plate-like shards are observed as well. All pumice grains are well preserved. The dimensions of the pumice fragments range from 80 x 60 μm to 250 x 100 μm .

At depths between 293 and 305 cm, there are abundant tephra with single grains of rutile, chromite, ilmenite and sponge-like (or moss-like) Al-silicates (Heiken, 1974; Heiken et al., 1985). In all the samples from the Oreste bog profile, grains of sponge-like Al-silicate were observed, ranging in size from 10 to 150 μm . In the Oreste bog these structures are abundant at the depth of 266 cm and comprise more than 60 % of the samples at depths of 278, 312 and 482 cm. At a depth of 482 cm these minerals change habit from sponge-like to needle-like. The chemical composition of this mineral is composed of Fe and Si, with traces of Mg, Al, Ca, K, P, S, Cl, and sometimes Ti.

Heiken (1974) noticed this structure in rhyolitic rocks and they have been described by him as moss-like. Unfortunately, Heiken (1974) did not show any chemical composition data or X-ray fluorescence spectra. Meunier (2005) has described these structures as dioctahedral smectites, originating either from dacitic or rhyolitic volcanic ashes in lakes, swamps, lagoons or shallow sea areas. SEM images and SEM-EDX spectra of this mineral in the profile of the Oreste bog are shown in Figure 7: 7 – 10.

5 Weathering and diagenesis of mineral particles in the peat bog

There are three principal mechanisms of mineral dissolution in acidic bogs: proton-promoted dissolution, in response to the low pH values which characterise acidic bog waters, ligand-promoted dissolution, as a result of the abundance of organic acids, and reductive dissolution, of Fe- and Mn-bearing

phases, in response to the anoxic conditions. Although these characteristics of bogs imply that the fluids should be aggressive and corrosive toward fine-grained mineral particles supplied by atmospheric transport, this hardly appears to be the case. In fact, plagioclase and alkali feldspars, mica, and even hornblende and pyroxene, occur commonly throughout the profile. Moreover, their distribution with depth is effectively uniform which indicates that their relative abundance has not been altered by six thousands years of burial in these acidic fluids. In contrast, ilmenite containing high mole percent pyromorphite is found only down to depths of approximately 50 cm, and magnetite down to ca. 77 cm. Assuming that the rates of deposition of these minerals from the atmosphere was constant over time, some Fe- and Mn-bearing accessory minerals, apparently have been lost by *in situ* weathering and diagenesis. The most likely explanation for the gradual disappearance of the Fe- and Mn-bearing minerals is reductive dissolution reactions which are probably coupled to the oxidation of organic matter. Except for these, the remarkable preservation of siliceous mineral particles from biogenic sources, rock-forming minerals, and volcanic ash suggests that variations in the vertical distribution of these unreactive mineral phases must reflect changes in their supply from the atmosphere, rather than due to chemical processes taking place within the bog. The minerals which constitute the AIA fraction, therefore, and their variation with time as peat accumulates, offers the promise of new information about the changing rates and sources of atmospheric mineral dusts.

6 Possible sources of terrigenous minerals

6.1 Input from soil dust

The primary, rock-forming minerals commonly found throughout the peat profile are often large: the maximum lengths found (μm), in decreasing order, are approximately mica 200, plagioclase 150, quartz 100, and pyroxene and amphibole 60; in general, these particles are far too large to have been derived from long-range transport. In fact, these dimensions are characteristic of locally-derived soil materials (Schütz, 1989), with the mountains surrounding the Oreste bog the most

likely dominant source. In contrast to these large particles, there is an abundance of much smaller material: these are the mineral grains in the fine fraction ($<10\ \mu\text{m}$) which can be seen in the SEM pictures as a groundmass surrounding the larger particles. In the absence of quantitative data about the particle size distribution, we assume that most of the mass of the AIA fraction is made up of these materials. Given their size, they certainly may have been transported much greater distances. The primary, rock-forming minerals which make up the AIA, therefore, were supplied both by local as well as long-range atmospheric transport.

All of the Ti and Zr-bearing accessory minerals, which are found in Oreste bog, are regarded as very stable minerals that are able to survive many cycles of weathering, sedimentary transport, diagenesis, metamorphism, and anatexis (Milnes and Fitzpatrick, 1989). Similarly, monazite is also considered very resistant to weathering (Allen and Hajek, 1989). The relatively homogeneous distribution of these accessory minerals is consistent with the effectively constant, vertical concentration profiles of Ti and Zr in the peat core (Sapkota et al., submitted). Taken together, the lack of variation in the relative abundance of primary and accessory minerals, combined with the uniform distribution of Ti and Zr concentrations, suggests that the peat bog has been subjected to effectively constant inputs of soil-derived mineral dusts. This finding, in turn, suggests that the climatic conditions in this region have been very stable for the last ca. 6000 years.

6.2 Volcanic input

In contrast to the uniform distribution of soil-derived mineral particles, there is an anomalous zone of elevated AIA concentrations which is dominated by large tephra grains and glass shards; this layer which is also enriched in Ti and Zr (Sapkota et al., submitted) provides clear evidence of a specific volcanic event. The Oreste bog is located on the territory bordering the Andean Austral Volcanic Zone (AVZ) (Stern et al. 1984). All six volcanoes in the AVZ have erupted andesites and dacites (Stern and Kilian, 1996), however, only two volcanoes are identified to

be active during the late Holocene: Mt. Burney and Mt. Augilera (Stern, 1990; Kilian et al., 2003). The Oreste bog is located approximately 400 km southeast (55°S) of Mt. Burney (52°S) and is known to have deposited tephra as far south as Tierra del Fuego (Kilian et al., 2003). The mid-Holocene explosion of Mt. Burney (ca. 4200 cal yr BP) is found at a depth in the Oreste Bog which, according to the age-depth model based on ^{14}C age dating (Sapkota et al., submitted), is contemporaneous with this age. The eruption of Mt. Burney, therefore, is the most likely source of the abundant tephra grains between 293 and 305 cm found in the bog.

In addition to the anomalous inputs from the Mt. Burney eruption, a few grains of pumice are commonly found in AIA samples throughout the peat profile from the Oreste bog. However, these materials are much smaller, and their distribution uniform. These volcanic materials were probably supplied to the bog indirectly, from the physical weathering and subsequent ablation and suspension of tephra particles which previously had been deposited on the soils of the region. Once again, the homogeneous distribution of these materials with depth through the peat bog supports the view of relatively constant climatic conditions during the past 6,000 years.

7 Conclusion

The ombrotrophic (ie rain-fed) section of the Oreste Bog (Isla Navarino, Chile) from southernmost South America, has been accumulating atmospheric mineral dusts for more than six thousand years. The following physical, mineralogical, and chemical properties of the peat profile indicate that relatively stable climatic conditions have prevailed for the past ca. 6000 yrs. First, except for one anomalous zone, the abundance of AIA is uniform with depth (time). Second, the size, morphology and distribution of primary, rock-forming minerals, as well as accessory phases, is also uniform. Third, although there are pronounced differences in density between primary minerals (quartz, plagioclase, mica) and accessory minerals (zircon, monazite, rutile, ilmenite, and titanite), the proportions of these light and heavy phases, respectively, are constant. Fourth, the siliceous particles of

biogenic origin are also distributed uniformly through the profile.

The presence of both small (<10 µm) as well as large particles (up to 200 µm) indicate that dusts have been supplied both by local as well as long range atmospheric transport. The zone of anomalous concentrations of AIA at a depth of 300 cm is dominated by particles of volcanic ash. Dating the peat profile using ¹⁴C and the development of an age-depth model suggest that these tephra grains can be attributed to the Mt. Burney eruption at ca. 4200 cal yr BP.

Acknowledgements

This project was funded by the Deutsche Forschungsgemeinschaft (DFG, SH 89/2-2 and SH 89/2-3). We are indebted to Dr. Vera Markgraf for providing the peat core, which she collected from the Oreste bog with funding from the National Science Foundation USA (NSF-EAR-9709145) and for her comments and suggestions. We thank Dr. Andriy Cheburkin for support with the SEM, Anastasiya Kurznel for editorial assistance.

References

- Allen, B.L.** and **Hajek, B.F.**, 1989. Mineral occurrence in soil environments. In: Dixon, J.B. and Weed, S.B. (Eds.), *Minerals in soil environments*. Soil Science Society of America, Wisconsin, USA, pp. 199 – 278.
- Andrejko, M.J., Cohen, A.D., and Raymond Jr., R.**, 1983. Origin of mineral matter in peat. In: Raymond Jr., R. and Andrejko, M. J. (Eds.), *Mineral matter in peat. Its occurrence, form, and distribution*. US DOE, Los Alamos, pp. 3 – 24.
- Biscaye, P.E., Grousset, F.E., Revel, M., Gaast, S.V., Zielinski, G.A., Vaars, A., and Kukla, G.**, 1997. Asian provenance of glacial dust (stage 2) in the Greenland Ice sheet project 2 Ice core, summit, Greenland. *Journal of Geophysical Research* 102, 26765 – 26781.
- Björck, S. and Clemmensen, L.B.**, 2004. Aeolian sediment in raised bog deposits, Halland, SW Sweden: a new proxy record of Holocene winter storminess variation in southern Scandinavia? *The Holocene* 14, 677 – 688.
- Carnelli, A.L., Theurillat, J.-P., and Madella, M.**, 2004. Phytolith types and type-frequencies in subalpine-alpine plant species of the European Alps. *Review of Paleobotany and Palynology* 129, 39 – 65.
- Clapperton, C.M.**, 1993. Quaternary geology and geomorphology of South America. Elsevier, Amsterdam, 779 pp.
- Delmonte, B., Petit, J.R., and Maggi, V.**, 2002. Glacial to Holocene implications of the new 27000-year dust record from the EPICA Dome (East Antarctica). *Climate Dynamics* 18, 647 – 660.
- Finney, H.R. and Farnham, R.S.**, 1968. Mineralogy of the inorganic fraction of peat from two raised bogs in northern Minnesota. *Proceedings of the 3rd International Peat Congress Quebec, Canada*, pp. 102 – 108.
- Gabrielli, P., Planchon, A.M., Hong, S., Hyuan Lee, K., Do Hur, S., Barbante, C., Ferrari, C.P., Petit, J.R., Lipenkov, V.Y., Cescon, P., and Boutron, C.F.**, 2005. Trace elements in Vostok Antarctic ice during the last four climatic cycles. *Earth and Planetary Science Letters* 234, 249-259.
- Gaudichet, A., Petit, J.R., Lefevre, R., and Lorius, C.**, 1986. An investigation by analytical transmission electron microscopy of individual insoluble microparticles from Antarctic (Dome C) ice core samples. *Tellus* 38B, 250 – 261.
- Goudie, A.S., and Midelton, N.J.**, 2001. Saharan dust storms: nature and consequences. *Earth-Science Reviews* 56, 179 – 204.
- Harrison, S.P. and Kohfeld, K.E.**, 2001. The role of dust in climate changes today, at the last glacial maximum and in the future. *Earth-Science Reviews* 54, 43 – 80.

- Heiken, G.**, 1974. An atlas of volcanic ash. Smithsonian Institution Press, Washington DC, USA, 101 pp.
- Heiken, G. and Wohletz, K.**, 1985. Volcanic ash. University of California Press, Berkeley, 246 pp.
- Heusser, C.J.**, 1998. Deglacial palaeoclimate of the American sector of the Southern Ocean: Late Glacial-Holocene records from the latitude of Canal Beagle (55 °S), Argentine Tierra del Fuego. *Palaeogeography, Palaeoclimatology, Palaeoecology* 141, 277 – 301.
- Huang, P.M.**, 1989. Feldspars, olivines, pyroxenes, and amphiboles. In: Dixon, J.B. and Weed, S.B. (Eds.), *Minerals in Soil Environments*. Soil Science Society of America, Wisconsin, USA, pp. 976 – 1039.
- Kilian, R., Hohner, M., Biester, H., Wallrabe-Adams, H.J., and Stern, C.R.**, 2003. Holocene peat and lake sediment tephra record from the southernmost Chilean Andes (53° - 55° S). *Revista Geologica de Chile* 30, 23 – 37.
- Kondo, R., Childs, C., and Atkinson, I.**, 1994. Opal Phytoliths of New Zealand. Manaaki Whenua Press, Lincoln, Canterbury, New Zealand. 80 pp.
- Kraemer, P.E.**, 2003. Orogenic shortening and the origin of the Patagonian orocline (56 °S. Lat). *Journal of South American Earth Sciences* 15, 731 – 748.
- Leinen, M., Prospero, J. M., Arnold, E. and Blank, M.**, 1994. Mineralogy of aeolian dust reaching the North Pacific Ocean. *Journal of Geophysical Research* 99, 21017 – 21023.
- Meunier, A.**, 2005. *Clays*. Springer. Berlin, Heidelberg.
- Milnes, A.R. and Fitzpatrick, R.W.**, 1989. Titanium and zirconium minerals. In: Dixon, J.B. and Weed, S.B. (Eds.), *Minerals in soil environments*. Soil Science Society of America, Wisconsin, USA, pp. 1131 – 1206.
- Nickling, W.G.**, 1983. Grain-size characteristics of sediment transported during dust storms. *Journal of Sedimentary Petrology* 53, 1011 – 1024.
- Olivero, E.B. and Martinioni, D.R.**, 2001. A review of the geology of Argentinean Fuegian Andes. *Journal of South American Earth Science* 14, 175 – 188.
- Piperno, D.R.**, 1988. *Phytolith analysis: An Archeological and Geological Perspective*. Academic Press Inc., San Diego, USA, 280 pp.
- Prospero, J.M.**, 1996. The atmospheric transport of particles to the ocean. In: Ittekkot, V., Schäfer, P., Honjo, S., and Depetris, P.J. (Eds.), *Particle flux in the Ocean*. John Wiley and Sons Ltd., pp. 19 – 52.
- Röthlisberger, R., Mulvaney, R., Wolf, E.W., Hutterli, M.A., Bigler, M., Sommer, S., and Jouzel, J.**, 2002. Dust and sea salt variability in central East Antarctica (Dome C) over the last 45 kyrs and its implications for southern high-latitude climate. *Geophysical Research Letters* 29, doi:10.1029/2002GL015186.
- Schütz, L.**, 1989. Atmospheric mineral dust - properties and source makers. In: Leinen, M. and Sarnthein, M. (Eds.), *Paleoclimatology and Paleometeorology: Modern and Past Patterns of Global Atmospheric Transport*. Kluwer Academic Publishers, Dordrecht, The Netherlands, pp. 359 – 383.
- Steinmann, P. and Shotyk, W.**, 1997. Geochemistry, mineralogy, and geochemical mass balance on major elements on two peat bog profiles (Jura Mountains, Switzerland). *Chemical Geology* 138, 25 – 53.
- Stern, C.R.**, 1990. The tephrochronology of southernmost Patagonia. *National Geographic Research* 6, 110 – 126.
- Stern, C.R., Futa, K. and Muehlenbachs, K.**, 1984. Isotope and Trace element data for Orogenic Andesites from the Austral Andes. In: Harmon, R.S. and Barreiro, B.A. (Eds.), *Andean Magmatism: Chemical and Isotopic*

constraints. Shiva Publishing Limited, UK, pp. 31 – 46.

- Stern, C.R. and Kilian, R.,** 1996. Role of subducted slab, mantle wedge and continental crust in the generation of adakites from the Andean Austral Volcanic Zone. *Contributions to Mineralogy and Petrology* 123, 263 – 281.
- Svensson, A., Biscaye, P.E., and Grousset, F.E.,** 2000. Characterization of Late Glacial continental dust in the Greenland Ice Core Project ice core. *Journal of Geophysical Research* 105, 4637 – 4656.
- Thomas, D.S.G.,** 1989. The nature of arid environments. In: Thomas, D.S.G. (Ed.), *Arid Zone Geomorphology*. Belhaven Press, London, pp. 1 – 8.
- Tuhkanen, S.,** 1992. The climate of Tierra del Fuego from a vegetation geographical point of view and its ecoclimatic counterparts elsewhere. *Acta Botanica Fennica* 145, 1 – 64.
- Vallelonga, P., Gabrielli, P., Rosman, K.J.R., Barbante, C., and Boutron, C.F.,** 2005. A 220 kyr record of Pb isotopes at Dome C Antarctica from analyses of the EPICA ice core. *Geophysical Research Letters* 32, doi:10.1029/2004GL021449.
- Wüst, R.A.J., Ward, C.R., Bustin, R.M., and Hawke, M.I.,** 2002. Characterization and quantification of inorganic constituents of tropical peats and organic-rich deposits from Tasek Bera (Peninsular Malaysia): implication for coals. *International Journal of Coal Geology* 49, 215 – 249.
- Wüst, R.A.J., and Bustin, R.M.,** 2003. Opalin and Al-Si phytoliths from a tropical mire system of West Malaysia; abundance, habit, elemental composition, preservation and significance. *Chemical Geology* 200, 267 – 292.

Chapter 4

Dusts source

-Chapter 4-
Holocene record of $^{87}\text{Sr}/^{86}\text{Sr}$ ratios in dust components of an ombrotrophic bog at the southernmost edge of South America: volcanic inputs, atmospheric soil dust, and comparison with ice core dust of the Eastern Antarctic Plateau

Bernd Kober*, Atindra Sapkota, Andriy K. Cheburkin and William Shotyk

Institute of Environmental Geochemistry, University of Heidelberg, Im Neuenheimer Feld 236, D-69120, Heidelberg, Germany

*Corresponding author; Tel: + 49 62 21 54 48 99, Fax: + 49 62 21 54 52 28;

Email: bernd.kober@urz.uni-heidelberg.de

Submitted to Earth and Planetary Science Letter, 2006

Abstract

$^{87}\text{Sr}/^{86}\text{Sr}$ ratios have been analysed of acid soluble (ASA) and insoluble (AIA) components in ashed peat from a 5.42 m core taken from the Oreste moorland bog on the Isla Navarino, Chile (55°13'13" S, 67°37'28" W). The data record covers 13 ka of peatland evolution. Peat was found to be an excellent archive of Sr isotopes in insoluble particles, and even of Sr isotope compositions of labile components. The ASA compositions are dominated by marine aerosols in the ombrotrophic peat layers (< 6 ka BP) and by remnants of soil fluids in the fen peat (6 – 13 ka BP). Four Holocene explosive eruptions of the “Mt. Burney” volcano released tephra from the Australandean Volcanic Zone over a distance of ~ 450 km to the bog. AIA of these peat layers have significantly reduced $^{87}\text{Sr}/^{86}\text{Sr}$ ratios due to the mantle Sr isotope signature of the tephra. Outside of these layers, the Sr isotope compositions of AIA in the ombrotrophic peat vary within a narrow range ($0.7087 < ^{87}\text{Sr}/^{86}\text{Sr} < 0.7090$, average: 0.70884 ± 0.00014). The Holocene data record indicates that release of dusts from the various Argentinian sediment deposits gives rise to well mixed air masses and stable signals over southern South America. Moreover, the observed average value is identical to $^{87}\text{Sr}/^{86}\text{Sr} = 0.7088 \pm 0.0002$ calculated from data reported for Eastern Antarctic ice core dust (ICD) during Glacial Stage 2. The Argentinian sediment deposits have been the only sources of dust in the Eastern Antarctic ice at least since the Late Pleistocene. The partly higher $^{87}\text{Sr}/^{86}\text{Sr}$ ratios published for ICD of earlier Glacial Stages are possibly due to episodic periglacial expansion of Patagonian ice sheets over the Argentinian plains east of the Andean crest. This eastward ice sheet growth was reported to have been larger during earlier glaciations than during the Last Glacial Maximum. Ice sheet transgressions during cold periods of the Quaternary could have forced episodic disruption of dust release from Patagonian sediment deposits south of 37-41°S which were reported to be less radiogenic than those in the more northern sediment deposits of Argentina.

Key words: $^{87}\text{Sr}/^{86}\text{Sr}$ ratio, ombrotrophic peat bog, Southern Chile, mineral aerosol, Antarctica, Patagonian glaciation

1. Introduction

Mineral aerosols are important atmospheric tracers for the modelling of air mass circulations and of atmospheric source-to-sink transport phenomena in space and time [1-7]. Dust particles can be investigated via their mineralogy, geochemistry and their radiogenic isotope compositions to identify the contributions from the possible source areas (“PSA”; [8-17]). Recent dust transport can be investigated by direct collection of aerosols from the atmosphere ([18-20]). Past transfers of dust particles are recorded by sediments [21,22], ice cores [23], snow deposits [24] and peat bogs [25]. All these natural archives can be used to analyse spatial and temporal variations in predominant source areas and depositional fluxes.

Various studies have used the tracer concept [26] for investigations of ice cores from Antarctica in order to discuss the origin of mineral aerosols stored in the ice, and to constrain the coupling of air masses over Antarctica to continental areas in the southern hemisphere [6,8,27]. Radiogenic isotope compositions of ice core dust demonstrated the great potential of Sr and Nd isotopes to constrain the PSAs by comparison of the isotope distributions in the dust with those of soils and sediments from South Africa, South America, Australia and New Zealand [6,28]. The data available to date have indicated that southern South America is the most important source area for dust to Antarctic ice. However, those data do not convincingly exclude contributions from other continents (Australia, South Africa) and do not yet allow straight-forward calculations of the relative importance of the PSAs based on mixing models [28]. The main reasons for the uncertainties are PSA isotope heterogeneities due to the radiogenic isotope evolutions of the soil and sediment particles within the source deposits as well as particle grain-size related fractionation. To help circumvent these principle systematic problems for the application of radiogenic isotopes as source tracers of Antarctic dust, fine grain size fractions (<5µm) of PSAs have been investigated [29,30]. The Sr and Nd isotope distributions showed that Nd isotopes vary less than Sr isotopes in the southern

hemisphere and that contributions from South Africa and Australia are improbable. Ice core dust data available to date are compatible with South American soil and sediment fractions <5 µm. But there remains an overlap with New Zealand and Antarctic dry valley data which does not allow dust transfer from these PSAs to the East Antarctic Plateau to be excluded [30]. Clearly, the distinction between single- or multiple-source paleorientation needs to be made. An unambiguous interpretation of the dust fluxes to the Antarctic ice shield is a prerequisite for the successful reconstruction of southern hemispheric circulation of air masses and of atmospheric transfer paths both for aerosols of natural and anthropogenic origin.

An alternative approach to constrain the present day as well as past radiogenic isotope composition of windblown particles deflated from southern South American sources would be to study mineral aerosols which are preserved in the ombrotrophic sections of peat bogs of southernmost South America. Ombrotrophic peat bogs are abundant in Tierra del Fuego [31] and they have been receiving mineral dust particles for thousands of years. Moreover, they are suitably located intermediately between the extensive loess plains of Argentina and the Antarctic continent.

The first aim of our study was to develop a protocol for the analysis of Sr isotopes in insoluble particles trapped by the peat matrix. The second aim was to apply Sr isotope compositions of insoluble particles in a peat bog from southern South America to constrain the Sr isotope composition of dust released from the Argentinian soils and sediment deposits and collected by the moorland enroute to the Antarctic continent.

2. Sample location and description

Southern South America is a region with intense volcanic activities. Particles from volcanoes of the Andean cordillera are widely distributed, and have been even observed in Antarctic ice [32]. Andean calc-alkaline volcanics have also been reported to be major sources of the Argentinian loess deposits ([28,33]) which cover an area of approximately 1.1×10^6 km² of Argentina

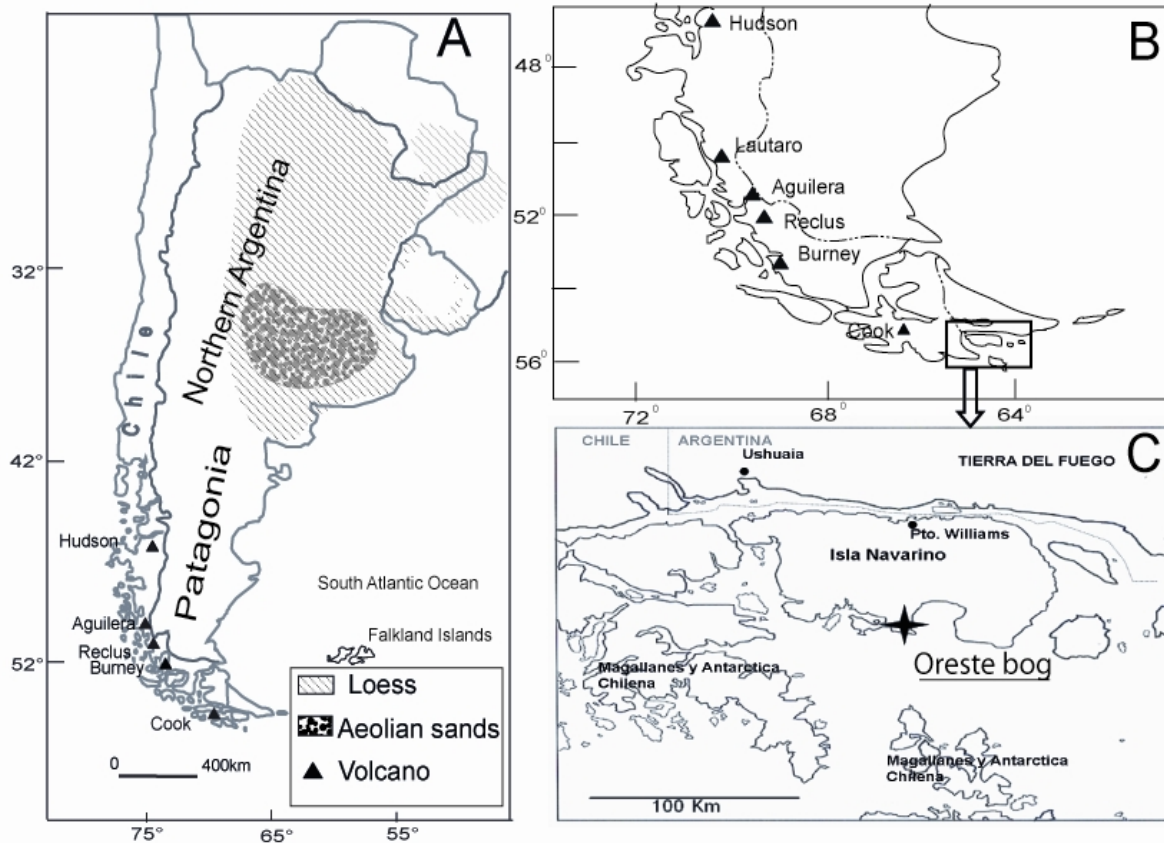


Fig. 1: Peat core sampling location of Oreste bog at the southernmost edge of South America: A: position of sampling area relative to the Andean cordillera and to the Argentinian sediment deposits; Argentinian loess areas plotted after [68]; (not plotted: Patagonian loess deposits) B: position of sampling area relative to the Australandean Volcanic Zone (AVZ) in Chile; C: Oreste bog on the Southern Isla Navarino/Chile ($55^{\circ}13'13''S$, $67^{\circ}37'28''W$).

([34], Fig. 1). The frequent particle transfer from Andean volcanoes to lake sediments [35,36] and peat bogs [37] delimits the undisturbed recording of remote particles deflated from the Argentinian sediment deposits. Therefore, we selected for our study a peat bog in a position maximum distance (approx. 450 km) from the southern Andean explosive volcanoes called the Australandean Volcanic Zone (AVZ, [38]; Fig. 1). The Oreste Bog is influenced by the air masses at the southernmost edge of South America south of the Argentinian sediment deposits (Fig. 1). It is located south of Tierra del Fuego on the west side of Bahía Windhound, Southern Isla Navarino, Chile ($55^{\circ}13'13''S$ and $67^{\circ}37'28''W$) (Fig. 1). It is a magellanic moorland bog with an average precipitation 800 mm yr^{-1} [39, 40]. The climate of the area is dominated by prevailing Westerlies [40]. The ombrotrophic bogs, including Oreste bog, within this maritime climate zone show rapid

growth, often overlying minerotrophic peat [31].

The rocks underlying the bog belong to the Late Jurassic-Early Cretaceous Rocas Verdes Marginal Basin with Upper Jurassic silicic volcanic rocks, Lower Cretaceous deep-marine volcanoclastic turbidites and slope mudstones, and Upper Cretaceous plutonic rocks [41].

The Oreste bog was cored in 1995 using a Livingston piston corer of 7.5 cm diameter to a depth of 542 cm. From 530 to 542 cm the peat was strongly minerogenic, containing silt and clay. The complete peat profile was sliced into 2 cm sections. The detailed description of the site location, geology and the preparation of samples for age dating, physical, chemical and mineralogical analysis is described elsewhere [42].

3. Analytical methods

To date, we know of no published Sr isotope analyses of mineral particle fractions of ombrotrophic peat. We have therefore established a protocol for the separation of Sr components in the organic matrix from those hosted in the insoluble particles. The bulk material was first dried and milled, then ashed at 550 °C overnight. The acid insoluble ash (AIA) was separated from the acid soluble ash (ASA) and collected on polycarbonate membrane filter (0.2 µm pore size) by leaching the peat ash with 1M HCl for 15 minutes followed by filtration. To remove the Sr components in the ASA quantitatively from the AIA fraction, 3 cleaning steps were carried out by repeatedly rinsing the deposits on the filters with 5 ml 1M HCl. The cleaning procedure was completed by final rinsing with 18 MΩ H₂O. It was found that after this cleaning procedure the contributions from any labile Sr remaining in processed residuum were within the range of the verified total-procedure Sr blanks: these were <1ng (including the filter procedures and extraction steps). These Sr blank contributions were negligible compared to the processed sample Sr (0.1-1µg in the case of insoluble fractions, 10 – 100 µg in the case of labile Sr).

Trace element distributions in bulk peat and in the generally small AIA fractions (2 – 4 mg, collected on the membrane filters) were determined using non-destructive and energy-dispersive miniprobe multielement (EMMA) XRF analyzer [43]. All chemical results are reported in detail by [42].

The insoluble fractions were digested using 2 ml 48 % HF + 1 drop HNO₃ (conc.). Strontium was extracted from the ASA and AIA sample solutions using ion exchange chromatography employing SrResin[®] (EiChrom) according to the extraction protocols e.g. of [44,45]. Strontium extracts were loaded to single Ta filaments and were analysed using a multicollector thermal ion mass spectrometer (MC-TIMS Finnigan MAT261). The average between-sample reproducibility was found to be 0.01 % (2σ) which was 1 – 2 times larger than the within-run precision. The ⁸⁷Sr/⁸⁶Sr ratios were internally normalized to ⁸⁶Sr/⁸⁸Sr = 0.1194. SRM987 (NIST) isotope standard was used

for routine monitoring and correction of instrumental bias and trends.

4. Results

4.1 Chemical and mineralogical trends in the peat column

The investigated peat core represents approximately 13 ka of peat accumulation (¹⁴C dating, [42]). The lowermost section between 542 cm and 425 cm shows a decreasing amount of AIA from more than 6 % at the bottom to less than 0.2 – 0.3 % at approximately 4 m (Fig. 2). This section represents the minerogenic part of the bog and records the decreasing importance of mineral particle transfer from local sources, having vanished ca. 6 ka ago. In the ombrotrophic part of the bog (above 425 cm) the amount of AIA remained rather constant (0.1 – 0.5 % of dry weight). AIA generally contains phytoliths, quartz, feldspars, biotite, sphene, zircon, rutile, monazite, ilmenite and clay minerals such as illite [42]. At depths of 50–60 cm, at 152 cm and again at ca. 300 cm significant contributions from volcanic eruptions such as pumice fragments were observed. In the fen peat some more dispersed pumice fragments were found, but no marked tephra layer was observed probably due to dilution of AIA by soil particles. The change from fen peat (dominated by local soil sources) to ombrogenic peat (increasingly influenced by remote sources) is recorded by the chemical composition of bulk peat and AIA as well. While the bulk Sr concentration of peat ash varies in a rather narrow range of 30 – 70 ppm (30 – 40 ppm in lowermost samples, 35 – 70 ppm above 450 cm), the bulk peat Sr/Ti ratio increased by an order of magnitude in the transition from minerotrophic to ombrotrophic peat. This change reflects the vanishing importance of locally-derived mineral particles and thus the decreasing flux of solid particles to the peat column (Fig. 2). In addition, it also indicates that over the whole history of peat accumulation the Sr input was profoundly influenced by a Sr component which is not associated with insoluble particles. Both SiO₂ and K₂O in AIA are diminished by approximately a factor of 2 in the course of the change in depositional conditions (Fig. 2).

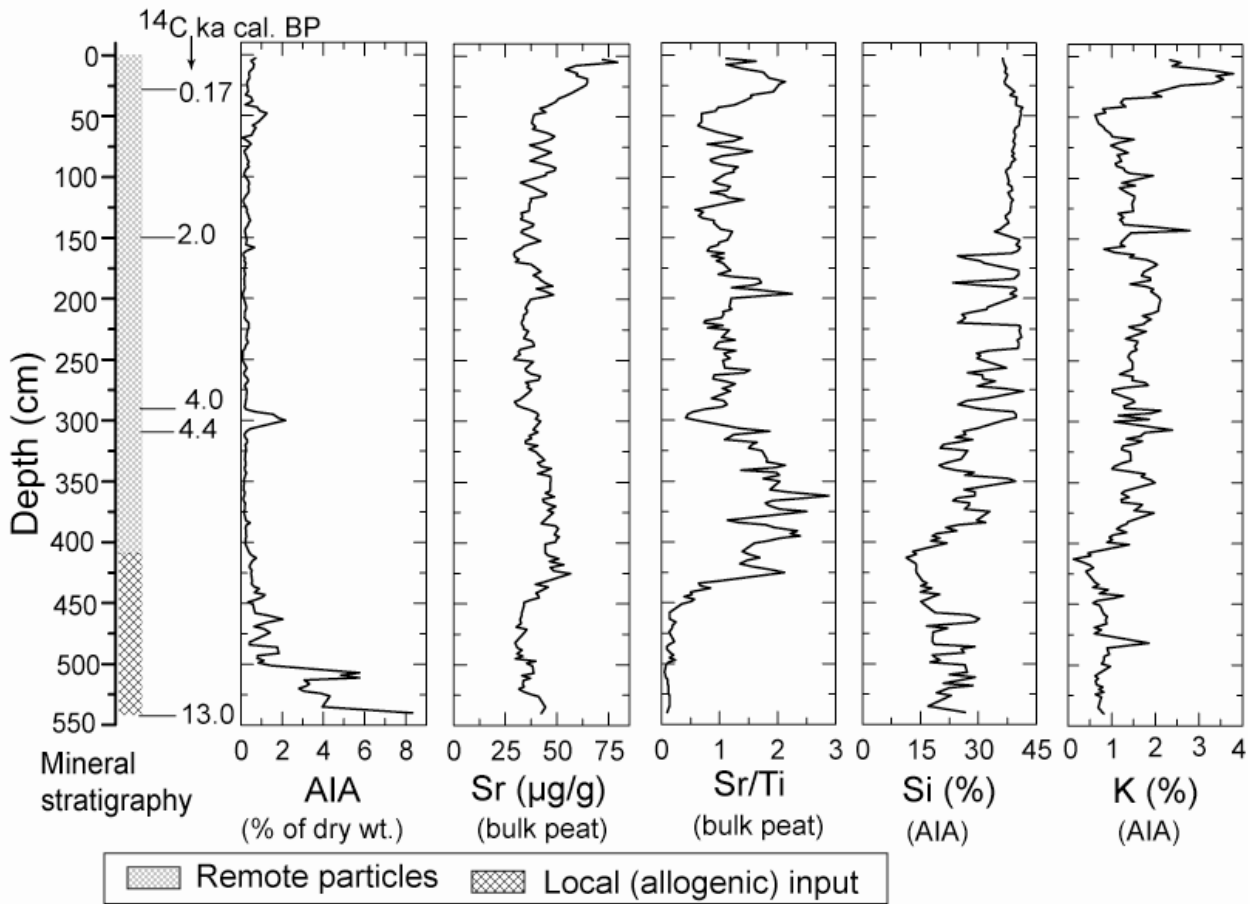


Fig. 2: Plots versus core depth for the peat core from the Oreste bog, Chile: relative amount of AIA in peat ash, ^{14}C dated layers (cal. BP), Sr concentrations and Sr/Ti ratios in bulk peat, Si and K concentrations in AIA. Larger amounts of tephra particles (pumices) are found in particular in the peat layer at ~ 300 cm, indicated also by increased amounts of AIA. Pumices found in the fen peat (below 425 cm) are too much dispersed in the bottom peat and too diluted by soil particles to clearly identify a single tephra layer.

This evolution indicates a significant dilution of AIA by non-silicate and K-poor insoluble particles in the fen peat compared to the ombrotrophic parts. The K_2O contents in the AIA of the ombrogenic sections roughly vary around 1.5 – 2 %. However, there are significant deviations from these values in the topmost peat, with >3 – 4 % in the uppermost 30 cm, and with a decrease of K_2O concentrations to <1 % at 50 – 60 cm, where a significant amount of tephra was observed.

4.2 Strontium isotopes

The $^{87}\text{Sr}/^{86}\text{Sr}$ ratios of AIA and ASA are listed versus core depth in Tab. 1 and plotted versus depth in Fig. 3. The ASA record forms a rather smooth trend over the core. The $^{87}\text{Sr}/^{86}\text{Sr}$ in ASA increased from 0.7067 in the fen peat to about 0.7091 in the topmost matrix. This trend is significantly different from the Sr isotope compositions

found in AIA. Sr isotope trends in the insoluble peat fractions are more complex and variable in the range 0.7055 – 0.7090, with two distinct characteristics: an apparent “background” aerosol with $^{87}\text{Sr}/^{86}\text{Sr}$ ratios > 0.7087, and four distinct less radiogenic peaks with $^{87}\text{Sr}/^{86}\text{Sr}$ ratios < 0.7080. The trends being different between ASA and AIA clearly indicate that the Sr components contained in the ASA are not in isotope equilibrium with Sr hosted in the AIA particles, neither in the ombrotrophic nor in the minerogenic parts of the bog. Instead, the data sets demonstrate that the AIA components preserved their individual Sr isotope composition over several thousand years of bog evolution despite the conditions of the anaerobic, organic-rich acidic environment of peat bogs (~ pH 4). This agrees with the conclusions of [46] and [47], that atmospherically deposited, fine grained silicate and non-silicate minerals

in peat bogs do not dissolve appreciably, or even measurably, after their deposition and fixation in the organic material. The AIA $^{87}\text{Sr}/^{86}\text{Sr}$ ratios show four local minima at approximately 50 – 60 cm, 150 cm, 300 cm and 500 – 520 cm in agreement with the observed abundant tephra particles. The

minimum $^{87}\text{Sr}/^{86}\text{Sr}$ values in these four layers are different and are in the range 0.7055 – 0.7080. Outside of these layers, the AIA Sr isotope compositions are rather uniform and in the ombrotrophic peat vary in the rather narrow range of $0.7087 < ^{87}\text{Sr}/^{86}\text{Sr} < 0.7090$.

Tab. 1 $^{87}\text{Sr}/^{86}\text{Sr}$ ratios of acid soluble (ASA) and acid insoluble (AIA) components in peat ash from the Oreste bog, Chile. Errors given are on the 95 % confidence level.

Depth (cm)	$^{87}\text{Sr}/^{86}\text{Sr}$ (AIA) \pm	$^{87}\text{Sr}/^{86}\text{Sr}$ (ASA) \pm
19	0.70862 0.00005	0.70910 0.00007
35	0.70900 0.00004	
60	0.70689 0.00003	0.70898 0.00005
90	0.70882 0.00009	
136	0.70872 0.00003	
158	0.70798 0.00005	
189	0.70894 0.00004	0.70901 0.00006
216	0.70886 0.00004	
245	0.70893 0.00012	
293	0.70547 0.00006	0.70856 0.00004
316	0.70829 0.00008	
368	0.70898 0.00006	
420	0.70869 0.00007	
471	0.70644 0.00007	0.70713 0.00010
491	0.70597 0.00006	
516	0.70820 0.00005	0.70668 0.00004

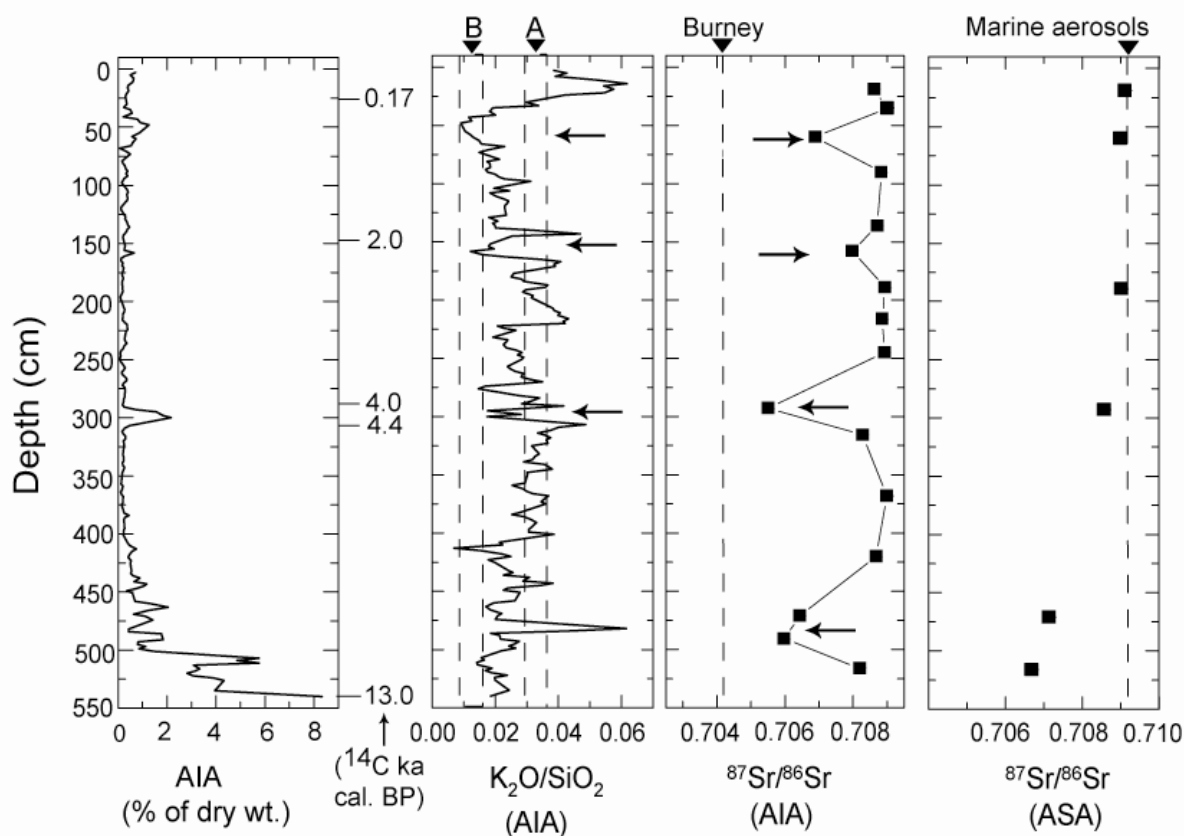


Fig. 3: Plots versus core depth for the peat core from the Oreste bog, Chile: K_2O/SiO_2 ratios and $^{87}Sr/^{86}Sr$ ratios in acid insoluble peat ash (AIA), $^{87}Sr/^{86}Sr$ ratios in acid soluble peat ash (ASA). The dates for the 4 eruptions of volcano Mt. Burney (Australandean Volcanic Zone (AVZ)) are given by the arrows (data from [37] and [53]). K_2O/SiO_2 ratios of Mt. Burney (“B”, AVZ) and Mt. Aguilera (“A”; AVZ) volcanoes are taken from [54] and [55].

5. Discussion

Strontium components can be derived from any of the following sources: marine aerosols (sea salt), aquatic inputs derived from chemical weathering in the watershed, local soil particles, dust components from long range atmospheric transport and tephra particles. The relative importance of these contributions can be reconstructed using the isotope composition of Sr in the ASA and in the AIA.

5.1 Sources of Sr in Acid Soluble Peat Ash (ASA)

The $^{87}Sr/^{86}Sr$ ratios found in ASA of the topmost 2 m of the investigated core vary merely within the range of 0.7090 – 0.7091 (Tab. 1, Fig. 3). This Sr isotope composition is nearly identical to the one of modern seawater (0.70918, [48]). The Sr isotope data, therefore, indicate that non-sea spray Sr which could have been released by leaching of Sr from solid particles (e.g. feldspars and

mica) is negligible. Given the mobility of Sr in acidic peat bog profiles [49], these results support the view that chemical weathering of silicate aerosols in peat is undetectable. Further, the Sr isotope data demonstrate the limited extent of upward migration of fluids from the fen peat into the ombrotrophic parts of the bog. This holds especially true for the 50 – 60 cm level where particles are abundant. There is clearly no significant transfer of Sr from remote dust particles and tephra components hosted in the bog to labile components in the organic matrix. Labile Sr in the ombrotrophic peat is dominated by sea spray aerosols. A slightly lower $^{87}Sr/^{86}Sr$ ratio of 0.7086 at approx. 3 m depth (another tephra dominated layer) may have been more influenced by minor transfer of less radiogenic Sr from fen peat fluids (~ 0.707 , Tab. 1, Fig. 3) than by release of Sr components leached from the less radiogenic tephra material. The ASA Sr composition in the fen peat material is significantly less

radiogenic (0.7067 – 0.7071) and in isotopic disequilibrium with the ombrotrophic parts. The Sr isotope composition of ASA in the basal levels of the bog is slightly more radiogenic than typical rocks of southernmost South America (0.703 – 0.706, e.g. [50]), possibly due to mixing of local Sr components carried in soil waters with sea spray strontium. Thus the ASA data are compatible with continuous transfer of sea spray to the bog over the whole Holocene. These inputs were mixed with soil strontium in the bottom (fen) parts of the bog. The labile Sr components or labile Sr mixtures (in ASA) were sufficiently well archived that they could be recovered upon ashing of the peat and leaching the ash using HCl. The fractionation scheme employed here appears to have successfully recovered this fraction of Sr, without contributions by the Sr hosted in insoluble mineral particles within the peat matrix.

5.2 Sources of Sr in Acid Insoluble Peat Ash (AIA)

The heterogeneous Sr isotope composition of AIA (Tab. 1, Fig. 3) cannot be due to a single source of insoluble particles in the core. The episodic and systematic changes of the $^{87}\text{Sr}/^{86}\text{Sr}$ ratios suggest episodic contributions from volcanic eruption centres to the accreting peatland. Various strong explosive eruptions have occurred in the Southernmost South Volcano Zone (SSVZ) and the Australandean Volcano zone (AVZ) during the Holocene whose tephra fans could have reached the moorland bogs of Isla Navarino. The strongest eruption during the Holocene is reported to be that of Mt. Hudson (SSVZ) dated at 7.7 – 7.8 ka cal. BP [51-53]. Further important eruptions were reported for Mt. Aguilera (AVZ; approx. 3.6 – 3.8 ka cal. BP, [37,53]) and for Mt. Burney with four strong Holocene eruptions including one documented by historical records (A.D. 1910) as well as those found dating from approx. 2 ka cal. BP, from 4.25 (\pm 0.12) ka cal. BP and from approx. 9.0 – 9.2 ka cal. BP [37,53]. Stern and Kilian [54] and Naranjo and Stern [55] showed that the the $\text{K}_2\text{O}/\text{SiO}_2$ ratios in the volcanic magmas are diagnostic of the various eruption centres and can be used to

attribute tephra glasses to the different eruption events [37]. The $\text{K}_2\text{O}/\text{SiO}_2$ ratios of AIA in the investigated core are plotted in Fig. 3 vs. depth and vary mostly in the range 0.02 – 0.04. However, at depths corresponding to Sr isotope ratios with reduced radiogeneity (Fig. 3) they are significantly lower than 0,02 and drop as low as 0.009 – 0.15. These $\text{K}_2\text{O}/\text{SiO}_2$ values rule out contributions from Mt. Hudson and Mt. Aguilera whose ratios are typically in the range of >0.02 (Mt. Hudson) and >0.03 (Mt. Aguilera), and instead favour tephra influx from Mt. Burney (0.009 – 0.016; [37]; Fig. 3). The 4 episodes of episodically reduced $^{87}\text{Sr}/^{86}\text{Sr}$ ratios of AIA in the studied peat are therefore interpreted as having arisen from four explosive eruptions of volcano Mt. Burney (AVZ) during the Holocene. The different minimum $^{87}\text{Sr}/^{86}\text{Sr}$ ratios of AIA in the four peat layers contaminated by tephra indicate different degrees of binary mixing of volcanic material with remote dust particles in the ombrotrophic peat as well as admixture of mineral aerosols with local soil particles in the fen peat. None of the 4 levels influenced by the Mt. Burney eruptions fully meets the Sr isotope composition of Mt. Burney magma (0.7042; [50, 51]). This indicates that in each of the four layers the analysed AIA was mixed with significant amounts of non-volcanic insoluble particles. This mixing process may have taken place during atmospheric transport, or within the peatland, subsequent to deposition. While the strontium contributed by tephra components makes up about 80 % of total strontium in AIA at a depth of ca. 3 m, the volcanic contributions to total strontium in AIA are significantly smaller in the case of other peaks, ranging from 20 % to 50 %. The Sr isotope data for the uppermost peak (at ca. 50 – 60 cm) is much less radiogenic than overlying and underlying analysed layers. This highly resolved response of Sr isotope compositions of the AIA to the young eruption event (ca. 0.1 ka ago) reflects the ability of the bog to preserve rapid changes in the composition of the AIA. Above and below the layers which are influenced by the eruption events, $^{87}\text{Sr}/^{86}\text{Sr}$ ratios of AIA are more radiogenic and fairly constant. The preservation of Sr

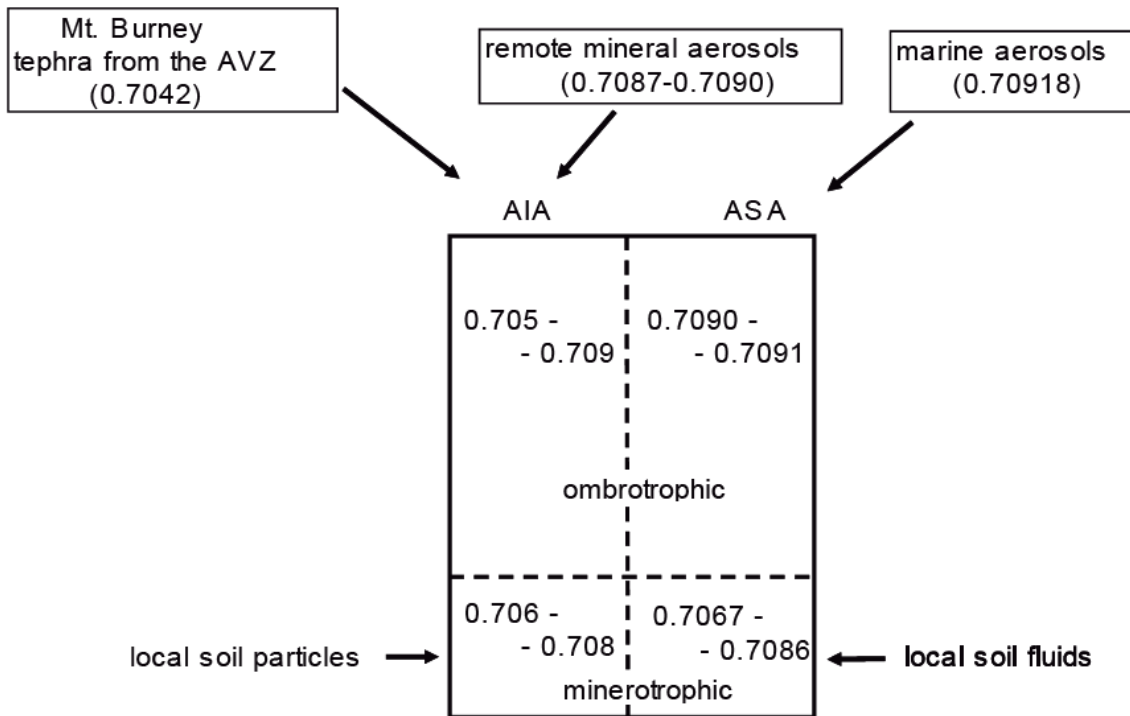


Fig. 4 Summary of Sr sources and their isotope compositions, derived from the Holocene Sr isotope compositions in acid insoluble (AIA) and acid soluble (ASA) components of ashed peat from the Oreste bog, Chile. The Sr isotope composition of Mt. Burney volcanoes is taken from [50] and [51].

isotope disequilibria between tephra influenced and tephra uninfluenced layers indicates that the Sr isotope data can indeed be used to constrain the average Sr isotope composition of remote dust components which were intercepted and preserved by the organic material during peatland evolution. All the ombrotrophic peat layers, when uninfluenced by eruption events, have similar AIA Sr isotope compositions ($^{87}\text{Sr}/^{86}\text{Sr} = 0.7087 - 0.7090$) with an average value of 0.70884 ± 0.00014 . The variation over the whole ombrotrophic part of the peat column is only 2 – 3 times larger than the experimental errors. Thus the AIA data demonstrate that dusts found in the organic matrix had a rather constant Sr isotope composition at least over the past 6 ka.

The results of the previous discussion of ASA and AIA components in the studied moorland bog are summarized in Fig. 4 in the light of seaspray aerosols, soil waters, locally-derived soil particles, mineral aerosols of volcanic origin and dust transferred from remote sources.

6. Implications

6.1 Sr isotope composition of dusts released from Argentinian sediments

The Sr isotope compositions of dust particles were reported to be rather complex tracers for the identification of PSAs [28,33]. Particle sorting during sediment transport can generate grain-size related fractionation of Sr isotope compositions [56-58]. The Argentinian loess deposits which were proposed to be major sources of Antarctic ice dust [6,28] were largely derived from pyroclastic materials released from Andean volcanoes with mantle isotope signatures [33]. Weathering of tephra and tephra related sediments can form K- and Rb-rich fine clays which can very rapidly evolve their Sr isotope compositions from mantle- to crustal-type signatures. Sediment deposits, even if predominately derived from weathering and erosion of mantle related volcanic ejecta with less radiogenic Sr, can evolve their Sr isotopes within rather short episodes during the Quaternary to more radiogenic compositions which resemble rocks and sediments with a longer lasting crustal

residence. Loesses and soils can host rather radiogenic particles in the finest fractions, mixed with coarser grains with less evolved Sr isotope compositions. Windblown microparticles from these sediment deposits carry Sr isotope compositions into the air, which are significantly more radiogenic than the bulk sediments.

The grain size related fractionation of Sr isotope compositions has been discussed in detail by Basile et al. [28], Smith et al. [33], and Delmonte et al. [30] in the context of the PSA discussion for Antarctic ice dust. Significantly higher $^{87}\text{Sr}/^{86}\text{Sr}$ ratios compared to bulk sediments have been observed by [6], [28] and [30] in the $<5\ \mu\text{m}$ fractions of southern hemispheric sediment areas as PSAs of mineral aerosols that reached the Eastern Antarctic Plateau. Argentinian bulk loesses north of $37 - 41^\circ\text{S}$ have $^{87}\text{Sr}/^{86}\text{Sr}$ ratios in the range of $0.7059 - 0.7123$ [33] while those south of $37 - 41^\circ\text{S}$ are characterized by generally lower ratios of $0.7060 - 0.7067$ [28]. The $<5\ \mu\text{m}$ sediment fractions are generally more radiogenic than the respective bulk sediments [6,28] and show a rather large spread in the range of $0.705-0.713$ with an average value calculated from the data set of [30] of 0.7083 ± 0.0023 . This straightforward averaging of the sediment data of [30] is somewhat arbitrary because it does not take into account the different but unknown source strengths of the various sediment areas. Despite this the result is an acceptable first order estimation of the Sr isotope composition of mineral aerosols mixed in the air masses over southern South America from the various Argentinian fine particle sources. The rather good agreement of this average value with the $^{87}\text{Sr}/^{86}\text{Sr}$ ratio of 0.70884 ± 0.00014 deduced from the analyses of AIA in the bog studied here supports the view that this archive is a suitable monitor of the mineral aerosol composition over Argentina. Moreover, the data demonstrate that mixing of fine particles in the atmosphere over southern South America appears to be highly effective over time and yields a Sr isotope composition in the mineral aerosols which was homogeneous and well-defined over at least the last 6 ka despite the Sr isotope

heterogeneities of source loesses and soils in Argentina.

6.2 Implications for the sources of Antarctic Ice Core Dust (ICD)

The data presented here indicate that the Argentinian sediment areas are a source of dust much more homogeneous and stable with respect to the Sr isotope composition of the atmospheric dust load than was assumed by e.g. [28] and [30]. The average $^{87}\text{Sr}/^{86}\text{Sr}$ ratio of $0.70884(14)$ can be directly compared to the ICD data of [6], [28] and [30]. The available Sr and Nd isotope ICD data for the Eastern Antarctic Plateau reported for the ice cores “Dome C” ($74^\circ39'\text{S}$, $124^\circ10'\text{E}$) and “Vostok” ($78^\circ28'\text{S}$, $106^\circ48'\text{E}$) was reviewed by [30], including new data for the “Dome C” area (ice core “EPICA Dome C”, $75^\circ06'\text{S}$, $123^\circ24'\text{E}$) and the ice core “Vostok”. The five available data sets, which were attributed to Glacial Stage 2, represent the period of 26.4 ka cal. BP to 15.9 ka cal. BP with an average value of $^{87}\text{Sr}/^{86}\text{Sr} = 0.70878(16)$. These results are fully compatible to the moorland bog data of the present study. This good agreement rules out significant contributions of dust from Antarctic dry valleys and from the southern island of New Zealand (cf. data of [30]) since the Last Glacial Maximum (LGM). Therefore, the Argentinian sediment deposits have been the predominant or even exclusive source of ICD at least since the LGM, except for two explosive volcanic events at 3,45 ka cal. BP and 6,87 ka cal. BP [8,32], as indicated by two ash layers in the ice core “Vostok”. Our conclusion of paleorientation of eastern Antarctic ICD to Argentina since the LGM confirms the conclusion of [33], that the severe climatic change at the end of the Pleistocene did not induce an effective change of dust mobilization phenomena in Argentina. The proposed more northern positions of the Westerlies and the Antarctic Polar Front during the late Pleistocene ([59,60]) did not induce mobilization of relatively more dust with significantly greater Sr radiogeneity from sediment deposits north of $37 - 41^\circ\text{S}$ [33]. Four data of [30] dated at approximately 60–62 ka cal. BP represent dust deposition in the course of Glacial Stage 4. These data yield an average $^{87}\text{Sr}/^{86}\text{Sr}$ of $0.7084(3)$ which

appears only slightly less radiogenic compared to the Glacial Stage 2 and the Holocene. This is again compatible with the concept of single-source paleorientation of ICD. It may however, indicate minor differences in the source strengths of the various Argentinian sediment areas in favour of more southern sediment deposits.

The $<5 \mu\text{m}$ sediment particle analyses of [30] confirm the conclusion of [33], that there is a Sr radiogeneity gradient, on average with decreasing $^{87}\text{Sr}/^{86}\text{Sr}$ ratios of the sediments and their fine fractions from north to south ($31^\circ\text{S} - 34^\circ\text{S}$: 0.7093 – 0.7137; average of 5 data: 0.7102(8); $41^\circ\text{S} - 53^\circ\text{S}$: 0.7046 – 0.7129; average of 13 data: 0.7076(26) – calculated from the data of [30]. The (arbitrarily) averaged sediment data of [30] are compared in Fig. 5 with the peat data and with the averaged ice core data from [6], [28] and [30], and plotted versus the date of glacial dust deposition on the Eastern Antarctic Plateau. This figure demonstrates that the ICD data match the averaged Argentinian sediment data well at about 60 – 63 ka cal. BP (0.7084(3) – stage 4), at 159 – 167 ka cal. BP (0.7083(2) – earlier episode of stage 6), and at 340 ka cal. BP (0.70846(4) – stage 10). This implies that during these different glacial episodes of strongly enhanced atmospheric dust load the orientation of air masses over the Eastern Antarctic Plateau to the Argentinian sediment deposits were similar to the Holocene. It can be assumed for the glacial episodes of stages 2, 4, parts of 6 and 10, that the principle phenomena of dust mobilization in Argentina and uptake into the atmosphere were similar to the Holocene, despite equatorwards displacement of the Westerlies as proposed e.g. by [61]. However, Fig. 5 also demonstrates, that this conclusion can be not generalized for some other glacial episodes: ~ 150 ka cal. BP (0.7096(11), later episode during stage 6), ~ 268 ka cal. BP (0.71113(3), stage 8), and ~ 421 ka cal. BP (0.71085(1), stage 12). The dust load over Eastern Antarctica during these episodes had a Sr isotope composition significantly more radiogenic than during the LGM and the Holocene. It is not possible to generate fine particle mixtures having similar radiogenic Sr

isotope compositions when contributions from most Argentinian sediment deposits would have been included, as is suggested by the fine fraction sediment data of [30] and the peat data of the present study for the Holocene. One possible explanation is that the ICD compositions in these cases could indicate a turnover of the Southern Hemispheric air circulations to conditions where significant dust contributions from other continental areas (S. Africa, Australia) came into play. The ϵ_{Nd} values for fine particles derived from South Africa, Australia and uncovered Antarctic sediment deposits are, however, mostly too negative to match the ICD dust data for the critical glacial episodes (sediment fine fractions [30]: -7 to -10: Australia; -10 to -25: South Africa; +5.7 to -12.5: Antarctica; ice core data ([28, 30]): -0.22 to -3.8: ICD of “stage 6”; -4.8: ICD of “stage 8”; -3.1: ICD of “stage 12”). The only area which would fit with its isotope compositions to the ICD data is the southern island of New Zealand. Its potential to release dust to the atmosphere, however, is believed to be not high enough to explain the strong and intensified atmospheric dust loads over Antarctica [30]. More likely, dust release from the areas south of $37 - 41^\circ\text{S}$ had been effectively diminished during the critical glacial episodes. As discussed above, South American sediment deposits north of $37 - 41^\circ\text{S}$ have matching (more radiogenic) Sr isotope compositions (Fig. 5), and the ϵ_{Nd} values match, too: -0.2 to -3.0: [30], -0.8 to -6.3 [33]. Dust compositions of the Glacial Stages 6, 8 and 12 are therefore compatible with the more northern sediment deposits of Argentina. Dust mobilization and atmospheric uptake during these glacial episodes in South America shifted more to the north relative to the Holocene situation. Effective reduction of dust release in the southern parts of Argentina may have been due to a stronger shift of the Westerlies to the north and a more northern position of the Antarctic Polar front than during the LGM. But we favour as a major controlling factor the episodic occurrence of periglacial ice sheets which diminished dust emissions from the Patagonian sediment deposits south of $37 - 41^\circ\text{S}$.

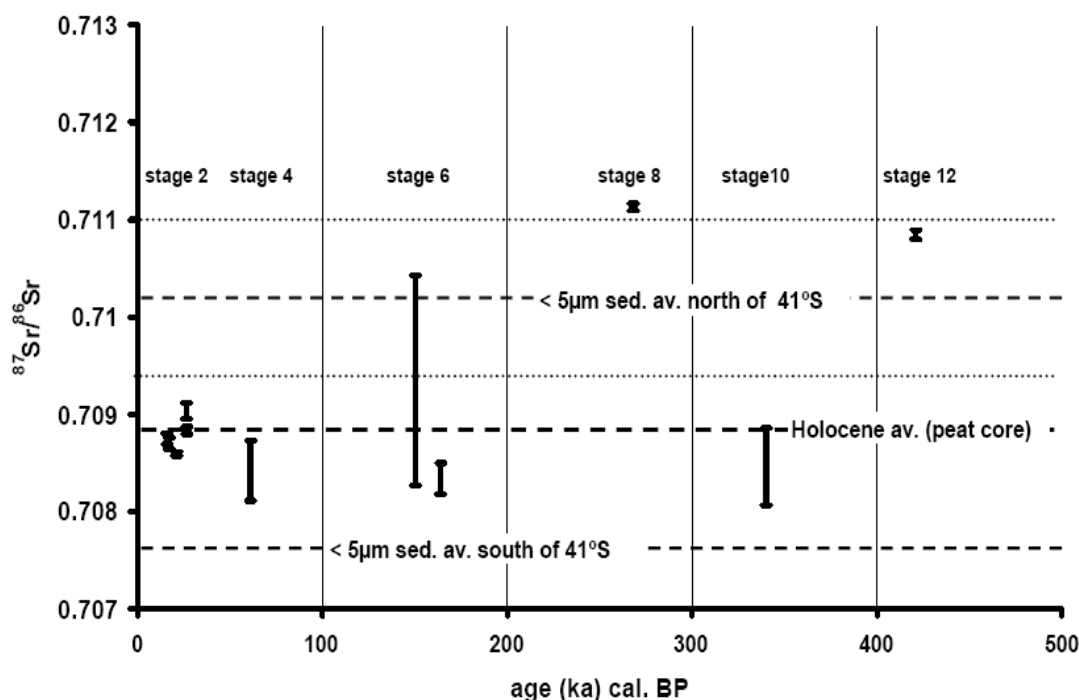


Fig. 5 Comparison of the Sr isotope composition in Holocene mineral aerosols collected by the Oreste peat bog (“Holocene reference”, present study) with Pleistocene Sr isotope compositions in glacial dusts of Glacial Stages 2 – 12, found in East Antarctic ice cores (ice cores “Dome C”, “EPICA Dome C” and “Vostok”; ICD data taken from [6],[28],[30]). The dotted lines indicate the mean of $^{87}\text{Sr}/^{86}\text{Sr}$ ratios of $<5\ \mu\text{m}$ fractions from various Argentinian sediments (fine fraction sediment data taken from [30]) averaged separately for sediments north and south of 41°S . The average Holocene dust composition concluded from the peat data are compatible with fine fraction sediment data if averaged for all Argentinian sediment deposits (north and south of 41°S : $^{87}\text{Sr}/^{86}\text{Sr} = 0.7083 \pm 0.0023$).

6.3 Possible influence of Patagonian ice sheets on Quaternary dust mobilization

At present two ice fields exist in southernmost South America high in the Andes between 43°S and 51°S . During the LGM these ice fields expanded to an ice sheet of a length of 1800 km and a width of up to a few 100 km between 38°S and 56°S , aligned along the Andean crest and migrated to the east over parts of the Patagonian high plains [62]. Model calculations of [63] showed that the size of the ice sheet may be due to a temperature drop of 6°C , and that the growth of the ice masses with formation of a coherent ice sheet settled most rapid in the North and South Patagonian ice field sector ($45 - 52^\circ\text{S}$). While in this ice field sector with maximum mass balance a large ice sheet expansion to the east occurred within 10 – 15 ka, the accumulation of ice masses kept in the

northern sector ($38 - 43^\circ\text{S}$) restricted to the mountain areas (field observations: [62], model calculations: [63]). Glaciation was accompanied by significant snow line depression [64], and was controlled by the degree of temperature drop and moisture increase and by topography ([63,64]). Marden 1994 [65] argued from field observations, that the ice sheets - centered on the Patagonian Andes - developed successively smaller during Quaternary glaciations. The implication of this is that the LGM ice sheet expansion estimated by [62] was one of the smaller ice sheets in the succession of Quaternary glaciations. Singer et al. [66] investigated a sequence of Pleistocene terminal moraines, which were deposited east of Lago Buenos Aires (46.5°S) in the course of glacier advances from the Patagonian ice cap onto the high plains adjacent to the Southern Andes. On the basis of K-Ar

chronology they concluded in agreement with [65], that the Patagonian ice sheets had a maximum extension at approximately 1100 ka BP, and that the overall pattern of Patagonian glaciation is one of diminishing eastward extent of ice during successive glacial advances over the past 1 Ma. This interpretation is compatible with the Sr isotope trends of ICD dusts from the various Glacial Stages and with the sediment data for Argentina plotted in Fig. 5. The maximum advance of the LGM ice sheet [62] was not far enough to the east to significantly influence dust release from Patagonian sediments. Thus the similarity of Holocene dust compositions (peat core Sr isotope data) and LGM dust compositions (ICD Sr isotope data) indicate rather stable conditions of dust deflation from Argentinian sediments during the LGM and the Holocene despite the temporary Patagonian glaciation.

For some of the earlier Glacial Stages (e.g. 8 and 12 – Fig. 5) the situation appears different. According to [65] and [66] the expansion of the ice sheet could have been so far to the east (especially in the Patagonian ice field sector 45 – 52°S [63]) that dust release from the southern Patagonian sediment deposits was strongly reduced. The remaining dust source areas during these times were thus strongly oriented toward the northern sectors with their significantly higher Sr isotope ratios in the dust particles (Fig. 5). On the other hand the data presented in Fig. 5 demonstrate that advances during Glacial Stages 4 and 10 could not have been much further to the east than during the LGM. A special situation is indicated by the data in Fig. 5 for Glacial Stage 6. Dust compositions at the beginning of this Glacial Stage (~ 170 ka BP) started with mixtures from sediment sources effectively distributed across Argentina. Within 15 – 20 ka Sr in the mineral aerosols became increasingly radiogenic, but not to the same extent as per stages 8 and 12 with orientations to Argentinian areas north of 37 – 41°S. These interpretations are consistent with growth of a Patagonian ice sheet within 15 – 20 ka (in agreement with typical times of ice sheet formation estimated by [63], with an eastern expansion greater than during the LGM, but

less than that seen during earlier Glacial Stages. Fine particle components in the southern sediment areas at approximately 150 ka BP were not as effectively immobilized by the ice sheet influence as during stages 8 and 12. Thus the Sr isotope data of stage 6 may indicate a transitional situation with a turnover from effective dust immobilization in sediment deposits south of 38–41°S during early Glacial Stages to insignificant dust immobilization in Patagonia since approximately 60 – 100 ka (Glacial Stages 4, 2 and the Holocene). Consequently, the Sr isotopes in the ICD record could reflect the vanishing influence of Patagonian ice sheets on dust mobilization from Patagonian loesses and soils, in agreement with the conclusions of [65] and [66].

7. Summary and conclusions

A peat core from the Oreste bog located at the southernmost edge of South America is an effective archive of mineral aerosols and provides a record of the variations in their Sr isotope composition. The applied analytical protocol of peat ashing, weak acid leaching and careful cleaning was successful in distinguishing the labile Sr components in the acid soluble peat ashes (ASA) from Sr components which constitute the insoluble mineral particles (AIA) in the peat column. The available data demonstrate that the information recorded by the Sr isotopes of the insoluble particles was not significantly altered by the special conditions of storage in the organic material and the acidic and anoxic fluids hosted therein. Thus the Sr isotope data can be used to discuss the origin of the insoluble particles found in the ombrotrophic peat layers in the light of South American volcanic explosive eruptions and of remote mineral aerosol deposition.

All the tephra which reached the study area during the Holocene, can be attributed to the four Holocene explosive eruptions of one eruption center in the AVZ, namely the Mt. Burney volcano. These four eruptions caused the Sr isotope signature in the AIA of the influenced peat layers to shift to less radiogenic values reflecting the mantle isotope signature of the volcanic contributions. The mantle-type Sr isotope

traces were not equilibrated in the bog environment which demonstrates the potential of Sr isotopes hosted in AIA as indicators of volcanic inputs. Outside of the tephra influenced layers in the peat column the insoluble components have a reproducible and homogeneous Sr isotope composition ($^{87}\text{Sr}/^{86}\text{Sr} = 0.70884 \pm 0.00014$) which was nearly constant over the past 6 ka of ombrotrophic peat bog development. The homogeneous Sr isotope composition represents the average mineral aerosol composition, which was collected by the studied bog from the air masses receiving dust inputs from across Southern South America.

The ASA Sr isotope data show that not only the insoluble particles but also the labile Sr components in the peat bog did not equilibrate their Sr isotope signatures. Labile Sr in the ombrotrophic parts of the bog are strongly dominated by marine Sr isotope composition indicating the important continuous influx of sea spray to the moorland. Labile Sr components in the minerogenic peat layers may represent a mixture of marine Sr with Sr of local soil fluids migrating through the bottom peat layers.

Application of the moorland bog as a monitor of Holocene mineral aerosols has revealed an unexpectedly constant Sr isotope composition in the air masses over Southern South America. This indicates highly effective and stable dust mixing in the atmosphere on large scales. The observed $^{87}\text{Sr}/^{86}\text{Sr}$ ratio (0.70884(14)) matches the sediment data of [30] well, when all the $<5 \mu\text{m}$ fractions reported for sampling areas between 31°S and 53°S are (arbitrarily) averaged (0.7083 ± 0.0023). This shows that at least since the middle Holocene all the sediment deposits exposed in Argentina contributed dust to the southern South American atmosphere. The peat bog data demonstrate how the Sr isotope signatures in South American dusts provide a well-defined tracer for the discussion of possible source areas of dust in Antarctic ice cores, with much greater importance than was previously considered e.g. by [28] and [33]. The stable Holocene mineral aerosol Sr isotope composition over southern South America

matches perfectly the Sr isotope composition of Antarctic ice core dust of 0.7088 ± 0.0002 during Glacial Stage 2, calculated from the eastern Antarctic ice core dust data (cores “Dome C” and “EPICA Dome C”, data of [6],[28],[30]). This finding indicates that the Argentinian sediments are the only sources of mineral aerosols which reached the East Antarctic Plateau at least since the LGM. Moreover, those data show the air mass circulations and source-to-sink processes relating South America and the Antarctic ice shield to have stable been throughout the Late Pleistocene and the Holocene. The higher $^{87}\text{Sr}/^{86}\text{Sr}$ ratios in ice core dusts found for earlier Glacial Stages [67,28,30] indicate conditions of dust uptake from Argentinian loess plains which differed from those of the Late Pleistocene/Holocene. The north-south gradient in the Sr isotope composition of the Argentinian sediments ([30,33]) shows that during some of the earlier Glacial Stages the Patagonian sediment areas did contribute significantly less to the mineral dust inventory of the South American atmosphere. Dusts from the less radiogenic sediment deposits south of $38 - 41^\circ\text{S}$ appear to have been immobilized during some of the glacial maxima of earlier Pleistocene periods. The Sr isotope composition of ice core dusts of these episodes could reflect the episodic expansion of North and South Patagonian ice sheets to the east of the Andean crest over the Patagonian high plains, much further [66] than was reported for the ice shield during the LGM [62]. This interpretation means that the Sr isotope composition of ice core dusts of the earlier Pleistocene indicates the degree of Patagonian ice sheet expansion and transgression over the high plains to the east, if referred to the peat bog data (Holocene) and the ice core dust data for the LGM. The Sr isotope data for the ICD, therefore, reflect the fading importance of Patagonian glaciation during successive Glacial Stages of the earlier Pleistocene in accordance with the conclusions of [65] and [66].

Acknowledgements

Financial support from the Deutsche Forschungsgemeinschaft (DFG, SH 89/2-3) is gratefully acknowledged. Thanks to Olena

Kurzelt for mineralogical analyses and Dietlinde Pingel for support with cleanroom wet chemistry and TIMS Sr isotope analyses.

References

- [1] J. Nriagu, Global inventory of natural and anthropogenic emissions of trace metals to the atmosphere, *Nature* 279 (1979) 409-411.
- [2] K.K. Turekian, J.K. Cochran, ^{210}Pb in surface air at Enewetak and the Asian dust flux to the Pacific, *Nature* 292 (1981) 522-524.
- [3] C.C. Patterson, D.M. Settle, Review of data on Aeolian fluxes of industrial and natural lead to the lands and seas in remote regions on a global scale, *Mar. Chem.* 22 (1987) 163-177.
- [4] H.B. Maring, R.A. Duce, The impact of atmospheric aerosols on trace metal chemistry in open ocean surface sea water, 1. Aluminum, *Earth. Planet. Sci. Lett.* 84, (1987) 381-392.
- [5] B. Hamelin, F.E. Grousset, P.E. Biscaye, A. Zindler, Lead isotopes in trade wind aerosols at Barbados. The influence of European emissions over the North Atlantic, *J. Geophys. Res.* 94 (1989) 16243-16250.
- [6] F.E. Grousset, P.E. Biscaye, M. Revel, J.-R. Petit, K. Pye, S. Joussaume, J. Jouzel, Antarctic (Dome C) ice-core dust at 18 ky BP: Isotopic constraints on origins, *Earth Planet. Sci. Lett.* 111 (1992) 175-182.
- [7] Y.L. Yung, T. Lee, J.T. Shieh, Dust: a diagnostic of the hydrologic cycle during the Last Glacial Maximum, *Science* 271 (1996) 962-963.
- [8] J.R. Petit, M. Briat, A. Royer, Ice age aerosol content from East Antarctic ice core samples and past wind strength, *Nature* 293 (1981) 391-394.
- [9] S.R. Taylor, S.M. McLennan, M.T. McCulloch, Geochemistry of loess, continental crustal composition and crustal model ages, *Geochim. Cosmochim. Acta.* 47 (1983) 1897-1905.
- [10] S.L. Goldstein, R.K. O’Nions, P.J. Hamilton, A Sm-Nd isotopic study of atmospheric dusts and particulates from major river systems, *Earth. Planet. Sci. Lett.* 70 (1984) 221-236.
- [11] A. Gaudichet, M.D. Angelis, R. Lefevre, J.R. Petit, Y.S. Korotkevitch, V.N. Petrov, Mineralogy of insoluble particles in the Vostok Antarctic ice core over the last climatic cycle(150 kyr), *Geophys. Res. Lett.* 15 (13) (1988) 1471-1474.
- [12] Y.J. Balkanski, D.J. Jacob, B.M. Gardner, W.C. Graustein, K.K. Turekian, Transport and residence times of tropospheric aerosols inferred from a global 3-dimensional simulation of Pb-210, *J. Geophys. Res.* 98 (1993) 20573-20586.
- [13] S. Jousoume, Paleoclimatic tracers – an investigation using an atmospheric general-circulation model under ice-age conditions. I. Desert dust, *J. Geophys. Res. Atmos.* 98 (1993) 2767-2805.
- [14] K.K. Anderson, A. Armengaud, C. Genthon, Atmospheric dust under glacial and interglacial conditions, *Geophys. Res. Lett.* 25 (1998) 2281-2284.
- [15] S. Gallet, B. Jahn, B.V.V. Lanoe, A. Dia, E. Rosselo, Loess geochemistry and its implications for particle origin and composition of the upper continental crust, *Earth. Planet. Sci. Lett.* 156 (1998) 157-172.
- [16] B.M. Jahn, S. Gallet, J.M. Han, Geochemistry of the Xining, Xifeng and Jixian sections, Loess Plateau of China: eolian dust provenance and paleosol evolution during the last 140 ka, *Chem. Geol.* 178 (2001) 71-94.
- [17] B. Delmonte, J.R. Petit, V. Maggi, Glacial to Holocene implications of the new 27000-year dust record from the EPICA Dome C (East Antarctica) ice core. *Clim. Dyn.* 18 (8) (2002) 647-660.
- [18] J.F. Hopper, H.B. Ross, W.T. Sturges, L.A. Barrie, Regional source discrimination of atmospheric aerosols in Europe using the isotope composition of lead, *Tellus* 43B (1991) 45-60.

- [19] H. Mukai, A. Tanaka, T. Fijii, M. Nakao, Lead isotope ratios of airborne particulate matter as tracers of long-range transport of air pollutants around Japan, *J. Geophys. Res.* 99 (1994) 3717-3726.
- [20] Y. Erel, A. Veron, L. Halicz, Tracing the transport of anthropogenic Pb in the atmosphere and in soils using isotope ratios, *Geochim. Cosmochim. Acta* 61 (1997) 4495-4507.
- [21] H. Shirahata, R.W. Elias, C.C. Patterson, Chronological variations in concentrations and isotopic compositions of anthropogenic atmospheric lead in sediments of a remote subalpine pond, *Geochim. Cosmochim. Acta* 44 (1980) 149-162.
- [22] B. Kober, M. Wessels, A. Bollhöfer, A. Mangini, Pb isotopes in sediments of Lake Constance, Central Europe constrain the heavy metal pathways and the pollution history of the catchment, the lake and the regional atmosphere, *Geochim. Cosmochim. Acta* 63 (1999) 1293-1303.
- [23] J.R. Petit, J. Jouzel, D. Raynaud, N.I. Barkov, J.M. Basile, M. Bender, J. Chappelaz, M. Davis, G. Delaygue, M. Delmonte, V.M. Kotyakov, M. Legrand, V.Y. Lypenov, C. Lorius, L. Pepin, C. Ritz, E. Saltzman, E. Stievenard, Climate and atmospheric history of the past 420000 years from the Vostok ice core, Antarctica, *Nature* 399 (1999) 429-436.
- [24] K.J.R. Rosman, W. Chisholm, C.F. Boutron, J.P. Chandelone, S. Hong, Isotopic evidence to account for changes in the concentration of lead in Greenland snow between 1960 and 1988, *Geochim. Cosmochim. Acta* 58 (1994) 3265-3269.
- [25] W. Shotyk, Atmospheric deposition and mass balance of major and trace elements in two oceanic peat bog profiles, northern Scotland and the Shetland islands, *Chem. Geol.* 138 (1997) 55-72.
- [26] K.A. Rahn, The chemical composition of the atmospheric aerosol, Technical Report, Graduate School of Oceanography, University of Rhode Island, Kingston, R.I. USA (1976) 265 pp.
- [27] C. Genthon, Simulations of desert dust and sea-salt aerosols in Antarctica with a general circulation model of the atmosphere. *Tellus* 44 (1992) 371-389.
- [28] I. Basile, F.E. Grousset, M. Revel, J.R. Petit, P.E. Biscaye, N.I. Barkov, Patagonian origin of glacial dust deposited in East Antarctica (Vostok and Dome c) during Glacial Stages 2., 4, and 6, *Earth Planet. Sci. Lett.* 146 (1997) 573-589.
- [29] B. Delmonte, J.R. Petit, I. Basile-Doelsch, A. Michard, B. Gemmiti, V. Maggi, M. Revel-Rolland, Refining the isotope (Sr-Nd) signature of potential source areas for glacial dust in East Antarctica, *J. Physique IV* 107 (2003) 365-368.
- [30] B. Delmonte, I. Basile-Doelsch, J.R. Petit, V. Maggi, M. Revel-Rolland, A. Michard, E. Jagoutz, F. Grousset, Comparing the EPICA and Vostok dust records during the last 220000 years: stratigraphical correlation and provenance in glacial periods, *Earth. Sci. Rev.* 66 (2004) 63-87.
- [31] J. Rabassa, A. Coronato, C. Roig, The peat bogs of Tierra del Fuego, Argentina, in: E. Lappalainen (Ed.), *Global peat resources*, International Peat Society, Finland (1996).
- [32] I. Basile, J.R. Petit, S. Tournon, F.E. Grousset, N. Barkov, Volcanic layers in Antarctic (Vostok) ice cores: source identification and atmospheric implications, *J. Geophys. Res.* 106 (2001) 31915-31931.
- [33] J. Smith, D. Vance, R.A. Kemp, C. Archer, P. Toms, M. King, M. Zarate, Isotopic constraints on the source of Argentinean loess with implications for atmospheric circulation and the provenance of Antarctic dust during recent glacial maxima, *Earth Planet. Sci. Lett.* 212 (2003) 181-196.
- [34] M.E. Teruggi, The nature and origin of Argentine loess, *J. Sediment. Petrol.* 27 (1957) 322-332.

- [35] V. Markgraf, J.P. Bradbury, A. Schwalb, S.T. Burns, C.R. Stern, D. Ariztegui, A. Gilli, F.S. Anselmetti, S. Stine, N. Maidana, Holocene paleoclimates of southern Patagonia: limnological and environmental history of Lago Cardiel, Argentina, *The Holocene* 13 (2003) 581-591.
- [36] A. Gilli, D. Ariztegui, F.S. Anselmetti, J.A. McKenzie, V. Markgraf, I. Hajdas, R. McCulloch, Mid-Holocene strengthening of the southern Westerlies in South America – sedimentological evidences from Lago Cardiel, Argentina (49°S), *Global Planet. Change* 49 (2005) 75-93.
- [37] R. Kilian, M. Hohner, H. Biester, H.J. Wallrabe-Adams, C.R. Stern, Holocene peat and lake sediment tephra record from the southernmost Chilean Andes (53-55°S), *Rev. Geol. Chile* 30 (2003) 23-37.
- [38] C.R. Stern, Active Andean volcanism: its geologic and tectonic setting, *Rev. Geol. Chile* 31 (2004) 161-206.
- [39] C.M. Clapperton, Quaternary geology and geomorphology of South America, Elsevier Science Publisher, Amsterdam, (1993).
- [40] S. Tuhkanen, The climate of Tierra del Fuego from a vegetation geographical point of view and its ecoclimatic counterparts elsewhere, *Acta Bot. Fennica* 145 (1992) 43-80.
- [41] E.B. Olivero and D.R. Martinioni, A review of the geology of Argentinean Fuegian Andes. *J. South Am. Earth Sci.* 14 (2001) 175 – 188.
- [42] A. Sapkota, A. K. Cheburkin, G. Bonani, W. Shotyk, Six millennia of atmospheric dust deposition in southern South America, Holocene (submitted)
- [43] A. Cheburkin, W. Shotyk, An Energy-dispersive Miniprobe Multielement Analyzer (EMMA) for direct analysis of Pb and other trace elements in peats, *Fres. J. Anal. Chem.* 354 (1996) 688-691.
- [44] E.P. Horwitz, Novel strontium-selective extraction chromatographic resin. Solvent Extract. Ion Exchange 10 (1992) 313.
- [45] C. Pin, C. Bassin, Evaluation of a strontium-specific extraction chromatographic method for isotopic analysis in geological materials. *Anal. Chim. Acta* 269 (1992) 249-255.
- [46] P. Steinmann, W. Shotyk, Geochemistry, mineralogy, and geochemical mass balance on major elements of two peat bog profiles (Jura Mountains, Switzerland), *Chem. Geol.* 138 (1997) 25-53.
- [47] G. LeRoux, D. Aubert, P. Stille, M. Krachler, B. Kober, A. Cheburkin, T. Noernberg, W. Shotyk, Reappraisal of lead atmospheric deposition in Central Western Europe using a new peat record from Southern Germany compared to snow, Herbarium samples and other bog studies, *Atmos. Environ.* 39 (2005) 6790-6801.
- [48] J.M. McArthur, Recent trends in strontium isotope stratigraphy, *Terra Nova* 6 (1994) 331-358.
- [49] W. Shotyk., D. Weiss, J.D. Kramers, R. Frei, A.K. Cheburkin, M. Gloor, S. Reese, Geochemistry of the peat bog at Etang de la Gruere, Jura Mountains, Switzerland, and its record of atmospheric Pb and lithogenic trace elements (Sc, Ti, Y, Zr, Hf and REE) since 12,370 ¹⁴C yr BP. *Geochim. Cosmochim. Acta.* 65 (2001) 2337-2360.
- [50] K. Futa, C.R. Stern, Sr and Nd isotopic and trace element composition of Quaternary volcanic centers of the southern Andes, *Earth. Planet. Sci. Lett.* 88 (1988) 253-262.
- [51] C.R. Stern, F.A. Frey, K. Futa, R.E. Zartman, Z. Peng, T.K. Kyser, Trace element and Sr, Nd, Pb and O isotopic composition of Pliocene and Quaternary alkali basalts of the Patagonian Plateau lavas of southernmost South America, *Contrib. Mineral. Petrol.* 104 (1990) 294-308.
- [52] C.R. Stern, Mid-Holocene tephra on Tierra del Fuego (54°S) derived from the Hudson Volcano (46°S): evidence

- for a large explosive eruption, *Rev. Geol. Chile* 18 (1991) 139-146.
- [53] J.A. Naranjo, C.R. Stern, Holocene tephrochronology of the southernmost part (42°30' - 45°S) of the Andean Southern Volcanic Zone, *Rev. Geol. Chile* 31 (2004) 225-240.
- [54] C.R. Stern, R. Kilian, The role of subducted slab, mantle wedge and continental crust in the generation of adakites from the Andean Austral Volcanic Zone, *Contrib. Mineral. Petrol.* 123 (1996) 263-281.
- [55] J.A. Naranjo, C.R. Stern, Holocene explosive activity of Hudson volcano, southern Andes, *Bull. Volcanology* 59 (1998) 291-306.
- [56] E.J. Dash, Strontium isotopes in weathering profiles, deep-sea sediments and sedimentary rocks, *Geochim. Cosmochim. Acta* 33 (1962) 1521-1552.
- [57] P.E. Biscaye, E.J. Dash, The rubidium - strontium isotope system in deep sea sediments: Argentine basin, *J. Geophys. Res.* 76 (1971) 5087-5096.
- [58] P.E. Biscaye, Strontium isotope composition and sediment transport in the Rio de la Plata estuary, *Geol. Soc. Am. Mem.* 133 (1972) 349-357.
- [59] M.H. Iriondo, N.O. Garcia, Climatications in the Argentine plains during the last 18000 years, *Palaeogeogr. Palaeoclimatol. Palaeocol.* 101 (1993) 209-220.
- [60] M. Iriondo, Patagonian dust in Antarctica, *Quatern. Intern.* 68-71 (2000) 83-86.
- [61] H.E. Wright, J.E. Kutzbach, T.W. Webb III, W.F. Ruddiman, F.A. Street-Parott, T.J. Bartlein, *Global climates since the Last Glacial Maximum*, Univ. of Minnesota Press Minneapolis (1993) 550 pp.
- [62] R.D. McCulloch, M.J. Bentley, R.S. Purves, N.R.J. Hulton, D.E. Sugden, C.M. Clapperton, Climatic inferences from glacial and paleoecological evidences at the last glacial termination, southern South America, *J. Quatern. Sci.* 15 (2000) 409-417.
- [63] D.E. Sugden, N.R.J. Hulton, R.S. Purves, Modelling the inception of the Patagonian icesheet, *Quatern. Intern.* 95-96 (2002) 55-64.
- [64] K. Haselton, G. Hilley, M.R. Strecker, Average Pleistocene patterns in the Southern Central Andes: controls on mountain glaciation and paleoclimate implications, *J. Geology* 110 (2002) 211-226.
- [65] C.J. Marden, Factors affecting the volume of Quaternary glacial deposits in Southern Patagonia, *Geografiska Annaler. Ser. A.* 76 (1994) 261-269.
- [66] B.S. Singer, R.P. Ackert, H. Guillou, $^{40}\text{Ar}/^{39}\text{Ar}$ and K/Ar chronology of Pleistocene glaciations in Patagonia, *GSA Bull.* 116 (2004) 434-450.
- [67] I. Basile, *Origines des aerosols volcaniques et continentaux de la carotte de glace de Vostok (Antarctique)*, PH D thesis Universite Joseph Fourier, Grenoble – I, France (1997).
- [68] M. Zarate, Loess of southern South America, *Quatern. Sci. Rev.* 22 (2003) 1987-2006.

Chapter 5

Atmospheric Deposition of Pb

-Chapter 5-

The paradigm of natural Pb in the atmosphere: 6000 years of soil dust deposition recorded by the Oreste peat bog, southern Patagonia

William Shotyk*, Atindra Sapkota, Andriy K. Cheburkin, and Bernd Kober

Institute of Environmental Geochemistry, University of Heidelberg, INF 236, D-69120 Heidelberg, Germany

*Corresponding author; email: shotyk@ugc.uni-heidelberg.de; tel +49 (6221) 54 4803; fax 54 5228

Submitted to Global Biogeochemical Cycle, 2006

Abstract

A peat core from Oreste Bog, Isla Navarino, Chile, in southernmost South America, was collected for detailed study. The 542 cm long core represents approximately 13,000 years of peat accumulation. Chemical analyses of the peat showed that the top 400 cm of peat is ombrotrophic, representing an archive of 6,000 years of atmospheric mineral dusts. Two cm slices of peat were dried and ashed, and the acid insoluble ash (AIA) fraction obtained by vacuum filtration after reaction with 1 M HCl for 15 min. Quantitative analyses of Pb, Ti, and other trace elements were undertaken in the AIA (ca. 2 - 3 mg) using non-destructive XRF, directly, employing the 0.45 µm membrane filters for sample support. Selected samples were further cleaned using HCl, digested, and measured for Pb isotopes (^{204}Pb , ^{206}Pb , ^{207}Pb , ^{208}Pb) using TIMS.

The average concentrations of Pb ($15.2 \pm 8.2 \mu\text{g/g}$) and Ti ($3190 \mu\text{g/g}$) in the AIA are effectively constant, and remarkably similar to their abundance in crustal rocks: these findings suggest that soil dust particles have dominated the natural fluxes of atmospheric Pb throughout the Holocene. Support for this hypothesis is provided by the Pb isotope data, with the average ratio of $^{206}\text{Pb}/^{207}\text{Pb}$ (1.196 ± 0.003) also similar to crustal values. Although supplementary mineralogical and isotopic ($^{87}\text{Sr}/^{86}\text{Sr}$) investigations reveal several zones impacted by volcanic ash, there is neither a significant change in the Pb concentrations nor its isotopic composition. The natural inputs of atmospheric Pb, therefore, can be attributed nearly exclusively to soil dusts derived from rock weathering. Based on these results and an earlier study of a bog in Europe, we estimate that the natural, global flux of atmospheric Pb was no greater than 4000 T/yr.

Unlike the deeper peat layers, however, AIA samples from the top 50 cm contain greater Pb concentrations (up to $49 \mu\text{g/g}$), and less radiogenic Pb isotope signatures $^{206}\text{Pb}/^{207}\text{Pb}$ (1.1810 ± 0.0005), due to recent, anthropogenic inputs.

Keywords: *peat bog, Pb, soil dust, anthropogenic input, southern South America*

Introduction

Studies of peat cores from ombrotrophic (ie rain-fed) bogs have shown that atmospheric Pb in Europe has been dominated by anthropogenic inputs for approximately 3,200 years (Shotyk et al., 1998). Atmospheric Pb contamination in the historical past was particularly notable during the Roman Period, as well as the Medieval Period (Shotyk et al., 1996). However, a detailed reconstruction using a peat core from England provided unambiguous evidence of atmospheric Pb contamination pre-dating the Roman invasion of Britain (LeRoux et al., 2004). Peat cores from ombrotrophic bogs continue to provide new insight into the long history of atmospheric Pb contamination in Europe (Martinez-Cortizas et al., 2002; Monna et al., 2004). The extensive use of gasoline lead additives during the second half of the 20th century certainly compounded the problem of atmospheric Pb contamination, but this was only the latest chapter in a long history of environmental pollution: in Switzerland, 75% of the anthropogenic Pb had already been deposited from the atmosphere before leaded gasoline was introduced (Shotyk et al., 2000). Detailed, high resolution reconstructions using peat cores dated with ²¹⁰Pb and employing accurate measurements of stable Pb isotopes (²⁰⁶Pb, ²⁰⁷Pb, ²⁰⁸Pb) have shown that the greatest intensity of atmospheric Pb contamination, dating from the late 20th century, pre-dates the maximum impact of gasoline Pb (Shotyk et al., 2002), in some cases by as much as 25 years (Shotyk et al., 2003, 2005).

Peat bogs are valuable archives not only because they provide a sensitive and accurate indication of recent changes in the deposition rates and sources of atmospheric Pb, but also because they extend far enough back in time to be able record the natural background rates of atmospheric Pb deposition, for comparison with modern values. Detailed studies of deeper peat layers pre-dating the beginning of atmospheric Pb contamination offer the promise of help in understanding the natural geochemical processes which regulated the sources and

fluxes of Pb from the lithosphere, via the atmosphere, to the biosphere (Shotyk et al., 2001). To date, most studies of atmospheric Pb deposition using peat cores from bogs have focused mainly on the relatively shallow surface layers representing peat accumulation from the past few centuries and dominated by anthropogenic Pb (Bränvall et al., 1997; Farmer et al., 1997; Kempter et al., 1997; Klaminder et al., 2003; MacKenzie et al., 1997, 1998; Martinez-Cortizas et al., 1997, 2002; Nieminen et al., 2002; Norton et al., 1997; Novak et al., 2003; Vile et al., 1995, 2000; Weiss et al., 1999, 2002). Few studies exist of atmospheric Pb in deeper peat layers, dating from pre-anthropogenic times. In order to be able to interpret the recent atmospheric Pb fluxes in a quantitative way, it is important to establish natural background values (concentrations, enrichment factors, and isotopic composition) and their variation. This information, in turn, is vital to understand the predominant sources, and chemical and mineralogical forms, of natural Pb in the atmosphere.

The first complete record of atmospheric Pb for the entire Holocene was obtained from the peat bog at EGR in Switzerland which yielded a record of atmospheric Pb extending back in time 14,500 years (Shotyk et al., 1998). Using Sc as a conservative, lithogenic element, the concentrations of Pb in the peat bog were found to be proportional to those of Sc until 3,200 years ago: this finding suggested that soil dust particles derived from weathering of crustal rocks were the main source of natural, atmospheric Pb. Support for this hypothesis was provided by measurements of Pb isotope ratios which yielded average values of $^{206}\text{Pb}/^{207}\text{Pb} = 1.20$ and $^{208}\text{Pb}/^{206}\text{Pb} = 2.07$ which are comparable with values for the Upper Continental Crust (Stacey and Kramers, 1975; Ben Othman et al., 1989; Kramers and Tolstikhin, 1997).

In contrast to the plethora of studies of atmospheric Pb employing peat bogs in the northern hemisphere, there are few, if any, studies of atmospheric Pb using peat bogs as archives in the southern hemisphere. As an independent evaluation of the soil dust

hypothesis, we have measured Pb in a peat core from an ombrotrophic bog in southernmost Patagonia which provides a record of atmospheric deposition extending back in time 6,000 years. Our main objective is to determine the extent to which soil dust particles derived from crustal weathering can explain the natural flux of atmospheric Pb.

Materials and methods

Sample collection and preparation

The Oreste bog is located near the Fondeadero Orestes anchoring ground on the west side of Bahía Windhound, Southern Isla Navarino, Chile ($55^{\circ}13'13''\text{S}$ and $67^{\circ}37'28''\text{W}$ 35m) (Figure 1). It is a magellanic moorland bog (maritime climate) located behind a *Nothofagus betuloides* forest, with an average precipitation 800 mm/yr (Rabassa et al., 1996). The climate of the area is determined by the prevailing westerlies (Tuhkanen, 1992) with a seasonal shifts of the storm tracks that crosses the belt of westerlies,

poleward in summer and toward the equator in winter (Pendall et al., 2001). The ombrotrophic bogs, including Oreste bog, in this maritime climate show rapid growth, often overlying minerotrophic peat (Rabassa et al., 1996). The dominant moorland taxa are *Sphagnum magellanicum*, *Drepanocladus sp.*, and *Astelia pumila* accompanied by *Carex*, *ericaceous* shrubs such as *Empetrum* and *Marrsippospermum grandiflorum*.

The central part of Isla Navarino is mountainous. This central belt is part of a Late Jurassic-Early Cretaceous marginal basin (the Rocas Verdes Marginal Basin) with the following rock types: Upper Jurassic silicic volcanic rocks, Lower Cretaceous deep-marine volcanoclastic turbidites and slope mudstones, and Upper Cretaceous plutonic rocks (Olivero and Martinioni, 2001). The geology of the area is dominated by Mesozoic quartzites, slates, phyllites, and low-grade schists.

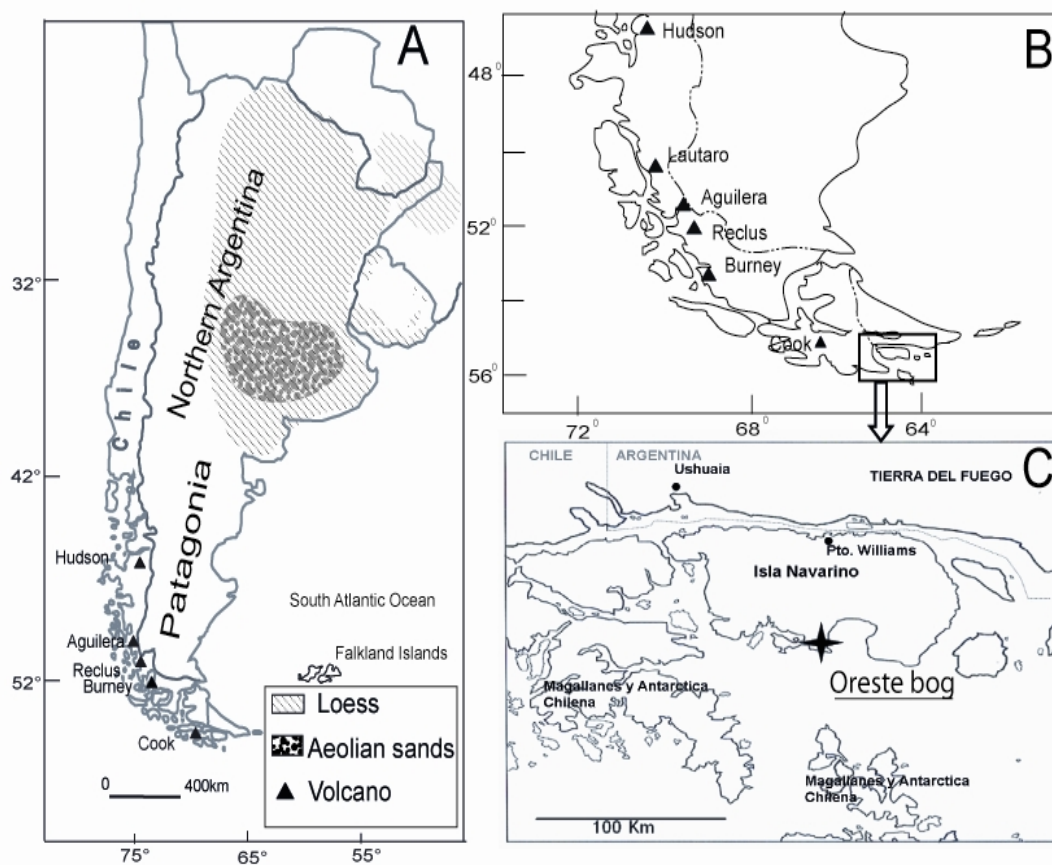


Figure 1: A) Map of South America featuring southern sediment deposit (Patagonian steppe) and northern Argentinian sediment deposit (after Zarate, 2003). B) Southern tip of South America with Austral Andean Volcanoes and the location of Isla Navarino (Chile) enclosed in a box where the Oreste bog is situated. C) Oreste bog on the Isla Navarino, Chile ($55^{\circ} 13' 13'' \text{S}$, $67^{\circ} 37' 28'' \text{W}$).

Sample preparation

Dry weight, density and macrofossils

While still frozen, each core section was cut precisely in the lab into 2 cm increments using a stainless steel band saw. The peat sub-samples obtained were irregular in shape, making it difficult to calculate volume and density. However, each peat sub-sample was photographed and image analysis software (ImageJ) used to calculate the volume of each slice. The accuracy of the volume calculated was estimated using an object of known volume to be approximately 1 %. Volumetric plugs (6 cm³) were taken from each slice to obtain macrofossils for paleobotanical studies as well as age dating using ¹⁴C. The remaining sub-samples of peat were dried overnight at 105 °C in clean polyethylene vessels, and crushed gently in that vessel, using a porcelain mortar.

Ash content and acid insoluble ash

Approximately 2 g of dried peat was combusted overnight at 550 °C that on ashing yielded ca. 20 mg. After ash content determination, the same peat ash was react with 1M HCl (Suprapur, Merck, Darmstadt, Germany) for 15min to dissolve any soluble minerals such as oxides, carbonates, sulphates, phosphates which might have formed during combustion (Steinmann and Shoty, 1997). The acid insoluble ash (AIA) fraction which consists of silicate as well as refractory oxides, were separated from the solution by filtration (0.2 µm Nuclepore polycarbonate membrane filters, ø 25 mm, Whatman International Ltd. Kent UK) under vacuum. Prior to use, the filters and the petri dishes used to hold them, were leached in high purity 1 % HNO₃ (prepared in-house, in a clean lab, distilled twice by sub-boiling), rinsed 3 – 4 times in MilliQ water (Millipore, Milford, MA, USA), then dried in a Class 100 laminar flow clean air cabinet. All of the handling of the AIA samples, including acid leaching, filtration and sample drying, were done in class 100 clean lab facilities. The samples of AIA were typically on the order of a few mg, and great care was exercised with every step of sample handling, preparation, and analysis.

Chemical analysis

XRF analysis of AIA

The abundance of Ti in the AIA was analyzed using non-destructive energy-dispersive X-ray fluorescence (XRF) spectroscopy. The TITAN XRF instrument (Cheburkin and Shoty, 2005) consists of a Co target, conventional X-ray tube and monochromator adjusted to the Co K- α line (6.93 keV). The high purity Ge X-ray detector has a resolution of 115 eV at 5.9 keV. Similarly, Pb in AIA was determined using the EMMA X-Ray Fluorescence analyzer (Cheburkin and Shoty, 1996). The design of the EMMA instrument is similar to the TITAN analyzer, and also employs monochromatic X-ray excitation. The main difference is that the EMMA analyzer employs a Mo target, conventional X-ray tube with Si(Li) detector, and a monochromator adjusted to the Mo K- α line (19.6 keV). The TITAN analyzer was operated at 17 kV and 2 mA while the EMMA analyzer operated at 45 kV and 10 mA. The acquisition time was 600 s using TITAN and 1200 second for EMMA.

The amount of AIA collected on filters varied with the yield of AIA, and ranged from 0.7 mg to 100 mg. The size of each filter provided a deposition surface of 1.8 cm² which meant the mass of sample on the filters ranged from 0.4 to 55 mg/cm². The variable sample mass creates several complications for the XRF analyses, including calibration. Additives could not be used because the same sample materials were also to be used for mineralogical and isotopic analyses. The problem of variations in sample size was solved simply by using variable amounts of each standard reference material (SRM). SRMs ranging from 2 to 100 mg were mixed with MilliQ water and filtered using the procedure described above for AIA (ie 0.2 µm Nuclepore polycarbonate membrane filters). The SRMs selected for calibration included W-1, DTS-1, G2 and MAG1 from the USGS; 1633a and 2710 from NIST; LKSD-1 and LKSD-4 from CCRMP.

Three SRMs with range in mass similar to that of the AIA, were analyzed using the TITAN and EMMA XRF instruments. The data obtained was used to

make two types of calibrations: (1) dependence of peak area with varying mass of sample (element concentrations being constant) and (2) dependence of peak area with varying element concentrations (sample mass being constant). The complete description of this calibration procedure will be described in a separate publication. In brief, it was possible to analyze the AIA samples using these XRF instruments, and obtaining a reproducibility of $\pm 12 - 15 \%$ (relative) for all elements of interest. The sensitivity of the analyses was dependent of the amount of material deposited on a filter, but was sufficient to analyze all of the elements of interest (Figure 2). Using the EMMA XRF, the absolute sensitivities (ng/cm^2) for some trace elements obtained using NIST 2783 SRM (atmospheric dust collected on filter media) were 0.45 Ni, 0.5 Cu, 0.9 Zn, and 0.8 Pb.

Pb isotope analyses

There exists a small risk of minor remnants of Pb from the acid soluble ash (ASA) fraction contaminating the residual AIA. In order to remove any Pb contributions from ASA, a further cleaning procedure which was applied to the insoluble components (AIA) collected on the filters. This final sample treatment followed the procedures developed previously for Sr isotope analyses of AIA from the same peat core (Kober et al., submitted). Specifically, three cleaning steps were carried out by repeatedly rinsing the deposits on the filters with 5 ml 1M HCl (Merck Suprapur). The cleaning procedure was completed by final rinsing with 18 M Ω H₂O. It was found that after this cleaning procedure the contributions from any labile Pb remaining in processed residuum were within the range of the verified total-procedure Pb blanks: these were < 0.3 ng (including the filter procedures and extraction steps). These Pb blank contributions were negligible compared to the processed sample Pb.

The insoluble fractions were digested using 2 ml 48 % HF + 1 drop HNO₃ (conc.); these were also Merck Suprapur reagents. All solutions were dried after digestion and the

residues redissolved in 2 ml of 2.4M HCl prior to the passage through the column. After conversion to the chloride form, Pb was separated using the lead selective extraction chromatographic SrResin[®] from EiChrom (Horwitz, et al., 1994), following the distribution factor dependencies for Pb as reported by Horwitz (1998). Further details of the extraction method have been reported by Weiss et al. (2004).

Lead extracts were loaded to single Re filaments (Si-gel technique) and were analysed using a multicollector thermal ion mass spectrometer (5-cup-TIMS Finnigan MAT261; Kober et al., 1999). The average between-sample reproducibility was found to be 0.05 – 0.1 % (2 σ) for Pb isotopes normalized to ²⁰⁴Pb. Raw TIMS data were calibrated versus NIST SRM 981 international Pb isotope standard with reference values of Galer and Abouchami (1998). Long term reproducibility of SRM981 analyses was below 0.03% (95% confidence level) for ratios normalized to ²⁰⁴Pb.

Results

Atmospheric Pb supplied by soil dust

The distribution of Pb and Ti in the AIA fraction, along with the corresponding Pb/Ti ratios, are shown in Figure 2. The average Pb concentration in the AIA is 15.2 ± 8.2 $\mu\text{g}/\text{g}$ which agrees remarkably well with the values of 14.8 $\mu\text{g}/\text{g}$ for the Earth's crust, and 17 $\mu\text{g}/\text{g}$ for the Earth's Upper Continental Crust, as reported by Wedepohl (1995). The similarity between the Pb concentrations in the AIA and the crustal values suggests that dust particles, derived from the physical and chemical weathering of rocks and soils, can account for effectively all of the natural inputs of atmospheric Pb during most of the past ca. 6,000 years. Although there is some variation, the standard deviation (8.2 $\mu\text{g}/\text{g}$) is only 53 % of the mean (15.2 $\mu\text{g}/\text{g}$) which indicates that the variation is sufficiently small that, for the purposes of the present paper, it can reasonably be ignored.

The Ti concentrations also are remarkably constant, and the distribution of this element relatively featureless. The average Ti concentration is 3190 $\mu\text{g}/\text{g}$ which

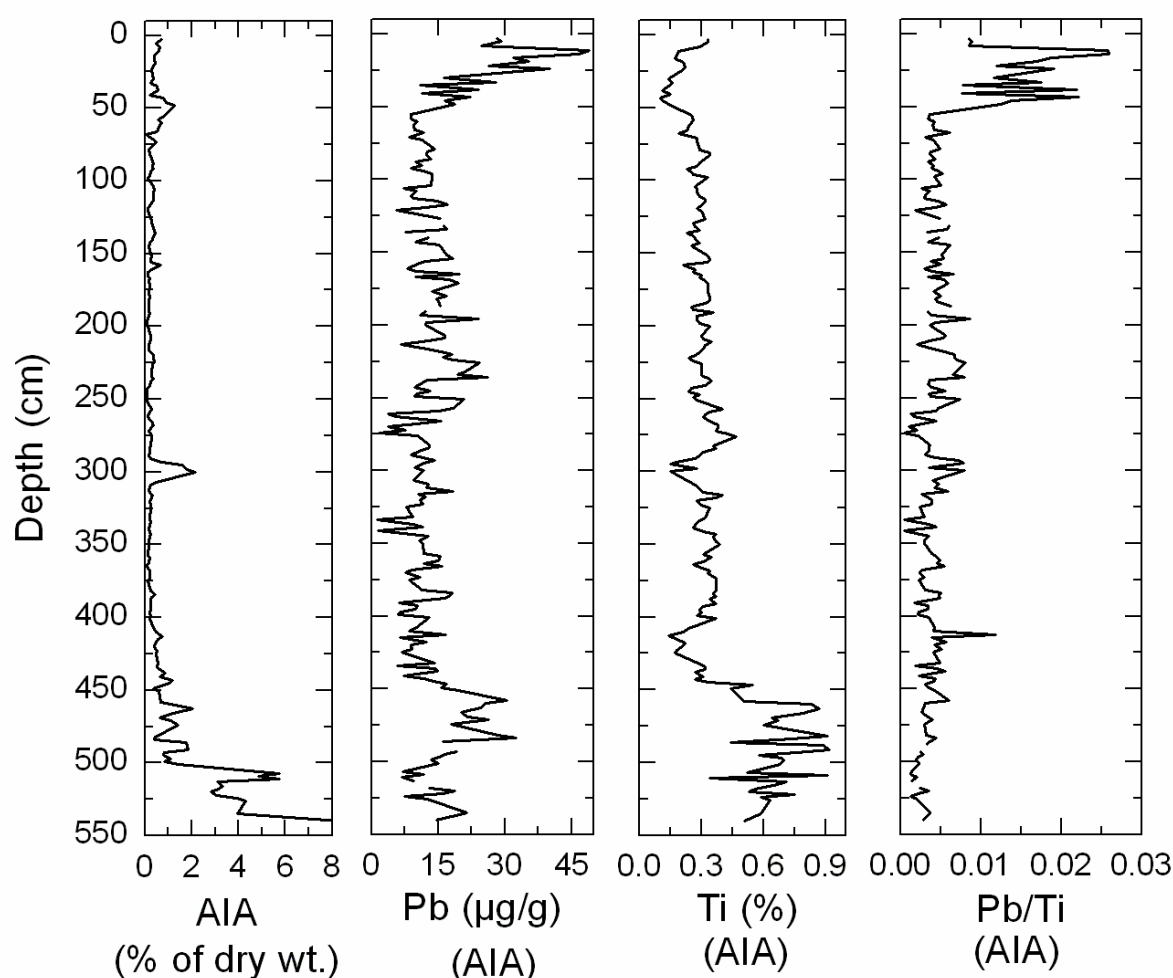


Figure 2: Relative amount of AIA (% of dry wt.); concentration profiles of Pb ($\mu\text{g/g}$) and Ti (%), and ratios of Pb to Ti in AIA.

again compares well with the value of 3117 $\mu\text{g/g}$ reported for the Upper Continental Crust (Wedepohl, 1995). The Pb and Ti concentrations in the AIA fraction yield an average Pb/Ti ratio of 4.76×10^{-3} ; this value agrees to within 13 % of the corresponding value for the Upper Continental Crust of 5.45×10^{-3} (Wedepohl, 1995). Given the similarity between the Pb and Ti concentrations of the AIA fraction and those of the Earth's Upper Continental Crust, the supply of natural, atmospheric Pb can be explained more or less exclusively by soil dust inputs, with the total flux depending only on the absolute rate of dust deposition.

Inputs of Pb from volcanic activities

Sr isotope analyses of AIA of the studied core from Oreste bog (Kober et al., submitted) have shown that the genesis of insoluble mineral particles archived by the bog is more complex than is suggested by the

smooth and homogeneous Ti and Pb concentrations across the core. The Sr isotopes demonstrate the episodic influx of volcanic particles derived from explosive eruptions of Mt. Burney volcano in the Australandean Volcanic Zone (AVZ) at A.D. 1910 (core depth 50 – 60 cm), at approximately 2.0 ka BP (~ 150 cm), at 4.2 ka BP (~ 300 cm) and at 9.0–9.2 ka BP (~ 470 – 490 cm). The importance of tephra transferred from volcanic eruption centers of the Southern Andes is supported by scanning electron microscopy (SEM) observations of large ($> 40 \mu\text{m}$) pumice particles using, found in abundance at the mentioned depths, particularly in the case of the sample from approximately 300 cm with elevated abundance of AIA (Figure 2). The Pb concentrations in the AIA samples from these depths, however, are not elevated, compared to the average concentration of Pb in AIA, even though the Sr isotope compositions

indicated contributions of tephra particles to the AIA particle mixtures in the respective layers in the range of 20 % up to 80 % (Kober et al., submitted). Specifically, the sample from a depth of 63 cm, contained only 9.5 µg/g Pb, compared to the average Pb concentration of 15.2 ± 8.2 µg/g. Similarly, the sample from a depth of 298 cm contained only 9.7 µg/g Pb. Despite the intensity of this volcanic eruption and the amount of mineral material which was deposited on the surface of the bog, this dust did not contribute any more Pb to the profile than the soil-derived dust particles which preceded it, nor the soil particles which followed it. Because the andesites and dacites of the Mt. Burney contains only about 5 µg/g Pb (Stern et al., 1984), tephra deposits from Mt. Burney are more likely to dilute the Pb in atmospheric mineral dust. Although there is documented and unambiguous evidence of volcanic inputs to the peat profile, have not significantly contributed to the Pb inventory.

Isotopic composition of natural, atmospheric Pb

The isotopic composition of Pb is summarized in Table 1 and in the form of the ratio $^{206}\text{Pb}/^{207}\text{Pb}$ in Figure 3. With the exception of the uppermost layers, the data show values which are typical for the Upper Continental Crust (Stacey and Kramers, 1975;

Ben Othman et al., 1989; Kramers and Tolstikhin, 1997). The Pb isotope composition found in the sample at 19 cm can be attributed to anthropogenic inputs. Excluding the anomaly in the top sample, the average ratio of $^{206}\text{Pb}/^{207}\text{Pb}$ is 1.196 ± 0.003 (Figure 3) which is a value typical for the Upper Continental Crust. The homogeneity of the Pb isotope composition of AIA in the peat profile over at least 6 ka of peat bog evolution indicates that not only the element concentrations in the mineral particle mixtures, but also their Pb isotope compositions were unaffected by the episodic volcanic particle influxes, despite the significant response of the reported Sr isotope ratios (Kober et al., submitted).

The averaged Pb isotope ratios of AIA in layers with volcanic input ($^{206}\text{Pb}/^{204}\text{Pb} = 18.71 \pm 0.03$, $^{207}\text{Pb}/^{204}\text{Pb} = 15.64 \pm 0.02$, $^{208}\text{Pb}/^{204}\text{Pb} = 38.62 \pm 0.07$) is identical to those in the layers without significant Sr isotope response due to volcanic contributions ($^{206}\text{Pb}/^{204}\text{Pb} = 18.67 \pm 0.02$, $^{207}\text{Pb}/^{204}\text{Pb} = 15.63 \pm 0.02$, $^{208}\text{Pb}/^{204}\text{Pb} = 38.57 \pm 0.03$). The good agreement of the Pb isotope data of volcanic influx from the AVZ with the average remote dust mixture indicates that the volcanic emissions from the AVZ approximate well the average elemental and Pb isotope composition of the remote soil dust sources.

Table 1: Pb isotope ratios of acid insoluble ash (AIA) of Oreste peat bog.

Depth (cm)	206/204	±	207/204	±	208/204	±	206/207	±	208/207	±
19	18.424	0.006	15.600	0.006	38.258	0.013	1.1810	0.0005	2.4524	0.0012
35	18.668	0.006	15.641	0.005	38.567	0.014	1.1936	0.0005	2.4658	0.0012
60	18.668	0.002	15.620	0.001	38.545	0.004	1.1952	0.0001	2.4677	0.0004
90	18.719	0.013	15.651	0.012	38.656	0.033	1.1961	0.0011	2.4699	0.0030
136	18.728	0.001	15.637	0.001	38.642	0.001	1.1976	0.0001	2.4712	0.0001
158	18.654	0.025	15.657	0.024	38.579	0.057	1.1914	0.0021	2.4640	0.0051
216	18.751	0.005	15.622	0.006	38.616	0.015	1.2003	0.0005	2.4719	0.0013
287	18.665	0.012	15.604	0.010	38.506	0.024	1.1962	0.0009	2.4677	0.0021
316	18.703	0.001	15.617	0.001	38.601	0.003	1.1976	0.0001	2.4717	0.0003
368	18.698	0.005	15.665	0.003	38.700	0.020	1.1936	0.0003	2.4705	0.0018
471	18.637	0.001	15.616	0.001	38.537	0.003	1.1934	0.0001	2.4678	0.0003
491	18.657	0.002	15.612	0.002	38.544	0.005	1.1950	0.0001	2.4688	0.0004
516	18.740	0.009	15.607	0.007	38.615	0.019	1.2008	0.0007	2.4743	0.0017

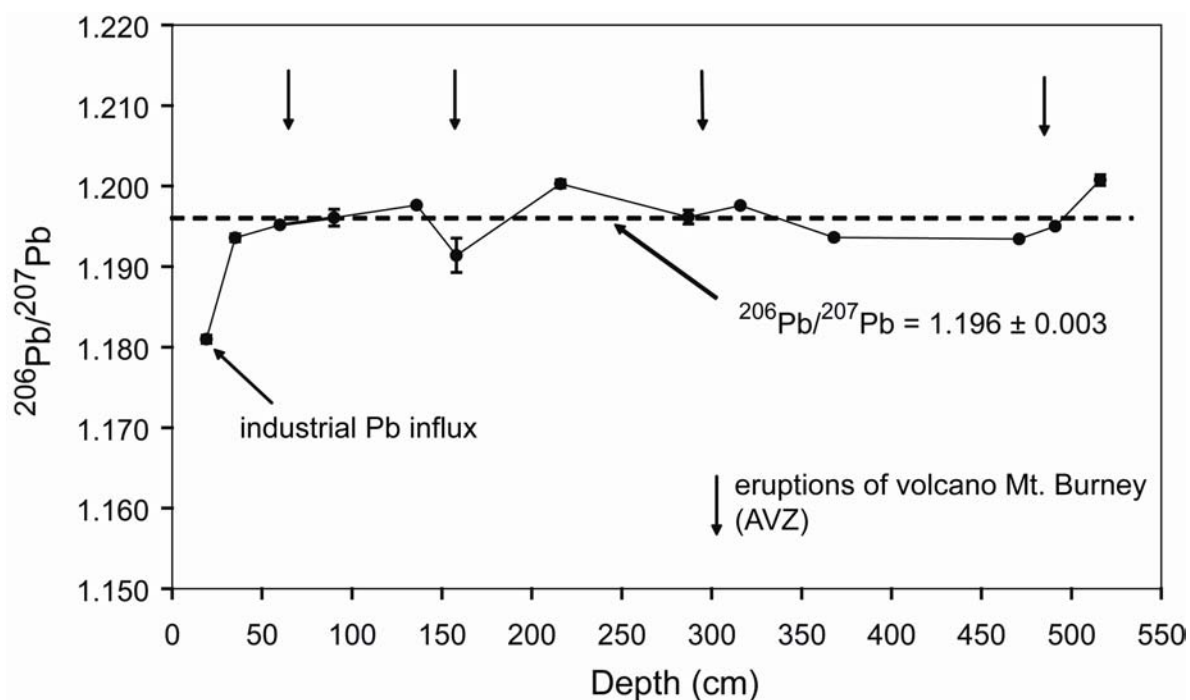


Figure 3: $^{206}\text{Pb}/^{207}\text{Pb}$ isotope ratios in selected AIA samples. Arrows correspond to layers impacted by volcanic ash inputs, as indicated by SEM micrographs as well as $^{87}\text{Sr}/^{86}\text{Sr}$ analysis (Kober et al., submitted).

The chemical and isotopic composition of basalts in southern South America is strongly influenced by the entrainment of terrigenous components in the course of slab subduction (Southern Andean arc magmas – e.g. Kilian and Behrmann, 2003), or by involvement of continental lithospheric mantle in the course of intrusional activities of more primitive OIB/MORB type and plume-related basalts which extruded in the Patagonian magmatic provinces east of the Andean Cordillera (Patagonian plateau basalts - e.g. Gorrington et al., 2003). The Southern Andean basalts as well as the Patagonian plateau basalts have been developed to rather similar Pb isotope compositions despite the strong differences in the magmatic phenomena and mixing sources. Kilian and Behrmann (2003) reported average Pb isotope ratios for the southernmost Southern Volcanic Zone (SSVZ: $^{206}\text{Pb}/^{204}\text{Pb} = 18.58$, $^{207}\text{Pb}/^{204}\text{Pb} = 15.60$, $^{208}\text{Pb}/^{204}\text{Pb} = 38.50$), the Australandean Volcanic Zone (AVZ: 18.6 – 18.7, 15.56 – 15.60, no $^{208}\text{Pb}/^{204}\text{Pb}$ given), for the Patagonian Batholith ($^{206}\text{Pb}/^{204}\text{Pb} = 18.67$, $^{207}\text{Pb}/^{204}\text{Pb} = 15.62$, $^{208}\text{Pb}/^{204}\text{Pb} = 38.62$) and for Andean S-type rocks (average of 65 Palaeozoic plutonic and metasedimentary rocks:

$^{206}\text{Pb}/^{204}\text{Pb} = 18.67$, $^{207}\text{Pb}/^{204}\text{Pb} = 15.64$, $^{208}\text{Pb}/^{204}\text{Pb} = 38.78$). Kay et al. (2004) published Pb isotope compositions of basalts e.g. from the southernmost Patagonian plateau magmatic provinces ($> 49^\circ\text{S}$: $^{206}\text{Pb}/^{204}\text{Pb} = 18.69 - 18.99$, $^{207}\text{Pb}/^{204}\text{Pb} = 15.62 - 15.66$, $^{208}\text{Pb}/^{204}\text{Pb} = 38.69 - 38.89$). All these basalt data together define a narrow Pb isotope ratio range which allows us to estimate rather precisely the average Pb isotope composition of the Southern South America crust to $^{206}\text{Pb}/^{204}\text{Pb} = 18.7$, $^{207}\text{Pb}/^{204}\text{Pb} = 15.6$, $^{208}\text{Pb}/^{204}\text{Pb} = 38.6$, yielding Pb isotope ratios of $^{206}\text{Pb}/^{207}\text{Pb} = 1.198$ and $^{208}\text{Pb}/^{207}\text{Pb} = 2.474$. This means that the average Pb isotope composition fully matches the average Pb isotope composition of AIA in the studied peat bog over much of the Holocene (~ 6 ka). Moreover, it indicates further that the average AIA peat core data precisely reflect the mean regional dust composition deflated from the soil and loess deposits of Argentina during the later Holocene.

The present data support the hypothesis that the southern South American dust sources as well as mineral dusts in the atmosphere over southern South America are related to the erosion of South American basaltic provinces and of tephra deposits

released by Andean volcanoes and Patagonian plateau volcanic centers, in agreement with conclusions reported in the literature (literature review given by Smith et al., 2003). Consequently, the apparently crustal type Pb isotope signature of Holocene eolian dust collected by the Oreste bog during the later Holocene at the southernmost edge of South America in fact is due to the specific magmatic features of the various (mafic = mantle-related) magmatic provinces and volcanic eruption centers in southern South America.

Recent, anthropogenic inputs of atmospheric Pb

At a depth of approximately 50 cm, the Pb concentrations increase, out of proportion with those of Ti, reaching a maximum of 49 µg/g Pb at a depth of 11 cm. This change is not restricted to a few samples, but rather to all of the samples from the top of the peat core. As we know of no natural geochemical process which would create an enrichment of Pb in the near-surface layers of the peat bog, we attribute these elevated values to recent inputs of anthropogenic Pb. Support for this interpretation is provided by the ratio $^{206}\text{Pb}/^{207}\text{Pb}$ which is 1.1810 ± 0.0005 at a depth of 19 cm, well below the average value for the profile of 1.196 ± 0.003 . The evolution of the isotopic composition of Pb to less radiogenic values, a process well documented in many environmental archives from the northern hemisphere (Shotyk et al., 2005a, b and references cited therein), can be most easily explained by the introduction of Pb-bearing aerosols derived from anthropogenic activities, including lead mining, smelting, and refining, coal burning, and the use of gasoline lead additives during the 20th century. Other factors contributing to the lower ratio $^{206}\text{Pb}/^{207}\text{Pb}$ include the smelting and refining of other sulphide ores (e.g. Cu, Ni, Zn), as well as the combustion of municipal solid waste.

Bollhöfer and Rosman (2000) reported $^{206}\text{Pb}/^{207}\text{Pb}$ ratios of 1.14 – 1.18 for recent aerosols emitted from areas of Brazil and Argentina, and of 1.06 – 1.18 for areas of Chile. Southern South America has been

reported to be the major source area of mineral aerosols in the Southern Hemisphere and particularly in the Antarctic atmosphere (Basile et al., 1997; Smith et al., 2003). The Pb isotope composition of mineral aerosols collected by Oreste bog during recent times ($^{206}\text{Pb}/^{207}\text{Pb} = 1.18$) is a mixture of natural dusts from soils and volcanoes ($^{206}\text{Pb}/^{207}\text{Pb} = 1.196$) and anthropogenic aerosols ($^{206}\text{Pb}/^{207}\text{Pb} = 1.06 - 1.18$), with most of the industrial particles in the topmost layers of the bog being found in the insoluble fraction. Using the average of aerosol Pb isotope compositions from nine cities in southern South America ($^{206}\text{Pb}/^{207}\text{Pb} = 1.12 \pm 0.04$; Bollhöfer and Rosman, 2000) for a rough estimation of the mean composition of anthropogenic emissions to the southern South American atmosphere, we calculate that roughly 20 – 50 % of the Pb found in topmost AIA of Oreste bog has been derived from anthropogenic sources, in agreement with the observed significantly increased Pb concentrations in top layers of the studied peat profile.

The mixture composition found in AIA of the top peat layers is more radiogenic than the highly variable Pb isotope composition of ice core dust reported for ice samples from Coats Land (Western Antarctica) for the years 1950 to 1990 ($^{206}\text{Pb}/^{207}\text{Pb} = 1.10 - 1.17$; Planchon et al., 2003) which suggests that the Pb isotope composition of recent aerosols in the Antarctic atmosphere may be significantly more heterogeneous than was previously suggested by the Pb isotope chronological standard curve for Antarctica ($^{206}\text{Pb}/^{207}\text{Pb} \sim 1.16 \pm 0.01$; Paula and Giraldez, 2003).

Comparison with the background atmospheric Pb flux in the N. Hemisphere

In the ombrotrophic peat bog at Etang de la Gruere in Switzerland, the concentrations of Pb were proportional to those of Sc from 14,500 cal. yrs. BP (when peat formation began) until to 3,200 cal. yrs. BP when anthropogenic Pb began to dominate atmospheric deposition in Europe. The correlation between Pb and Sc, a conservative, lithogenic element showed that

the Pb fluxes were controlled and regulated by the fluxes of soil dust. The dust flux was at a minimum in the peats dating from 6,000 to 9,000 cal yrs BP, corresponding to the Holocene Climate Optimum (HCO) when vegetation cover was at its greatest extent. At this time, the average peat accumulation rate was 0.45 mm/yr which, combined with the average Pb concentrations in the bulk peat samples (230 ± 40 ng/g) yielded a “background” rate of atmospheric Pb deposition of $10 \mu\text{g}/\text{m}^2/\text{yr}$ Pb.

In the Oreste bog, the average rate of accumulation of Pb can be calculated as the product of the average peat density ($0.06 \text{ g}/\text{cm}^3$), accumulation rate ($0.08 \text{ cm}/\text{yr}$), Ti concentration ($34 \mu\text{g}/\text{g}$), and Pb/Ti ratio ($15.2/3190$) which yields $7.8 \mu\text{g}/\text{m}^2/\text{yr}$ Pb. This “background” rate of atmospheric Pb deposition for the southern hemisphere obtained using the peat core from the Oreste bog ($7.8 \mu\text{g}/\text{m}^2/\text{yr}$ Pb) is in remarkably good agreement with that obtained using the peat bog at EGR in the northern hemisphere ($10 \mu\text{g}/\text{m}^2/\text{yr}$ Pb). Although the dust flux recorded by EGR during the mid-Holocene ($0.23 \pm 0.12 \text{ g}/\text{m}^2$) is half that of Oreste bog ($0.43 \pm 0.12 \text{ g}/\text{m}^2$), the Pb/Ti ratio in the peat samples from EGR was approximately 40 % greater.

Pre-anthropogenic flux of Pb to the global atmosphere

In a previous paper, we used the background Pb flux at EGR ($10 \mu\text{g}/\text{m}^2/\text{yr}$) and extrapolating to the continental land area ($147 \times 10^6 \text{ km}^2$), obtaining an estimated natural flux of 1480 T/yr Pb to the continents (Shotyk et al., 2004). Assuming that the natural flux of Pb to the oceans is comparable to the continental flux, the total natural flux to the global atmosphere was estimated to be ca. $3 \times 1480 = 4440$ T/yr. If the natural flux of atmospheric Pb in the southern hemisphere is ca. 20% less than in the northern hemisphere, and if two-thirds of the total flux originates in the northern hemisphere (with its correspondingly larger land mass), then a better estimate of the total flux of natural atmospheric Pb would be 4150 T/yr; this latter estimate brings us slightly closer to the original estimate by Patterson and Settle

(1987) (2600 T/yr). Mather et al. (2003) have used data from the literature to estimate a mean annual emission rate of soil dust to the atmosphere at 2150 Tg/yr. Using mean Pb concentrations of $14.8 \mu\text{g}/\text{g}$ for the Earth’s crust, or $17 \mu\text{g}/\text{g}$ for the Earth’s Upper Continental Crust (Wedepohl, 1995) we calculate mean annual Pb emission rates of 3180 T/yr and 3650 T/yr, respectively. Thus these different and independent estimations all favor a total flux of natural atmospheric Pb in the range 2000 – 4000 T/yr. Either way, the calculations suggest that the approach described here - using chemical analyses of Pb in peat dating from pre-anthropogenic times - is reasonable approximation of the global atmospheric Pb deposition rates – both for the Holocene and for recent times.

The results presented here contrast with the current estimated flux of natural Pb to the global atmosphere (12,000 T/yr) published by Pacyna and Pacyna (2001). It is suggested by our data and the estimations of Mather et al. (2003) and Patterson and Settle (1987) that the current estimated flux of natural Pb to the global atmosphere proposed by Pacyna and Pacyna (2001) is an overestimate by a factor of 3 - 6.

Acknowledgements

Dr. Vera Markgraf collected the peat core from Oreste bog in 1995 under a grant from National Science Foundation (NSF-EAR-9709145), and generously provided the peat core. Ms. Stephanie Janssen (University of Köln) prepared the samples for age dating. We thank Ms. Olena Kurzel for the XRF and SEM analysis. We gratefully acknowledge the assistance of Ms. Dietlinde Pingel in preparing the cleanroom wet chemistry for Pb isotope extraction and in analyzing Pb isotopes using TIMS.

References

- Basile, I., F. E. Grousset, M. Revel, J. R. Petit, P. E. Biscaye, and N. I. Barkov (1997), Patagonian origin of glacial dust deposited in east Antarctica (Vostok and Dome c) during glacial stages 2., 4, and 6, *Earth and Planet. Sci. Lett.*, 146, 573-589.

- Ben Othman, D., W. M. White, and J. Patchett (1989), The geochemistry of marine sediments, island arc magma genesis, and crust-mantle recycling, *Earth and Planet. Sci. Lett.*, *94*, 1-21.
- Bollhöfer, A., and K. J. R. Rosman (2000), Isotopic source signatures for atmospheric lead: the Southern Hemisphere, *Geochim. Cosmochim. Acta*, *64*, 3251-3262.
- Bränvall, M. L., R. Bindler, O. Emteryd, M. Nilsson, and I. Renberg (1997), Stable isotope and concentration records of atmospheric lead pollution in peat and lake sediments in Sweden, *Water Air Soil Pollut.*, *100*, 243-252.
- Cheburkin, A. K., and W. Shotyk (1996), An Energy-dispersive Miniprobe Multielement Analyzer (EMMA) for direct analysis of Pb and other trace elements in peats, *Fresenius J. Anal. Chem.*, *354*, 688-691.
- Cheburkin, A. K., and W. Shotyk (2005), Energy-dispersive XRF spectrometer for Ti determination (TITAN), *X-Ray Spectrom.*, *34*, 69-72.
- Farmer, J. G., A. B. Mackenzie, C. L. Sugden, P. J. Edgar, and L. J. Eades (1997), A comparison of the historical lead pollution records in peat and freshwater lake sediments from central Scotland, *Water Air Soil Pollut.*, *100*, 253-270.
- Galer, S. J. G., and W. Abouchami (1998), Practical application of lead triple spiking for correction of instrumental mass discrimination, *Miner. Mag.*, *62*, 491-492.
- Gorring, M., B. Singer, J. Gowers, and S. M. Kay (2003), Plio-Pleistocene basalts from the Meseta del Lago Buenos Aires, Argentina: evidence for asthenosphere-lithosphere interactions during slab window magmatism, *Chem. Geol.*, *193*, 215-235.
- Horwitz, E. P., M. L. Dietz, S. Rhoads, C. Felinto, N. H. Gale, and J. Houghton (1994), A lead selective extraction chromatographic resin and its application to the isolation of lead from geological samples, *Anal. Chim. Acta*, *292*, 263-273.
- Horwitz, E. P. (1998), Extraction Chromatography of Actinides and Selected Fission Products: Principles and Achievement of Selectivity, *International Workshop on the Application of Extraction Chromatography in Radionuclide Measurement*, IRMM, Geel, Belgium, 9-10.
- Kay, S. M., M. Gorring, and V. A. Ramos (2004), Magmatic sources, setting and causes of Eocene to recent Patagonian plateau magmatism (36°S to 52°S latitude), *Rev. Asoc. Geol. Argent.*, *59*, 556-568.
- Kempton, H., M. Görres, and B. Frenzel (1997), Ti and Pb concentrations in rainwater-fed bogs in Europe as indicators of past anthropogenic activities, *Water Air Soil Pollut.*, *100*, 367-377.
- Kilian, R., and J. H. Behrmann (2003), Geochemical constraints on the sources of Southern Chile Trench sediments and their recycling in arc magmas of the Southern Andes, *J. Geol. Soc.*, *160*, 57-70.
- Klaminder, J., I. Renberg, R. Bindler, O. Emteryd (2003), Isotopic trends and background fluxes of atmospheric lead in northern Europe: Analyses of three ombrotrophic bogs from south Sweden, *Global Biogeochem. Cycles*, *17*, 1
- Kober, B., M. Wessels, A. Bollhöfer, and A. Mangini (1999), Pb isotopes in sediments of Lake Constance, Central Europe constrain the heavy metal pathways and the pollution history of the catchment, the lake and the regional atmosphere, *Geochim. Cosmochim. Acta*, *63*, 1293-1303.
- Kramers, J. D., and N. Tolstikhin (1997), Two terrestrial lead isotope paradoxes, forward transport modeling, core formation and the history of the continental crust, *Chem. Geol.*, *139*, 75-110.
- LeRoux G., D. Weiss, J. Grattan, N. Givelet, M. Krachler, A. K. Cheburkin, N.

- Rausch, B. Kober, and W. Shotyk (2004), Identifying the sources and timing of ancient and medieval atmospheric metal pollution in England by a peat profile, *J. Environ. Monit.*, *6*, 502-510.
- MacKenzie A. B., J. G. Farmer, C. L. Sugden (1997), Isotopic evidence of the relative retention and mobility of lead and radiocaesium in Scottish ombrotrophic peats, *Sci. Total Environ.*, *203*, 115-127.
- MacKenzie A. B., E. M. Logan, G. T. Cook, I. D. Pulford (1998), Distributions, inventories, and isotopic composition of lead in ^{210}Pb -dated peat cores from contrasting biogeochemical environments: Implications for lead mobility, *Sci. Total Environ.*, *223*, 25-35.
- Martinez-Cortizas, A., X. Pontevedra Pomba, J. C. Novoa Munoz, and E. Garcia-Rodeja (1997), Four thousand years of atmospheric Pb, Cd, and Zn deposition recorded by the ombrotrophic peat bog of Penido Vello (northwestern Spain), *Water Air Soil Pollut.*, *100*, 387-403.
- Martinez Cortizas, A., E. Garcia-Rodeja, X. Pontevedra Pombal, J. C. Novoa Munoz, D. Weiss, and A. K. Cheburkin (2002), Atmospheric Pb deposition in Spain during the last 4600 years recorded by two ombrotrophic peat bogs and implications for the use of peat as archive, *Sci. Total Environ.*, *292*, 33-44.
- Mather, T. A., D. M. Pyle, and C. Oppenheimer (2003), Tropospheric volcanic aerosol, in *Volcanism and the Earth's atmosphere*, *Geophys. Monogr. Ser.*, vol. 139, edited by A. Robock and C. Oppenheimer, pp. 189-212, AGU, Washington, D. C.
- Monna, F., C. Petit, J.-P. Guillaumet, I. Jouffroy-Bapicot, J. Dominik, R. Losno, H. Richard, J. Leveque, and C. Chateau (2004), History and environmental impact of mining activity in Celtic Aeduan territory recorded in a peat bog (Morvan, France), *Environ. Sci. Tech.*, *38*, 665-673.
- Nieminen, T., L. Ukonmaanaho, and W. Shotyk (2002), Enrichment of Cu, Ni, Zn, Pb and As in an ombrotrophic peat bog near a Cu-Ni smelter in SW Finland, *Sci. Total Environ.*, *292*, 81-89.
- Norton, S. A., G. C. Evans, and J. S. Kahl (1997), Comparison of Hg and Pb fluxes to hummocks and hollows of ombrotrophic Big Heath Bog and to nearby Sargent Mt. Pond, Maine, USA *Water Air Soil Pollut.*, *100*, 271-286.
- Novak M., S. Emmanuel, M. A. Vile, Y. Erel, A. Veron, T. Paces, R. K. Wieder, M. Vanecek, M. Stepanova, E. Brizova, J. Hovorka (2003), Origin of lead in eight Central European Peat Bogs determined from isotope ratios, strengths and operation times of regional pollution sources, *Environ. Sci. Tech.*, *37*, 437-445.
- Olivero, E. B., and D. R. Martinioni (2001), A review of the geology of the Argentinean Fuegian Andes, *J South Am. Earth Sci.*, *14*, 175-188.
- Pacyna, J. M., and E. G. Pacyna (2001), An assessment of global and regional emissions of trace metals to the atmosphere from anthropogenic sources worldwide, *Environ. Rev.*, *9*, 269-298.
- Patterson, C. C., and D. M. Settle (1987), Magnitude of the lead flux to the atmosphere from volcanoes, *Geochim. Cosmochim. Acta*, *51*, 675-681.
- Paula, A. H., and M. C. Geraldies (2003), Holocene Pb isotope chronological standard curve: a review of the record of the anthropogenic activity in the last 6000 years, Short papers – IV South American Symposium on Isotope Geology, pp. 465-468, Salvador, Brazil, 24-27 August.
- Pendall, E., V. Markgraf, J. V. C. White, and M. Dreier (2001), Multiproxy record of Late Pleistocene-Holocene climate and vegetation changes from a peat bog in Patagonia, *Quat. Res.*, *55*, 168-178.
- Planchon, F. A. M., K. Van De Velde, K. J. R. Rosman, E. W. Wolff, C. P. Ferrari, and C. F. Boutron (2003), One hundred fifty-year record of lead isotopes in Antarctic snow from Coats Land,

- Geochim. Cosmochim. Acta*, 67, 693-708.
- Rabassa, J., A. Coronato, and C. Roig (1996), The peat bogs of Tierra del Fuego, Argentina, in *Global peat resources*, edited by E. Lappalainen, International Peat Society, Finland, pp. 261-265.
- Shotyk, W., A. K. Cheburkin, P. G. Appleby, A. Fankhauser, and J. D. Kramers (1996), Two thousand years of atmospheric arsenic, antimony, and lead deposition recorded in a peat bog profile, Jura Mountains, Switzerland, *Earth Planet. Sci. Lett.*, 145, E1-E7.
- Shotyk, W., D. Weiss, P. G. Appleby, A. K. Cheburkin, R. Frei, M. Gloor, J. D. Kramers, S. Reese, and W. O. Van der Knaap (1998), History of atmospheric lead deposition since 12,370 ¹⁴C yr BP recorded in a peat bog profile, Jura Mountains, Switzerland, *Science*, 281, 1635-1640.
- Shotyk, W., P. Blaser, A. Grünig, and A. K. Cheburkin (2000), A new approach for quantifying cumulative, anthropogenic, atmospheric lead deposition using peat cores from bogs: Pb in eight Swiss peat bog profiles, *Sci. Total Environ.*, 249, 281-295.
- Shotyk, W., D. Weiss, J. D. Kramers, R. Frei, A. K. Cheburkin, M. Gloor, and S. Reese (2001), Geochemistry of the peat bog at Etang de la Gruure, Jura Mountains, Switzerland, and its record of atmospheric Pb and lithogenic trace elements (Sc, Ti, Y, Zr, Hf and REE) since 12,370 ¹⁴C yr BP, *Geochim. Cosmochim. Acta*, 65, 2337-2360.
- Shotyk, W., D. Weiss, M. Heisterkamp, A. K. Cheburkin, and F. C. Adams (2002a), A new peat bog record of atmospheric lead pollution in Switzerland: Pb concentrations, enrichment factors, isotopic composition, and organolead species, *Environ. Sci. Tech.*, 36, 3893-3900.
- Shotyk, W., M. Krachler, A. Martinez-Cortizas, A. K. Cheburkin, and H. Emons (2002b), A peat bog record of natural, pre-anthropogenic enrichments of trace elements in atmospheric aerosols since 12,370 ¹⁴C yr BP, and their variation with Holocene climate change, *Earth Planet. Sci. Lett.*, 199, 21-37.
- Shotyk, W., M. E. Goodsite, F. Roos-Barraclough, J. Heinemeier, R. Frei, G. Asmund, C. Lohse, and T. H. Stroyer (2003), Anthropogenic contributions to atmospheric Hg, Pb, and As deposition recorded by peat cores from Greenland and Denmark dated using the ¹⁴C ams “bomb pulse curve”, *Geochim. Cosmochim. Acta*, 67, 3991-4011.
- Shotyk, W., M. Krachler, and B. Chen (2004), Antimony in recent peat from Switzerland and Scotland: comparison with natural background values (5,320 to 8,020 ¹⁴C yr BP), correlation with Pb, and implications for the global atmospheric Sb cycle, *Global Biogeochem. Cycles*, 18(GB), 1016, doi:10.1029/2003GB002113.
- Shotyk, W., M. E. Goodsite, F. Roos-Barraclough, N. Givélet, G. LeRoux, D. Weiss, A. K. Cheburkin, K. Knudsen, J. Heinemeier, W. O. Van der Knaap, S. A. Norton, and C. Lohse (2005), Accumulation rates and predominant atmospheric sources of natural and anthropogenic Hg and Pb on the Faroe Islands, *Geochim. Cosmochim. Acta*, 69, 1-17.
- Shotyk, W., J. Zheng, M. Krachler, C. Zdanowicz, R. Koerner, and D. Fisher, (2005), Predominance of industrial Pb in recent snow from Devon Island, Arctic Canada, *Geophys. Res. Lett.*, 32(L2), 1814, doi:10.1029/2005GL023860.
- Smith, J., D. Vance, R. A. Kemp, C. Archer, P. Toms, M. King, and M. Zarate (2003), Isotopic constraints on the source of Argentinian loess – with implications for atmospheric circulation and the provenance of Antarctic dust during recent glacial maxima, *Earth Planet. Sci. Lett.*, 212, 181-196.
- Stacey, J. S., and J. D. Kramers (1975), Approximation of terrestrial lead isotope evolution by a two-stage model, *Earth Planet. Sci. Lett.*, 26, 207-221.

- Steinmann, P., and W. Shotyk (1997), Geochemistry, mineralogy, and geochemical mass balance on major elements on two peat bog profiles (Jura Mountains, Switzerland), *Chem. Geol.*, 138, 25-53.
- Stern C. R., K. Futa, and K. Muehlenbachs (1984), in *Andean Magmatism: Chemical and Isotopic constraints*, edited by R. S. Harmon and B. A. Barreiro, pp. 31-46, Shiva Publishing Limited, UK.
- Tuhkanen, S. (1992) The climate of Tierra del Fuego from a vegetation geographical point of view and its ecoclimatic counterparts elsewhere, *Acta Bot. Fenn.*, 145, 1-64.
- Vile, M. A., M. J. Novak, E. Brizova, R. K. Wieder, and W. R. Schell (1995), Historical rates of atmospheric Pb deposition using ^{210}Pb dated peat cores: corroboration, computation, and interpretation, *Water Air Soil Pollut.*, 79, 89-106.
- Vile M. A., R. K. Wieder, M. Novak (1999), Mobility of Pb in Sphagnum-derived peat, *Biogeochem*, 45 35-52.
- Wedepohl K. H. (1995), The composition of the continental crust, *Geochim. Cosmochim. Acta*, 59, 1217-1232.
- Weiss, D., W. Shotyk, P. G. Appleby, A. K. Cheburkin, and J. D. Kramers (1999a), Atmospheric Pb deposition since the Industrial Revolution recorded by five Swiss peat profiles: enrichment factors, fluxes, isotopic composition, and sources *Environ. Sci. Tech.*, 33, 1340-1352.
- Weiss, D., W. Shotyk, M. Gloor, and J. D. Kramers (1999b), Herbarium specimens of *Sphagnum* moss as archives of recent and past atmospheric Pb deposition in Switzerland: isotopic composition and source assessment, *Atmos. Environ.*, 33, 3751-3763.
- Weiss, D., W. Shotyk, E. A. Boyle, J. D. Kramers, P. G. Appleby, and A. K. Cheburkin (2002), Constraining lead sources the North Atlantic Ocean: recent atmospheric lead deposition recorded by two ombrotrophic peat bogs in Scotland and Eastern Canada, *Sci. Total Environ.*, 292, 7-18.
- Weiss, D. J., B. Kober, A. Dolgoplova, K. Gallagher, B. Spiro, G. LeRoux, T. F. D. Mason, M. Kylander, and B. J. Coles (2004), Accurate and precise Pb isotope ratio measurements in environmental samples by MC-ICP-MS, *Int. J. Mass Spectrom.*, 232, 205-215.
- Zarate, M. A. (2003), Loess of southern South America, *Quat. Sci. Rev.*, 22, 1987-2006.

Appendixes

-Appendix I- Suggested protocol for collecting, handling and preparing peat cores and peat samples for physical, chemical, mineralogical and isotopic analyses

Nicolas Givelet^{a,‡}, Gaël Le Roux^b, Andriy Cheburkin^b, Bin Chen^b, Jutta Frank^b, Michael E. Goodsite^c, Heike Kempter^b, Michael Krachler^b, Tommy Noernberg^c, Nicole Rausch^b, Stefan Rheinberger^b, Fiona Roos-Barraclough^{#a}, Atindra Sapkota^b, Christian Scholz^b, and William Shotyk^{b*}

^aInstitute of Geological Sciences, University of Berne, Baltzerstrasse 1-3, CH-3012 Berne, Switzerland.

^bInstitute of Environmental Geochemistry, University of Heidelberg, Im Neuenheimer Feld 236, D-69120 Heidelberg, Germany. E-mail: shotyk@ugc.uni-heidelberg.de; Tel: +49 (6221) 54 4803; Fax: +49 (6221) 54 5228

^cDepartment of Chemistry, University of southern Denmark, Campusvej 55, DK-5230 Odense M.

[‡]Present affiliation: Institute of Environmental Geochemistry, University of Heidelberg, Germany. E-mail: givelet@ugc.uni-heidelberg.de

[#]Present affiliation: Chemical Analytical R&D, Cilag, Switzerland.

*To whom correspondence should be addressed

Journal of Environmental Monitoring 6, 481-492 (2004)

Abstract

For detailed reconstructions of atmospheric metal deposition using peat cores from bogs, a comprehensive protocol for working with peat cores is proposed. The first step is to locate and determine suitable sampling sites in accordance with the principal goal of the study, the period of time of interest and the precision required. Using the state of the art procedures and field equipment, peat cores are collected in such a way as to provide high quality records for paleoenvironmental study. Pertinent field observations gathered during the fieldwork are recorded in a field report. Cores are kept frozen at -18 °C until they can be prepared in the laboratory. Frozen peat cores are precisely cut into 1 cm slices using a stainless steel band saw with stainless steel blades. The outside edges of each slice are removed using a titanium knife to avoid any possible contamination, which might have occurred during the sampling and handling stage. Each slice is split, with one-half kept frozen for future studies (archived), and the other half further subdivided for physical, chemical, and mineralogical analyses. Physical parameters such as ash and water contents, the bulk density and the degree of decomposition of the peat are determined using established methods. A subsample is dried overnight at 105 °C in a drying oven and milled in a centrifugal mill with titanium sieve. Prior to any expensive and time consuming chemical procedures and analyses, the resulting powdered samples, after manual homogenisation, are measured for more than twenty-two major and trace elements using non-destructive X-Ray fluorescence (XRF) methods. This approach provides lots of valuable geochemical data, which documents the natural geochemical processes, which occur in the peat profiles and their possible effect on the trace metal profiles. The development, evaluation and use of peat cores from bogs as archives of high-resolution records of atmospheric deposition of mineral dust and trace elements have led to the development of many analytical procedures which now permit the measurement of a wide range of elements in peat samples such as lead and lead isotopes ratios, mercury, arsenic, antimony, silver, molybdenum, thorium, uranium, rare earth elements. Radiometric methods (the carbon bomb pulse of ¹⁴C, ²¹⁰Pb and conventional ¹⁴C dating) are combined to allow reliable agedepth models to be reconstructed for each peat profile.

Introduction

The use of peat cores from bogs in paleoenvironmental studies has increased dramatically during the last decade.¹⁻⁶ The reasons for this are not only that peat cores from ombrotrophic bogs are excellent archives of many kinds of atmospheric particles: soil dust, volcanic ash, phytoliths, anthropogenic aerosols, and many trace elements but peat bogs are also economically attractive archives because the concentrations of trace elements such as mercury (Hg) and lead (Pb), are sufficiently high that they are much more accessible by conventional methods of analysis than other archives of atmospheric deposition such as ice cores. Unlike glacial ice which is restricted to Alpine and Polar regions, peatlands are widely distributed across the globe, accounting perhaps 5% of the land area of the Earth.⁷ There is growing evidence that undisturbed bogs have faithfully preserved the historical records of a wide range of trace metals, despite the low pH and abundance of dissolved organic acids in the waters, and the seasonal variations in water table (and impact which this may have on redox state). In the case of a metal such as lead, for example, the historical record of atmospheric Pb deposition is so well preserved in undisturbed bogs⁸ that our ability to read and interpret the peat bog records is largely independent of chemical processes taking place within the bog itself, but can depend to a large extent on the methods used to collect, handle, and prepare the samples for analysis.⁹ Moreover, the lack of a commonly used, validated protocol has hindered the interpretation and comparison of peat core metal profiles from different laboratories within the international community. Therefore, to compare the published peat bog records with one another or to other archives (e.g. lake sediments, ice cores, tree rings), and for detailed reconstructions of atmospheric metal deposition, a comprehensive protocol for working with peat cores is warranted.

Since the first cores for chemical analysis were collected at Etang de la Gruère in the Jura Mountains, Switzerland, in the autumn of 1990,¹⁰ many changes and developments have been made with respect to

the practical aspects of this work. The present paper shows that the effects of core compression during sampling, the spatial resolution obtained by core cutting, as well as the accuracy and precision of peat core slicing can very much affect the measured record of trace element concentrations and enrichment factors (EF). Moreover, in this paper we have summarized the refinements made to the methodological procedures and analyses which have been developed by our research group over the years, to share these with the international community. We hope that the protocol described here can serve as a guideline for future paleoenvironmental studies using peat cores from bogs. Improvements to the description of the coring sites and the cores themselves, the accuracy and precision of slicing techniques and sub-sampling, as well as the physical and chemical analytical methods employed and the dating methods used to model the age-depth relationship, will help to ensure that the results obtained by different research teams are directly comparable.

Background to the problem

Comparison of two peat bog records of atmospheric lead pollution from Etang de la Gruère in Switzerland (EGR) have shown that while the general agreement between the two cores (EGR, cores 2F and 2K) is very good, there are also some differences.⁹ One difference is revealed by the concentration profiles of anthropogenic Pb. The 2F core reveals two pronounced peaks of nearly identical Pb EF during the 20th century, but in the 2K core the more recent of these two is less pronounced (Fig. 1). Here, possible reasons for this difference are explored: differential core compression during sample collection, the relative thick peat slices (3 cm) used to represent the individual samples, and from the imprecision of the cutting technique used to section the cores.

Effects of core compression on anthropogenic Pb concentrations

A summary of some physical and chemical properties of the two peat cores is given in Figure 1. In general, both profiles contain a zone of enhanced peat humification

from ca. 20 to 60 cm which is visible upon inspection of the cores in the field (darker colour, finer texture, fewer visible plant remains). This zone is also revealed in each core by the elevated bulk density values at these depths, as well as reduced pH values and lower yields of extractable porewater (Fig. 2). However, there are some discernible differences between the two cores. First, the ash content profile shows significantly higher maximum ash content in the 2F core (8.6 %) compared with 2K (6.9 %). Second, the maximum bulk density in the 2F core (0.15 g cm^{-3}) exceeds that of 2K (0.13 g cm^{-3}). Both of these changes suggest that the 2F core experienced compression in the vertical

direction, relative to the 2K core. At the time which core 2F was collected (26. August, 1991), the bog surface was very dry; with the depth to water table approximately 70 cm below the peat surface. During these conditions, it is very difficult to obtain a peat monolith without compressing the core, especially with the abundance of roots of Ericaceous shrubs and Eriophorum fibres which dominate the near surface layers of the peat profile. Comparison of the ash content and bulk density profiles introduces (Fig. 1) the suspicion that the 2F core was compressed, relative to 2K, during core retrieval.

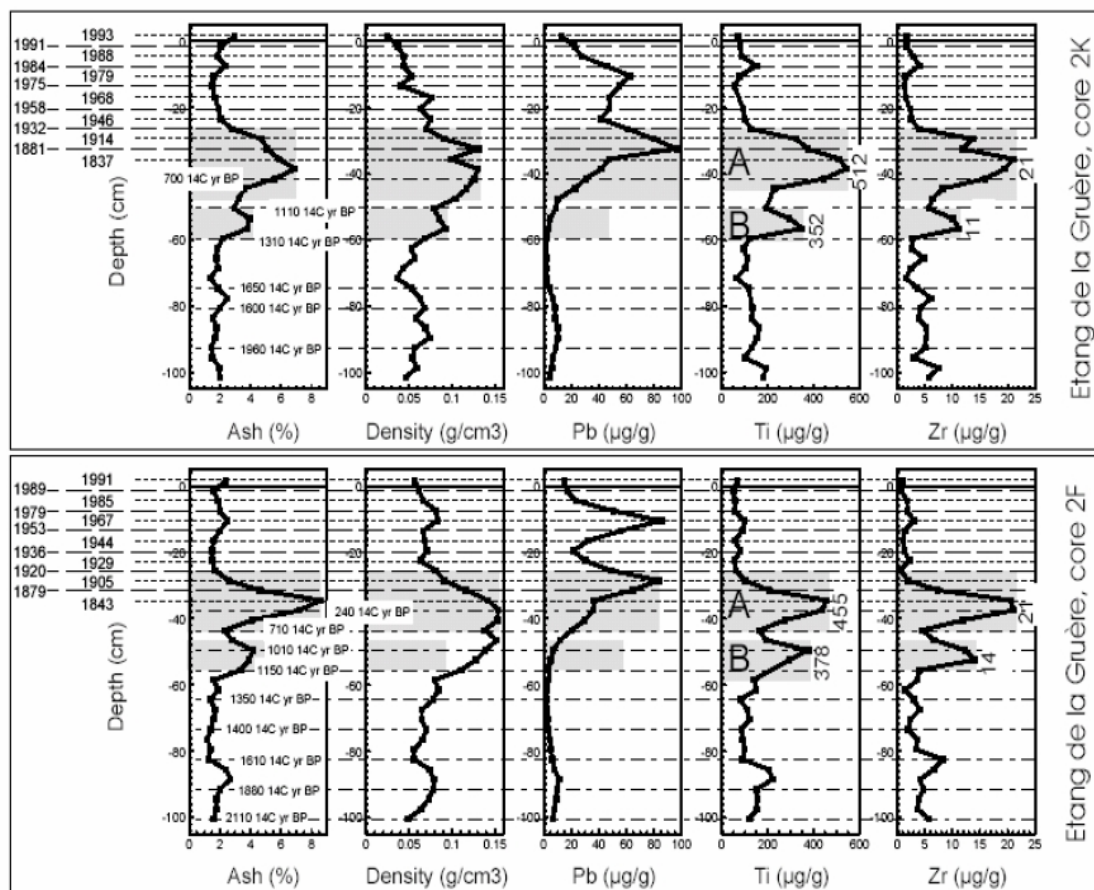


Fig. 1. a) Ash content, bulk density, concentrations of Pb, Ti, Zr, and Pb EF in the 2K core. b) ash content, bulk density, concentrations of Pb, Ti, Zr, and Pb EF in the 2F core. Maximum concentrations of Ti and Zr are indicated beside the peaks identified by the shaded bars. Pb EF calculated using Sc (relative to Earth's Crust). Age dates shown on the right hand side of box b) were obtained using ^{210}Pb , age dates within box b) are radiocarbon ages, expressed as conventional radiocarbon years Before Present.

The abundance and distribution of total Pb concentrations exhibit striking differences: in 2F, there are two nearly identical peaks in Pb concentration, whereas in the 2K core the deeper, older peak is clearly superior (Fig. 1). The concentrations of Pb at these depths exceed the LLD ($0.4 \mu\text{g g}^{-1}$) by more than two orders of magnitude, and in this concentration range the accuracy and precision of the Pb measurements using EMMA XRF are better than 5%.¹¹ Thus, the difference in the abundance and distribution of Pb cannot be explained in terms of analytical error. Titanium and Zr both show two pronounced peaks in each core, but the ratios between the two peaks differ (Fig. 1): in the 2K core, the ratio of Ti and Zr in peak A to peak B are 1.5 and 1.9, respectively; the corresponding ratios in 2F are 1.2 and 1.5, respectively. Thus, soil-derived mineral

material is relatively more abundant in the A peak of the 2K core than the A peak of the 2F core. To say it another way, Pb, Ti, and Zr are relatively more abundant in the B peak of core 2F compared with core 2K. This difference may simply reflect the extent of natural variation with a given area at a given time, as observed previously using Sphagnum mosses collected from a given bog during a single year.¹² However, if both Pb and Ti have been accidentally increased at any point in the 2F peat core by vertical compression while coring, then both elements would increase in concentration to the same extent, and this would have no net effect on anthropogenic Pb calculated as described earlier. Thus, the direct effect of compression in the 2F peat core on the concentrations of Pb and Ti cannot explain the differences in the relative abundance of anthropogenic Pb between the two cores.

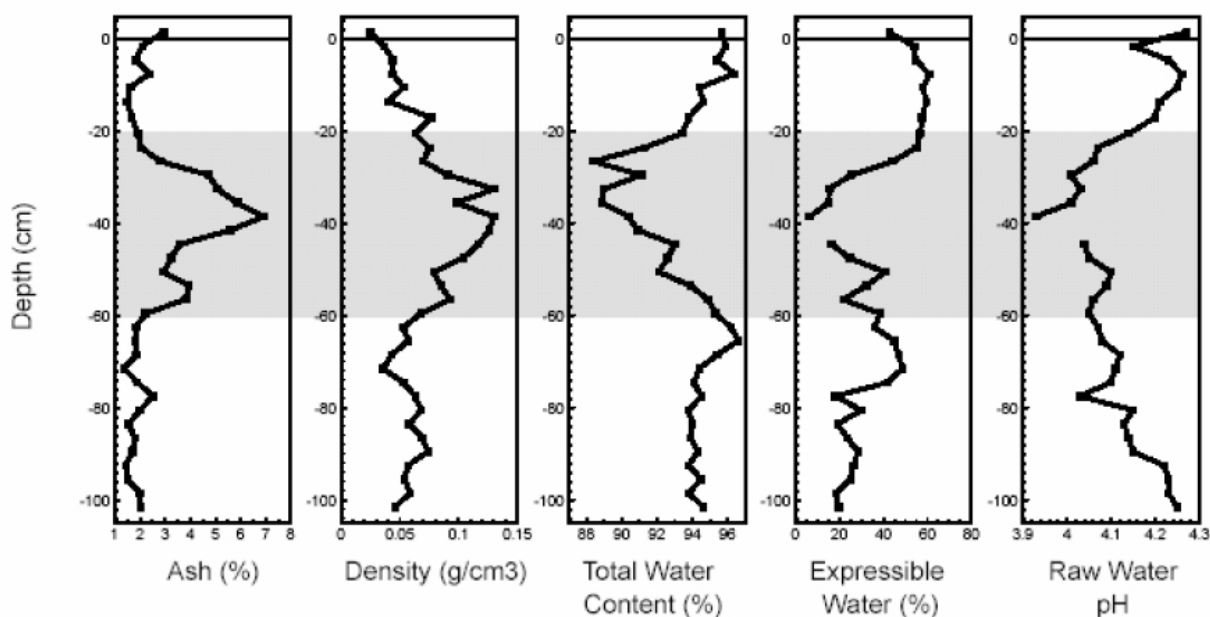


Fig. 2. Ash concentration, bulk density, total water content, expressible water, and raw water pH, 2K core.

Effects of core compression on the age-depth relationship

To further evaluate the possibility that the 2F core may have been compressed and to try to understand the possible importance of this process, the age depth relationship has been plotted for the entire length of both cores (Fig. 3a) and for only the uppermost layers which were dated using ^{210}Pb (Fig. 3b). Both graphics show clearly that there has been some vertical displacement of the 2F core, relative to 2K. First, the arrows in Fig. 3a show an inflection point where age does not measurably change with depth; in the 2F core, this is found between 64 and 74 cm, but in the 2K core from 74 to 81 cm. The change in ^{210}Pb age with depth shows that the 2F core has certainly been compressed, relative to 2K, in particular in the range ca. 10 to 30 cm (Fig. 3b). Also shown in Fig. 3c is the incremental age, in calendar years, for the individual slices of 2K samples pre-dating ca. 1980. This information is included to emphasize the

increase in age of each peat slice with increasing depth. In the range where the 2F core was compressed, the individual peat slices represent from 4 to 33 years of peat accumulation. The effect of compression on age therefore becomes increasingly important with depth, as a greater proportion of older material becomes compressed into a given volume. The extent of compression can be estimated by assuming that any given ^{210}Pb age should be found at the same depth in each core. Assuming this ideal case, the vertical difference between the two cores is approximately 3 cm at 1920, 6 cm at 1940, 12 cm at 1960, and 4 cm at 1980 (Fig. 3c).

Despite these differences and the causes to which they are due, compression of the peat core will affect the activity of ^{210}Pb and the concentrations of Pb and Sc. Compression of the peat core alone, therefore will not affect the chronology or intensity of the changes in anthropogenic Pb concentrations.

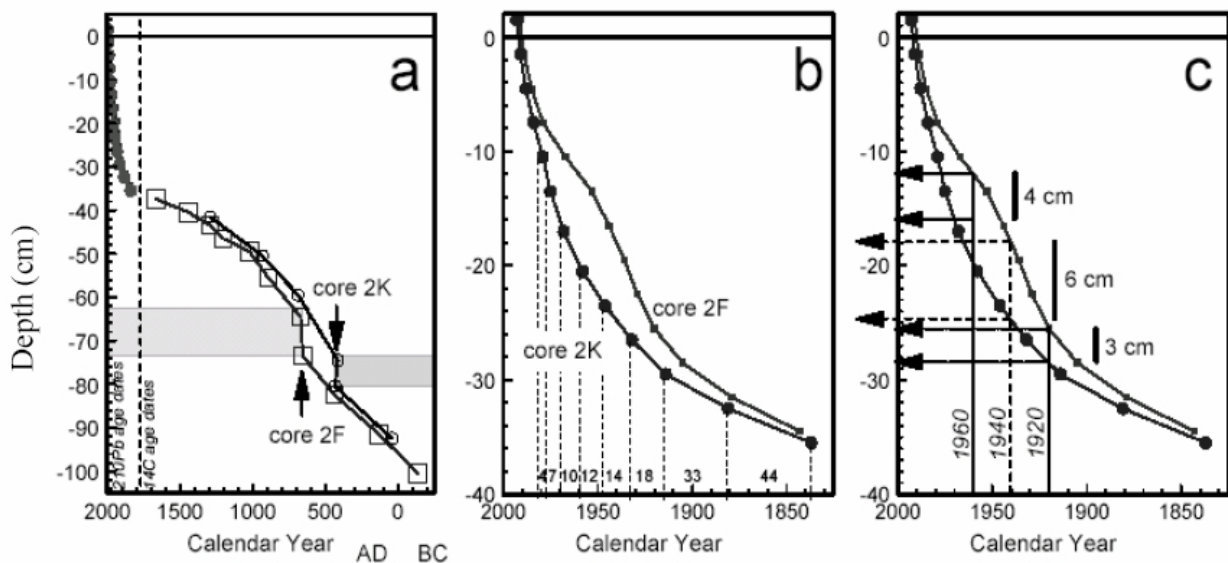


Fig. 3. a) Age-depth relationship in the two peat cores. Vertical dashed line distinguishes ^{210}Pb from ^{14}C age dates. Notice that both ^{14}C curves show an inflection, indicated by the arrows, but that this section is deeper in the 2K core (shaded bar on right) compared to 2F (shaded bar on left). b) ^{210}Pb age dates of the two peat profiles. Numerical values between vertical dotted lines indicate the number of calendar years represented by each slice. c) Assuming that the ^{210}Pb age should represent the same depth in each peat core, the dotted line indicates the vertical displacement (cm) between the two cores at AD 1920, the dashed line at AD 1940, and the solid line at AD 1960.

Effects of hand slicing of peat cores on the chronology of anthropogenic Pb

When the two peat cores were sectioned, they had been removed from the bog and were cut fresh, at ambient temperature, by hand using a bread knife. A measuring tape was attached to the cutting board and used to guide the eye while positioning the knife blade. While the intended thickness of each slice was 3 cm, no effort was made to determine the accuracy or precision of the cuts. Using the green plant material as a guide to the location of the living, biologically active layer, this section was cut away first, and is the first sample of each core. Strictly speaking, however, this material is living plant matter, and not peat. After cutting away the living layer, the top of

the core became the “zero” depth, and all subsequent cuts, in increments of ca. 3 cm, were made relative to this point. Given the differential compression between the two cores and the differences in age-depth relationship, modelling of curve smoothing and combined smoothing plus compression scenarios indicates that the thickness and position of peat core slicing can significantly affect the intensity of a peak in anthropogenic Pb (Fig. 4.) by incorporating overlying and underlying material of lower anthropogenic Pb concentration. Not only could this process affect the calculated concentration of anthropogenic Pb per slice, but also the chronology of the enrichment, as determined using ^{210}Pb , as material of younger and older age becomes incorporated into any given slice.

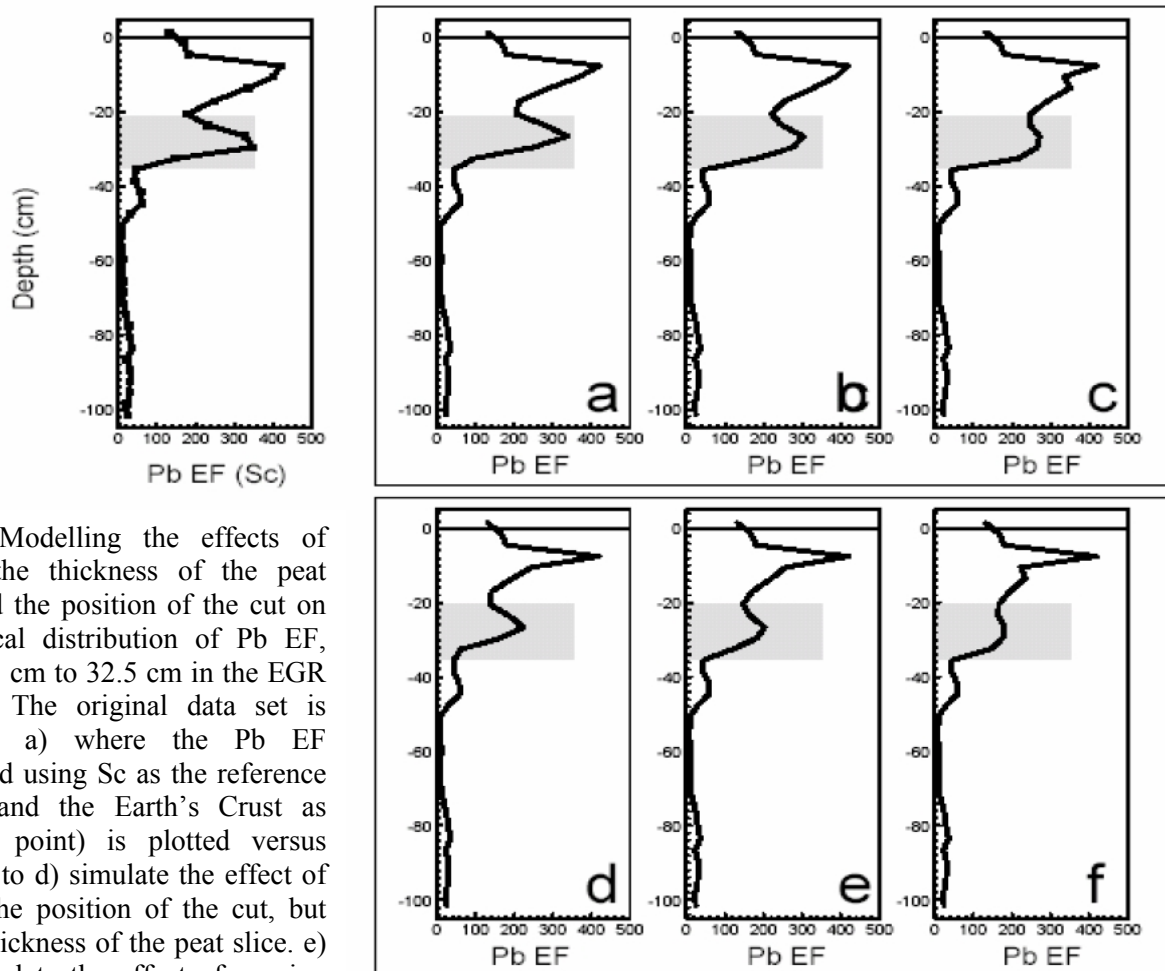


Fig. 4. Modelling the effects of varying the thickness of the peat slices and the position of the cut on the vertical distribution of Pb EF, from 10.5 cm to 32.5 cm in the EGR 2F core. The original data set is given in a) where the Pb EF (calculated using Sc as the reference element and the Earth’s Crust as reference point) is plotted versus depth. b) to d) simulate the effect of varying the position of the cut, but not the thickness of the peat slice. e) to g) simulate the effect of varying both the position of the cut and the thickness of the slice.

Effect of the thickness of a peat slice on the signal resolution

The resolution and magnitude of any given peak depends on the thickness of the slice. The thinner the slice is, the better will be the resolution of the record. Moreover, as shown in Fig. 1, over a small vertical distance (ca. 50 cm), there are extreme changes in Pb concentration, as well as significant changes in ash content and bulk density. Therefore the thickness of the slices is of greatest importance in the uppermost peat layers which represent the most critical time period in terms of pollution reconstruction (i.e. the past two centuries since the start of

industrialisation). However, even in the lower peat layers, the thickness of the slices is also important. For example, short-lived events such as the deposition of volcanic ash can be clearly resolved using 1 cm slices (Fig. 5). Thicker slices, however, not only provide poorer resolution (Fig. 5), but they also prevent the event from being accurately agedated. Taken together, the available evidence suggested that the protocol used during the past decade had to be improved. Specifically, cutting the cores very precisely into 1 cm slices will maximize the signal/noise ratio of the peaks in metal concentration and therefore greatly contribute to improving the accuracy, reproducibility and reliability of peat bog archives (Fig. 6).

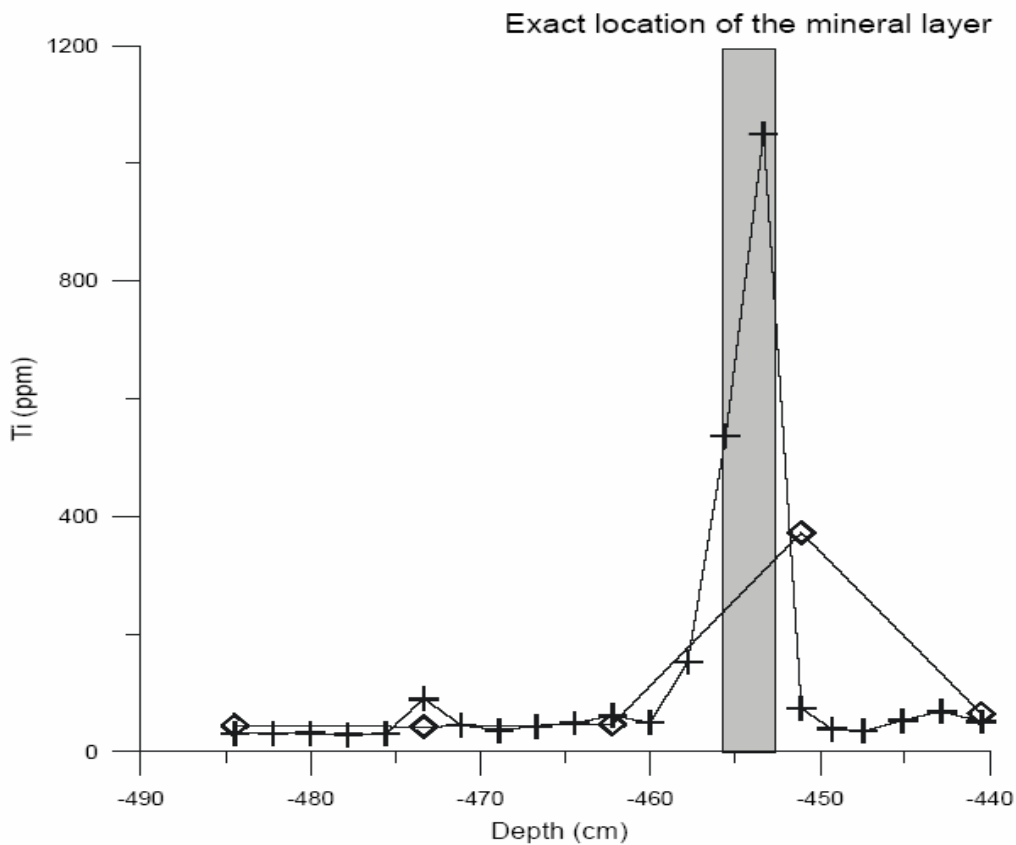


Fig. 5. Concentration of Ti (ppm) between 440 and 490 cm depth from a peat core from the Black Forest, Germany. Titanium concentrations were measured in every second sample, cut into 1 cm slices; those are reported as crosses (+) whereas average Ti concentrations for five samples (10 cm peat section) are indicated by diamonds (◇).

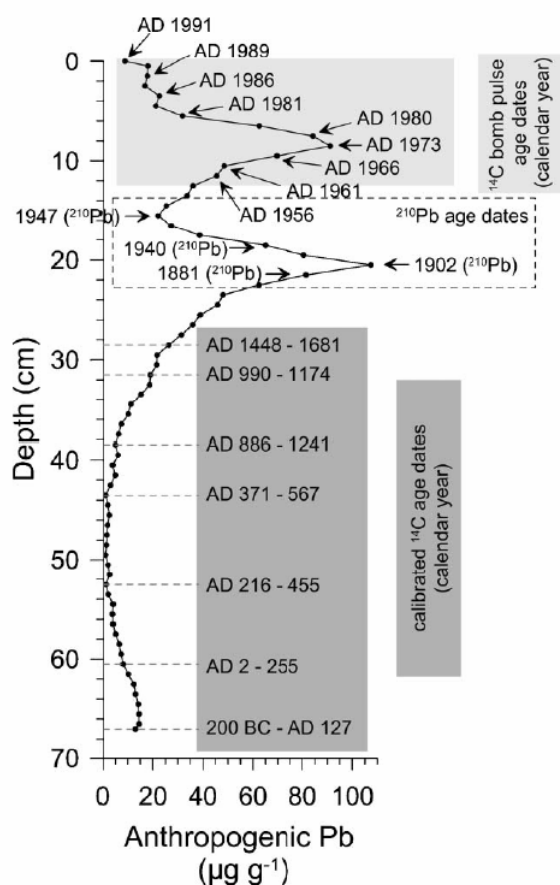


Fig. 6. Concentration of Pb (ppm) for the Wardenaar peat profile 2G from Étang de la Gruère, Switzerland (Shotyk, unpublished). This core was collected the same year as the EGR 2F core (i.e. 1991). It shows the kind of resolution, which can be obtained using 1 cm slices (compare the 2F and 2K cores (Fig. A1-1) which were cut into 3 cm slices) and accurate age dating. The upper layer age dates have been calculated using the ^{14}C “atmospheric bomb pulse curve”.

Improvements and proposed protocol

Since EGR 2F and 2K cores were collected in 1991 and 1993, respectively, several changes have been made in the collection, handling and preparation of peat cores to improve the accuracy and precision of peat bog records of atmospheric dust and trace metal deposition. The most important changes are summarised below.

Field sampling strategy

The success of paleoenvironmental studies using peat cores as archives largely depends on the ability to select appropriate peatlands which have preserved high-quality paleoenvironmental records. Therefore careful selection of sites and coring locations

within the sites are critical elements of field research. Although, the strategy will vary depending on the purpose of the study and the site itself, several general considerations can be helpful to design suitable field sampling strategies and for retrieving peat cores. Since comprehensive field observations are a very valuable aspect of the survey, pertinent information that should be recorded are listed and discussed below.

Site selection

To reconstruct the deposition history of atmospheric particles using peat cores, selection criteria should include the morphology of the peatland (topography and depth of peat accumulation), character of peat (visual inspection of the botanical composition, degree of decomposition, moisture content and abundance of mineral matter), possible damages to the peatland and to the peatland hydrology (peat cutting, drainage, dams), possible use of the peatland for forestry or agriculture, and distance from human activities.

Not all peatlands are appropriate for the reconstruction of the changing rates of atmospheric metal deposition and it is worthwhile to pay particular attention on the selection of the peatland.

The quality of the paleoenvironmental record for many trace elements is mainly controlled by the trophic status of the peatland as revealed by e.g. the botanical composition and abundances of mineral matter. Ombrotrophic (“rain-fed”) bogs should be favored over other types of peatlands, as they receive water solely from atmospheric precipitation (rain, snow) falling onto their surface. Ideally, the most valuable part of a bog is the raised dome. Neither groundwater nor surface water runoff from other areas can reach the raised part of the bog, as it is above the level of the local groundwater table. Moreover, ombrotrophic bogs provide records with better time resolution than minerotrophic deposits, mainly due to the lower degree of organic decomposition. Both biological and chemical characteristics that can be used in the field and in the lab to establish the existence of an ombrotrophic zone are presented elsewhere in detail.¹³ The

mineralogical and chemical composition of the basal sediment on which the peatland is resting should be also considered. Weathering of minerals from the underlying rocks and sediments could be an important source of ions which migrate upward into the peat by diffusion.¹⁰ There is a great difference between the trophic status of peat profile in a bog forming on calcareous versus granitic substratum, with carbonate weathering clearly supplying more metals to the basal peat layers. Therefore, ombrotrophic bogs underlain by granites are chemically less affected by upward diffusion of ions and should be favoured over bogs growing on carbonate rocks.

If ombrotrophic bogs are common in temperate and boreal latitudes, they are scarce in sub-Arctic and Arctic latitudes.⁷ Therefore at high latitudes, minerotrophic peat deposits may have to be used as archives of atmospheric metals even though they are fed both by atmospheric and terrestrial inputs. Recent studies have shown that at some predominantly minerotrophic peatlands, mercury and lead may be supplied exclusively by the atmosphere and therefore can still provide a record of the changing rates of atmospheric deposition of those elements.¹⁴⁻¹⁷ Such reconstructions, however, must be interpreted with great caution and on an element by element basis because some metals of interest e.g. nickel¹⁸ and uranium¹⁹ are certainly enriched in minerotrophic peat due to weathering inputs.

Before selecting the exact site for collecting peat profiles at a peatland, the site morphology must be known. If this is not the case, it could be established by depth profiling at least two transects at 90°. This process will help selecting the deepest ombrotrophic part of a bog or the deepest organic accumulation of a minerotrophic peat deposit. Comparison of mercury and lead fluxes to hummocks and hollows of ombrotrophic bogs suggest that cores from both locations are recording trends in atmospheric deposition of Hg and Pb, but that hollow cores are recording lower input values than hummock cores, apparently due to a larger component of dry and occult (fog) deposition at hummocks than at hollows.²⁰

Therefore sampling sites located in “lawns”, or at the transition between hollow and hummock are considered to be optimal and therefore recommended.

Prior to peat core collection, permission to retrieve geologic and environmental samples should be secured from the owner of the land if necessary. This is especially important in the case of nature reserves and other protected areas where many of the remaining central European raised bogs are found.

Core collection

The low density and the unsaturated environment of the topmost layers of a peat bog make the collection of good quality peat cores challenging. It is difficult to cut these layers as they are easily trampled and compressed. Moreover, the upper layers of a peat bog represent the past decades which is the most critical and interesting period in terms of atmospheric pollution, not only for trace metals and organic contaminants, but also for fallout radionuclides. The main concern about this section is to collect surface layers as an undisturbed continuous peat profile extending as far back in time as possible in an effort to reach “natural background” values. By using procedures developed by our research group, all fieldwork is completed in such a way as to minimize the impact on the environment, utilizing the latest techniques and best available technology for sampling, handling and preparing the materials.

Modified Wardenaar corer

The topmost layers of peat can be collected using a 10 cm × 10 × 100 cm Wardenaar peat profile cutter²¹ which is commercially available. Our 1 m Wardenaar corer with XY dimensions 15 cm × 15 cm, was home-made using a Ti-Al-Mn alloy and includes a serrated cutting edge; this new cutting edge cuts more easily through dwarf shrubs (e.g. *Ericaceous* shrubs) and *Eriphorum* root fibres. This feature, combined with the larger cross sectional area means that any given slice undergoes less compression in the Z (vertical) dimension. Moreover, the enlargement of the XY dimensions to 15 cm

of the new Wardenaar corer compared to the older version (10 cm) provides enough peat sample material to conduct a wide range of analyses and still to be able to preserve part of the material as an archive for futures work, even using thin slices (i.e. 1 cm). The state of the art of the modified Wardenaar corer and the best way to collect a good quality peat core from the surface layers of a bog are described in detail elsewhere.²²

During extraction, some compression of the peat core is unavoidable. However, the compression can be measured, using the bog surface as a reference. After extraction, the Wardenaar corer is laid horizontally on the bog surface, on a large sheet of plastic; the top half of the Wardenaar corer is removed, exposing the peat monolith. This core is described visually in the field (length, colour, texture, plant remains, moisture, special layers) and photographed. The core is inspected for modern plants of the bog surface which may have “contaminated” the outside of the core; these are carefully removed using a small knife. The exposed surface and two sides of the core are wrapped in polyethylene cling film. A wooden core box built specifically for the Wardenaar core is lined with plastic (a large sheet, or two large sheets, is made using plastic garbage bags). The plastic-lined wooden core box is placed over the peat core. Two people lift the bottom half of the Wardenaar corer, flip it carefully backward 180°, allowing the peat core to slide down into the box. The surface of the core is wrapped in polyethylene cling film, with the film pressed down around the sides of the core and ends using a plastic spatula.

The core is covered with plastic, labelled and the lid attached using screws. In this way, handling of the core in the field is kept to a minimum.

Belarus corer

A Belarus (Macaulay) peat sampler is used for deeper peat layers.²¹ Two versions of this corer are actually used: stainless steel and titanium (Ti). The titanium corer, which is much lighter, was constructed using the same alloy as for the Wardenaar corer.

Cores are removed from two holes adjacent to the hole from the Wardenaar core,

approximately 20 cm apart, in parallel overlapping design. Peat cores are carefully packed onto plastic-semi tubes which are lined with polyethylene cling film: while still in the peat corer, the peat sample (a semi-cylinder ca. 50 cm long and 10 cm wide) is wrapped with polyethylene cling film and a plastic semi-tube is placed on top; the corer is gently flipped backwards 180°, and holding the semi-tube, the core is carefully slid away from the corer. Again, the cores are described and photographed without touching them. The core is wrapped with polyethylene cling film, labelled, and packed in rows in a transport aluminium box.

Motorized corer for frozen peat

A unique peat sampler was designed and built by Mr. Tommy Nørnberg for obtaining continuous samples of frozen peat in the Arctic. Up to 10 meters of frozen peat in 70 cm sections can be removed using this corer. The sampler and the coring technique is described in detail elsewhere (Noernberg et al.). Cores are kept cool until they can be frozen: this is done soon as possible after collection, and kept frozen at -18 °C until they can be prepared in the laboratory. Cores collected from frozen peat deposits are shipped frozen back to the laboratory.

Field observations

Pertinent field observations that should be gathered during the fieldwork include sampling date and time, sampling site significance and location. The precise location of the core collection should be indicated on a topographical map and the GPS coordinates recorded. Because it may be very useful to return to the coring site at some future date, burying a plastic soda pop bottle containing a handful of steel just below the surface of the coring site will allow the exact site of core collection to be found later, using a metal detector. This also helps to avoid possible further peat collection at the same location, as the peat stratigraphy may have been affected by the coring session. Notes on colour, component, length, depth, core compression and other details (e.g. layers of wood, charcoal) are also information that should be recorded. As noted earlier, core

compression during sample collection can be a problem, because of secondary effects on the metal concentration profiles and/or the age-depth relationship. Therefore, coring in spring or early summer when the peatland is at its wettest is recommended. Additional pertinent information that should be recorded includes maximum depth of peat accumulation at the collection site and possible disturbance. Collection of representative surface plant species may serve as a valuable reference for the plant material which constitutes the fossil botanical assemblage of the peat cores.

In order to achieve consistency in recording such data, a field report should be written. This primarily provides a public report of the fieldwork, detailing how and where peat and other geologic or environmental samples were taken for subsequent dating and analysis. The Field Report format developed by M.E. Goodsite is highly recommended²⁴ and is available for downloading for free use at <http://www.rzuser.uni-heidelberg.de/~i12/eergebnisse.htm>.

Samples preparation

To have a rapid, approximate description of the geochemistry of a peat core, a sacrificial core may be sliced immediately in the field using a serrated stainless steel knife into 3 cm slices. Using plastic gloves, each slice is placed in a plastic bag and the bag squeezed by hand to express the pore water. The pore waters may be analyzed for pH, major element cations and anions, and DOC.¹⁰ Slicing the core by hand with a knife has some advantages, as it can provide a rapid survey of the geochemistry of the peat profile if the pore waters are analysed. However it only provides an approximate description of the geochemistry, and this preparation procedure is not suitable to reconstruct high-resolution records of atmospheric metal contamination.

Slicing the cores

With respect to high-resolution records, Wardenaar, Belarus and Nørnberg peat cores are cut frozen in the lab into 1 cm increments using a stainless steel band saw

with stainless steel blades. The width of the blade is 1 mm, so ca. 10% of each slice is lost during cutting. The accuracy of the thickness of these slices is better than ± 1 mm. For Belarus and Nørnberg cores, a slicing system was designed and constructed as described elsewhere.²³ A similar system made of an Omega SO 200a band saw and a precision cutting table is used to slice the Wardenaar cores. Because the cores are large and long, they are heavy (~23 kg) and the cutting table is necessary for precise cutting. The individual slices are subsequently placed on a polyethylene cutting board and the outer 1 cm of each slice is trimmed away using a 13 × 13 cm polyethylene plate and either an acid rinsed ceramic knife or a Ti knife (Fig. 7). The outside edges are systematically discarded, as those could have been contaminated during the sampling and preparation procedures by layers enriched in mineral matter such as tephra layers (e.g. Faroe Island cores), or where there are very high metal concentrations (due to intense atmospheric pollution). The cutting board and knife are rinsed with deionised water three times between each slice. Then slices are packed into labelled zip-lock plastic bags for storage and further preparation.

Sub-sampling Strategy

Great care has to be focused on the orientation of each slice during the slicing session with respect to its original position when it was in the peat monolith. To guarantee the reconstruction of high-resolution records, peat material for a given analysis should be sub-sampled along a conceptual micro-core within the Wardenaar core and therefore at a similar location within the oriented slices.

A sub-sampling strategy is defined for each individual core depending of the main objective of the study. An example of the approach we use is shown in Fig. 7. Two 6 × 6 cm squares are removed using a polyethylene plate. The squares are divided into four triangles by cutting each square along its diagonal. Each triangle is identified with respect to its position within the peat slice, packed into labeled bags and reserved for previously defined analyses (Fig. 7). Part

of the material is archived at -18 °C for possible future studies, and the remainder of the sub-samples will be processed for physical, chemical, mineralogical and isotopic analyses.

Drying and milling

The peat samples are dried at 105 °C in acid-washed Teflon bowls, and macerated in a centrifugal mill equipped with a Ti rotor and 0.25 mm Ti sieve (Ultra centrifugal Mill ZM 1-T, F.K. Retsch GmbH and Co., Haan, Germany). This yields a very fine, homogeneous powder with average particle size of ca. 100 µm (and Gaussian particle size distribution). For finer powder (e.g. for slurry sampling AAS), the direction of the sieve can be reversed. For samples rich in mineral matter (e.g. tephra layers) and for organic-rich sediments, an agate ball mill is used instead. The powdered samples are manually homogenised and stored in airtight plastic beakers. The milling is carried out in a Class 100 laminar flow clean air cabinet to prevent possible contamination of the peat samples by lab dust. In the laboratory, all of the sample handling and preparation is carried out using clean laboratory techniques. Peat powder stored for longer than one year in humid conditions should be re-dried prior to analysis following similar procedures for certified standard reference materials (e.g. plant SRMS from NIST, BCR, or IAEA).

Acid digestion procedures

Other elements in solid peat samples can be quantified for a wide selection of trace elements using instrumental neutron activation analysis (INAA). As no certified reference material for trace elements in ombrotrophic peat was available until recently, INAA data served as a reasonable benchmark for the development of other analytical procedures requiring dissolution of peat samples. In this context, several digestion procedures for the acid dissolution of peat have been developed and evaluated using open vessel digestion as well as closed vessel digestion procedures on a hot plate or using microwave energy. No matter which digestion approach is considered, it is essential to completely destroy the silicate

fraction of peat in order to release the trace elements that are hosted in the silicates. This can be achieved by the addition of HF or HBF₄ to the acid mixture, whereas the use of HBF₄ provides many advantages in that context and thus is highly recommended.^{30,31}

Analyses

Physical analyses

The precision of the bulk density measurements is of great importance for the reconstruction of records of metal contamination as the bulk density data is used to calculate the rates of metal accumulation. Until recently, the centers of the peat slices were sub-sampled using a sharpened stainless steel tube (16 mm diameter) and these plugs used to determine the dry bulk density. The height of each plug was measured to an accuracy of 0.1 mm and the volume calculated. After recording wet weights, plugs were dried at 105 °C overnight and the dry mass was weighed to 1 mg. Later, in order to decrease the discrepancy of the diameter of the plugs induced by the operator, a hand-operated stainless steel press was used to recover plugs of 20 mm diameter with an accuracy of 0.1 mm.²³ However, with respect to the heterogeneity of peat material within a slice, especially the upper layers of modern accumulation, and the unknown, possibly important uncertainties in the measurement of the volume and weight of a small plug of peat material, we found that the determination of bulk density was an important source of error in the calculation of rates of metal accumulation. For example, the calculation of Hg accumulation rates in a peat core from southern Ontario using the minimum and the maximum value of bulk density determined using four plugs for each slice show the calculated Hg accumulation rates of mercury may be ± 10 % of the accumulation rate value calculated using the average bulk density value of the four plugs (Fig. 8). This is mainly explained by the heterogeneity of the peat material within a given slice, especially in the surface peat layers which are poorly decomposed. Therefore the use of larger volume samples, such as the 6 × 6 cm rectangle as recommended in the previous section, should improve the quality of the

bulk density measurement because they are more representative of the slice, thereby also improving the accuracy of the rate of metal accumulation calculation.

The degree of decomposition of the peat is measured by colorimetry on alkaline peat extracts at 550 nm using a Cary 50 UV-visible spectrophotometer. The powdered peat samples (0.02g) are placed in test tubes and 8 % NaOH soln. (10 ml) is added. The samples are shaken then heated 95 ± 5 °C for 1 hour, then made up to 20 ml with deionised water, shaken and left to stand for 1 hour before being re-shaken and filtered through Whatman no. 1 filter papers. Samples are diluted with an equal quantity of deionised water directly before colorimetric measurement. The percentage of light absorption (% absorbance) in these extracts may be used as a proxy of peat humification.²⁵

Chemical analyses

The development, evaluation and use of peat cores from ombrotrophic bogs as archives of high-resolution reconstructions of atmospheric deposition of mineral dust and trace elements have led to the development of many analytical procedures which now permit the measurement of a wide range of elements in peat samples. Prior to any expensive and time consuming chemical procedure and analysis, measurement of major and trace elements in peat samples using the non-destructive and relatively inexpensive X-Ray Fluorescence (XRF) method is performed on all peat samples first. This method provides invaluable geochemical data that helps to document the natural geochemical processes which occur in the peat profiles and their possible effect on the distribution of trace

elements. Calcium (Ca) and strontium (Sr), for example, can be used to identify mineral weathering reactions in peat profiles, manganese (Mn) and iron (Fe) redox processes, bromine (Br) and selenium (Se) atmospheric aerosols of marine origin. Titanium (Ti) and zirconium (Zr) are conservative, lithogenic elements whose abundance and distribution reflects the variation in mineral matter concentration in the peat core.²⁶ One gram of dried, milled peat may be analysed for these and other major and trace elements simultaneously (Y, K, Rb, Cr, Ni, Cu, Zn, As and Pb) using the EMMA XRF.^{11,27} Titanium (Ti) may be analysed precisely using the new TITAN XRF spectrometer which provides a lower limit of detection for Ti of only $1 \mu\text{g g}^{-1}$. Both instruments measure the sample in powder form. Because the method is non-destructive, these same samples can be used again for other measurements (Fig. 7). Complete details about the design and construction of this instrument are presented in a separate publication.²⁸

Mercury

Solid peat samples can be analysed for Hg using a direct mercury analyser (LECO AMA 254).²⁹ The main advantage of this approach is that no acid digestion of the peat sample is necessary. After air-drying overnight in a Class 100 laminar flow clean air cabinet, three subsamples, previously removed from a pre-selected, fresh portion of each slice, are analysed for total Hg, and the results of the three subsamples are averaged (Fig. 7). The detection limit of the instrument is 0.01 ng Hg and the working range is 0.05 to 600 ng Hg, with reproducibility better than 1.5%

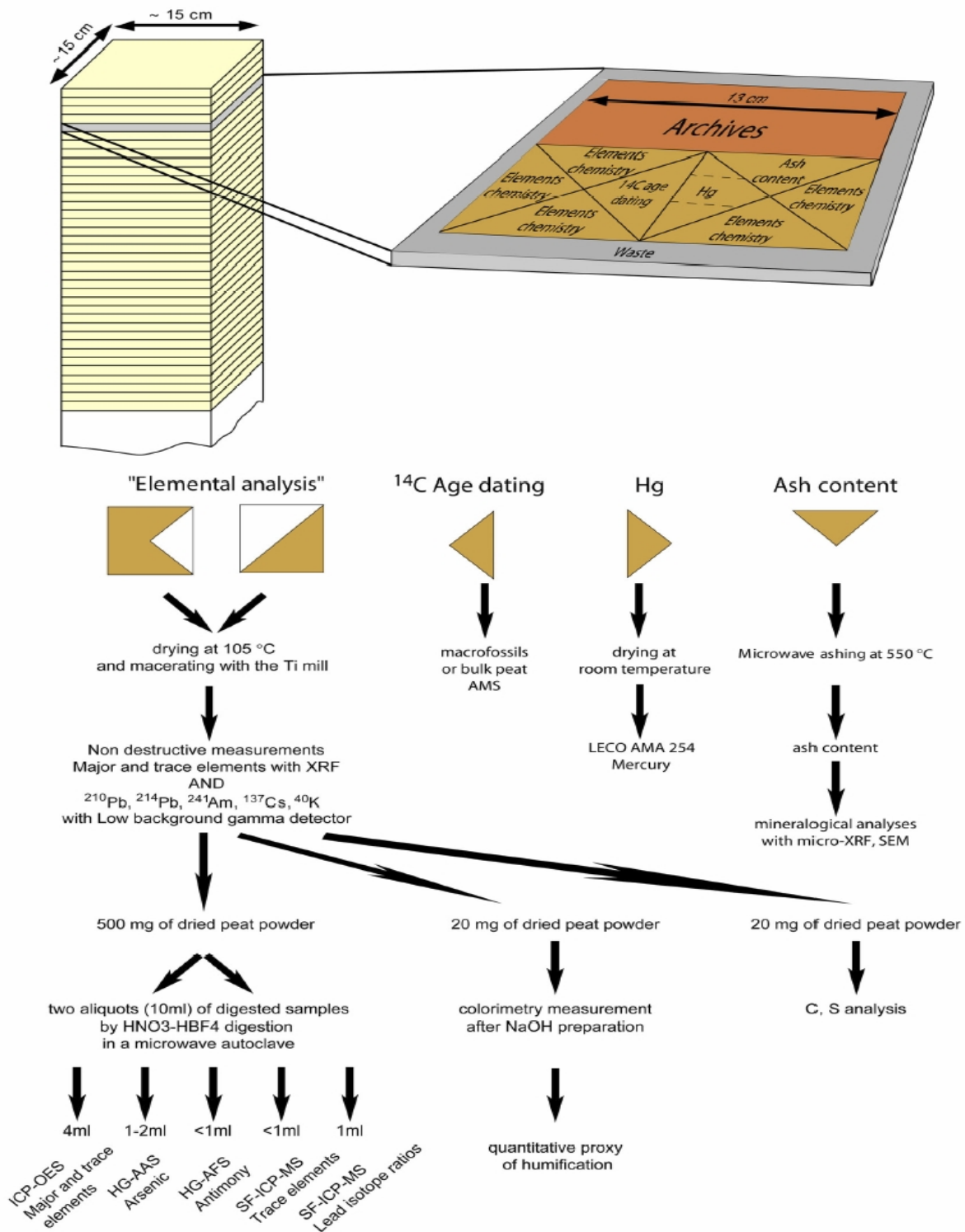


Fig. 7. Analytical flow chart and sub-sampling strategy for a peat slice from a Wardenaar core. The outside edges of the slices are systematically removed to waste to ensure that only the uncontaminated part of each sample is used for study. Part of the slice is archived for possible future studies. Peat triangles are sub-sampled, oriented to ensure that, for any given analysis, the sub-samples are taken from the same position in each slice.

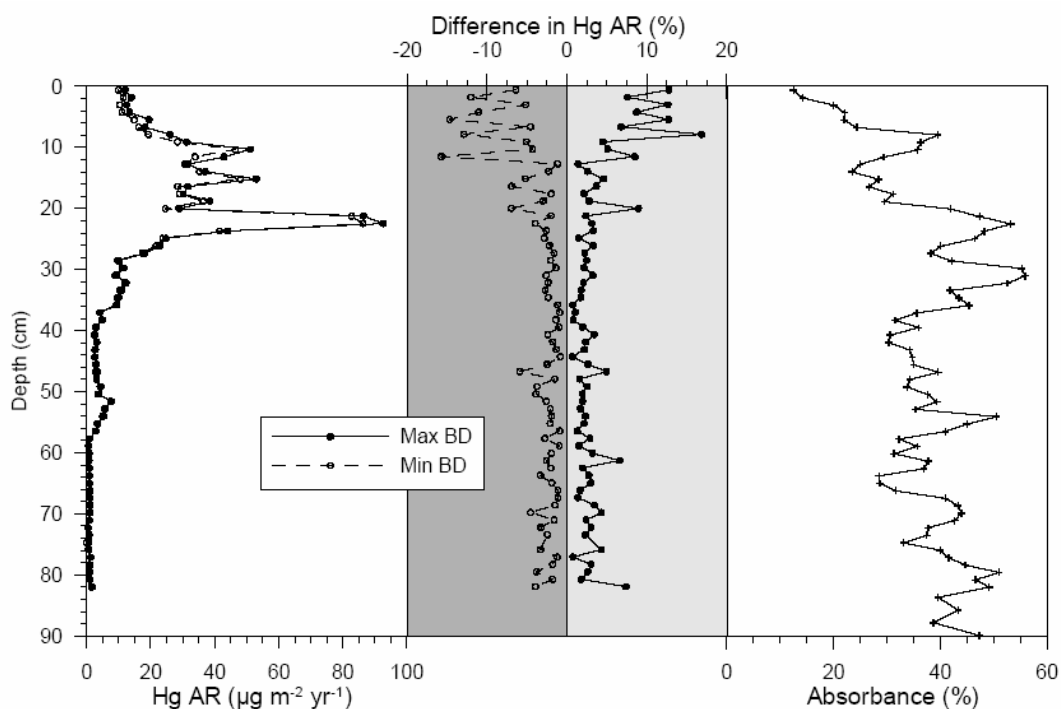


Fig. 8. Comparison of mercury accumulation rate profiles calculated using a) minimum bulk density value and b) maximum bulk density value for a peat core from southern Ontario, Canada. The corrected absorbance is an indicator of the degree of peat humification

Quantification of trace elements

Trace elements in these digestion solutions have been determined using ICP-MS, ICP-OES, HG-AAS and HG-AFS.³²⁻³⁷ The large variety of analytical instruments available allowed several inter-method comparisons which greatly benefit the quality of the analytical results (Fig. 7). Both ICP-MS and ICP-OES were used to analyse more than 25 elements, whereas work to date with HG-AAS and HG-AFS mainly focused on the determination of low concentrations of arsenic and antimony in peat.^{37,38} Using ICP-MS, a powerful multi-element technique with low detection limits, it has been possible to establish complete chronologies of Ag, Tl, Pb, Cd,³⁹ Mo, U, Th¹⁹, the REE³⁰ and V, Cr, Ni.¹⁸ A method has also been developed to determine major elements in acid digested peat samples using ICP-OES and this has been successfully applied to the determination of Al, Ca, K, Mn, Ti, Fe, Na, Sr, Mg concentrations. Again, measurements of international, certified, standard reference materials yielded results which are in good agreement with the certified values.

Lead isotope measurements

Lead isotope ratios in peat can largely help to identify the predominant anthropogenic sources of Pb. Lead isotope measurements can be performed using ICP-MS. We recently developed a method using sector field inductively coupled mass spectrometry (ICP-SF-MS) after acid digestion of peat powders using a high-pressure and high-temperature microwave autoclave.⁴⁰ The accuracy and precision of the ICP-SMS protocol was further evaluated using thermal ionisation mass spectrometry (TIMS) of selected samples and an in-house peat reference material. In general, the Pb isotope ratios determined using ICP-SMS deviated from the TIMS values by less than < 0.1%. Given the throughput of the ICP-SMS compared to the TIMS (which requires chemical separation of Pb), the ICP-SMS approach offers great promise for environmental studies to fingerprint the predominant sources of anthropogenic Pb. In a few cases when improved accuracy and precision are needed, the Pb isotope ratios in these selected samples may also be measured using thermal ionisation mass spectrometry (TIMS).

Quality control

Decreasing limits and thresholds require accuracy, comparability and traceability of analytical measurements for the determination of elemental content in peat material. Certified Standard Reference Materials of coals and plants from the National Institute of Science and Technology (USA), the International Atomic Energy Agency (Vienna), South Africa, the European Community, Poland, the Czech Republic, and China are analysed in triplicate as blind standards. However, to guarantee accuracy, quality control, quality assurance or validation of a measurement by means of certified reference material, the assessment of analytical results in certified reference materials must be as accurate as possible and every single step has to be fully evaluated. To date, the lack of a common certified peat reference material has hindered the quality assurance of the generated analytical data from different laboratories in the international community. There are ongoing efforts to fill the lack of a common certified peat reference material for working with peat material by developing a multi-element reference material for low-ash peat to be used by the international community.^{41,42}

Mineralogical analyses

Mineralogical analyses of the inorganic fraction could be of particular importance to identify the origin and type of anthropogenic and natural particles deposited on the surface of the peat bog. However because of the very low inorganic content in ombrotrophic peat, it is very difficult to extract the deposited atmospheric particles. Moreover in the case of a general study also including bulk peat geochemistry, there may be only a small quantity of peat available for mineralogical analyses. Finally the extraction method used is dependent on the type of mineral investigated because the reagents and temperature used could modify the minerals by oxidation (e.g. sulphides) or dehydration (e.g. clays). However, prior to mineralogical analyses, samples should not be milled. Many methods for extracting minerals grains from the bulk peat matrix are available from the

literature, some of them designed for the extraction of specific fractions such as tephra glasses^{43,44} or recent anthropogenic particles. One method used in our laboratory and proposed by Steinman and Shoty⁴⁵ is to ash the peat at 550 °C, remove the carbonates and other inorganic components formed during the ashing process using dilute HCl. These samples are then ready for optical microscopy and could also be analysed after preparation using Scanning electron Microscope (SEM w/EDAX). Another approach is to digest the peat with 65% H₂O₂ in a Teflon beaker on a hot plate. Every ca. three days, the reagents are poured off and a new solution of 65% H₂O₂ is added until there is no visible trace of organic matter. However, this procedure is time-consuming and could last more than two weeks. It is possible to use an ultrasonic bath to mechanically extract the minerals before and after each H₂O₂ attack. Individual mineral grains which are large enough could be also directly analysed by microscopic techniques such as microbeam XRF.⁴⁶

Age dating

Establishing high quality chronologies is a critical feature of paleoenvironmental studies, especially for the last few hundred years which have witnessed so many changes. A reliable and detailed chronology is essential if peat bogs are to be compared with other high-resolution archives such as polar ice, laminated lake sediments, tree rings, bryophytes, including herbarium specimens. Multiple techniques can be used to develop peat chronologies including analyses of short-lived radioisotopes (²¹⁰Pb, ¹³⁷Cs, ²⁴¹Am, ¹⁴C bomb pulse), historical pollen, chronostratigraphic markers, tephra layers, and fly-ash particles.⁴⁷

Radiocarbon age dating

It should be relatively straightforward to establish radiocarbon-based chronologies for most Holocene peats used for paleoenvironmental reconstructions. However, there are a number of problems to be considered in radiocarbon dating peat. In the past, ¹⁴C age dating was typically done using the decay counting method on bulk samples. This method had the disadvantage of

wasting a large amount of material, because several grams of dry peat was needed. Moreover, radiocarbon age dating of bulk samples can be problematic as it may lead to ^{14}C age inversions in cases where older peat layers have been penetrated by younger plant roots.⁴⁸ Therefore macrofossils of Sphagnum moss, specifically selected and cleaned are ideal for radiocarbon dating as mosses have no root systems and therefore cannot introduce younger carbon to lower layers. Careful sample selection and cleaning (removing roots of other plants), pre-treatment (washed water followed by an acid-base-acid treatment) circumvents other potential problems such as the mobility of carbon in the peat profiles. However some movements of carbon can occur, especially of dissolved organic carbon; the translocation of younger carbon to deeper horizons by vascular plant roots or the possible “reservoir” effect involving translocation of older carbon to contemporary vegetation also are real concerns.

Age dates of plant macrofossils younger than AD 1950 can be obtained using ^{14}C by directly comparing the absolute concentration of ^{14}C in the sample to the general-purpose curve derived from annually averaged atmospheric $^{14}\text{CO}_2$ values in the northernmost northern hemisphere: post-1950 ^{14}C concentrations in the atmosphere are elevated compared to natural levels due to atomic weapons testing. This approach which effectively matches the ^{14}C concentrations (percent modern carbon, or PMC) in successive plant macrofossils to the increase (since AD 1950) and subsequent decrease (since AD 1963) in ^{14}C concentrations is the so called “bomb pulse curve of ^{14}C ” and has been successfully used to date peat accumulation in Denmark and in southern Greenland.⁴⁹ This comparatively new dating method has been found to provide high-resolution age dates which are accurate to ± 2 years.

Radiometric age dating

^{210}Pb is widely used for dating environmental records in natural archives such as lake sediments, peat bogs and marine sediments spanning the last 130 years or so.⁵⁰

Assessing ^{210}Pb dates in conjunction with dates from longer time-scale dating methods such as ^{14}C can be beneficial in a number of respects. Age dating peat profiles by combining independent dating methods helps to provide a reliable long time-scale chronology. The main advantage of ^{210}Pb age dating is that it can be done in-house using low background gamma spectrometry and therefore eventually reduces the cost of age dating. In contrast, ^{14}C age dating of plant macrofossils can be done only at those labs with Acceleration Mass Spectrometry (AMS) facilities.

When building up an age dating strategy, an important question is what are we trying to date? The age dating strategy will be different if we try to provide dates for a few events such as the concentration peaks in a record or if we establish a chronology for an entire record. In the case of dating specific events, the optimum strategy would be to direct all the effort at these particular periods.⁵¹ Therefore great attention is required in selecting material sent to the laboratory, to be sure that the most important events are dated. To establish a precise chronology for the entire peat profile, a regular interval of sample selection will guarantee the generation of an accurate age-depth model and therefore of a reliable peat chronology.

Modelling the age-depth relationship

Chronology reconstruction is based on a series of radiometric dates, sometimes supplemented by other markers (e.g. tephra layers...). As independent check, various models can be applied, all of which have underlying assumptions, even if they are not explicitly stated. The choice of model varies but is most often subjective, favouring linear model based on R^2 values, using central calibrated dates, and assuming continuous peat accumulation often without evaluating this assumption.

Without a large number of dates there is no convincing reason for preferring one regression to another or for using the same regression for all profiles.⁵² We are forced to return to a subjective evaluation of curve fitting as well as our knowledge of peatland system. If we want to estimate maximum

possible error then we should perhaps evaluate the age-depth function obtained from a range of models which would give us an error range. Of course, this still excludes the error ranges on the calibrated ages used to generate the age-depth relationship. As far we are aware, there is no available method to deal with these errors, because the probability distribution of calibrated ages is non-normal.⁵³

Conclusion

The protocol described here is time consuming and expensive. There is no need to apply it to poor quality cores. We recommend that for the study of the uppermost layers a peat bog, three Wardenaar cores should be collected. The first one could be used to investigate the quality and the suitability of the peat deposit for paleoenvironmental purposes. This core could be visually inspected, described, and cut by hand in the field. Measurement of the pH and the calcium concentration in the porewater can be used to determine the trophic status of the peat profile, and the chlorine concentration to reveal the influence of marine aerosols. As first approximation of the chronology, Pb could be measured using XRF which would clearly indicate the beginning of industrialisation. In Europe, this approach would also identify the Roman period, if this is present in the peat core. If the core is in good agreement with the selection criteria define during the first step of the study (ombrotrophic peat deposit, time period of interest), then the second core should be cut into 1 cm slices and the protocol proposed in this paper could be followed. The third core should be storage intact at -18 °C as an “archive” which could be used in future studies.

Acknowledgements

Special thanks to Dr. A. Smirnov (1st Ti Wardenaar and Ti Belarus corer) and Mr H.-P. Bärtschi (Stainless steel Belarus corer) for assistance with field equipment. Financial support was provided by the Swiss National Science Foundation (grants 21-061688.00 and 21-5669.98 to W. S.), the International Arctic Research Center (IARC) and Cooperative

Institute for Arctic Research (CIFAR), Fairbanks, Alaska (grant to W. S., H.F. Schöler and S.A. Norton), the Danish Cooperation for Environment in the Arctic (DANCEA) grant to M.E. G., W. S. and G. Asmund. This paper summarises twenty years of field studies by W.S., coring a great variety of peat bogs; I wish to thank my co-authors for all of the questions, comments, and suggestions which have led to so many improvements with all aspects of this work. In addition, I am indebted to the Swiss NSF for many years of generous financial support.

References

1. A. B. MacKenzie, E. M. Logan, G. T. Cook and I. D. Pulford, *Sci. Total Environ.*, 1988, 222, 157.
2. M. A. Vile, M. Novak, E. Brizova, R. K. Wieder and W. Schell, *Water, Air, Soil Pollut.*, 1995, 79, 89.
3. J. G. Farmer, A. B. Mackenzie, C. L. Sugden, P. J. Edgar and L. J. Eades, *Water, Air, Soil Pollut.*, 1997, 100, 253.
4. A. Martínez Cortizas, X. Pontevedra Pombal, E. García-Rodeja, J. C. Nóvoa Muñoz and W. Shotyk, *Science*, 1999, 284, 939.
5. M. Novak, S. Emmanuel, M. A. Vile, Y. Erel, A. Veron, T. Paces, R. K. Wieder, M. Vanecek, M. Stepanova, E. Brizova and J. Hovorka, *Environ. Sci. Technol.*, 2003, 37, 437.
6. F. Monna, C. Pettit, J.-P. Guillaumet, I. Jouffroy-Bapicot, C. Blanchot, J. Dominik, R. Losno, H. Richard, J. Lévêque and C. C. Chateau, *Environ. Sci. Technol.*, 2004, 38, 665.
7. D. J. Charman, *Peatland and Environmental Change*, John Wiley and sons, Chichester, 2002.
8. W. Shotyk, D. Weiss, P. G. Appleby, A. K. Cheburkin, R. Frei, M. Gloor, J. D. Kramers and W. O. Van Der Knaap, *Science*, 1998, 281, 1635.
9. W. Shotyk, D. Weiss, M. Heisterkamp, A. K. Cheburkin, P. G. Appleby and F. C. Adams, *Environ. Sci. Technol.*, 2002, 36, 3893.
10. W. Shotyk and P. Steinmann, *Chem. Geol.*, 1994, 116, 137.

11. A. K. Cheburkin and W. Shotyk, *Fresenius J. Anal. Chem.*, 1996, 354, 688.
12. D. Weiss, W. Shotyk, J. D. Kramers and M. Gloor, *Atmos. Environ.*, 1999, 33, 3751.
13. W. Shotyk, *Environmental Review*, 1996, 4, 149.
14. N. Givelet, F. Roos-Barraclough, M. E. Goodsite, A. K. Cheburkin and W. Shotyk, *Environ. Sci. Technol.*, accepted for publication.
15. W. Shotyk, *Sci. Total Environ.*, 2002, 292, 19.
16. F. Roos-Barraclough and W. Shotyk, *Environ. Sci. Technol.*, 2003, 37, 235.
17. W. Shotyk, M. E. Goodsite, F. Roos-Barraclough, R. Frei, J. Heinemeier, G. Asmund, C. Lohse and T. S. Hansen, *Geochim. Cosmochim. Acta*, 2003, 67, 3991.
18. M. Krachler, C. Mohl, H. Emons and W. Shotyk, *Environ. Sci. Technol.*, 2003, 37, 2658.
19. M. Krachler and W. Shotyk, *J. Environ. Monit.*, 2004, this issue.
20. S. A. Norton, G. C. Evans and J. S. Kahl, *Water, Air, Soil Pollut.*, 1997, 100, 271.
21. I. E. Belokopytov and V. V. Beresnevich, *Torf. Prom.*, 1955, 8, 9.
22. T. Noernberg, M. E. Goodsite, W. Shotyk and N. Givelet, in preparation.
23. T. Noernberg, M. E. Goodsite and W. Shotyk, *Arctic*, accepted for publication.
24. M. E. Goodsite and W. Shotyk, Long term deposition of atmospheric Hg, Cd, Pb and persistent organic pollutants (POPs) in peat cores from Arctic peatlands (Bathurst Island), post expedition field and status report, Institute of Environmental Geochemistry, Heidelberg, 2001.
25. C. J. Caseldine, A. Baker, D. J. Charman and D. Hendon, *Holocene*, 2000, 10, 649.
26. W. Shotyk, D. Weiss, J. D. Kramers, R. Frei, A. K. Cheburkin, M. Gloor and S. Reese, *Geochim. Cosmochim. Acta*, 2001, 65, 2337.
27. A. K. Cheburkin and W. Shotyk, *X-Ray Spectrometry*, 1999, 28, 145.
28. A. K. Cheburkin and W. Shotyk, *X-ray Spectrometry*, 2004, 33.
29. F. Roos-Barraclough, N. Givelet, A. Martinez-Cortizas, M. E. Goodsite, H. Biester and W. Shotyk, *Sci. Total Environ.*, 2002, 292, 129.
30. M. Krachler, C. Mohl, H. Emons and W. Shotyk, *J. Anal. At. Spectrom.*, 2002, 17, 844.
31. M. Krachler, C. Mohl, H. Emons and W. Shotyk, *Spectrochimica Acta Part B*, 2002, 57, 1277.
32. M. Krachler, M. Burow and H. Emons, *Analyst*, 1999, 124, 777.
33. M. Krachler, M. Burow and H. Emons, *Analyst*, 1999, 124, 923.
34. M. Krachler, M. Burow and H. Emons, *J. Environ. Monit.*, 1999, 1, 477.
35. M. Krachler, W. Shotyk and H. Emons, *Anal. Chim. Acta*, 2001, 432, 303.
36. M. Krachler, H. Emons, C. Barbante, G. Cozzi, P. Cescon and W. Shotyk, *Anal. Chim. Acta*, 2002, 458, 387.
37. B. Chen, M. Krachler and W. Shotyk, *J. Anal. At. Spectrom.*, 2003, 18, 1256.
38. W. Shotyk, M. Krachler and B. Chen, *Global Biogeochem. Cycles*, 2004, 18.
39. W. Shotyk and M. Krachler, *J. Environ. Monit.*, 2004, this issue.
40. M. Krachler, G. Le Roux, B. Kober and W. Shotyk, *J. Anal. At. Spectrom.*, 2004, 19, 354.
41. C. Barbante, W. Shotyk, H. Biester, A. K. Cheburkin, H. Emons, J. G. Farmer, E. Hoffman, A. Martinez-Cortizas, J. Matschullat, S. A. Norton, J. Schweyer and E. Steinnes, *Proceeding of the 11th Conference on Heavy Metals in the Environment*, Ann Arbor, Michigan, USA, 2000.
42. C. Yafa, J. G. Farmer, M. C. Graham, J. R. Bacon, R. Bindler, I. Renberg, A. K. Cheburkin, A. Martinez-Cortizas, H. Emons, M. Krachler, W. Shotyk, X. D. Li, S. A. Norton, I. D. Pulford, J. Schweyer, E. Steinnes and D. Weiss, *Proceeding of the 6th*

- International Symposium on Environmental Geochemistry, Edinburgh, Scotland, 2003.
43. C. Persson, *Sveriges Geologiska undersökning*, 1971, 65,A. J. Dugmore, A. J. Newton and D. E. Sugden, *J. Quaternary Sci.*, 1992, 7, 173.
 44. P. Steinmann and W. Shotyk, *Chem. Geol.*, 1997, 138, 25.
 45. A. K. Cheburkin, R. Frei and W. Shotyk, *Chem. Geol.*, 1997, 135, 75.
 46. I. Renberg, R. Bindler and M.-L. Brännvall, *Holocene*, 2001, 11, 511.
 47. D. Weiss, W. Shotyk, J. Rieley, S. Page, M. Gloor, S. Reese and A. Martinez-Cortizas, *Geochimica and Cosmochimica Acta*, 2002, 66, 2307.
 48. M. E. Goodsite, W. Rom, J. Heinemeier, T. Lange, S. Ooi, P. G. Appleby, W. Shotyk, W. O. van der Knaap, C. Lohse and T. S. Hansen, *Radiocarbon*, 2001, 43, 1.
 49. P. G. Appleby, P. Nolan, F. Oldfield, N. Richardson and S. Higgitt, *Sci. Total Environ.*, 1988, 69, 157.
 50. D. Mauquoy, B. Van Geel, M. Blaauw and J. Van der Plicht, *Holocene*, 2002, 12, 1.
 51. R. J. Telford, E. Heegaard and H. J. B. Birks, *Quat. Sci. Rev.*, 2004, in press.
 52. K. D. Bennet, *Holocene*, 1994, 4, 337.

-Appendix II-

Analytical procedures for the determination of selected major (Al, Ca, Fe, K, Mg, Na, and Ti) and trace (Li, Mn, Sr, and Zn) elements in peat and plant samples using inductively coupled plasma-optical emission spectrometry

Atindra Sapkota, Michael Krachler*, Christian Scholz, Andriy K. Cheburkin and William Shotyk

Institute of Environmental Geochemistry, University of Heidelberg, Im Neuenheimer Feld 236, D-69120 Heidelberg, Germany.

*Corresponding author; Email: krachler@ugc.uni-heidelberg.de; Tel: + 49 (6221) 54 48 48; Fax: + 49 (6221) 54 5228.

Analytica Chimica Acta 540 (2005) 247-256

Abstract

A simple, robust and reliable analytical procedure for the determination of Al, Ca, Fe, K, Li, Mg, Mn, Na, Sr, Ti and Zn in peat and plant materials by inductively coupled plasma-optical emission spectrometry (ICP-OES) was developed. A microwave heated high pressure autoclave was used to digest powdered sample aliquots (approximately 200 mg) with different acid mixtures including nitric acid (HNO₃), tetrafluoroboric acid (HBF₄) and hydrogen peroxide (H₂O₂). The optimized acid mixture for digestion of plant and peat samples consisted of 3 mL HNO₃ and 0.1 mL HBF₄, in addition to H₂O₂ which was sub-boiled into the PTFE digestion tubes during heating of the autoclave. Using HNO₃ alone, recoveries of Al and Ti were too low by 40% and 160%, respectively, because HNO₃ could not fully liberate the analytes of interest from the silicate fraction of the plant and peat matrix. However, for all other elements (such as Mn, Sr and Zn), the use of HBF₄ was less critical. The accuracy of the analytical procedure developed was evaluated with peat and plant reference materials of different origin and composition. The ICP-OES instrument was optimized using solutions of plant reference materials considering RF power, nebulizer pressure, auxiliary gas flow and rinse time. Scandium was used as an online internal standard (IS) as it showed less than 3% drift in sensitivity over time which was lower compared to other potential IS such as Rh (20%) and In (6%). The combination of most sensitive and less sensitive wavelengths allowed to obtain low detection limits and highest possible dynamic range. The achieved procedure detection limits ranged from 0.05 µg g⁻¹ (Li) to 15 µg g⁻¹ (Ca) and allowed a precise quantification of all elements. Comparative X-ray fluorescence spectrometric measurements of solid peat and plant samples generally agreed well with results obtained by digestion/ICP-OES. To overcome interferences caused by Na, K and Li, a solution of 10 µg g⁻¹ CsCl₂ was successfully used as an ionization buffer. The good agreement between the found and certified concentrations in plant and peat reference materials indicates that the developed analytical procedure is well suited for further studies on the fate of major elements in plant and peat matrices.

Keywords: *microwave digestion; ICP-OES; plant; peat; major elements*

1. Introduction

Major and trace elements have widespread implications in industrial, geological, geochemical and environmental studies. Studies of major and trace elemental composition of mineral dust are necessary to better understand geochemical cycle of these dusts and their relationship to climate changes [1-3]. The transport and deposition of mineral dust from arid and semi-arid continental regions has been investigated since many years [1,2,4]. There is a growing interest in the use of plants as bioindicators and peat bogs as archives of atmospheric mineral dust deposition [3,5-7]. Ombrotrophic peat bogs are the most appropriate medium for that purpose as they receive mineral dust particles exclusively from air. However, precise and accurate analytical procedures for the reliable determination of major and trace elements are needed to reconstruct atmospheric mineral dust deposition rates, and to quantify possible changes due to weathering and diagenesis.

To this end, peat samples have to be digested prior to multi-elemental analysis by most instrumental techniques. At present, sample digestion is commonly carried out by heating the samples with acids in open or closed vessels, increasingly by means of microwave irradiation. This method involves the total or partial decomposition of the sample, destroying most of the organic matter. Sample preparation for subsequent elemental analysis is always a crucial step of the analytical procedure. Many factors such as level of contamination, homogeneity of samples, reproducibility and completeness of digestion, suitability of the analytical technique employed, time needed for sample preparation and economic aspects should be considered [8-11]. In comparison to open vessel microwave-assisted digestion, closed vessel microwave-assisted acid digestion has been extensively used for sample digestion [8,9]. Closed vessel microwave-assisted digestion techniques are superior sample pretreatments allowing shorter heating time, reducing cross contamination and minimizing loss of volatile analytes. However, simply employing a closed pressurized digestion system will not give accurate and precise results. Digestion efficiency largely depends

on various parameters such as the method of heating, working pressure as well as kind and volume of acids specifically required to dissolve the sample matrices. Several studies dealing with closed vessel microwave acid digestion of peat and plant matrices have been reported [8,9,11]. Various authors showed that the digestion procedure, specifically, the composition of the acid mixture, has a dominant influence on the results obtained when determining major and trace elements [8,9,11,12]. The main reagents used for digestion of sample matrices such as plant, peat and air particulates are different combinations of nitric acid (HNO_3), hydrofluoric acid (HF) and hydrogen peroxide (H_2O_2). Common practice for the digestion of plant matrices is the addition of H_2O_2 to HNO_3 . Addition of H_2O_2 to the digestion mixture increases the oxidation power of HNO_3 during digestion and enhances the attack of organic material present in the sample. However, mixtures of $\text{HNO}_3/\text{H}_2\text{O}_2$ alone cannot dissolve all of the siliceous material present in the sample, thus leading to poor recoveries for many elements [8,9,13]. Other elements such as As and Se are not bound to the silicate fraction of plant materials or peat and consequently do not require complete dissolution of the siliceous matrix for their accurate quantification [14,15]. Hydrofluoric acid in combination with boric acid (H_3BO_3) is commonly used in the acid mixtures to dissolve silicates present in the samples and to complex “excess HF” in the digestion solutions. In the past few years, however, comparative studies clearly demonstrated the advantages of using tetrafluoroboric acid (HBF_4) over the combination of HF and H_3BO_3 for complete digestion of peat [8,9].

Inductively coupled plasma-optical emission spectrometry (ICP-OES) has been widely used for multielemental analysis [11,16,17]. Analytical qualities such as relatively low detection limits, capacity for simultaneous, rapid and precise determinations over wide concentration ranges have made ICP-OES the method of choice for multielemental analysis and preferred instrumentation over other techniques such as atomic absorption

spectrometry (AAS), flame atomic emission spectrometry (FAES), instrumental neutron activation analysis (INAA) and X-ray fluorescence (XRF) spectrometry. Even though several previous studies reported on the multielement analysis of plant and airborne particulate materials using ICP-OES [11,15,18], no modern investigations of peat samples can be found in the literature. The analytical procedures used to determine major elements developed for plant and particulate matter might not be successfully applied to dissolve peat samples as their composition frequently differs. Besides the plant derived organic material in various stages of decay and humification, the presence of an inorganic mineral fraction, predominantly derived from atmospheric soil dust, makes peat a difficult-to-digest matrix.

The aim of this study was to develop and evaluate an analytical procedure for the digestion of peat materials elucidating the potential of HBF_4 , followed by the determination of selected major elements by ICP-OES. In order to evaluate the digestion and ICP-OES procedures, the seven major (Al, Ca, Fe, K, Mg, Na, and Ti) and four trace (Li, Mn, Sr, and Zn) elements were determined in several certified peat and plant reference materials. Additional measurements of the investigated elements in the solid samples by XRF helped to evaluate the completeness of the digestion procedure and the suitability of the developed analytical procedure.

2. Experimental

2.1. Determination of elements by ICP-OES

ICP-OES measurements were carried out using a Vista MPX instrument with Charge Coupled Devices (CCD) simultaneous detection systems (Varian Inc., Victoria, Australia). Plasma torch alignment was performed by using a Mn solution ($5 \mu\text{g g}^{-1}$) at emission line 257.61 nm. During measurements, chemical attack of instrumental parts such as nebulizer, spray chamber and plasma torch as well as residue formation should be minimized. As the sample solutions contained HBF_4 which is corrosive to quartz, an HBF_4 resistant Inert V-groove nebulizer (Varian Inc.) was used.

Similarly, an inert Ertalyt[®] (Polyethylene Terephthalate) Sturman-Masters spray chamber (Varian Inc.) was employed to improve plasma stability and to minimize matrix interferences.

2.2. Reagents and standards

All solutions were prepared with high-purity water of 18.2 M Ω cm resistivity obtained from a MilliQ-system (Millipore, Milford, MA, USA). Reagents used for the sample digestion were nitric acid (65%, analytical-reagent grade, Merck, Darmstadt, Germany), tetrafluoroboric acid solution (HBF_4 , ~ 50%, Purum, Fluka, Buchs, Switzerland) and hydrogen peroxide (30%, Baker analysed, J.T. Baker, Deventer, Holland). The purity of the nitric acid was further increased by sub-boiling distillation (MLS, Leutkirch, Germany). Please note that the potential toxicity of HBF_4 should be considered similar to that of HF, even though non-conclusive assessment data indicate that the harmful action of HBF_4 might be less compared to HF.

Aliquots of an ICP multi-element standard solution (1000 mg L⁻¹ CertiPUR[®], Merck) containing Al, Ca, Mg, Na, K, Fe, Mn, Sr, Zn, and Li were mixed with a stock standard solution of Ti (1000 mg L⁻¹ CertiPUR[®], Merck). In this manner, one stock solution with all elements with the same concentration (10 mg L⁻¹) was obtained and used for the preparation of all calibration solutions. Calibration solutions ranged from 0.01 mg L⁻¹ to 10 mg L⁻¹ and were prepared daily by adequate dilution of the stock standard solution. Scandium (0.5 mg L⁻¹, CertiPUR[®], Merck) was used as an internal standard element to monitor matrix effects and sensitivity drifts of the ICP-OES instrument. Cesium chloride (CsCl_2 , 10 $\mu\text{g g}^{-1}$) (Optical Grade, Life Technologies, Paisley, Scotland) was used as ionization buffer to correct the interferences caused by high concentrations of alkali elements.

2.3. Sample digestion in the microwave autoclave

Sample aliquots of approx. 200 mg were digested in 20 mL polytetrafluoroethylene (PTFE) vessels in the

microwave autoclave (ultraCLAVE II, MLS, Leutkirch, Germany) using 3 mL HNO₃ and 0.1 mL HBF₄. Additionally, a total volume of 30 mL H₂O₂ placed in a PTFE vessel inside the reaction chamber was subboiled into the 40 digestion vessels during heating of the autoclave. Blank solutions were prepared by applying the same procedure and reagent solutions without sample. The microwave autoclave can digest up to 40 samples in the reaction chamber simultaneously under identical experimental conditions. The starting pressure of the reaction chamber with sample vessels inside was set to 50 bar with Ar. Then the vessels were heated in the microwave autoclave for 76 min reaching a temperature of 240 °C and a pressure of approximately 110 bar. The digestion program consisted of 5 steps: room temperature to 60 °C in 9 min; 60-125 °C in 25 min; 125-160 °C in 10 min; 160-240 °C in 12 min; heated at 240 °C for 20 min. Before opening the reaction chamber, the digests were allowed to cool for about 35 min to well below the boiling point of the acid mixture at atmospheric pressure. After digestion, sample and blank solutions were quantitatively transferred into 15 mL polypropylene tubes (Falcon[®], Becton Dickinson, Meylan Cedex, France) and the volume was made up with high-purity water.

2.4. Quality control

At an early stage of this work no certified peat reference material was available and only one peat material was in the process of certification to become a peat reference material for selected major and trace elements [19]. Therefore, to ensure the accuracy of the developed analytical procedures, a number of certified plant reference materials were analyzed. Reference materials with certified or recommended elemental concentrations were Bush Branches and Leaves (GBW 07602) from Institute of Geophysical and Geochemical Exploration, Langfang, China; Tomato Leaves (NIST 1573a), Apple Leaves (NIST 1515), Peach Leaves (NIST 1547), and Pine Needles (NIST 1575), all from National Institute of Standards and Technology, Gaithersburg, USA; Oriental Tobacco Leaves (CTA-OTL-1) and Virginia Tobacco Leaves

(CTA-VTL-2), both from Institute of Nuclear Chemistry and Technology, Warszawa, Poland and Hay Powder (IAEA-V-1) from International Atomic Energy Agency, Vienna, Austria.

Additionally three peat materials were considered for quality control assurance. Two in-house bulk peat reference materials (Peat 1 and 2) with different chemical matrix characteristics (botanical composition, ash content, concentration of elements) were employed for the development of adequate digestion procedures for small amounts of peat. Peat 1 consists of a fen peat from the Holland Marsh, Ont., Canada and was sample coded as OGS 1878P. Peat 2 was a bulk peat sample collected at Schöpfenwald Moor, near Interlaken, Switzerland. “Reference” values for these in-house materials were obtained as follows: Elemental concentrations in Peat 1 were determined by instrumental neutron activation analysis (INAA) at a commercial laboratory (ACTLABS, Activation Laboratories Ltd, Ancaster, Ont., Canada). Selected elemental concentrations in Peat 2 were quantified by ICP-OES in an accredited laboratory at the Research Center of Juelich, Germany using well established analytical procedures. Several elements in the plant and peat materials were additionally determined in-house by Titan XRF [20]. Details of the preparation and analytical application of these internal peat reference materials is presented elsewhere [8,9,21,22]. Description of the third low ash peat reference (Peat 3, NIMT /UOE/ FM/ 001), which is now certified and available, is provided elsewhere [19].

All reference materials were used as bottled. The moisture content of the reference materials was determined on 200 mg sample aliquots by an electronic moisture analyzer (MA 100H, Sartorius, Göttingen, Germany). The reliability and analytical performance of the moisture determination procedure were described elsewhere [10].

3. Results and discussion

The availability of peat reference materials certified for the major elements considered in this investigation was limited to Peat 3 [19]. However, for many of the elements studied here in Peat 3 (Al, Ca, Fe,

Na and Ti) only information values are reported. Peat 1 and 2 only provide elemental concentrations from inter-laboratory comparisons and these are not certified values. Thus, to evaluate the accuracy of an analytical procedure for the determination of the selected elements in peat, certified reference materials of similar composition are required. Peat consists of an accumulation of decay products of plant materials as well as mineral particles. Considering this, various certified reference materials of plant origin were also used to optimize and evaluate the digestion and quantification procedure.

3.1. Optimization of ICP-OES parameters

As signal intensities of analytes depend on the sample matrix, it is important to optimize ICP-OES parameters such as RF power, nebulizer pressure, auxiliary gas flow rate, sample uptake and rinse time. Emission intensities are mostly affected by the first two parameters, whereas other parameters have relatively small effects and are usually adjusted to accommodate memory effects due to particular sample type such as organic materials or dissolved solids. In this study, plant reference materials were utilized rather than aqueous standard solutions to optimize the instrumental parameters. Based on high signal/blank ratios at lines of least interference, the optimum values for all parameters were obtained (Table 1). Furthermore, the employed ICP-OES instrument allows different spectral wavelengths to be selected for the quantification of elements. Since elements of interest in real samples may occur over wide concentration ranges, one single emission line may not be sufficient to cover these wide ranges. Therefore, two emission lines i.e. the most sensitive line to cover the lower concentration range and a less sensitive line to cover the upper concentration range was selected for the detection of analyte signals. This approach helps to achieve the best detection limits and highest possible dynamic range. Based on the sensitivity and likelihood of occurrence of spectral interferences, the most appropriate of the spectral lines for the analytes of concern are given in Table 1. The wavelengths reported in column 1 of Table 1

were used for quantification throughout this study, whereas the second emission line was used as an independent check of accuracy of the measurements.

Table 1: Operational parameters used for the determination of elements by ICP-OES.

Method Parameters		
RF Power (kW)		1.20
Plasma Flow (L min ⁻¹)		15.0
Aux Flow (L min ⁻¹)		1.50
Nebulizer Pressure (kPa)		240
Sample Uptake (s)		30
Rinse Time (s)		20
Pump Rate (rpm)		18
Replicate Time (s)		20
Stabilization Time (s)		15
Replicates		3
Element	Emission line (nm) ^a	Emission line (nm) ^b
Al	237.312	396.152*
Ca	317.933	370.602
Fe	238.204*	261.382
K	769.897	766.491*
Li	670.783*	610.365
Mg	285.213	280.270
Mn	257.610*	259.372
Na	589.592*	588.995
Sr	407.711*	421.552
Ti	334.188	334.941
Zn	213.857*	202.548

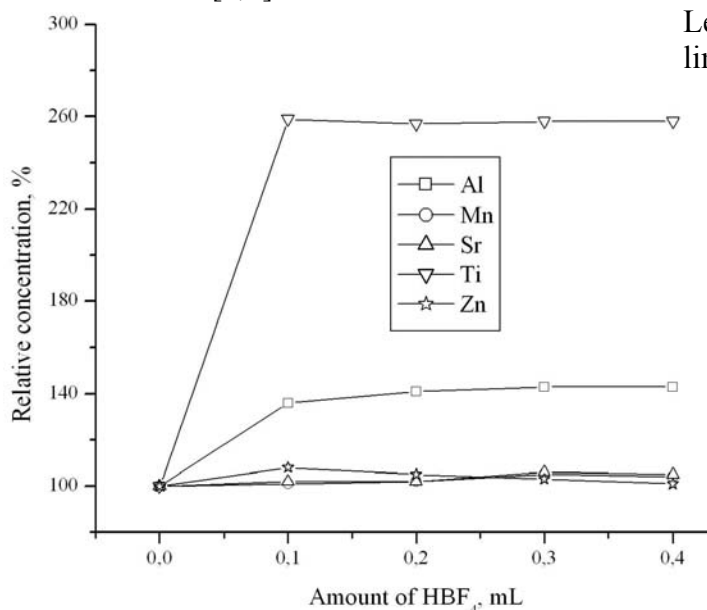
^a Concentrations reported in this study are based on this emission line; ^b Wavelength used for independent accuracy check; * indicates the most sensitive emission line. Please note that because of the high concentrations of Ca, Mg, and Ti in the analyte solutions only less sensitive emission lines were employed.

3.2. Influence of digestion procedure in microwave autoclave

Complete breakdown of siliceous material requires, besides HNO₃, hydrofluoric acid (HF) which has some serious analytical drawbacks [8,9]. Therefore, HBF₄ is preferable for the complete dissolution of silicate-containing materials such as peat and plant matrices for subsequent trace element analysis as described in details elsewhere [8,9].

Initial experiments focused on the establishment of the digestion efficiency of

plant samples using different amounts of HBF_4 (0; 0.1; 0.2; 0.3; and 0.4 mL). Two replicate digestions were carried out for the reference material Bush Branches and Leaves adding variable amounts of HBF_4 to 3 mL HNO_3 . Results of the analysis of these digestion solutions using HNO_3 alone were set to 100% and all other concentrations of selected elements were plotted relative to this first data point (Fig. 1). As shown in Fig. 1, the addition of small volumes (0.1 mL) of HBF_4 distinctly increased the measured concentrations of Al and Ti by 40% and 160% respectively, indicating an association of the two elements with the silicate fraction. Concentrations of Al and Ti remained fairly constant when the amounts of HBF_4 were further increased. However, for other elements such as Mn, Sr, and Zn the addition of HBF_4 to HNO_3 did not increase or decrease the measured concentrations (Fig. 1) indicating that Mn, Sr and Zn are predominately bound to other crystalline or amorphous phases. Similarly, elements such as Ca, Fe, K, Li, Mg and Na behaved similarly to Mn, Sr and Zn. These results demonstrate that the use of 3 mL HNO_3 and 0.1 mL HBF_4 is sufficient to completely dissolve the silicate fraction of plant samples for subsequent elemental analysis (Fig. 1). Further details on the use of HBF_4 for digestion of plant and peat samples and subsequent trace element analysis can be found elsewhere [8,9].



3.3. Detection limits

The ICP-OES instrument employed in this study used an axially viewed configuration that generally provides better detection limits than radially viewed plasmas [23]. For the calculation of the detection limits, ten separate blank solutions were analyzed. The solution detection limit of the ICP-OES procedure was calculated as the concentration equal to 3 times the standard deviation of the signals of the blank solutions. The solution quantification limit was equal to ten times the standard deviation of the signals of the ten blank solutions. The procedure detection and quantification limits of the investigated elements were calculated as the concentration equal to 3 and 10 times the standard deviation of the signals of the blank solutions, multiplied by the dilution factor of 500. The procedure quantification limit represents the lowest concentration of major elements in plant and peat samples that can be reliably quantified with the developed analytical approach (digestion/ICP-OES). The detection limits for all elements studied are summarized in Table 2. Elemental concentrations of Al, Fe, Li, Sr, Ti and Zn determined in the samples, were at least 40 times higher than the procedure detection limit. Similarly, concentrations of Ca, K, Mg, and Mn are 100 times higher than the corresponding procedure detection limits. In the case of Na, its concentration is 20 times higher in all samples except for Peach Leaves and Apple Leaves i.e. only 4 times higher than detection limit thus giving rise to poor precision.

Fig. 1. Concentrations of selected elements determined in digests of the reference material Bush Branches and Leaves after addition of variable amounts of HBF_4 to the digestion mixture containing 3 mL HNO_3 .

Table 2: Detection and quantification limits of the developed digestion/ ICP-OES procedure

Element	Solution detection limit ^a ($\mu\text{g L}^{-1}$)	Solution quantification limit ^b ($\mu\text{g L}^{-1}$)	Procedure Detection limit ^c ($\mu\text{g g}^{-1}$)	Procedure quantification limit ^d ($\mu\text{g g}^{-1}$)
Al	3	10	1.50	5.00
Ca	30	100	15.0	50.0
Fe	4	13	2.00	6.50
K	23	77	11.5	38.5
Li	0.10	0.33	0.05	0.16
Mg	15	49	7.50	24.5
Mn	0.3	1	0.15	0.50
Na	12	40	6.00	20.0
Sr	0.2	0.5	0.10	0.25
Ti	0.4	1.5	0.20	0.75
Zn	0.2	1	0.10	0.50

^aConcentrations corresponding to 3 standard deviations of the blank. ^bConcentrations corresponding to 10 standard deviations of blank. ^cConcentrations corresponding to 3 standard deviations of the blank related to a sample mass of 200 mg finally diluted in 100 mL. ^dConcentrations corresponding to 10 standard deviations of the blank related to a sample mass of 200 mg finally diluted in 100 mL.

3.4. Selection of internal standards for ICP-OES

Precision or sensitivity of analytical instruments is often affected by intensity fluctuations. Calibration curves and optimized instrumental parameters may change between the time the first calibration is performed and the time of sample measurement. Studies on ICP-OES performance have shown that small changes of parameters such as sample uptake rate, size of aerosol droplets, Ar pressure in the spray chamber, plasma robustness or RF power may give rise to drift of sensitivity [24-26]. This deteriorated performance hampers the repeatability of measurements and more importantly, leads to inaccurate results. In order to obtain the highest possible accuracy and precision, corrections for these effects are necessary. In that context, the use of an internal standard is of utmost importance to reduce the errors in ICP-OES caused by drift and matrix effects due to variations in the sensitivity encountered during a large series of sample analyses [17]. One approach to internal standardization is to add a well defined amount of an element to function as an internal standard, to an exactly known

quantity of sample solution. Another way of correcting the analyte signals is to use internal standards side by side with analytes operating using the same physical parameters (e.g. pump speed, Ar pressure) which is known as online internal standardization. However, small changes in the pump speed within and between sample uptake and online internal standard solution uptake might result in poor precision of analyte concentrations. Although, the internal standard addition technique is a much more accurate approach, it is more time consuming for a large sets of samples compared to online internal standardization. Online internal standardization with an axially viewed ICP-OES was evaluated and found appropriate for long series of measurements [27]. It has been shown that under robust plasma conditions, when the drift is assumed to be mainly a change in the sample transport efficiency, the use of only a single internal standard element such as Ar, Y, Sr, and Sc is sufficient [17,24,27]. Initial experiments carried out with peat digests in this study elucidated the potential of Sc, Rh, and In as internal standard elements, but Sc was ultimately found to be the best choice (Fig. 2).

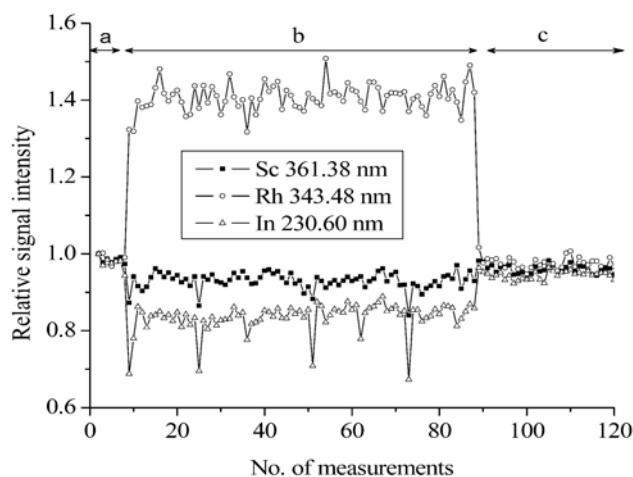


Fig. 2. Variation of signal intensities observed for the potential internal standard elements Sc (361.38 nm), Rh (343.48 nm) and In (230.60 nm) during a measurement sequence of peat digests.

As shown in Fig. 2, relative signal intensities for Sc, Rh and In were similar during the measurement of the first 10 samples which consisted of standards and blanks. Upon introduction of peat digests (section b in Fig. 2) Rh signals increased and In signals decreased from the initial line whereas the Sc response remained fairly stable. Upon further dilution (5000 times) of the peat digests (section c), all three potential internal standard elements returned to their initial values again. It is important to note here, that this drift was largely reproducible and related to the sample matrix. The analytical signals obtained from the analysis of several certified reference materials have been normalized using In, Rh or Sc as potential internal standard elements. By far the best agreement between experimental and certified values was obtained employing Sc as the internal standard element. Consequently Sc was chosen as internal standard at a concentration of $100 \mu\text{g kg}^{-1}$ and was continuously supplied online to the instrument throughout all measurements.

3.5. Interference study

The so-called alkali effect or interference in the Ar plasma due to easily ionized elements such Na and K is a well known phenomena in ICP-OES [28]. High concentrations of any of these elements in the

sample promote rapid ionization of Na and K and thereby increase their free atom population in the plasma. This increment enhances the signal intensity of other elements of same group such as Li, Na or K and thus suppresses the real analyte signal. In the present study, considerable signal suppression was only observed when high amounts of either Na or K ($> 100 \mu\text{g g}^{-1}$ in the analyte solution) were analyzed with the ICP-OES instrument.

Signal suppression due to Na and/or K was further evaluated utilizing spike solutions of different concentrations of Na and K. First, a set of solutions with different K concentrations ($0, 10, 100, 500$ and $1000 \mu\text{g g}^{-1}$) was added to a set of solutions each containing $5 \mu\text{g g}^{-1}$ Na and $1 \mu\text{g g}^{-1}$ Li. Similarly, another set of solutions was prepared with constant amounts of K ($5 \mu\text{g g}^{-1}$) and Li ($1 \mu\text{g g}^{-1}$), but with varying concentrations of Na ($0, 10, 100, 500$ and $1000 \mu\text{g g}^{-1}$). Both sets of solutions were run at identical instrumental parameters as used for peat and plant reference materials. Each set was measured twice, with and without addition of CsCl_2 ($10 \mu\text{g g}^{-1}$) solution acting as an ionization buffer to suppress the ionization effects of Na and K. Recoveries of Na, K and Li expressed as percentage of the target values are presented in Fig. 3a + b. As highlighted in Fig. 3a, recovery of Li gradually increased from 108% to 160% when the addition of K was increased from $0 \mu\text{g g}^{-1}$ to $1000 \mu\text{g g}^{-1}$. In comparison, when CsCl_2 was used Li concentrations varied only between 93% and 101%. A similar behavior was observed for Na with recoveries varying between 95% and 152% and between 95% and 106% for analyses without and with an ionization buffer. Additionally, the effect of varying Na concentrations on the Li and K signals is summarized in Fig. 3b.

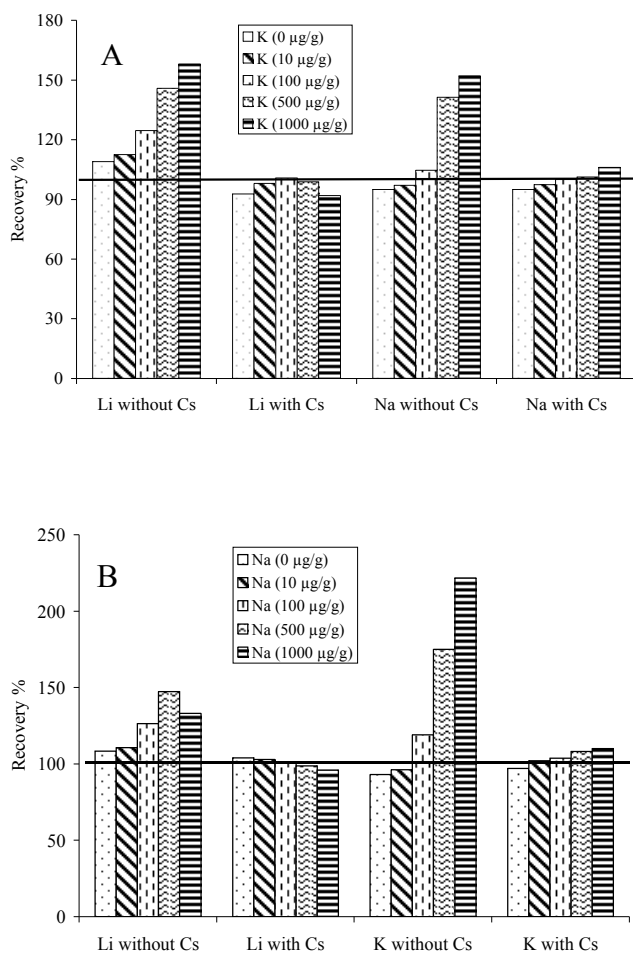


Fig. 3. Recoveries expressed as % of Na, K and Li illustrating the signal variation caused by different amounts of Na and K in the analyte solution. (a) Sample series with $5 \mu\text{g g}^{-1}$ Na, $1 \mu\text{g g}^{-1}$ Li and variable K concentrations; (b) Sample series with $5 \mu\text{g g}^{-1}$ K, $1 \mu\text{g g}^{-1}$ Li and variable Na concentrations.

For this experiment, concentrations of K ($5 \mu\text{g g}^{-1}$) and Li ($1 \mu\text{g g}^{-1}$) were kept constant whereas Na concentrations were varied between 0 and $1000 \mu\text{g g}^{-1}$. As shown in Fig. 3b, Li concentrations ranged from 108% to 147% as the concentration of Na increased from $0 \mu\text{g g}^{-1}$ to $1000 \mu\text{g g}^{-1}$ in the absence of an ionization buffer. In contrast, when CsCl_2 was added to the analyte solutions Li concentrations only varied from 96% to 104% despite the increasing Na concentrations. Similarly, recoveries for K varied between 93% and 222% and between 97% and 110% without and with an ionization buffer. Taken together, these data indicate that the use of an ionization buffer (CsCl_2)

was effective for correcting the signal suppression due to the alkali effect.

3.6. Element determinations in plant reference materials

For the verification and cross-examination of the accuracy of the developed digestion/ICP-OES procedure, all powdered samples were also analyzed for Ti, Zn, Sr, Mn, Fe, K, and Ca in-house using XRF spectrometry. Concentrations of these elements determined by ICP-OES and XRF are presented in Tables 3 and 4, respectively, together with their certified or information values. Lithium values determined by ICP-OES in the plant reference materials agreed well with the certified Li concentrations provided for Virginia Tobacco Leaves, Bush Branches and Leaves as well as Oriental Tobacco Leaves. Unfortunately, there are no certified or information values for Li in the other plant reference materials where concentrations of Li were much lower ($0.2 \mu\text{g g}^{-1}$ to $1 \mu\text{g g}^{-1}$). Except for Oriental Tobacco Leaves (Table 4), concentrations of Al in all reference materials were in good agreement with certified values varying within 95-105% of the target values. Concentrations of Al in Hay Powder and Virginia Tobacco Leaves are information values and thus must be considered with caution. For the remaining elements Ca, Fe, K, Mg, Mn, Sr, Ti, and Zn, the recoveries ranged between 95-105% of the certified mean values for all reference materials. Similarly, Na concentrations also ranged between 95-105% of the target value except for Virginia Tobacco Leaves, Peach Leaves and Apple Leaves where the recoveries were 163% (of the information value), 133% and 125% respectively. Signal suppression due to high K concentrations in the analyte solutions as well as Na concentrations close to the procedure detection limit are most likely the reasons for these inaccuracies established for Peach Leaves and Apple Leaves.

XRF analysis revealed that elemental concentrations for Ti, Zn, Sr, Mn, Fe, K and Ca were 90-120% relative to certified and/or non certified values. Certified values for Ti are rarely provided for plant reference materials, making a comparison with Ti data

obtained using XRF an essential part of this study. Comparing the concentrations of Ti determined by XRF and ICP-OES, good agreement was obtained for Virginia Tobacco Leaves, Bush Branches and Leaves, Pine Needles and Tomato Leaves (Tables 3 and 4). For Hay Powder, Apple Leaves and Oriental Tobacco Leaves, Ti concentrations differed between XRF and ICP-OES by ~ 30%. Reasons for this large variation of the Ti

concentrations might be possible sample contamination, inhomogeneity of samples or differences in detection limits. Referring to the solid sample, ICP-OES has a detection limit of $0.2 \mu\text{g g}^{-1}$ whereas the limit of detection for Ti provided by XRF amounts to $1.2 \mu\text{g g}^{-1}$. However, in the absence of a certified value for Ti for these reference samples, the values obtained here should be considered with caution.

Table 3: Elemental concentrations (mean \pm standard deviation, $\mu\text{g g}^{-1}$ dry mass) in four plant reference materials as determined by ICP-OES (n = 8) and XRF (n = 3).

Element	Hay Powder	Virginia Tobacco Leaves	Bush Branches and Leaves	Pine Needles
	ICP-OES XRF Certified	ICP-OES XRF Certified	ICP-OES XRF Certified	ICP-OES XRF Certified
Al	59 ± 2	1935 ± 33	2200 ± 80	558 ± 14
	-	-	-	-
	$47 (30-87)^b$	1682^b	2140 ± 180	545 ± 30
Ca ^a	2.15 ± 0.07	3.54 ± 0.03	2.24 ± 0.07	0.41 ± 0.01
	2.08 ± 0.07	3.55 ± 0.03	2.30 ± 0.20	0.42 ± 0.01
	$2.16 (2.10-2.22)$	3.60 ± 0.15	2.22 ± 0.07	0.41 ± 0.02
Fe	182 ± 7	1071 ± 20	1023 ± 37	197 ± 3
	165 ± 30	1031 ± 15	1001 ± 95	252 ± 13
	$186 (177-190)$	1083 ± 33	1020 ± 40	200 ± 10
K ^a	1.94 ± 0.42	1.05 ± 0.01	0.86 ± 0.01	0.37 ± 0.00
	2.07 ± 0.07	1.12 ± 0.03	0.91 ± 0.07	0.38 ± 0.01
	$2.10 (1.96-2.25)$	1.03 ± 0.04	0.85 ± 0.03	0.37 ± 0.02
Li	0.68 ± 0.04	24.1 ± 1.5	2.6 ± 0.05	0.21 ± 0.1
	-	-	-	-
	-	23.0 ± 1.9	2.4 ± 0.30	-
Mg ^a	0.136 ± 0.003	0.51 ± 0.01	0.287 ± 0.009	0.112 ± 0.002
	-	-	-	-
	$0.136 (0.133-0.145)$	0.51 ± 0.023	0.287 ± 0.011	-
Mn	52 ± 1	79.1 ± 2.0	59 ± 1	671 ± 11
	50 ± 1	71.1 ± 2.4	62 ± 4	687 ± 8
	$47 (44-51)^b$	79.7 ± 2.6	58 ± 3	675 ± 15
Na	491 ± 4	508 ± 69	1.08 ± 0.03^a	67 ± 5
	-	-	-	-
	$500 (440-570)^b$	312^b	1.10 ± 0.06^a	-
Sr	43.8 ± 1.7	116 ± 1	347 ± 15	4.8 ± 0.1
	42.2 ± 1.4	118 ± 1	362 ± 5	4.5 ± 0.2
	-	110 ± 12	345 ± 7	4.8 ± 0.2
Ti	7 ± 2	82.5 ± 1.5	98 ± 4	18.3 ± 1.0
	11 ± 1	85 ± 10	89 ± 6	22.3 ± 1.7
	-	76.3^b	95 ± 13	-
Zn	24 ± 1.2	42.2 ± 0.7	21.6 ± 1.6	56 ± 3
	22 ± 1.4	42.4 ± 1.0	24 ± 3	73 ± 6
	$24 (23-25)$	43.3 ± 2.1	20.6 ± 1.0	-

^aConcentration in percentage (%); ^binformation value; - not determined

Concentrations of other elements such as Ca, Fe, K, Mn, Sr and Zn quantified by both instrumental techniques differed by not more than 10%. The cross-examination of the digestion/ICP-OES procedure with XRF for the elements considered in this study demonstrates the reliability of the analytical procedures developed. Aluminum in combination with Si is abundant in igneous rocks. Complete recovery of Al element is an

efficient tool for validating the completeness of the digestion procedure for dissolving silicates. Titanium-bearing minerals like ilmenite (FeTiO_3), sphene (CaTiSiO_5) and rutile (TiO_2) are important accessory minerals in many rocks [29]. Therefore, the recovery results provided by Ti also indicates the complete digestion of the investigated plant materials.

Table 4: Elemental concentrations (mean \pm standard deviation, $\mu\text{g g}^{-1}$ dry mass) in four plant reference materials as determined by ICP-OES (n = 8) and XRF (n = 3).

Element	Tomato Leaves	Peach Leaves	Apple Leaves	Oriental Tobacco Leaves
	ICP-OES XRF Certified	ICP-OES XRF Certified	ICP-OES XRF Certified	ICP-OES XRF Certified
Al	593 \pm 18	246 \pm 16	269 \pm 9	2310 \pm 30
	-	-	-	-
Ca ^a	598 \pm 12	249 \pm 8	286 \pm 9	1740 \pm 290
	4.62 \pm 0.36	1.56 \pm 0.01	1.47 \pm 0.03	3.34 \pm 0.06
	4.80 \pm 0.03	1.50 \pm 0.03	1.80 \pm 0.14	3.44 \pm 0.07
Fe	5.05 \pm 0.09	1.56 \pm 0.02	1.53 \pm 0.02	3.17 \pm 0.12
	361 \pm 12	214 \pm 12	79 \pm 3	1250 \pm 10
	368 \pm 8	261 \pm 11	90 \pm 3	1090 \pm 30
K	368 \pm 7	218 \pm 14	83 \pm 5	-
	2.72 \pm 0.26	2.45 \pm 0.17	1.51 \pm 0.30	1.55 \pm 0.03
	2.67 \pm 0.011	2.46 \pm 0.03	1.87 \pm 0.13	1.74 \pm 0.03
Li	2.70 \pm 0.05	2.43 \pm 0.03	1.61 \pm 0.02	1.56 \pm 0.05
	1.0 \pm 0.06	0.25 \pm 0.10	0.22 \pm 0.10	24.0 \pm 1.9
Mg ^a	-	-	-	-
	-	-	-	23.0 \pm 1.8
	1.1 \pm 0.2	0.422 \pm 0.010	0.266 \pm 0.007	0.459 \pm 0.065
Mn	-	-	-	-
	1.2 ^b	0.432 \pm 0.008	0.271 \pm 0.008	0.447 \pm 0.021
	250 \pm 8	99 \pm 4	54 \pm 1	408 \pm 3
Na	226 \pm 7	100 \pm 5	61 \pm 4	393 \pm 5
	246 \pm 8	98 \pm 3	54 \pm 3	412 \pm 14
Sr	144 \pm 14	32 \pm 3	30.8 \pm 1.1	360 \pm 5
	-	-	-	-
Ti	136 \pm 4	24 \pm 2	24.4 \pm 1.2	345 ^b
	88 \pm 1	53 \pm 2	25 \pm 0.9	216 \pm 3
	86 \pm 3	52 \pm 1	24 \pm 0.5	237 \pm 2
Zn	85 ^b	53 \pm 4	25 \pm 2	201 \pm 20
	59 \pm 1	25 \pm 4	16.0 \pm 1.1	120 \pm 10
Zn	57 \pm 3	-	24.9 \pm 2.4	93 \pm 5
	-	-	-	-
	31.9 \pm 2.1	17.7 \pm 0.8	12.5 \pm 1.5	46.8 \pm 3.1
Zn	32.0 \pm 2.0	19.4 \pm 0.1	15.0 \pm 0.3	52.0 \pm 1.0
	31.9 \pm 0.7	17.9 \pm 0.4	12.5 \pm 0.3	49.9 \pm 2.4

^aConcentration in $\mu\text{g g}^{-1}$; ^binformation value; - not determined

Table 5 Elemental concentrations (mean \pm standard deviation, % dry mass) in three peat reference materials as determined by ICP-OES (n = 8 for in-house, n = 4 for Juelich) and XRF/ INAA (n = 15 for Peat 1; n = 3 for Peat 3).

Element	Peat 1 ICP-OES XRF INAA	Peat 2 ICP-OES (in-house) ICP-OES (Juelich)	Peat 3 ICP-OES XRF Certified
Al	0.45 \pm 0.03 - 0.75 \pm 0.01	0.23 \pm 0.001 -	0.37 \pm 0.006 - 0.37 \pm 0.034 ^b
Ca	4.11 \pm 0.12 3.94 \pm 0.72 3.92 \pm 0.35	0.26 \pm 0.001 0.28 \pm 0.004	885 \pm 5 ^a 705 \pm 51 ^a 683 \pm 198 ^{a, b}
Fe	0.99 \pm 0.30 0.81 \pm 0.10 0.77 \pm 0.10	750 \pm 2 ^a 782 \pm 14 ^a	860 \pm 8 ^a 1075 \pm 32 ^a 921 \pm 84 ^{a, b}
K	0.32 \pm 0.06 0.28 \pm 0.05 0.20 \pm 0.03	453 \pm 39 ^a 452 \pm 16 ^a	0.057 \pm 0.003 0.034 \pm 0.004 -
Li ^a	3.02 \pm 0.02 - -	0.85 \pm 0.10 - -	1.0 \pm 0.05 - -
Mg	0.36 \pm 0.06 - -	117 \pm 14 ^a 125 \pm 3 ^a	0.071 \pm 0.002 - 0.058 \pm 0.017
Mn ^a	233 \pm 6 242 \pm 7 120 \pm 17	4.6 \pm 0.5 4.4 \pm 0.1	7.18 \pm 0.15 14 \pm 1 7.52 \pm 0.41
Na	0.33 \pm 0.08 - 0.27 \pm 0.03	186 \pm 47 ^a 145 \pm 17 ^a	632 \pm 22 ^a - 817 \pm 307 ^{a, b}
Sr ^a	190 \pm 2 193 \pm 19 191 \pm 2	13.3 \pm 1.6 13.2 \pm 0.3	23 \pm 1 23 \pm 1 -
Ti ^a	290 \pm 5 250 \pm 50 -	243 \pm 40 - -	364 \pm 6 278 \pm 12 357 \pm 18 ^b
Zn ^a	40 \pm 2 38 \pm 3 38 \pm 3	4.2 \pm 0.6 4.0 \pm 0.3	29.6 \pm 1.4 35 \pm 2 28.6 \pm 1.9

^aConcentration in $\mu\text{g g}^{-1}$; ^binformation value; - not determined

3.6. Element determinations in peat samples

Table 5 summarizes the concentrations of the 11 elements determined in three peat reference materials as obtained by the microwave digestion/ICP-OES procedure developed in this study. Concentrations of Li in these peat reference materials ranged between 0.85 $\mu\text{g g}^{-1}$ and 3 $\mu\text{g g}^{-1}$ and not discussed further here as no certified or information values available. Results for all other elements obtained by INAA/XRF (Peat 1), by an ICP-OES procedure routinely applied at the Research Center Juelich (Peat 2, closed pressurized digestion procedure on a hotplate with HNO_3

and 200 μL HF at 180 $^\circ\text{C}$ for 5 h) as well as the certified concentrations of Peat 3 [19] are included in this Table for comparison. Concentrations of all elements, except Al and Mn, determined in Peat 1 in this study agreed very well with the concentrations derived from INAA/XRF (Table 5). Peat 1 was of minerotrophic origin with a high ash content containing mineral inputs from the surrounding environment, making it a particularly difficult-to-digest material. A high amount of residue was always observed after the digestion of Peat 1. Therefore, the discrepancies between Al concentrations determined by ICP-OES and INAA in Peat 1

in this study may be due to the association of Al with minerals with a high silicate content resulting in incomplete dissolution of Al in solution. It is important to note here, that Peat 1 represents a worst case scenario (~ 22% ash) and contains far more mineral matter than typical sphagnum peats which usually have 1-3% ash. As demonstrated in Tables 3-5, for other peat and plant materials, the digestion/ICP-OES approach allowed an accurate determination of Al in the samples. Elemental concentrations of Peat 3 determined by ICP-OES in this study were also in good agreement with the elemental concentrations provided elsewhere [19]. However, comparing in-house ICP-OES and XRF concentrations in Peat 3, Mn concentrations determined by XRF were almost 100% higher. As Mn concentrations in the other reference materials obtained by both techniques were in good agreement, it was likely that inhomogeneity and/or potential contamination of the peat sample with Mn might be the reason behind this discrepancy. For the elements Ca, Fe, K, Mg, Mn, Na, Sr, and Zn values determined in-house in Peat 2 by ICP-OES agreed well with other ICP-OES results (closed pressurized digestion: 200 mg sample + 2 mL HNO₃ + 200 µL HF for 5 h at 180 °C). In general, the good agreement of results provided by the other two peat samples (Peat 1 + 3) and elements indicates that the digestion and ICP-OES quantification procedures produced reliable results.

4. Conclusions

A simple, robust and reliable analytical procedure for the simultaneous determination of 7 major and 4 trace elements in plant and peat specimens was developed. The microwave autoclave employed for dissolution of plant and peat samples provides an efficient, reliable and time saving tool for sample digestion. Complete dissolution of the silicate fraction liberating all elements from the peat or plant matrix was not possible with nitric acid alone. Complete recovery observed for Al and Ti in plant samples demonstrated the effectiveness of HBF₄ addition. The combination of 3 mL HNO₃ and 0.1 mL HBF₄ was the optimal digestion acid mixture for about 200 mg of powdered peat or plant

samples releasing the elements studied into the analyte solution at a temperature of 240 °C.

For ICP-OES, the combination of most and less sensitive emission lines for the quantification of elements helped to achieve the best detection limits and large dynamic ranges. The procedure detection limits ranged from 0.05 µg g⁻¹ (Li) to 15.0 µg g⁻¹ (Ca), demonstrating the potential of the analytical approach to quantify the major and trace elements in plant and peat samples. The accuracy of the ICP-OES technique used for the analysis of the elements Al, Ca, Fe, K, Li, Mn, Mg, Na, Sr, Ti and Zn was evaluated by using several plant and peat reference materials. Robust ICP-OES operating conditions employing only one internal standard is sufficient to correct the signal to background ratio adequately. Online internal standardization allows a correction for the drift in sensitivity, measuring the analyte signal and internal standard signal simultaneously under the influence of similar physical parameters. As an online internal standard, Scandium (Sc) was used as it showed less than 3% drift within a measurement sequence. In both plant and difficult-to-digest peat matrices, the accuracy for most of the elements was + 5% of the accepted concentration. The accuracy of ICP-OES results was further evaluated using XRF analyses of solid samples and was found to agree with the ICP-OES values to within 10%. Cesium chloride (CsCl₂, 10 µg g⁻¹) was successfully used as an ionization buffer to mask the signal suppression caused by high concentrations of Na and K in the samples. The generally good agreement between the reported concentrations and certified or inter-laboratory concentrations underpins the reliability of the proposed microwave and ICP-OES procedure for the analysis of major elements in peat and plant samples.

Acknowledgements

Financial support from the Deutsche Forschungsgemeinschaft (SH 89 / 2-1 and SH 89 / 2-2) is gratefully acknowledged.

References

- [1] A. Avila, M. Alarcon, I. Queralt, *Atmos. Environ.* 32 (1998) 179.
- [2] M.A.H. Eltayeb, J. Injuk, W. Maenhaut, R.E.V. Grieken, *J. Atmos. Chem.* 40 (2001) 247.
- [3] W. Shotyk, *Chem. Geol.* 138 (1997) 55.
- [4] N.J. Middleton, A.S. Goudie, *Trans. Inst. Br. Geogr.* 26 (2001) 165.
- [5] W. Shotyk, D. Weiss, P.G. Appleby, A. Cheburkin, R. Frei, M. Gloor, J.D. Kramers, S. Reese, W.O. Van Der Knaap, *Science* 281 (1998) 1635.
- [6] P. Steinmann, W. Shotyk, *Chem. Geol.* 138 (1997) 25.
- [7] W. Shotyk, M. Krachler, A. Martinez-Cortizas, A.K. Cheburkin, H. Emons, *Earth Planet. Sci. Lett.* 6180 (2002) 1.
- [8] M. Krachler, C. Mohl, H. Emons, W. Shotyk, *Spectrochim. Acta B* 57 (2002) 1277.
- [9] M. Krachler, C. Mohl, H. Emons, W. Shotyk, *J. Anal. At. Spectrom.* 17 (2002) 844.
- [10] M. Krachler, *Fresenius J. Anal. Chem.* 371 (2001) 944.
- [11] E.V.M. Carrilho, M.R. Gonzalez, A.R. Nogueira, G.M. Cruz, J.A.N. Brega, *J. Agric. Food Chem.* 50 (2002) 4164.
- [12] G.C.L. Araujo, M.H. Gonzalez, A.G. Ferreira, A.R. Nogueira, J.A. Nobrega, *Spectrochim. Acta B* 57 (2002) 2121.
- [13] M. Krachler, H. Emons, C. Barbante, G. Cozzi, P. Cescon, W. Shotyk, *Anal. Chim. Acta* 458 (2002) 387.
- [14] J. Frank, M. Krachler, W. Shotyk, *Anal. Chim. Acta* 530 (2005) 307.
- [15] J. Barciela Garcia, M. Krachler, B. Chen, W. Shotyk, *Anal. Chim. Acta* (2005), in press.
- [16] A. Robache, F. Mathe, J.C. Gallo, R. Guillermo, *Analyst* 125 (2000) 1855.
- [17] H. Kola, P. Peramaki, *Spectrochim. Acta B* 59 (2004) 231.
- [18] M. Grotti, C. Ianni, R. Frache, *Talanta* 57 (2002) 1053.
- [19] C. Yafa, J.G. Farmer, M.C. Graham, J.R. Bacon, C. Barbante, W.R.L. Cairns, R. Bindler, I. Renberg, A. Cheburkin, H. Emons, M.J. Handley, S.A. Norton, M. Krachler, W. Shotyk, X.D. Li, A. Martinez-Cortizas, I.D. Pulford, V. MacIver, J. Schweyer, E. Steinnes, T.E. Sjøbakk, D. Weiss, A. Dolgoplova, M. Kylander, *J. Environ. Monit.* 6 (2004) 493.
- [20] A.K. Cheburkin, W. Shotyk, *X-Ray Spectrom.* 34 (2005) 69.
- [21] M. Krachler, W. Shotyk, H. Emons, *Anal. Chim. Acta* 432 (2001) 303.
- [22] M. Krachler, W. Shotyk, *J. Environ. Monit.* 6 (2004) 418.
- [23] F.V. Silva, L.C. Trevizan, C.S. Silva, A.R. Nogueira, J.A. Nobrega, *Spectrochim. Acta B* 57 (2002) 1905.
- [24] A. Lorber, Z. Goldbart, M. Eldan, *Anal. Chem.* 56 (1984) 43.
- [25] X. Romero, E. Poussel, J.M. Mermet, *Spectrochim. Acta B* 52 (1997) 487.
- [26] J.W. Olesik, L.J. Smith, E.J. Williamsen, *Anal. Chem.* 61 (1989) 2002.
- [27] J.C. Ivaldi, J.F. Tyson, *Spectrochim. Acta B* 51 (1996) 1443.
- [28] J. Nölte, *ICP Emission Spectrometry: A Practical Guide*, Wiley-VCH Verlag GmbH, Weinheim, 2003.
- [29] V. M. Goldschmidt, in: A. Muir (Ed.), *Geochemistry (The International Series of Monographs on Physics)* Clarendon Press, Oxford, 1954.

-Appendix III- Atmospheric deposition of trace elements (Cr, Cu, Zn and Rb) in southern South America (a brief overview)

1 Introduction

In the Northern Hemisphere, peat bogs, as an environmental archive have clearly documented how the human activities altered the atmospheric composition of trace elements such as Pb (Shotyk et al., 1998), Hg (Roos-Barracough et al., 2006), Cu (Monna et al., 2004), Zn (Rausch et al., 2005), and V, Cr, and Ni (Krachler et al., 2003). In southern hemisphere, however, many studies on atmospheric deposition of trace elements are limited to either Antarctic ice cores with more focus on the early Holocene and Glacial-interglacial period (Hong et al., 2004; Hong et al., 2003) and/or lower latitudes of South America (Espí et al., 1997). In a recent study of trace elements (e.g. Cu, Zn, Cd, Pb) in firn- and ice-core from Antarctica, corresponding to 4500 BC – AD 1989, Cu and Pb concentrations were found to be consistent with increasing anthropogenic emissions of these elements in the Southern Hemisphere (Vallelonga et al., 2004). However, this needs to be studied in detail to estimate the contribution of different sources such as South America and / or Australia.

In southernmost South America, to date only one study has been reported on the enrichment of trace elements in sediments from coastal zone of the Beagle Channel (Tierra del Fuego, Argentina), suggesting human impact on the sediments (Amin et al., 1995). However, no studies on atmospheric metal deposition have been reported, despite the growing number of industries and mining activities in southern South America (Amin et al., 1995). Therefore, there is a great potential to use peat bog as an archive of atmospheric deposition of major and trace elements and to understand the human impact on natural environment of southern South America. This is a first geochemical study of a peat bog as an environmental archive in that region. Here

trace elements including Cr, Cu, and Zn in the Oreste bog (Isla Navarino, Chile) are presented. It is hoped that the data presented here will be helpful for future studies on trace element deposition in southern South America.

2 Material and methods

Detailed description of sample collection and preparation for the geochemical study of Oreste peat is described in Chapter 2. Chromium and Ti in the AIA were analysed using non-destructive and energy-dispersive TITAN analyzer. Similarly, Cu, Zn and Rb and Zr in AIA were measured using EMMA X-Ray Fluorescence (XRF) analyzer. (Analytical procedures presented in Chapter 2)

The calibrated age obtained for the peat macrofossil at 500 cm was ~ 6000 cal yrs BP and the peat accumulation rate was ~ 0.8 mm /yr (Chapter 2).

3 Results and discussions

3.1 Abundance and distribution of Cr, Cu, Zn and Rb

The concentration profiles of Cr, Zn, Cu and Rb along with Ti are shown in Figure 1. Chromium is a trace element and commonly found in heavy minerals such as chromite. The average concentration of Cr in the Oreste bog is $39 \pm 19 \mu\text{g/g}$, which is close to that the Upper Continental Crust (UCC) ($35 \mu\text{g/g}$) (Wedepohl, 1995) and may reflect that the Cr input is effectively controlled by soil derived dust. The similarity between Cr concentration and Ti concentration, assuming Ti as a surrogate of mineral dust (Shotyk et al., 2002), and being effectively constant above ~ 425 cm (Figure 1) suggest that the atmospheric deposition of mineral dust is effectively constant for the past ca. 6000 years. Notably, Cr and Ti show a few other remarkable features such as depletion at ca. 425 cm, 300 cm and 50 cm, indicating changes in mineralogy, as a result of changes in source area or changes in wind strength or both (figure 1). The changes in mineralogy are further supported by the concentration profile of Rb, where it shows relatively depleted concentration at ~ 425 cm but elevated (relatively) concentration at ~ 300

cm and 50 cm. Notably, the concentration of Cr at ~ 300 cm was below the detection limit of XRF ($1 \mu\text{g/g}$). On the other hand, Zn and Cu show relatively constant concentration between ~ 425 cm and 50 cm with values of $139 \pm 72 \mu\text{g/g}$ and $24 \pm 15 \mu\text{g/g}$ respectively. Above 50 cm, both Zn and Cu are elevated by a factor of about 2x. Nonetheless, the relatively constant Ti and Cr, compared to the increased Cu and Zn, suggest different source area or mineral composition than for Ti and Cr.

3.2 Enrichment of elements

The major and trace elements of clay and silt size particles derived from the earth's crust are expected to have the similar composition to the average crustal materials compared to the aerosols composition with anthropogenic input (pollution derived) (Rahn, 1976; Schütz, 1989). Rubidium is a dispersed element with no significant anthropogenic sources and is found in common rock-forming minerals such as K-feldspar and biotite, substituting for K^+ . Similarly, Ti is a conservative element in the weathering environment and is found commonly in accessory minerals such as ilmenite, rutile,

and sphene. Therefore, the ratio of metals (for example, Cr, Zn, and Cu) to Rb or Ti (Figure 2 and 3) in the AIA may indicate either the element derived exclusively from soil dust or from any other sources such as anthropogenic input.

The Cr/Rb ratios are similar to the earth's crust and are relatively constant above 425 cm, except at ca. 300 cm and 50 cm where Cr/Rb is depleted. Similarly, Ti/Rb ratios are also relatively constant except at ca. 300 cm and 50 cm, where Ti/Rb ratio is depleted. Notably, the lower ratio of Ti/Rb at ~ 300 cm and 50 cm (Figure 2) corresponds to the identified volcanic ash and their relatively larger particle sizes (Chapter 2 and 3), which indicates the changes in mineralogy from abundance of heavy minerals towards light mineral phases. The relatively constant ratios of Cr/Rb and Ti/Rb may indicate that the host mineral phases for these elements behave similarly during atmospheric transport and are predominantly from particular area(s). At 300 cm and 50 cm, where abundant volcanic particles are found (Chapter 2 and 3), the heavy minerals containing Ti and Cr are depleted; it is indicated by the lower ratio of Cr/Rb and Ti/Rb (Figure 2).

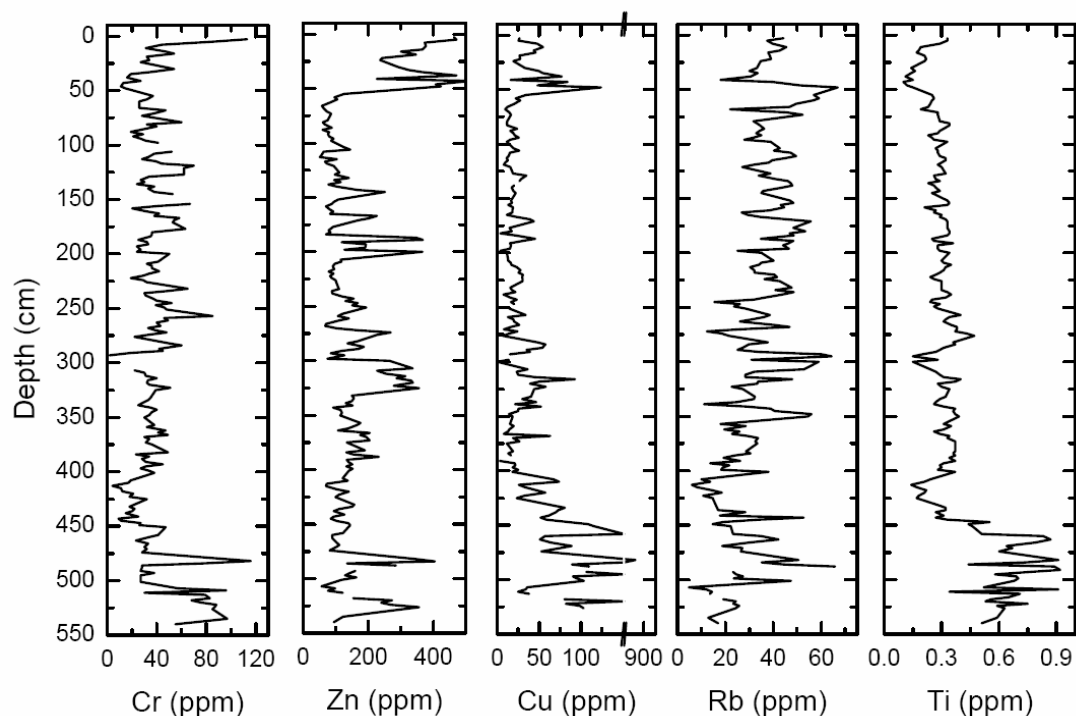


Figure 1: Concentration profile of Cr, Zn, Cu, Rb and Ti in Acid insoluble ash (AIA).

Copper and Zn are also depleted at ca. 300 cm. On the other hand, the ratio of Cr/Ti is relatively constant within the peat profile, whereas Zn/Ti and Cu/Ti are elevated by larger proportion above ~ 50 cm (Figure 3). The concentration and size distribution of mineral particles are a function of grain size fractionation during transport (Schütz, 1989) and are similar to bulk crust in composition in the smaller size fraction ($< 10 \mu\text{m}$), compared to the bigger particle sizes (10 – 60 μm) (Eltayeb et al., 2001; Schütz and Rahn, 1982). Titanium and Rb with no known anthropogenic sources, the elevated ratios of Zn and Cu above 50 cm (Figure 2 and 3) suggest that these two elements are derived from anthropogenic sources. The elevated ratios of Cu and Zn above 50 cm may probably due to the human activities in southern South America after the arrival of Spanish farmers at 17th century and the growing industrial activities (for example, mining, smelting, waste incineration etc.) that extended to southernmost part of Tierra del Fuego (Ushuaia).

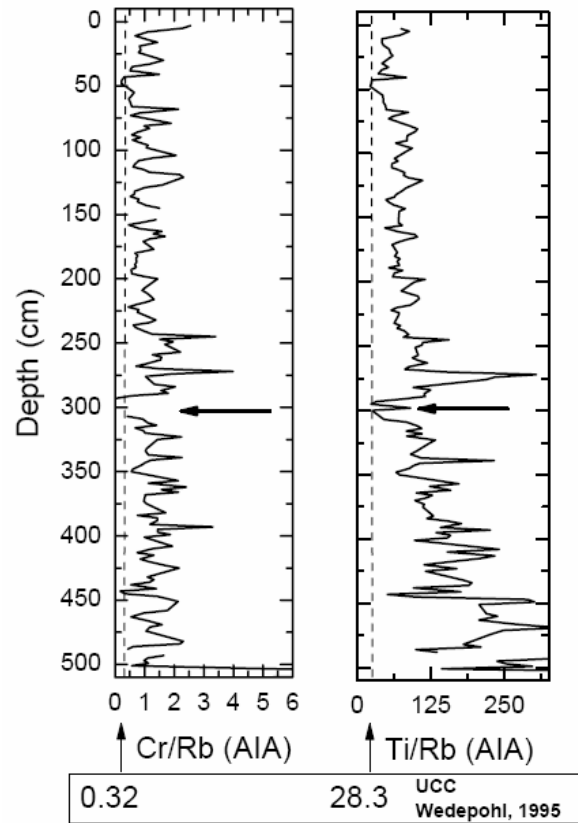


Figure 2: Cr/Rb, Ti/Rb in AIA from Oreste peat profile

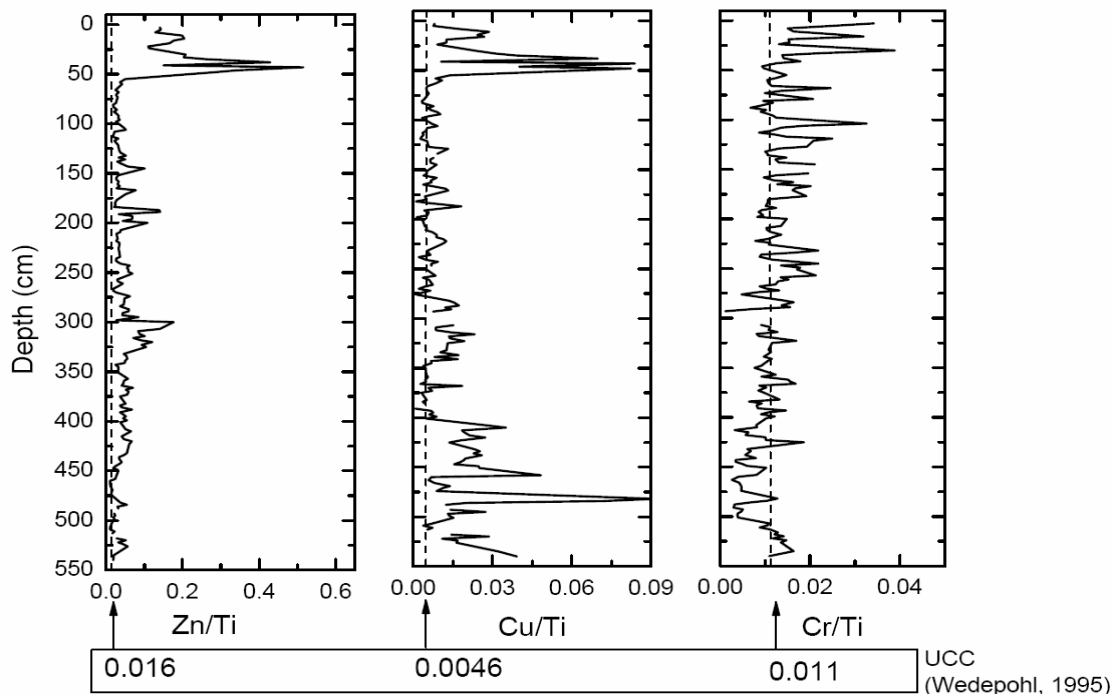


Figure 3: Zn/Ti, Cu/Ti, and Cr/Ti in AIA from the Oreste peat profile

Summary

This study utilized the peat bog as an environmental archive and documented the brief information about the input of trace elements in southernmost South America. It shows that the anthropogenic input of trace elements such as Cu and Zn has been increased possibly at the beginning of 18th century. However, the concentration of Cr shows that not all elements are enriched because of human activities. Nonetheless, further studies with better peat core and age dating are required, mainly for the upper part of the peat, for the detailed reconstruction of changing rates of atmospheric deposition of trace elements and to understand the impact of natural and human activities. The data presented here, though preliminary, may serve as a background for the forthcoming studies.

References

- Amin, O., Ferrer, L. and Marcovecchio, J., 1995. Heavy metal concentrations in littoral sediments from the Beagle Channel, Tierra del Fuego, Argentina. *Environmental Monitoring and Assessment*, 41: 219-231.
- Espi, E., Boutron, C.F., Hong, S., Pourchet, M., Shotyk, W. and Charlet, L., 1997. Changing concentrations of Cu, Zn, Cd, and Pb in a high altitude peat bog from Bolivia, South America, during the past 300 years. *Water Air and Soil Pollution*, 100: 289-296.
- Eltayeb, M.A.H., Injuk, J., W. Maenhaut and Grieken, R.E.V., 2001. Elemental composition of mineral aerosol generated from Sudan Sahara sand. *J. Atmos. Chem.*, 40: 247-273.
- Hong, S., Boutron, C.F., Gabrielli, P., Barbante, C., Ferrari, C.P., Petit, J.R., Lee, K. and Lipenkov, V.Y., 2004. Past natural changes in Cu, Zn and Cd in Vostok Antarctic ice dated back to the penultimate interglacial period. *Geophysical Research Letters*, 31(doi: 10.1029/2004GL021075).
- Hong, S., Boutron, C.F., Ferrari, C.P., Petit, J.R. and Lipenkov, V.Y., 2003. Changes in the natural lead, cadmium, zinc, and copper concentrations in the Vostok Antarctic ice over, the last glacial-interglacial cycles (240,000 years). *Journal de Physique IV*, 107: 629-632.
- Krachler, M., Mohl, C., Emons, H. and Shotyk, W., 2003. Atmospheric deposition of V, Cr, and Ni since the Late Glacial: Effects of climate cycles, human impacts, and comparison with crustal abundances. *Environmental Science and Technology*, 37: 2658-2667.
- Monna, F., Petit, C., Dominik, J.-P., Losno, R., Richard, H., Leveque, J. and Château, C.C., 2004. History and environmental impact of mining activity in Celtic Aeduan Territory recorded in a peat bog. *Environmental Science and Technology*, 38: 665-673.
- Rahn, K.A., 1976. The chemical composition of the atmospheric aerosol (Technical report, Graduate School of Oceanography, University of Rhode Island, Kingston).
- Rausch, N., Nieminen, T., Ukonmannaho, L., LeRoux, G., Krachler, M., Cheburkin, A.K., Bonani, G. and Shotyk, W., 2005. Comparison of atmospheric deposition of copper, nickel cobalt, zinc, and cadmium recorded by Finish peat cores with monitoring data and emission records. *Environmental Science and Technology*, 39: 5989-5998.
- Roos-Barraclough, F., Givelet, N., Cheburkin, A.K., Shotyk, W. and Norton, S.A., 2006. A ten thousand year record of atmospheric mercury accumulation in peat from Caribou Bog, Maine, and its correlation to bromine and selenium. *Environmental Science and Technology*, 40: 3188-3194.
- Schütz, L., 1989. Atmospheric mineral dust-properties and source makers. In: *Paleoclimatology and Paleometeorology: Modern and past patterns of global atmospheric transport*, (ed. M. Leinen and M. Sarnthein), 359-383.
- Schütz, L. and Rahn, K.A., 1982. Trace-element concentrations in erodible

- soils. *Atmos. Environ.*, 16(1): 171-176.
- Shotyk, W., Krachler, M., Martinez-Cortizas, A., Cheburkin, A.K. and Emons, H., 2002. A peat bog record of natural, pre-anthropogenic enrichments of trace elements in atmospheric aerosols since 12 370 ¹⁴C yr BP, and their variation with Holocene climate change. *Earth and Planetary Science Letters*, 6180: 1-17.
- Shotyk, W. et al., 1998. History of atmospheric lead deposition since 12,370 ¹⁴C yr BP from a peat bog, Jura Mountains, Switzerland. *Science*, 281: 1635-1640.
- Wedepohl, K.H., 1995. The composition of the continental crust. *Geochimica et Cosmochimica Acta*, 59(7): 1217-1232.

-Appendix IV- Cleaning of Acid insoluble ash (AIA) for Sr isotope measurements

To separate the silicate and refractory oxide minerals in the peat, about 2 g of peat was ashed at 550°C (overnight), and then leached with 1M HCl. The insoluble ash was separated by filtration (Chapter 2 and 4). Strontium is enriched in carbonates in weathering profiles (Dasch, 1969) and may have a distinct Sr isotopic signature which can eventually affect the Sr isotopic composition of insoluble silicates. Similarly, the presence of biogenically deposited calcium carbonate, which has the same isotopic composition as seawater, in the sediment can mask the ratio in the detrital material (Dasch et al., 1966). However, the HCl leaching procedure already removed about 85 to 99 % Sr in the peat ash. For example, AIA from the depth of 35 cm (B4) contained 136 µg Sr in 2.7 g dry peat (51 µg/g) and on leaching with HCl, 115 µg Sr was removed in acid soluble ash (ASA) and only 21 µg Sr was left in 31.5 mg AIA, i.e. ~ 85 % removal. Similarly, AIA from depth of 213 cm (I5) contained only 2 µg Sr (AIA weight: 4 mg; 510 µg/g), whereas in dry peat the amount of Sr was 70 µg (dry weight: 2 g; 34 µg/g), i.e. 97 % removal. To confirm that the separated AIA contained no labile Sr fraction, two AIA samples (B4 and I5) were used to optimize the rinsing steps. Both samples were rinsed four times in 5ml ultrapure 1M HCl (Merck, Darmstadt), and finally in MilliQ water (18 MΩ). Then Sr in all solutions was measured by using ICP-OES (operational parameters in Appendix II). The concentration of Sr in the AIA already decreased by ~ 95% during the first rinse and remained constant afterwards (< 1%) (Figure 1). Therefore, it was decided that rinsing AIA four times for Sr isotopes measurement (Chapter 5) were sufficient: three times in HCl and final cleaning in MilliQ water.

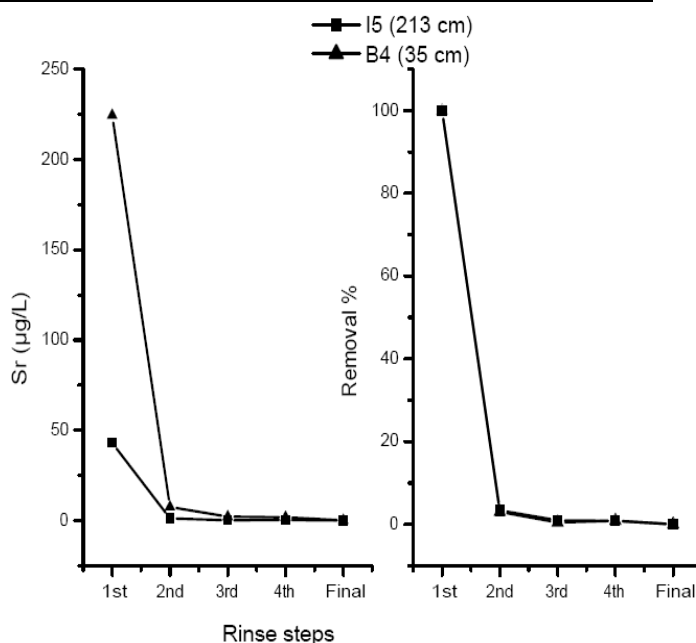


Figure 1: Sr concentration in the AIA from the depth of 35 cm (B4) and 213 cm (I5) (Left). Removal percentage of Sr calculated by using 1st rinse as a reference point (right). (Steps 1-4th: 1M HCl (5 ml); Final (5th): MilliQ water)

References

- Dasch, E.J., Strontium isotopes in weathering profiles, deep-sea sediments, and sedimentary rocks, *Geochim. Cosmochim. Acta* 33 (1969) 1521-1552
- Dasch, E.J., Hills, F.A., Turekian, K.K., Strontium isotopes in deep-sea sediment, *Science* 153 (1966) 295-297

-Appendix V-
**Titanium in an ombrotrophic peat
 profile from Valle de Andorra
 (Ushuaia, Tierra del Fuego) as
 indicator of atmospheric deposition
 of mineral dust for the last ca. 1300
 years**

Abstract

Titanium concentration in the ombrotrophic peat monolith of 1 m long collected from valle de Andorra (Ushuaia, Tierra del Fuego) was used as a proxy of atmospheric mineral dust. The average calculated mineral dust deposition rate was $1.2 \pm 0.5 \text{ g / m}^2 \text{ / yr}$. The ash content and the Ti concentration suggested periods of elevated mineral input for the last ca. 1300 yrs. The morphology of the identified mineral grains (quartz, feldspar, pyroxene, sphene, etc.) and their particle dimensions ($> 20 \times 20 \mu\text{m}$) in the acid insoluble ash (AIA) from selected samples suggested that mineral dusts were transported by frequent wind storms and possibly also from nearby sources (short distance).

1 Introduction

The dominant sources of Ti in the earth's crust are rutile (TiO_2), ilmenite (FeTiO_3) and titanite (CaTiSiO_5) and are found in similar abundance in rocks and soils (Goldschmidt, 1954; Rahn, 1976). Additionally, Ti in the atmospheric mineral dust is dominantly crustal derived with no known anthropogenic sources. Therefore, the changes in its concentration can be affected by the changes in amount of mineral deposition, composition of minerals and particle sizes, changes in source area and / or combined effect of all of them.

Ombrotrophic peat bogs receive mineral matter only from the atmosphere. Because of the conservative behavior of Ti (resistant to chemical weathering) and its immobility in the peat profile, the concentrations of Ti in bulk peat are sensitive indicators of the changing rates of soil dust

deposition. Apart from this, Ti is generally abundant in the peat, therefore making the measurement of its concentration much easier with a little sample preparation. Titanium in the peat has already been successfully used as an indicator of human impact on soil erosion (Hölzer and Hölzer, 1998) and a surrogate of the past atmospheric dust deposition (Shotyk et al., 2002). Use of Ti as a proxy of atmospheric dust is shown in the recent Antarctic ice core study, where the Ti concentrations in the insoluble mineral particles show close correlation with the observed mineral dust (Marino et al., 2004).

Here, Ti concentration in the peat profile from southern South America is being used as a surrogate of atmospheric dust.

2 Materials and methods

The Valle de Andorra (Andorra valley) is located ca. 10 km to the northeast of Ushuaia, Tierra del Fuego, Argentina ($54^\circ 45' \text{ S}$, $68^\circ 18' \text{ W}$, ca. 180 m asl) (Figure 1). The vegetation was predominantly composed of *Sphagnum magellanicum*, which grows on the highest hummock microforms of $> 60 \text{ cm}$ to the local water tables, *Marsippospermum grandiflorum*, and *Carex curta*. Other species such as *Sphagnum sect.*, *Cuspidata* and *Tetroncium magellanicum* are present at the pool margins of the hummock, although pool microforms are not common (Mauquoy et al., 2004). *Empetrum rubrum* and *Nothofagus antarctica* are also present at the microforms with lower local water tables. The average precipitation in this area is 450 – 600 mm / yr (Mauquoy et al., 2004).

The Andorra valley is surrounded by mountains higher than 500 m (mostly about 1000 m) from north-northwest (Monte Cortes and Cerro Vinciguerra), west (Sierra Valdivieso and Monte Tonelli) and southwest (Montes Marcial). On the channel of south-southeast lies the city of Ushuaia. The Andorra valley bog is surrounded by *Nothofagus* forest and is restricted to the mid-way of the mountains. The Ushuaia including the Andorra valley lies in the Central Cordillera which is a part of the Patagonian Andes orocline. The Central Cordillera is roughly parallel to the Beagle channel and is mountainous with the highest mountain peaks

(between ca. 1500 and 2400 m), mainly in Cordillera Darwin, Sierra de Sorondo and Sierra de Alvear, including Isla Navarino, eastern Hoste, and adjacent islands (Olivero and Martinioni, 2001). Ushuaia lies on the northern side of the Isla Navarino and is separated by the Beagle channel. The Central Cordillera is a part of a Late Jurassic-Early Cretaceous marginal basin (the Rocas Verdes Marginal Basin) and consists of highly deformed Paleozoic-Jurassic schists and granitic rocks, Upper Jurassic silicic volcanic rocks, Lower Cretaceous deep-marine volcanoclastic turbidites and slope mudstones, and Upper Cretaceous plutonic rocks (Olivero and Martinioni, 2001). The geology of Ushuaia consists of Lower Cretaceous marine sedimentary rocks (Kraemer 2003). The basement rocks along the southwestern part of Isla Grande de Tierra del Fuego and along the coast of the Beagle Channel (west of Ushuaia) are commonly exposed and contain highly deformed chlorite-sericite and biotite-garnet schists, greenstones, and amphibolites (Olivero and Martinioni, 2001).

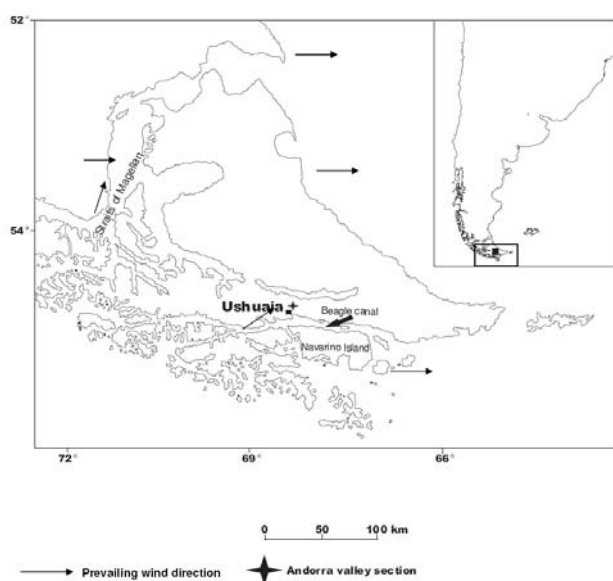


Figure 1: (A) Map of South America with a box index indicating the sampling site. (B) Map of southern South America (Tierra del Fuego) and the Andorra valley bog at Ushuaia (Mauquoy et al., 2004). Also shown on the map is the prevailing wind direction (Tuhkanen, 1992).

In 2001, a peat monolith of 1m depth was collected from the hummock using a

metal box (50 x 15 x 10 cm). The monolith was sliced into 1cm sections and macrofossil samples were collected from every 1 cm intervals for pollen analysis. Similarly, *Sphagnum* leaves and/or stems were collected from 13 samples for ^{14}C AMS age dating. Detailed description of pollen study, age dating and calibration is provided elsewhere (Mauquoy et al., 2004). The calibrated age obtained from the base of the monolith (99.5 cm) is AD 660, representing ca. 1300 yr record of peat accumulation (~ 0.7 m / yr) (Mauquoy et al., 2004). Similarly, the colorimetric measurement of an alkali extracts as a proxy of peat humification (Caseldine et al., 2000) has shown that the degree of humification is relatively stable (Mauquoy et al., 2004).

Peat sub-samples were dried overnight at 105 °C in a clean polyethylene vessels and milled to a fine powder using a Titanium centrifugal mill (ZM 1-T, F. K. Retsch GmbH and Co., Hann, Germany). Major and trace elements in the homogenized peat powder were analyzed using a non-destructive, energy-dispersive TITAN XRF and miniprobe multielement analyzer (EMMA XRF). The detailed description about the in-house design of TITAN and EMMA XRF analyzer and their application is described elsewhere (Cheburkin and Shotykh, 1996; Cheburkin and Shotykh, 2005). Standard reference materials such as NIST (1515, 1547, 1575, 1635 and 1632b) and BCR-60 were used to calibrate the instrument. The detection limits for selected elements are 1.5 $\mu\text{g/g}$ for Ti, 1 $\mu\text{g/g}$ for Cr, 0.9 $\mu\text{g/g}$ for Mn, 0.6 $\mu\text{g/g}$ for Br, 0.7 $\mu\text{g/g}$ for Rb, 1 $\mu\text{g/g}$ for Sr, 10 $\mu\text{g/g}$ for Ca and 2 $\mu\text{g/g}$ for Zr.

Dried and milled peat samples ($\sim 1 - 2$ g) were combusted at 550 °C, overnight and the ash content were measured. For mineralogical study of selective samples, the peat ash was leached in 1M HCl for 15 minutes in order to dissolve soluble fraction of carbonates, oxides/hydroxides, and phosphates, much of which may have been formed during combustion from the biological fraction. Afterwards, the acid insoluble ash (AIA) was collected on polycarbonate membrane filter of 0.2 μm pore size by using a Milipore vacuum filtration kit.

The AIA samples were then coated with graphite and high resolution Scanning Electron Microscope (SEM) LEO-440, equipped with OXFORD Energy-Dispersive X-ray Spectrometer (EDS) was used to study the morphology, size and chemical composition of AIA. The acceleration voltage was 20 kV, beam current 0.8 to 2 nA.

3 Results

3.1 Ash content and concentration of major and trace elements

The average ash content of the peat monolith is 2.15 ± 0.90 % and shows many elevated peaks (Figure 2). Notably, the ash contents have virtually no peak at the depths of 75 – 70 cm (I), 30 – 20 cm (II), and 7 – 0 cm (III).

The concentrations of major elements such as Ti, Ca, and Sr are shown in the Figure 2. Notably, Ti concentration profile corresponds with the ash content, including the peaks (Figure 2). The concentration of Ca and Sr are relatively constant (Figure 2).

Other lithogenic trace elements such as Cr, Rb, and Zr are also measured in the peat samples, but are generally below the detection limit. They are shown here for their few notable characters because they share few peaks similar with the ash content and Ti concentrations (Figure 2, 3, and 4).

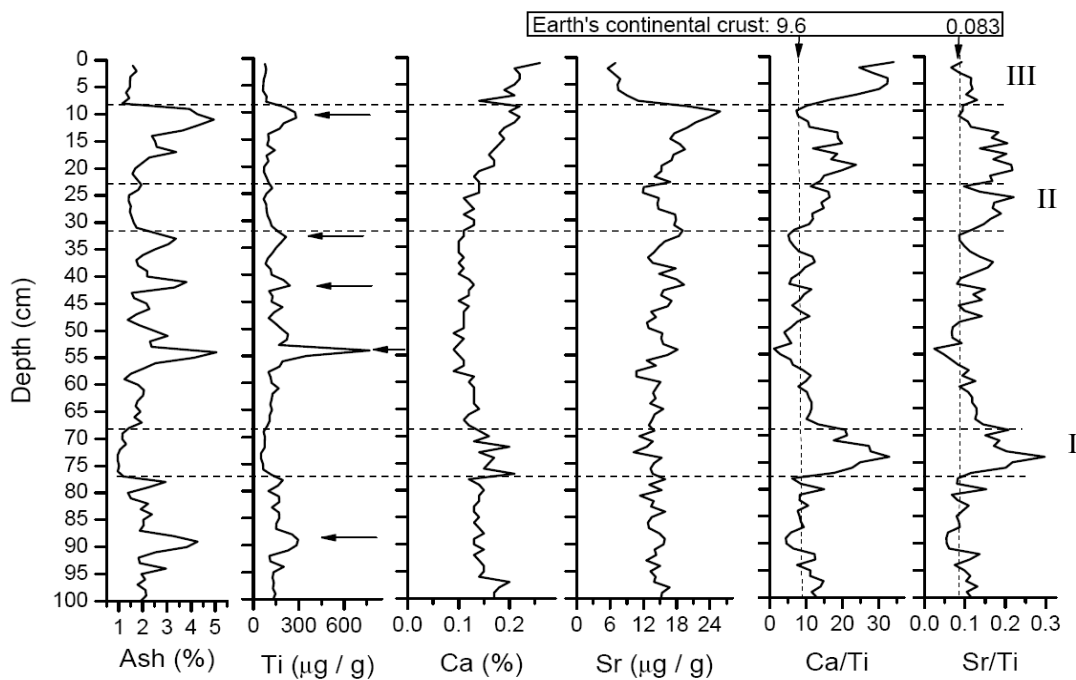


Figure 2: Distribution of ash content; concentration profiles of Ti, Ca and Sr; ratio of Ca/Ti and Sr/Ti in the bulk peat from Andorra valley.

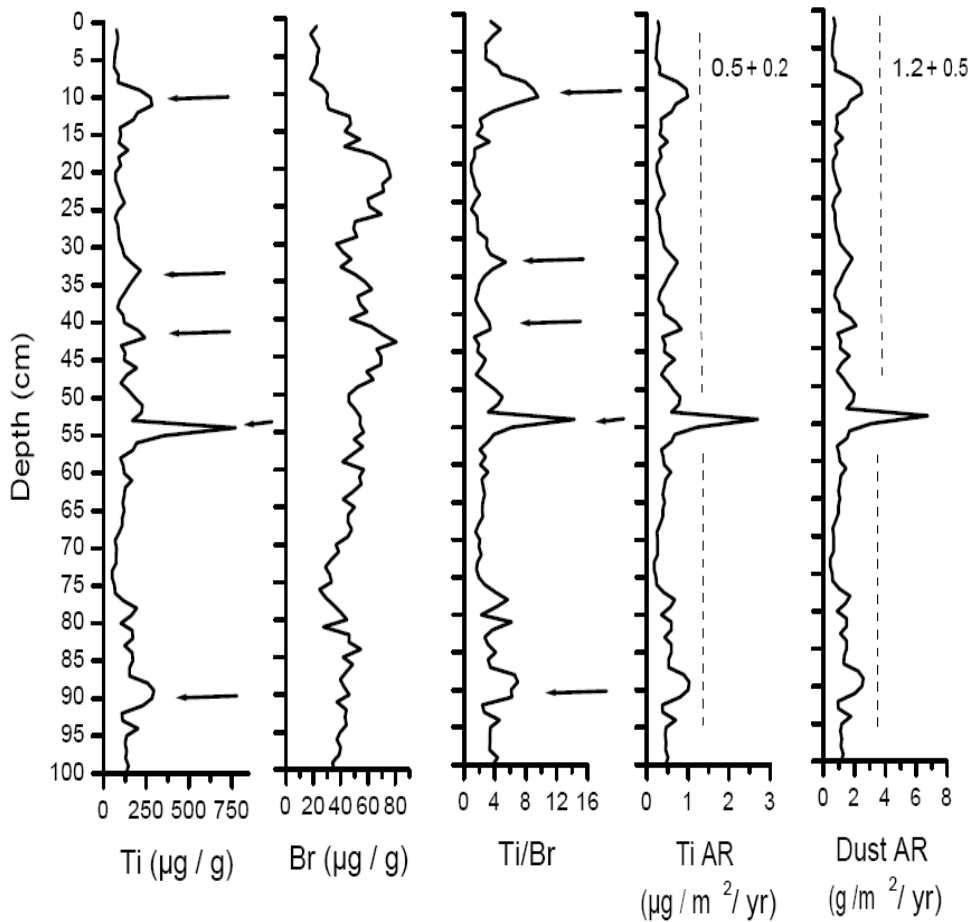


Figure 3: Concentration of Ti ($\mu\text{g/g}$), Br ($\mu\text{g/g}$), and ratio of Ti/Br in the bulk peat; Also shown is the calculated Ti AR ($\mu\text{g}/\text{cm}^2/\text{yr}$) and dust AR ($\text{g}/\text{m}^2/\text{yr}$)

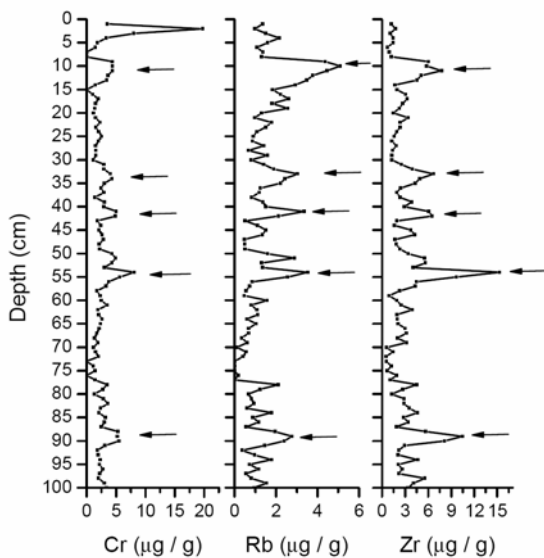


Figure 4: Concentration profiles of Cr, Rb, and Zr in Andorra Valley bulk peat. Horizontal arrows indicate peaks corresponding to ash content and Ti concentrations.

3.2 Mineralogy of inorganic fraction

Motivated by the observed peak in the ash content and Ti concentrations (Figure 2), selected samples (from depth of 11, 55 and 89 cm) were used for mineralogical study. The mineralogical composition is predominantly composed of quartz and feldspar with particle dimensions greater than $20 \times 20 \mu\text{m}$ (Figure 5 A and B). Other identified minerals are pyroxene (Figure 5 C and D) and Ti-bearing minerals such as sphene (Figure 5 E), ilmenite (Figure 5 F) and rutile (Figure 5 G and H). The Ti-bearing minerals are found either predominantly associated with quartz (Figure 5 G and H) or as a single grain with particle dimensions larger than $20 \times 20 \mu\text{m}$ (Figure 5 E and F). The particle size of pyroxene ranges from $60 \times 15 \mu\text{m}$ to $80 \times 10 \mu\text{m}$ (Figure 5 C and D).

4 Discussions

4.1 Ombrotrophic character of peat

The average ash content (2.15 ± 0.90 %) of the peat is well within the range of characteristic nature of ombrotrophic peat bog (Figure 2). Additionally, the concentration of Ca and Sr are useful indicator to access the input of elements in the peat bog because the concentration of these elements can be affected by biological intake, mineral dissolution in the underlying peat, and input of surface waters. The stable concentration profile of Sr (14 ± 3 $\mu\text{g} / \text{g}$) and Ca (0.14 ± 0.04 %), and their Ti normalized profile (Ca/Ti and Sr/Ti) reflect that the Sr and Ca are supplied only by atmospheric deposition of mineral matter (Figure 2).

4.2 Input of Ti and atmospheric mineral dust

The concentrations of Ti and ash contents show remarkably similar profiles with at least four clear peaks (Figure 2). These peaks can be the result of higher inputs of mineral matter, slower rate of peat accumulation and/or increase in peat humification (loss of organic fraction). However, the accumulation of peat (0.7 mm / yr) and the degree of peat humification observed for the peat monolith (100 cm) from Andorra valley are generally constant (Mauquoy et al., 2004). Therefore, they may not be responsible for the observed peak for ash contents and Ti concentrations. Another approach to correct the effect of peat humification in elemental peak is to normalize the elemental concentration by Br as Br tends to increase with increasing humification (Steinmann and Shoty, 1997), as a result of fixation of Br in organic matter. The Ti/Br profile shows that nearly all of the samples containing peaks in Ti and ash concentrations have peaks in Ti/Br (Figure 3). This is evidence that the increase in Ti and ash content is caused by the elevated atmospheric input of mineral matter and not by peat decomposition.

Additionally, the peaks of Ti and ash content correspond with the peaks of Cr, Rb and Zr (Figure 2 and 4). Chromium is commonly associated with an accessory minerals of spinel group of minerals (for

example, chromite). Rubidium is a dispersed element controlled by substitution with K^+ (1.33 Å) (potassium) and is found commonly in K-bearing minerals such as micas, K-feldspar and certain clay minerals (e.g. kaolinite) (Faure, 1986). Similarly, if Ti and Zr are enriched, it is possibly contributed by two types of mineral: a Ti-Fe containing mineral (e.g. ilmenite where Zr often found enriched) and Ti-Zr containing mineral (for example, Zirconite) (Eltayeb et al., 2001). Therefore, the abundance of feldspar, quartz, pyroxene, and Ti-bearing minerals either as a single grain or associated with rock-forming minerals (Figure 5) may indicate that either these elements share a common mineral host or that they behave similarly during the formation, atmospheric transport and deposition.

4.2.1 Accumulation rates of atmospheric mineral dust

Titanium concentration combined with peat accumulation rate (I) and dry bulk density (ρ) allow the calculation of atmospheric dust accumulation rate (AR) (Shoty et al., 2002) (equation 1)

$$\text{Dust AR } (\mu\text{g}/\text{cm}^2/\text{yr}) = 250 \times \text{Ti } (\mu\text{g}/\text{g}) \times \rho \text{ (g}/\text{cm}^3) \times \text{I (cm}/\text{yr}) \quad (1)$$

where 250 is the concentration factor use to convert the Ti concentration to an equivalent mineral dust concentration, assuming an average Ti crustal abundance of 0.40 % (4010 $\mu\text{g}/\text{g}$) (Wedepohl, 1995).

The average dust AR is on the order of 1.2 ± 0.5 $\text{g}/\text{m}^2/\text{yr}$ for the past ca. 1300 yrs, calculated by using the average peat accumulation rate (0.7 mm / yr), typical ombrotrophic peat density (0.05 g cm^{-3}), and the Ti concentration in the peat profile. Considering the stable climatic conditions of southern South America for the last ca. 6000 yrs (Heusser, 1998; Markgraf et al., 1992), peaks observed in the ash content and Ti may reflect the abrupt change in local wind strength, source area or both.

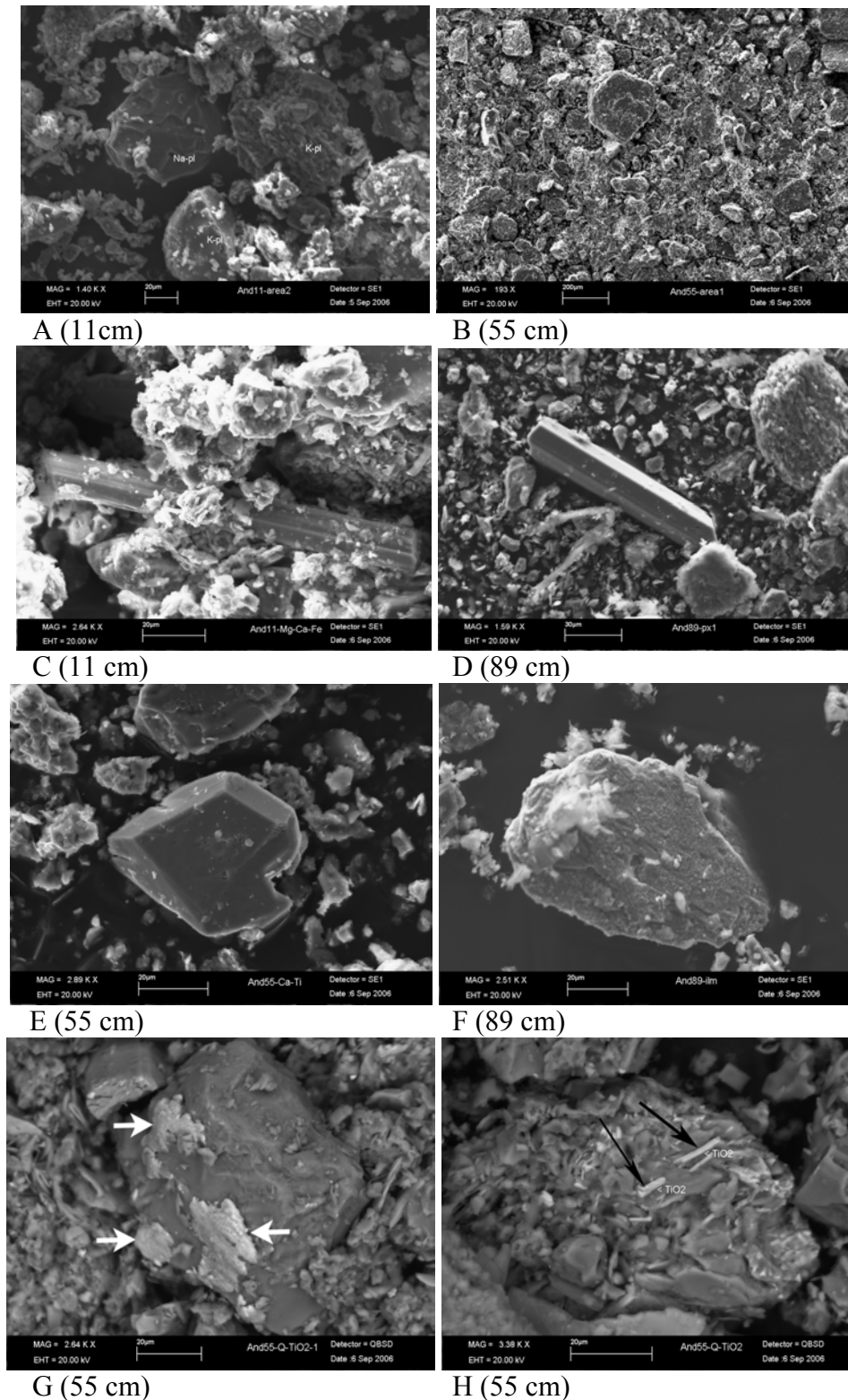


Figure 5: Morphology of AIA components from selective depths: A (11cm) and B (55 cm) - silicate minerals (quartz, feldspar, etc., > 10-20 µm); C (11 cm) and D (89 cm) - pyroxene (from 60 × 15 µm to 80 × 10 µm); E (55 cm) – sphene (> 20 × 20 µm); F (89 cm) – ilmenite (> 20 × 20 µm); G (55 cm) and H (55 cm) – (indicated by arrows) rutile associated with quartz (quartz > 20 × 20 µm). The scales for the SEM micrographs are 20 µm for A, C, E, F, G, and H. For B and D, the scales are 200 µm and 30 µm respectively.

Generally, clay and fine-grained silt with diameters less than 10 – 20 μm are able to remain suspended long enough and travel long distances while particles larger than $> 10 - 20 \mu\text{m}$ (coarse-grained silt and fine-grained sand) are transported in short term suspension (Herrmann et al., 1999; Schütz, 1989). The physical fractionation then influences the chemical fractionation of many elements. As in the case of Ti, its concentration is enriched in the 10 – 20 μm fractions compared to the clay size particles ($< 5 \mu\text{m}$). Notably, the predominant particle sizes of the inorganic fraction of selected samples (depth of 11, 55 and 89 cm) are larger than $20 \times 20 \mu\text{m}$ (Figure 5). Additionally, considering the occurrence of Ti-bearing minerals in crystal form and inclusion in larger grains of quartz and feldspars as an indicator of minerals derived from relatively unweathered source and unaltered during transportation, they may suggest nearby source area (short distance). Therefore, this may reflect the strong wind and bringing both coarse-grained local mineral matter and fine-grained long distant dust to the bog.

For comparison with the calculated dust AR values for Andorra valley, very few reliable data are available for southern South America. While few modeling studies have shown that the deposition rate is about $0.5 \text{ g} / \text{m}^2 / \text{yr}$ (Ginoux et al., 2001; Mahowald et al., 2006), some other study has shown that the deposition rate is $1-10 \text{ g} / \text{m}^2 / \text{yr}$ (Tegen and Fung, 1994) for the southern South America. Notably, the calculated average dust AR is higher by a factor of about two than in the Oreste bog which is situated further south ($55^\circ 13' 13'' \text{ S}$ and $67^\circ 37' 28'' \text{ W}$ 35m) ($0.43 \pm 0.12 \text{ g} / \text{m}^2 / \text{yr}$) calculated over the past 6000 yrs (A. Sapkota, Chapter 2). The difference in calculated dust AR rates might also be affected by the predominant influence of westerlies, which extends between 40° and 56° S , and the cyclonic circumpolar vortex centered on Antarctica (Thompson and Solomon, 2002). Additionally, the local topography may also cause distortion on the wind direction as in the case of Ushuaia (Andorra valley), where southwest is the prevailing wind direction (Tuhkanen, 1992).

In the mountainous channels such as Beagle Channel, local influence may modify the general wind direction, therefore resulting in turbulent local wind of hurricane, the williwaw, and blow downs from the mountains and the main land (Tuhkanen, 1992). While the larger mineral grains (for example, $> 75 \mu\text{m}$) can also be transported in suspension long distances during major dust outbreaks, this is uncommon (Betzer et al., 1988). On the other hand, the ash contents and Ti concentrations have shown many peaks (Figure 2), which may suggest frequent wind storms, except at zones I, II and III (Figure 2). Cooler and/or wetter conditions have been suggested for the zone III (ca. AD 1030 – 1100) and zone II (ca. AD 1800 – 1930) (Mauquoy et al., 2004). While the Andorra valley is surrounded by a chain of mountains from north-northwest to the southwest and the regional vegetation cover already at maximum at southern South America (Markgraf et al. 1992), the dust deposition at zone- I and II suggest the long range transport. For the rest of the periods, some of which are suggested to be warm and/or drier (Mauquoy et al., 2004), wind erosion of the local relief probably by seasonal changes in storm tracks can be more responsible for the elevated deposition of mineral than by the long-range transport of larger mineral grains. Alternatively, niveo-eolian transport, which is attributed to cold dry, snowy conditions and a high frequency of strong wind (Bjorck and Clemenson, 2004; Fisher and Loope, 2005), may also be responsible for the larger particle sizes.

5 Conclusions

The ash content and Ti concentration in the bulk peat from ombrotrophic peat from Andorra valley have revealed information about the frequent changes in atmospheric input of mineral dust for the last ca. 1300 yrs. The inorganic fraction (AIA) taken from the elevated ash contents and Ti concentrations were composed of relatively larger particles. Therefore, the sources of these minerals can be the nearby soil and/or rock debris that are subjected to erosion by frequent windstorms. This implies that although the climatic condition for the past ca. 6000 years were

relatively stable in southern South America, the dust deposition in the atmosphere varied significantly in space and time depending on the local or regional wind strength and the distance from source.

Acknowledgements

Financial support was provided by the Deutsche Forschungsgemeinschaft (DFG, SH 89/2-1 and SH 89/2-2). We thank Dr. Dmitri Mauquoy for generously providing us the peat core.

References:

- Björck S., and Clemmensen L. B. (2004) Aeolian sediment in raised bog deposits, Halland, SW Sweden: a new proxy record of Holocene winter storminess variation in southern Scandinavia? *Holocene* **14**, 677-688.
- Caseldine C. J., Baker A., Charman D. J., and Hendon D. (2000) A comparative study of optical properties of NaOH peat extracts: implications for humification studies, *Holocene* **10**, 649-658.
- Chadwick O. A., Derry L. A., Vitousek P. M., Huebert B. J., and Hedin L. O. (1999) Changing sources of nutrients during four million years of ecosystem development. *Nature* **397**, 491-497.
- Cheburkin A. and Shotyk W. (1996) An Energy-dispersive Miniprobe Multielement Analyzer (EMMA) for direct analysis of Pb and other trace elements in peats. *Fres. J. Anal. Chem.* **354**, 688-691.
- Cheburkin A. K. and Shotyk W. (2005) Energy-dispersive XRF spectrometer for Ti determination (TITAN). *X-Ray spectrometry* **34**, 69-72.
- Eltayeb M. A. H., Injuk J., W. Maenhaut, and Grieken R. E. V. (2001) Elemental composition of mineral aerosol generated from Sudan Sahara sand. *J. Atmos. Chem.* **40**, 247-273.
- Faure G. (1986) *Principles of Isotope Geology*. John Wiley and Sons.
- Fisher T. G. and Loope W. L. (2005) Aeolian sand preserved in Silver Lake: a new signal of Holocene high stands of Lake Michigan. *Holocene* **15**, 1072-1078.
- Ginoux P., Chin M., Tegen I., Prospero J. M., Holben B., Dubovik O., and Lin S.-J. (2001) Sources and distributions of dust aerosols simulated with the GOCART model. *J. Geophys. Res.* **106**(D17), 20,255-20,273.
- Goldschmidt V. M. (1954) Geochemistry. In *The International Series of Monographs on Physics* (ed. A. Muir), pp. 730. Clarendon Press, Oxford.
- Herrmann L., Stahr K., and Jahn R. (1999) The importance of source region identification and their properties for soil-derived dust: the case of Harmattan dust sources for eastern West Africa. *Contrib. Atmos. Phy.* **72**, 141-150.
- Heusser C. J. (1998) Deglacial paleoclimate of the American sector of the Southern Ocean: Late Glacial-Holocene records from the latitude of Canal Beagle (55°S), Argentine Tierra del Fuego. *Palaeoeco., Palaeoclim., Palaeoeco.* **141**, 277-301.
- Hölzer A. and Hölzer A. (1998) Silicon and titanium in peat profiles as indicators of human impact. *Holocene* **8**, 685-696.
- Kraemer P. E. (2003) Orogenic shortening and the origin of the Patagonian orocline (56 °S Lat.). *J. South Am. Earth Sci.* **15**, 731-748.
- Mahowald N. M., Muhs D. R., Levis S., Rasch P. J., Yoshioka M., Zender C. S., and Luo C. (2006) Change in atmospheric mineral aerosols in response to climate: Last glacial period, preindustrial, modern, and doubled carbon dioxide climates. *J. Geophys. Res.* **111**(D10202, doi:10.1029/2005JD006653).
- Marino F., Maggi V., Delmonte B., Ghermandi G., and Petit J. R. (2004) Elemental composition (Si, Fe, Ti) of atmospheric dust over the last 220 kyr from the EPICA ice core (Dome C, Antarctica). *Ann. Glaciol.* **39**, 110-118.
- Markgraf V., Dodson J. R., Kershaw A. P., McGlone M. S., and Nicholls N. (1992) Evolution of late Pleistocene

- and Holocene climates in the circum-South Pacific land areas. *Clim. Dyn.* **6**, 193-211.
- Mauquoy D., Blaauw M., Geel B. v., Borrromei A., Quattrocchio M., Chambers F. M., and Possnert G. (2004) Late Holocene climatic changes in Tierra del Fuego based on multiproxy analysis of peat deposits. *Quat.Res.* **61**, 148-158.
- Olivero E. B. and Martinioni D. R. (2001) A review of the geology of Argentinean Fuegian Andes. *J. South Am. Earth Sci.* **14**, 175-188.
- Rahn K. A. (1976) The chemical composition of the atmospheric aerosol, pp. 1-253. Graduate School of Oceanography, University of Rhode Island.
- Schütz L. (1989) Atmospheric mineral dust-properties and source makers. In *Paleoclimatology and Paleometeorology: Modern and past patterns of global atmospheric transport* (ed. M. Leinen and M. Sarnthein), pp. 359-383, Kluwer Academic Publisher.
- Shotyk W., Krachler M., Martinez-Cortizas A., Cheburkin A. K., and Emons H. (2002) A peat bog record of natural, pre-anthropogenic enrichments of trace elements in atmospheric aerosols since 12370 ¹⁴C yr BP, and their variation with Holocene climate change. *Earth Planet. Sci. Lett.* **6180**, 1-17.
- Steinmann P. and Shotyk W. (1997) Geochemistry, mineralogy, and geochemical mass balance on major elements on two peat bog profiles (Jura Mountains, Switzerland). *Chem. Geol.* **138**, 25-53.
- Tegen I. and Fung I. (1994) Modelling of mineral dust in the atmosphere: Sources, transport, and optical thickness. *J. Geophys. Res.* **99**, 22897-22914.
- Thompson D. W. J. and Solomon S. (2002) Interpretation of recent southern Hemisphere climate change. *Science* **296**, 895-899.
- Tuhkanen S. (1992) The climate of Tierra del Fuego from a vegetation geographica point of view and its ecoclimatic counterparts elsewhere. *Acta Bot. Fennica* **145**, 1-64.
- Wedepohl K. H. (1995) The composition of the continental crust. *Geochim. Cosmochim. Acta* **59**(7), 1217-1232.

Hiermit erkläre ich, Atindra Sapkota, geb. 02.12.1977 in Kathmandu, Nepal, an Eides statt, das ich die vorgelegte Dissertation selbst verfasst und mich dabei keiner anderen als der von mir ausdrücklich bezeichneten Quellen und Hilfen bedient habe.

Ich, Atindra Sapkota, geb. 02.12.1977 in Kathmandu, Nepal, erkläre zudem an Eides statt, dass ich an keiner anderen Stelle ein Prüfungsverfahren beantragt habe, dass ich die Dissertation nicht in dieser oder anderer Form bereits anderweitig als Prüfungsarbeit verwender habe und dass ich sie an keiner anderen Fkultät als Dissertation vorgelegt habe.

Heidelberg, 31st October 2006

-Curriculum Vitae-

Personal details:

First name: Atindra
Surname: Sapkota
Place of Birth: Nepal
Date of Birth: 1977.12.02
Marital Status: Single

Education

- 2003 – 2006 PhD
Institute of Environmental Geochemistry, University of Heidelberg
Germany
- 2001 – 2003 Master of Science
Applied Environmental Measurement Techniques, AEMT
Chalmers University of Technology
Göteborg, Sweden
- 1997 – 2000 Bachelor of Science
Environmental Science
Kathmandu University (affiliated institution: St. Xavier's College)
Kathmandu, Nepal
- 1995 – 1996 Proficiency Certificate in Science
(Major subjects: Biological group)
Tribhuvan University (affiliated institution: Nepal Science Campus)
Kathmandu, Nepal.
- 1982 – 1993 Primary and Secondary School
Bhrikuti Secondary School
Kathmandu, Nepal

List of publications and the author's contribution

This thesis is based on the following articles, which are included in the text as separate chapters (2, 3, 4 and 5) and appendixes (I and II).

Chapter 2

Atindra Sapkota, Andriy K. Cheburkin, Georges Bonani and William Shotyk. Six millennia of atmospheric dust deposition in southern South America (Isla Navarino, Chile). The Holocene. Manuscript submitted (2006)

This paper was initiated and planned jointly by A. Sapkota, A. Cheburkin and W. Shotyk. A. Sapkota was responsible for the preparation of bulk peat sample as well as extraction and isolation of acid insoluble mineral materials (AIA) from the bulk peat. A. Cheburkin with the help of O. Kurzel performed XRF analysis of bulk peat and AIA. G. Bonani provided the radiocarbon age datings. A. Sapkota prepared the manuscript and W. Shotyk did revision and helped for further improvement of the manuscript.

Chapter 3

Olena Kurzel, Atindra Sapkota, William Shotyk. Characterization of atmospheric mineral dusts preserved in an ombrotrophic peat bog from southernmost Southern Hemisphere, Oreste Bog, Tierra del Fuego, Chile. Quaternary Research. Manuscript submitted (2006)

This paper was initiated and planned jointly by O. Kurzel, A. Sapkota and W. Shotyk. O. Kurzel was responsible for the preparation of the article and co-authors assisted her. A. Sapkota extracted mineral materials from peat and O. Kurzel identified minerals by employing SEM. W. Shotyk did the revision and helped for improvement of the manuscript.

Chapter 4

Bernd Kober, Atindra Sapkota, Andriy K. Cheburkin and William Shotyk. Holocene record of $^{87}\text{Sr}/^{86}\text{Sr}$ ratios in dust components of an ombrotrophic bog at the southernmost edge of South America: volcanic inputs, atmospheric soil dust, and comparison with ice core dust of the Eastern Antarctic Plateau. Earth and Planetary Science Letters. Manuscript submitted (2006)

This paper was initiated and planned jointly by B. Kober, A. Sapkota and W. Shotyk. Data interpretation was performed by B. Kober with the assistance of A. Sapkota. The article was prepared by B. Kober and revised by W. Shotyk. A. Cheburkin provided XRF data and assisted in the interpretation of data. Extraction and isolation of AIA were done by A. Sapkota. Sample digestions and TIMS analyses were done by B. Kober and D. Pingel.

Chapter 5

William Shotyk, Atindra Sapkota, Andriy K. Cheburkin, and Bernd Kober. The paradigm of natural Pb in the atmosphere: 6000 years of soil dust deposition recorded by the Oreste peat bog, southern Patagonia. *Global Biogeochemical Cycles*. Manuscript submitted (2006)

The preparation of the manuscript was done by W. Shotyk. Co-authors assisted in the preparation of manuscript and interpretation of data. Extraction and isolation of mineral dusts from peat were performed by A. Sapkota. B. Kober provided Pb isotope data. A Cheburkin provided XRF data.

Appendix I

Nicolas Givelet, Gaël Le Roux, Andriy Cheburkin, Bin Chen, Jutta Frank, Michael E. Goodsite, Heike Kempter, Michael Krachler, Tommy Noernberg, Nicole Rausch, Stefan Rheinberger, Fiona Roos-Barraclough, Atindra Sapkota, Christian Scholz, and William Shotyk. Suggested protocol for collecting, handling and preparing peat cores and peat samples for physical, chemical, mineralogical and isotopic analyses. *Journal of Environmental Monitoring* 6 (2004): 481-482.

This paper was prepared jointly by N. Givelet, G. Le Roux and W. Shotyk. Co-authors assisted in the development and improvement of the manuscript. A. Sapkota contributed to the parts “Acid digestion procedures” and “Quantification of trace elements”.

Appendix II

Atindra Sapkota, Michael Krachler, Christian Scholz, Andriy K. Cheburkin and William Shotyk. Analytical procedures for the determination of selected major (Al, Ca, Fe, K, Mg, Na, and Ti) and trace (Li, Mn, Sr, and Zn) elements in peat and plant samples using inductively coupled plasma-optical emission spectrometry. *Analytica Chimica Acta* 540 (2005) 247-246.

This publication was prepared by A. Sapkota. Co-authors assisted in the sample preparation, ICP-OES analysis and in the interpretation of the data. A. Cheburkin was responsible for XRF analyses. M. Krachler and W. Shotyk revised the manuscript and assisted in further improvement.